CHARLES UNIVERSITY

Faculty of Science

Developmental and Cell Biology

Cecilia Aquino Perez

New molecular mechanisms involved in cell cycle control

Doctoral Thesis

Supervisor: MuDr. Libor Macůrek, PhD.

Laboratory of Cancer Cell Biology
Institute of Molecular Genetics AS CR, v.v.i.

Prague, 2022

DECLARATION

I hereby declare that I wrote this work independently and that I did my best to acknowledge all people involved in the production of this work and referenced the relevant literature. I did not use this work or a substantial part of it to obtain another academic degree or equivalent.

Prague, 2022 Cecilia Aquino Perez

PROHLÁŠENÍ

Prohlašuji, že jsem tuto závěrečnou práci zpracovala samostatně a že jsem uvedla všechny použité informační zdroje a literaturu. Tato práce ani její podstatná část nebyla předložena k získání jiného nebo stejného akademického titulu.

Praha, 2022 Cecilia Aquino Perez

ACKNOWLEDGEMENT

I would like to thank my supervisor MuDr. Libor Macůrek for all his help, guidance and advice throughout the years of my PhD studies. I would also like to thank my partner, friends and family for all the support and encouragement. Lastly, I would like to thank the Department of Developmental and Cell Biology of Charles University for the studentship that allowed me to conduct this thesis.

Table of Contents

List of abbreviations

BC	Breast cancer
BFA	Brefeldin A
cDNA	Complementary DNA
DAPI	4', 6-Diamidino-2-Phenylindole, Dihyrdrochloride
DBS	Double strand breaks
DCSI	Ductal carcinoma *in situ*
DDR	DNA damage response
DMSO	Dimethyl sulfoxide
dsDNA	Double stranded DNA
EC	Error correction
EGFP	Enhanced green fluorescent protein
ER	Endoplasmic reticulum
FACS	Fluorescent activated cell sorting
FBS	Fetal Bovine Serum
FGF	Fibroblast growth factor
FUCCI	Fluorescent ubiquitination-based cell-cycle indicator
GFP	Green fluorescent protein
HR	Homologous recombination
IEG	Immediate early gene
IF	Immunofluorescence
IR	Ionizing radiation
KD	Knock-down
KO	Knock-out
M	Mitosis
MAT	Metaphase to Anaphase transition
mRNA	Messenger ribonucleoprotein acid
MTOCs	Microtubule organizing centers
MTs	Microtubules
NE	Nuclear envelope
ORC	Opening reading frame
Oris	DNA replication origin
PBD	Polo box domain
PBS	Phosphate buffered saline
PBST	Phosphate buffered saline supplemented with 0.1% Tween
PCR	Polymerase chain reaction
PrCA	Pancreatic cancer
pre-RC	Pre-replicative complex

PTKs	Protein kinases
qPCR	Quantitative real-time PCR
RFs	Replication forks
RFP	Red fluorescent protein
SAC	Spindle assembly checkpoint
SDSA	Synthesis-dependent strand annealing
SMC	Structural maintenance of chromosomes
ssDNA	Single stranded DNA
SUMO	Sumoylation
UV	Ultraviolet
VGMs	Vesiculated Golgi membranes
WB	Western Blot
WT	Wild Type

List of Genes

53BP1	Tumor suppressor p53-binding protein1
ACPs	Adenomatous colorectal polyps
ACTA1	Actin coding gene
ACTG1	Actin, cytoplasmic 2
ACTN4	Alpha-actinin-4
Akt	Protein kinase B (PKB)
APC/C	Anaphase-promoting complex/Cyclosome
ASK1/Dbf4	Apoptosis signal-regulated kinase 1/Dumbbell former 4 protein
ANXA6	Annexin A6
ANK3	Ankyrin-3
ANKRD28	Serine/threonine-protein phosphatase 6 regulatory Ankyrin repeat subunit A
Arp2/3	Actin related protein 2/3
Asf1	Anti-silencing function 1
Asl	Asterless
ATAD5	ATPase family AAA domain-containing protein5
ATF2	Activating transcription factor 2
ATM	Ataxia-telangiectasia mutated
ATP	Adenosine tri-phosphate
ATR	Ataxia-telangiectasia mutated and Rad3-related
ATRIP	ATR interacting protein
AURKA	Aurora A kinase coding gene
BLM	Bloom syndrome protein
BORA	Protein aurora borealis
BARD1	BRCA1 Associated RING Domain 1
BRCA1/2	Breast cancer type ½ susceptibility protein
BUB1	Budding uninhibited by benzimidazole kinase 1
BUBR1	Budding uninhibited by benzimidazole kinase-related 1
B-Myb	Myb-related protein B
BRCT	BRCA1 C terminus
BRD8	Bromodomain containing 8
BRIX1	Ribosome biogenesis protein BRX1 homolog
β-TrCP	Beta-transducin repeat-containing protein
CAFs	Chromatin assembly factors
CAK	CDK activating kinase
CBP	CREB-binding protein
CCAN	Constitutive centromere associated network
CCNA2	Cyclin A coding gene
CCNB1	Cyclin B1 coding gene
CCNE	Cyclin E1 coding gene

Cdh1	Epithelial cadherin gene
CDK	Cyclin dependent kinase
Cdc25	Cell division control protein 25
Cdc	Cell division control protein
CDCA	Cell division cycle associated 2 also known as PP1 regulatory subunit 81
CENPs	Centromere proteins -A, -B, -C, -E
CHFR	Checkpoint with forkhead and ring finger domains
Chk1	Checkpoint kinase 1
Chk2	Checkpoint kinase 2
CIP/KIP	CDK interacting protein/kinase inhibitory protein
CK1s	Casein kinase 1
CKAP2	Cytoskeleton-associated protein 2
CKIs	Casein kinase inhibitors
CLASP	CLIP-associating proteins
CLIP	Class II-associated invariant chain peptide
CMG	Cdc45/MCM2-7GINS complex
CMV	Cytomegalovirus
CPB	Cryptic polo box
CPC	Chromosome passenger complex
CRPC	Castration-resistant prostate cancer
CRM1	Chromosomal maintenance 1, also known as exportin 1
CSPP	Centrosome/spindle associated protein
CSNK1A	Casein kinase 1 Alfa
CSNK1D	Casein kinase 1 Delta
CSNK1E	Casein kinase 1 Epsilon
CtIP	Carboxy-terminal binding protein
CTNNA1	Catenin alpha-1 coding gene
CTNNB1	Catenin beta-1 coding gene
CUL3	E3 ubiquitin ligase cullin 3
CYK4	GTPase MgcRacGAP
DAPI	4’, 6-Diamidino-2-Phenylindole, Dihyrdrochloride
DCAF15	DDB1 and CUL4 associated factor 15
DDK	DBF4-dependent kinase
Dma1	Defective in mitotic arrest 1
DNA-PKs	Extracellular-regulated kinases
E2F1	E2F Transcription factor 1
EB1	End-binding protein 1
EBNA1BP2	Probable rRNA-processing protein EBP2
ECT2	Epithelial cell transforming 2
EG5	Kinesin related motor protein

EGF	Epidermal growth factor
ELG1	Telomere length regulation protein ELG1 (Also ATAD5)
Emi1	Early mitotic inhibitor-1
ERKs	Extracellular signal-regulated kinases
EXO1	Exonuclease 1
FAM72D	Family with sequence similarity 72 isoform D
FAM83D	Family with sequence similarity 83 isoform D or Spindle protein CHICA
FAM110A	Family with sequence similarity 110 isoform A
FAM110B	Family with sequence similarity 110 isoform B
FAM110C	Family with sequence similarity 110 isoform C
FBXO31	F-box only protein 31
FBP	F-box protein
Fnk	Fibroblast growth factor-inducible kinase
FOXM1	Forkhead box protein M1
G2E3	G2/M phase specific E3 ubiquitin protein ligase
Gαi	α-subunit of three guanine nucleotide binding proteins
GAS2L3	Growth Arrest Specific 2 like 3
GEF	Guanine-nucleotide exchange factor
GINS	"Go-ichi-ni-san" proteins = Sid5, Psf1, Psf2, Psf3 proteins
GM130	Cis-Golgi matrix protein
GP210	Nuclear pore glycoprotein-210
GSK3-β	Glycogen synthase kinase 3 beta
GST	Glutathione S-transferase
GTSE1	G2 and S phase-expressed protein 1
γTuSC	Gamma-Tubulin small complex
HDM2	Human double minute 2
HEC1	High expressed in cancer protein 1
HNRNPDL	Heterogeneous nuclear ribonucleoprotein D-like
HERC2	Hect domain and RCC1-like domain-containing protein 2
Hrr25	HO and radiation repair
JAK/STAT	Janus kinase/Signal transducer and Activators of Transcription
JNKs	C-Jun N-terminal kinases
KAP	Kinase associated phosphatase
KAP1	KRAB domain-associated protein 1
KIFs	Kinesin proteins superfamily
KLH	Keyhole Limped Hemocyanin
KMN	Knl1 complex/Mis12 complex/Ndc80 complex protein network
KMTs	Kinetochore attached to MTs
KNL1	Kinetochore null protein 1
LAS2	Lung adenoma susceptibility protein 2 precursor

LBR	Lamin B receptor
LGN	TPR/GoLoco multidomain scaffolding protein
Lis1	Lissencephaly gene product 1
MAC	Membrane attack complex
MACF1	Microtubule-actin cross-linking factor 1
MAD1/2	Mitotic arrest deficient 1/2
MAPKs	Mitogen activated protein kinases
MAPs	Microtubule-associated proteins
MARCKSL	MARCKS-related protein 1
MCC	Mitotic checkpoint complex
MCM2-7	Minichromosome maintenance 2-7 heteroexamer
MDC1	Mediator of DNA damage checkpoint protein 1
MDM2	Mouse double minute 2 homolog
MDMX	Murine double minute X
MEF2	Myocyte enhancer factor-2
MEK	Mitogen-activated protein kinase kinase
Mik1	Mitosis inhibitor protein kinase 1
MIS12	4-subuinit missegregation 12 complex
MK2	Mitogen-activated protein kinase (MAPK)-activated protein kinase 2
MKLP	Kinesis Motor protein 1 and 2
MKP	Mitogen-activated protein kinase phosphatase
MOV10	Putative helicase MOV-10
MPF	Maturation-promoting factor
MPM-2	Anti-Mitotic proteins antibody 2
MPS1	Monopolar spindle protein kinase 1
MRE11	Meiotic recombination 11 homolog 1
MRN	MRE11/RAD50/NBS1 hetero-hexamer complex
MuvB	Also known as the LIN complex
MVB12B	Multivesicular body subunit 12B
Myb	Myeloblastosis proto-oncogene
Myt1	Myelin transcription factor 1
NBS1	Nijmegen breakage syndrome protein 1
NDC1	Nucleoporin NDC1 - Component of the nuclear pore complex
Ndc80	Kinetochore complex component 80
NDEL1	Nuclear distribution protein nudE-like 1
NDUFA13	NADH dehydrogenase 1 alpha subcomplex subunit 3
NEB	Nuclear envelope breakdown
NEKs	Never in mitosis A-related kinases
NEURL1b	Neuralized E3 ubiquitin protein
NF-KB	Nuclear factor kappa-light-chain-enhancer of activated B cells

NF-Y	Nuclear factor Y transcription factors
NHEJ	Non-homologous end-joining
NPCs	Nuclear pore complexes
NPAT	Nuclear protein, coactivator of histone transcription
NSCLC	Nuclear filamentous 2
NUF2	Nuclear mitotic apparatus, kinetochore protein Nuf2
NuMA	Non-small cell lung cancer
NUMA1	Nuclear mitotic protein 1
NUPs	Nucleoporins
OCRL	Lowe oculocerebrorenal syndrome protein, also known as Inositol polyphosphate 5-phosphatase
P21	Protein 21
P53	Protein 53
PALB2	Partner and Localizer of BRCA2
PCNA	Proliferating cell nuclear antigen
PDE9A	Phosphodiesterase 9A
PDGF	Platelet derived growth factor
PI3K	Phosphatidylinositol-3 kinase
PIF1	ATP-dependent DNA helicase PIF1
PKA	Protein kinase A
PKCε	Protein kinase C epsilon
PKs	Protein kinase
PLKs	Polo–like kinases
Plo	Serine/threonine-protein kinase plo1
Plx	Pollux protein
Pol	Polymerase
POM121	Nuclear envelope pore membrane protein 121
PP1	Protein phosphatase 1
PP2A	Protein phosphatase 2A
PP6	Protein phosphatase 6
PPP6C	Serine/threonine-protein phosphatase 6 catalytic subunit
PPP6Rs	Serine/threonine-protein phosphatase 6 regulatory subunits
pRB	Retinoblastoma protein
PRC2	Polycomb repressive complex 2
PRC1	MT bundling protein required for cytokinesis 1
Prk	Protein kinase C-related kinase
RAC1	Ras-related C3 botulinum toxin substrate 1
RAD50	Double strand break repair protein
RAD51AP	RAD51 associated protein 1
Raf	Ras-effector (Also known as MAPK or MEKK)

RanBP2	Ran binding protein 2
Ras	Rat sarcoma virus
RCC1	Ran guanine exchange factor 1
RFC	Replication factor C
RHINO	PHD finger protein rhinoceros
RIF1	Replication timing regulatory factor 1
RLF-M	Replication licensing factor-M
RNFs	Ring finger proteins
ROCK	Rho-associated protein kinase
RPA	Replication protein A
RPL34	60S ribosomal protein L34
RPL37A	60S ribosomal protein L37a
SCF	Skip1/Cdc53/F-box containing complex
Sid4	Separation initiation protein 4
Skp1/2	S-phase kinase-associated protein ½
SMADs	From the fusion of *C. elegans Sma* genes and the *Drosophila Mad*, Mothers against decapentaplegic
SNARE	Soluble-N-ethylmaleimide sensitive factor activating protein receptor
Snk	Serum-inducible protein kinase
SPC24/25	Spindle pole component 24/25
SPTAN1	Spectrin alpha chain, non-erythrocytic 1
Srs2	ATP-dependent DNA helicase Srs2
STAU1	Double-stranded RNA-binding protein Staufen homolog1
STLC	S-trityl-L-cysteine
SUN1	SUN domain-containing protein 1
TAO	Thousand and one aminoacid protein kinases
TFIIH	Transcription factor II F
TGF-β	Transforming growth factor β
TIAM1	T-cell lymphoma invasion and metastasis-inducing protein 1
Tip60	Tat-interactive protein 60
TMED2	Transmembrane emp24 domain-containing protein 2
TOPBP1	DNA topoisomerase 2-binding protein 1
TP53	Tumor protein 53
TRAIP	TRAF interacting protein
TRIM32	E2 ubiquitin-protein ligase TRIM32
TRIM49A	Tripartite motif containing 49-A
TTBK1/2	Tau-tubulin binding kinases 1 and 2
TUBB8	Beta-tubulin coding gene
TUB1AC	Alfa-tubulin coding gene
UBE2C	Ubiquitin conjugation enzyme E2 C
VCP	Valosin containing protein

VDAC3	Voltage-dependent anion-selective channel protein 3
VEGF	Vascular endothelial growth factor
VPRBP	DDB1-and CUL4-associated factor 1
VRK1	Vaccina-related kinase 1-3
Wee1	Mitosis inhibitor protein Wee1
WRN	Werner helicase protein
Wnt	Wingless-INT
XMAP215	Family of highly conserved group of MT-associated proteins
XRCC1	Base excision repair factor X-ray cross-complementing group 1
YWHAE	14-3-3 protein epsilon

List of figures

List of Tables

ABSTRACT (in English)

In this doctoral, thesis we aimed to find and study novel mechanisms regulating cell cycle phase transitions in non-stressed conditions and in context of the cell response to various types of stress. First, we focused on studying Polo-like kinase 3 that has previously been implicated in activation of the cell cycle checkpoint after DNA damage. For this, we employed CRISPR/Cas9- mediated gene editing to knock-out PLK3 in RPE cells while in parallel performing RNA interference assays and submitting the cells to different types of stress. The main observation was that in both systems PLK3 was disposable for response to DNA damage, hypoxia and osmotic stress. Through mass spectrometry analysis of purified EGFP-PLK3 we identified PP6 and its regulatory subunits PPP6R1 and PPP6R3 as novel PLK3 interactors. We observed that PLK3 is phosphorylated in its conserved residue Thr-219 and that PP6 depletion boosted PLK3 phosphorylation status but did not affect its kinase activity. The possible regulation of PLK3 trough PP6 is interesting and its biological relevance will be addressed by future research. Next, we performed a transcriptomic analysis in human RPE-FUCCI cells aiming to identify new regulators of the cell cycle. We selected Family with sequence similarity 110 member A (FAM110A) for further characterization as the protein was highly expressed in G2 cells and localized to the mitotic spindle and spindle poles throughout mitosis. Through siRNA-mediated depletion of FAM110A we observed an impairment in chromosomal congression, delayed Metaphase-to-Anaphase transition and misorientation of the mitotic spindle. By implementing a mass spectrometry analysis of purified mitotic FAM110A we identified the CK1 family isoforms CK1ε and CK1δ, alongside with the cytoskeletal proteins tubulin, actin, α/β-catenin and α-actinin as potential interactors. Through *in vivo* and *in vitro* assays, we showed that CK1δ interacted with FAM110A through its C-terminal domain. In addition, CK1 phosphorylated Ser-252-255 residues, which proved to be necessary for FAM110A's binding to tubulin and for chromosomal alignment during metaphase. Following with other cytoskeletal interactors, FAM110A interaction with actin proved to be relevant for chromosomal congression and during actin dynamics during mitosis. These observations pave an interesting path for future studies over FAM110A potential cytoskeletal cross-talk regulation roles during mitosis.

ABSTRAKT (v Czech)

V této doktorské práci jsme se zaměřili na nalezení a pochopení nových mechanismů řídících buněčný cyklus v normálních podmínkách i v kontextu buněčné odpovědi na různé formy stresu. Nejdříve jsme se zaměřili na studium Polo-like kinázy 3, která byla již dříve popsána v aktivaci kontrolních bodů cyklu v důsledku poškození DNA. Pomocí technologie CRISPR/Cas9 jsme cíleně inaktivovali gen PLK3 v lidských RPE buňkách a paralelně rovněž potlačili expresi PLK3 pomocí RNA interference. Hlavním pozorováním bylo zjištění, že PLK3 není nezbytná pro kontrolu buněčné odpovědi na poškození DNA, hypoxii a osmotický stres. Metodou hmotnostní spektrometrie jsme identifikovali fosfatázu PP6 a její regulační podjednotky PPP6R1 a PPP6R3 jako nové interakční partnery PLK3. Dále jsme pozorovali, že PLK3 je fosforylována na konzervovaném zbytku Thr219 a že deplece PP6 zvyšuje úroveň fosforylace PLK3 ovšem bez vlivu na její enzymatickou aktivitu. Tyto výsledky naznačují možnou regulaci funkce PLK3 prostřednictvím PP6 a biologická relevance tohoto pozorování bude předmětem dalšího studia. Dále jsme provedli transkriptomovou analýzu v lidských RPE-FUCCI buňkách s cílem nalézt potencionální nové regulátory buněčného cyklu. V dalším studiu jsme se zaměřili na Family with sequence similarity 110 member A (FAM110A), jehož exprese byla vysoká v G2 fázi buněčného cyklu a protein lokalizoval na pólech dělícího vřeténka v průběhu mitozy. Po depleci FAM110A jsme pozorovali poruchy kongrese chromozomů, oddálený přechod mezi metafází a anafází a porušenou orientaci dělícího vřeténka. Pomocí hmotnostní spektrometrie mitotického FAM110A jsme identifikovali kinázy CK1ε a CK1δ a cytoskeletální proteiny tubulin, actin, α/β-catenin a α-actinin jako nové interakční partnery FAM110A. Pomocí *in vitro* a *in vivo* experiment jsme prokázali, že CK1δ interaguje s C-terminální částí FAM110A a fosforyluje oblast Ser-252-255. Tato modifikace FAM110A je nezbytná pro vazbu tubulinu a pro správnou organizaci chromosomů v průběhu metafáze. Rovněž interakce FAM110A s dalšími cytoskeletálními proteiny byla nezbytná pro kongresi chromosomů a dynamiku aktinu v průběhu mitozy. Tato pozorování naznačují možnou funkci FAM110A v propojení cytoskeletálních systémů v průběhu mitozy a dávají základ pro další výzkum.

1. INTRODUCTION

1.1. The cell cycle

The eukaryotic cell cycle is a series of highly controlled molecular processes that lead to the complete duplication of a single cell into two identical daughter cells. The purpose if this process is controlled proliferation by completely and accurately duplicating the genome and then precisely segregating the two copies between the two future daughter cells. This purpose defines the two major phases of the cell cycle: Phase S, were DNA duplication occurs and M phase were chromosome segregation and cell division take place. This two major phases are separated by two "buffer" or "gap phases" known as G1 phase between M phase and S phase and G2 phase between S phase and M phase (**Figure 1**); together, G1/S/G2 are known as interphase (Malumbres and Barbacid 2009).

Cell cycle transitions between phases are regulated by cyclin-CDK protein kinases, protein phosphatases and ubiquitin-protein ligases. An important aspect of this regulation is the fact that only cyclins present an oscillatory nature during the cell cycle, while the presence of the rest of the participating proteins remains constant (Malumbres and Barbacid 2009). Therefore, the cyclins are regulated by timely transcription and ubiquitin-mediated proteasomal degradation.

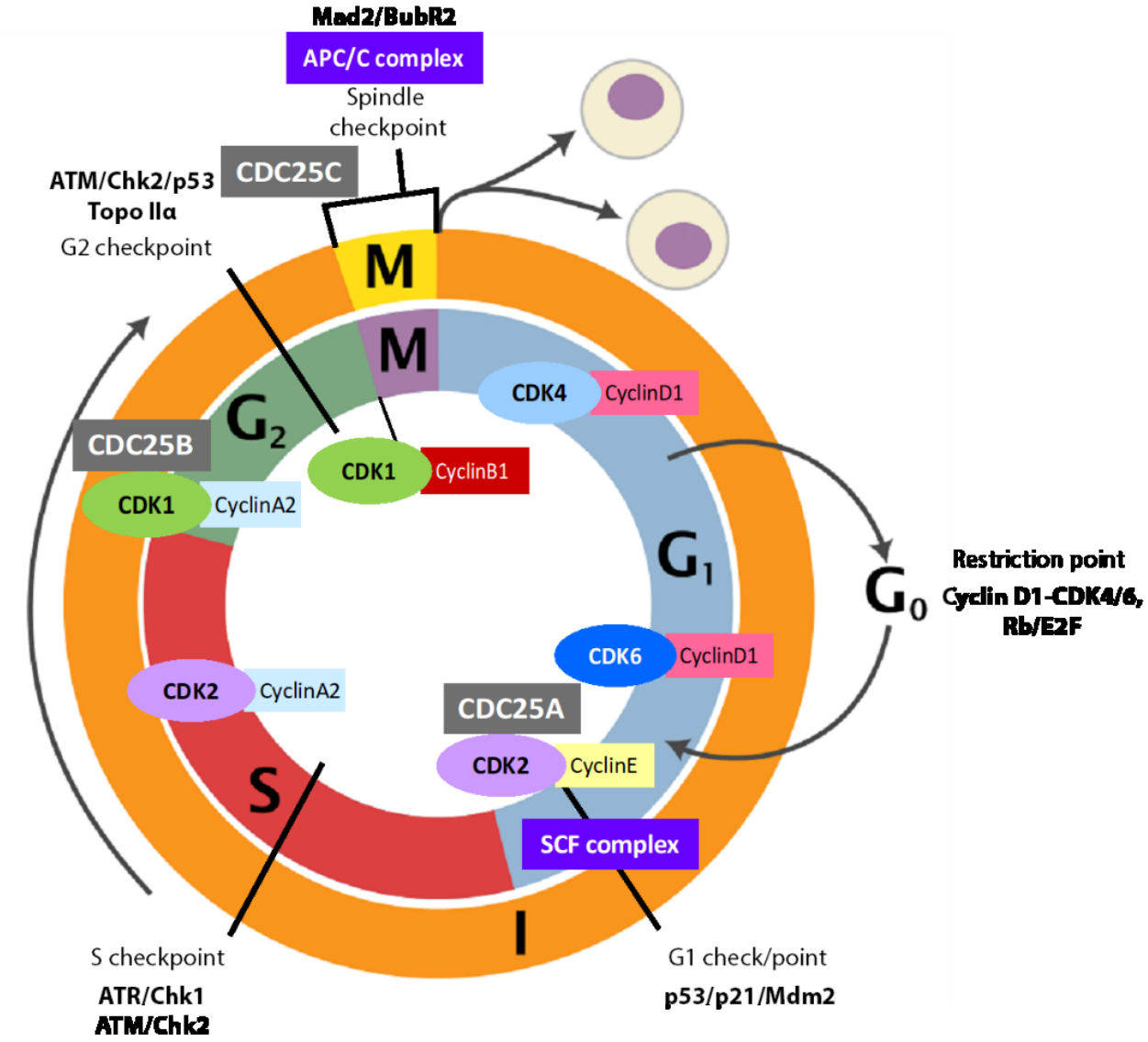

Figure 1. The Eukaryotic cell cycle. The eukaryotic cell cycle is composed of two major phases (S phase and Mitosis) separated by two gap phases (G1 and G2). Cell cycle transitions between this phases are regulated by CDKs that are activated by phase-specific cyclins, activated/deactivated by phosphatases and targeted for proteasome destruction by ubiquitin-protein ligases. Throughout the progression of the phases, checkpoints work as a surveillance mechanism that monitors the order, integrity and fidelity of the major events in the cell cycle in order to prevent deregulated proliferation. On first instance the restriction point happens during G0 and is overcome when the cell compromises to enter a new cycle. The G1 checkpoint where the cell arrest in the presence of either new or inherited DNA damage, the S checkpoint ensures correct and complete DNA replication and deals with DNA insults that occur during genomic duplication, the G2 checkpoint that will prevent cells from entering mitosis when there is presence of severe DNA damage and the spindle checkpoint that verifies the mitotic spindle formation and integrity to ensure proper chromatid segregation.

1.2. Protein kinases as the master regulators of the cell cycle

Progression through the cell cycle is controlled by activity of the PKs (Protein kinases) (Pines 1994). At first glance we have the widely known CDKs (Cyclin dependent kinases) which are evolutionary conserved master regulators of the cell cycle in all eukaryotes. CDKs depend on a cyclin subunit in order to be activated and to excerpt their control functions during transitions between individual phases of the cell cycle (Lukasik, Zaluski et al. 2021). The MAPKs family (Mitogen activated protein kinases) are in charge of responding to extracellular stimuli. MAPKs are further subdivided in ERKs (Extracellular-regulated kinases) that respond to growth factors and mitogens, JNKs (C-Jun N-terminal kinases) that respond to cellular stresses like osmotic or heat shock and p38s (p38 mitogen-activated protein kinases) that respond to stress, inflammatory cytokines and apoptotic signals (Pearson, Robinson et al. 2001, Yu, Sun et al. 2020). In addition, several families of other protein kinases are implicated in specialized functions throughout the cell cycle. For example NEK1 (Never in mitosis A-related kinases) participate during DNA damage response and in cell cycle checkpoint control (Chen, Chen et al. 2008) alongside the ATM/ATR kinases and DNA-PK that are the main regulators of the DNA damage response (Blackford and Jackson 2017). Other crucial families are Polo-like kinases and kinases of Aurora family that both contribute to control of the bipolar spindle formation, correct attachment of microtubules to the kinetochores and cytokinesis (Lee, Jang et al. 2014, Willems, Dedobbeleer et al. 2018). More recently, Casein kinase 1 family has been attributed with key cell cycle regulatory functions, ranging from Cdc25 family regulation and DNA damage response to orchestrating delicate mitotic functions (Knippschild, Gocht et al. 2005). Throughout the extension of this work, functions of CDKs, PLKs and CK1s families will be described in detail.

1.2.1. Cyclin-dependent kinases: critical regulators of the Cell cycle

CDKs (Cyclin-dependent kinases) are a subfamily of the PTKs (protein kinases). The human CDK family has 13 members that can interact with 29 cyclins or cyclin-related proteins; however, only ten of this 29 cyclins have been reported as directly involved in control and regulation of the mammalian cell cycle (Malumbres and Barbacid 2005).

Human CDKs can be classified in two groups: The interphase CDKs (CDK2, CDK4 and CDK6) and the mitotic CDK (CDK1), nevertheless other CDKs have also been reported to participate in the regulation of non-cell cycle related processes. For instance, human CDK5 is active in post-mitotic neurons, phosphorylating a plethora of substrates that participate in the neuronal actin cytoskeleton remodeling, both in healthy and diseases states (Shah and Rossie 2018). Another example is CDK7 and cyclin H, who aside from phosphorylating and activating CDK1 and CDK2, also control transcription trough association with TFIIH and by phosphorylating the carboxyl-terminal domain of the RNA Pol II largest subunit (Fisher

2005). In the case of CDK8, it has been reported to be needed for the expression of several β-catenin transcription targets (Firestein, Bass et al. 2008) and that its increased kinase activity is needed to repress E2F1 apoptotic targets (Morris, Ji et al. 2008). In future sections of this text we will focus on describing the functions of conventionally known CDKs throughout the Cell cycle in detail.

1.2.2. The Polo-like kinase family

Polo-like kinases are a family of evolutionary conserved Ser/Thr PKs that play critical roles during cell cycle progression, DNA damage response and G2/M checkpoint regulation (Korns, Liu et al. 2022). Originally, the first ortholog was discovered in the model organism *Drosophila melanogaster* when Glover's group found weak hypomorphic alleles of the genes encoding for *Polo* and *Aurora* and saw that homozygous embryos presented monopolar spindle poles due to centrosome maturation failure and failed to achieve cytokinesis (Sunkel and Glover 1988, Carmena, Riparbelli et al. 1998). Later on the protein was also detected in *Saccharomyces cerevisiae, S. pombe* and in *Xenopus* (Cdc5, Plo1 and Plxs respectively) (Glover 1989, de Carcer, Manning et al. 2011). In humans, the Polo-like family is comprised of five members (PLK1 - 5); in vertebrates, PLK1 duplication produced PLK2 and PLK3 and later on, PLK5 came out from a second duplication; PLK4 turned up from a PLK1-like protein (de Carcer, Manning et al. 2011). The PLK family present differential functions and regulation mechanisms throughout the cell cycle (Takai, Hamanaka et al. 2005) that have been shown to be relevant in oncogenesis and tumor progression, proving to be interesting subjects of study (Korns, Liu et al. 2022).

1.2.2.1. PLKs Structure, Activation and Regulation

The conserved nature of the PLKs among species can be observed in their structure and domains; all members of the PLK family share a similar structure within their N-terminal catalytic domain and the distinct PBD (Polo box domain) at their C-terminal region (Zitouni, Nabais et al. 2014). Plk1 – 4 present a catalytic domain at their N-terminal piece responsible for the phosphorylation of serine/threonine residues; on the contrary PLK5 catalytic domain is cut by half and has no activity therefore themed "pseudo-kinase domain" (Lowery, Lim et al. 2005). PLK1, PLK2, PLK3 and PLK5 have their PBD composed of two PBs in tandem (PB1 and PB2), while PLK4 presents a "Cryptic PB" and a third PB (PB3) that may assist during protein-protein interactions allowing PLK4 to homodimerize to perform its functions and exhibits a low level of homology with PLK1's PB1 and PB2 (Park, Soung et al. 2010) (**Figure 2**).

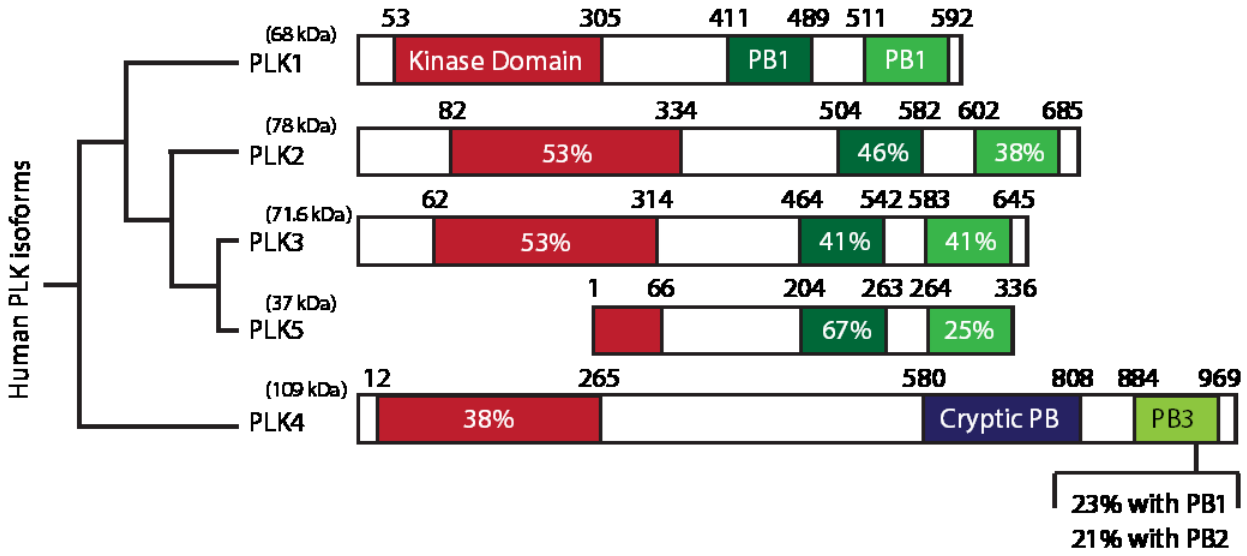

Figure 2. Protein architecture of the PLK family isoforms. Schematic diagram of human PLK1 – 5 isoforms; each one contains a catalytic kinase domain at their N-terminal region and a tandem of two repeats of the PBD domain (PB1, PB2) at their C-terminal region. Sequence identities with the corresponding domains in PLK1 are given in percentages. Numbers indicate the positions of amino acid residues for each given protein (Lee, Park et al. 2014).

The PBD is responsible for PLKs intracellular localization and works as a phospho-recognition module that regulate their functionality and substrate specificity (Elia, Rellos et al. 2003). For instance, mutations in the PBD of PLK1 prevent it from properly localizing to the spindle poles, it is believed that PLK2 (also known as Snk) and PLK3 (Also known as Fnk or Prk) are regulated in a similar manner (Lowery, Lim et al. 2005). In the case of PLK4 (also known as Sak23), the cryptic polo-box (CPB) function is to form a stable homodimer (Leung, Hudson et al. 2002, Slevin, Nye et al. 2012) and bind to a target in a manner that does not require a phosphorylated motif (Liu, Kim et al. 2020). On the other hand, whether the PBD of Plk5 also binds to a phospho-epitope is not known, however since it lacks a functional catalytic domain it seems to lack any function throughout the cell cycle; nonetheless it is highly expressed in non-proliferating neuronal cells (de Carcer, Escobar et al. 2011).

The PLKs kinase catalytic domain contains a conserved activation T-loop where key residues for enzymatic activation and ATP-binding are located: In the case of PLK1 the ATP binding residue is its Lys-82, for PLK2 it's Lys-111, for PLK3 it's Lys-91 and for PLK4 it's Lys-51. For enzymatic activation, the residue located at the T-loop in PLK1 is Thr-210, for PLK2 is Thr-239, for PLK3 is Thr-219 and for PLK4 IS Thr-169. Human PLK5 lacks any residue that resembles the previously described ones however, mouse PLK5 contains a complete kinase domain and a PBD (Lee, Jang et al. 2014).

1.2.2.2. PLKs Biological Functions

The PLK family have important and diverse functions during cell cycle control (Korns, Liu et al. 2022). PLK1 functions throughout the cell cycle are the widest studied and best characterized of all the PLKs family members. PLK1 plays crucial roles during the G2/M transition, progression through mitosis, functional maturation of centrosomes , cilia disassembly and in establishment of mitotic spindle bipolarity; it has been shown that PLK1 is needed for γ-Tub and MPM-2 recruitment to centrosomes (Lane and Nigg 1996, Casenghi, Meraldi et al. 2003). PLK1 is also needed for successful mitotic entry, progression and exit through APC/C regulation as well as participating in the SAC recovery process and proper cytokinesis (Toyoshima-Morimoto, Taniguchi et al. 2002, Zhou, Aumais et al. 2003, Macurek, Lindqvist et al. 2008). A detailed description of all PLK1 functions in the cell cycle are provided throughout this work.

Up to date, the functions of PLK2 and PLK3 are the least well studied, however some functions during the cell cycle regulation have been described. For instance, PLK2 has been involved in centriole duplication during S phase (Cizmecioglu, Krause et al. 2012) while PLK3 has been linked to DNA replication aiding through the G1-S phase transition by phosphorylating transcription-related proteins Topo Iiα and DNA Pol δ (Iida, Matsuda et al. 2008) Additionally, PLK3 is localized to the Golgi Apparatus and is involved in Golgi dynamics regulation throughout G2 phase and during Golgi fragmentation for mitotic entry (Lopez-Sanchez, Sanz-Garcia et al. 2009) and it has been reported to be activated upon cellular stress and DNA damage (Bahassi el, Conn et al. 2002, Zimmerman and Erikson 2007). PLK2 has been functionally linked to PLK4, since both of them localize to the centrioles during the M/G1 transition where both are in charge of duplicating the centrioles once G1 phase is restored, this function is conserved from *Drosophila* to mammals (Kleylein-Sohn, Westendorf et al. 2007). Additionally, it has been reported that depletion of PLK2 impairs embryonic development and placenta establishment in mice due to decreased cell proliferation (Ma, Charron et al. 2003). Asl (Asterless) functions as a scaffold protein by binding to PLK4 on its Cryptic PBD; during interphase it promotes PLK4 homodimerization and auto-phosphorylation and during mitosis it stabilizes it, targeting it to centrioles where its responsible for initiating centriole duplication (Klebba, Galletta et al. 2015). In order to prevent cells from double duplicating its centrioles, PLK4 auto-phosphorylates, priming itself for ubiquitin-mediated degradation and thus preventing the generation of multipolar spindles (Slevin, Nye et al. 2012).

1.2.2.3. PLKs and cancer

As mentioned throughout this work, the PLK family shows multiple functions throughout the cell cycle, thus roles in both mitotic and non-mitotic cancer development have been described for the PLK isoforms (Lee, Jang et al. 2014). For instance PLK1 has important roles during the SAC regulation and errors in this process can lead to faulty cell division which is a hallmark of cancer (Jang, Ji et al. 2007). Overexpression of PLK1 contributes to cancer development as it promotes excessive proliferation, which has been reported in cancers like gliomas, head and neck squamous carcinomas and breast malignancies (Degenhardt and Lampkin 2010). Other isoforms have roles in tumor development as well; PLK2 is a transcriptional target of stabilized p53 and PLK3 gets activated upon DDR and allegedly is capable of phosphorylating p53 in its Ser-20 residue (Xie, Wu et al. 2001). Parallel to this, overexpression of PLK3 has proven to suppress proliferation by impairing cytokinesis and by inducing apoptosis (Conn, Hennigan et al. 2000). Because of all the previously mentioned characteristics, PLKs isoforms are a good target for cancer therapy; for instance PLK1 inhibition to prevent centrosomal maturation has been proved to be an effective strategy to induce apoptosis in a tumor-selective manner (Lane and Nigg 1996). Currently several PLK1 inhibitors are under clinical studies (Degenhardt and Lampkin 2010).

1.2.3. The Casein Kinase 1 family

The members of the casein kinase 1 (CK1) family are known to be constitutive kinases that play key roles in diverse biological processes trough regulation of several cellular signal transduction pathways (Cheong and Virshup 2011). The CK1 family belongs to the Serine/Threonine-specific PTKs category (Manning, Whyte et al. 2002), they were named after their ability to phosphorylate the milk protein casein *in vitro,* however, casein is not a physiological substrate of the CK1 family (Venerando, Ruzzene et al. 2014). Numerous substrates have been reported to be targeted by the CK1 family isoforms for phosphorylation, thus involving them in an ample catalog of biological processes (Knippschild, Gocht et al. 2005). Amongst this biological processes, both canonical and non-canonical functions have been ascribed to the CK1 family (Knippschild, Gocht et al. 2005, Fulcher and Sapkota 2020).

The CK1 genes form a unique branch of the PTKs kinome tree and are evolutionary conserved within eukaryotes having several orthologues identified in animals, fungi, plants and protozoans (Hoekstra, DeMaggio et al. 1991, Casas-Mollano, Jeong et al. 2008, Wang, Liu et al. 2011, Tan, Dai et al. 2013). Being a small group, they show the closest relative sequence similarity with tau-tubulin binding kinases I and 2 (TTBK1/2), and the vaccinia-related kinase 1-3 (VRK1 – 3) (Cheong and Virshup 2011, Fulcher and Sapkota 2020). There are six human CK1 isoforms (α, δ, ε, γ1, γ2 and γ3) that are encoded by independent genes and post-transcriptionally processed to yield several splice variants.

1.2.3.1. CK1s Structure, activation and regulation

CK1 family members possess a highly conserved amino-terminal kinase domain (55-98% identical) that is adjacent to a more variable carboxyl-terminal extension which in turn show little homology between CK1 members (Cheong and Virshup 2011) (**Figure 3**). CK1 kinases do not require phosphorylation on the activation loop and have been reported to act as monomeric, constitutively active enzymes. They exclusively use ATP as a phosphate donor and are cofactor independent. CK1 family members are ubiquitously expressed and are considered to exist in a constitutive active state (Schittek and Sinnberg 2014). Nevertheless, the majority of studies reporting this constitutive activity have been performed *in vitro*, using purified catalytic domains, therefore failing to capture any potential interaction/regulation with other enzymes or accessory proteins *in vivo* (Cruciat, Dolde et al. 2013).

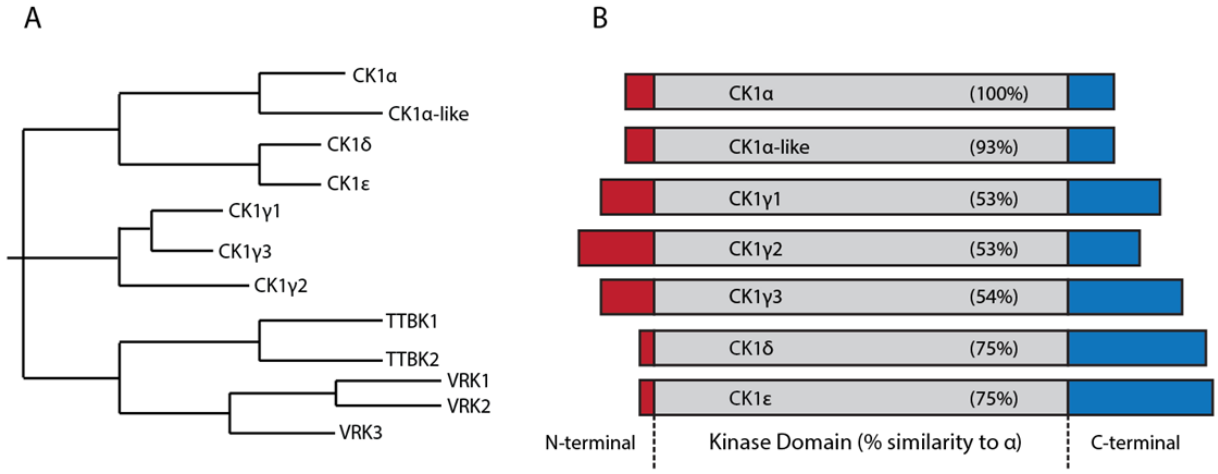

Figure 3. Protein architecture of the CK1 family isoforms. A. Phylogenetic tree of the CK1 family of protein kinases and their relation with the kinases with the closest sequence similarity (Manning, Whyte et al. 2002). **B.** Schematic diagram of the CK1 isoforms architecture; percentage values represent the sequence similarity of the kinase domain of each CK1 isoform relative to the CK1α kinase domain (Fulcher and Sapkota 2020).

The kinase domain of CK1 is similar with the rest of the PTKs, presenting its catalytic cleft in between the binding sites for ATP and its substrates, with a smaller N-terminal domain and a large C-terminal domain (Knippschild, Gocht et al. 2005). The activation of isoforms α, δ, and ε is inhibited by auto-phosphorylation of the C-terminal residues, thus regulating their catalytic activity (Graves and Roach 1995, Budini, Jacob et al. 2009). In addition, the C-terminal domain has shown to play key roles regulating the kinase ability to recognize substrates such as relief of the auto inhibition (Cegielska, Gietzen et al. 1998). Because it is considered that CK1 C-terminal domain is relatively small (regarding that of other PTKs), the interaction with functional partners or regulatory subunits may be necessary for their proper cellular regulation

(Fulcher and Sapkota 2020). In this sense, several potential regulatory mechanisms for CK1 have been investigated and described, such as activation trough phosphorylation by PKA (Giamas, Hirner et al. 2007), binding to 14-3-3 proteins (Clokie, Falconer et al. 2009) and the previously described timely auto-inhibition (Cegielska, Gietzen et al. 1998).

1.2.3.2. CK1s Biological Functions

Amidst the most deeply studied pathways where CK1 isoforms exercise their kinase activity we find membrane transport processes (Lampe and Lau 2004), ribosome biogenesis (Zemp, Wandrey et al. 2014), cellular morphology regulation (Robinson, Menold et al. 1993), vesicular transport (Gross, Hoffman et al. 1995), modulation of the Wnt/β-catenin and Hedgehog pathway during development (Price 2006), regulation of the circadian rhythms (Eide and Virshup 2001, Ebisawa 2007), ciliogenesis (Greer, Westlake et al. 2014), microtubule assembly (Peng, Moritz et al. 2015) and most relevant for our field, during DNA repair regulation (Hoekstra, Liskay et al. 1991, Winter, Milne et al. 2004, Knippschild, Wolff et al. 2005).

1.2.3.3. CK1s in DNA Damage Response

During DNA damage response Chk1 activation is supported by claspin and said binding has been reported to be mediated by CK1γ1 phosphorylation (Meng, Capalbo et al. 2011). Several studies have shown that p53 is stabilized through CK1 phosphorylation during the apoptotic response and cell cycle arrest (Dumaz, Milne et al. 1999) and that prior Ser-15 phosphorylation is required for this interaction (Dumaz and Meek 1999), showing CK1 modification to be sequential, creating an auto-regulatory feedback loop (Knippschild, Milne et al. 1997). CK1α has been reported to mediate MDM2-p53 interaction by phospho-priming p53 for further phosphorylation by CK1δ and CK1ε, which enhances MDM2-p53 interaction (Kulikov, Winter et al. 2006). However MDM2 phosphorylation in its Ser-118 and Ser-121 by CK1δ has been shown to target it for proteasomal degradation by $SCF^{-\beta TRCP}$ depending on the cell context (Inuzuka, Tseng et al. 2010). Hypoxia response regulation via CK1δ can also induce p53 stabilization (Kalousi, Mylonis et al. 2010). CK1δ and CK1ε have also been reported to phosphorylate Cdc25A, inhibiting and subsequently enhancing its proteasomal-mediated degradation upon DNA damage (Honaker and Piwnica-Worms 2010, Piao, Lee et al. 2011).

1.2.3.4. CK1s in Mitosis

The after mentioned processes are very well described functions performed by the CK1 family, however, recently novel functions during proper mitotic spindle positioning and chromosomal segregation have been described (Brockman, Gross et al. 1992, Behrend, Stoter et al. 2000, Milne, Looby et al. 2001, Peng, Moritz et al. 2015, Fulcher, He et al. 2019). The first roles for CK1 during mitosis where reported in lower

eukaryotes. Using the model organism *S. pombe*, it was shown that CK1 is a key modulator of the SAC. It was established that CK1 phospho-primes Sid4 for subsequent Dma1 (RNF8 in humans) ubiquitination and targeted degradation, thus establishing the SAC; Sid4 is a scaffold protein in charge of recruiting Plo1 to the spindle poles under normal conditions (Johnson, Chen et al. 2013). Parallel to this, it was shown in *S. cerevisiae* that Hrr25 (CK1D in humans) forms part of the γTuSC (γ-tubulin small complex), depending on its kinase activity for the association; further it was reported that Hrr25 mediated –phosphorylation of γTuSC promoted its integrity and functionality (Peng, Moritz et al. 2015). CK1δ and the γTuSC are highly conserved, therefore it is speculated that similar regulatory mechanisms may have a general similarity in the majority of eukaryotes.

In the case of human cells CK1δ has been reported to localize to centrosomes displaying a high affinity towards MTs under DDR and stress, suggesting that this isoform might have regulatory functions upon cell division checkpoint establishment (Behrend, Milne et al. 2000, Stoter, Bamberger et al. 2005, Peng, Moritz et al. 2015). Additionally, it was observed that specifically inhibiting both CK1δ/ε caused mitotic arrest (Behrend, Milne et al. 2000). CK1δ appears to be constitutively expressed in invasive extravillous trophoblasts, localizing to the centrosomes and to the mitotic spindle; it was also reported that CK1δ-specific inhibition caused structural alterations in the centrosomes, favored the formation of multipolar spindles and impaired proper mitotic progression (Stoter, Bamberger et al. 2005). More recently, CK1α has been reported to mediate mitotic spindle positioning through its scaffold protein FAM83D and that disruption of their normal interaction lead to a delayed MAT (metaphase to anaphase transition) (Fulcher, He et al. 2019). Putting this information into perspective, a recent phosphoproteomic analysis of cell cycle progression showed that around 50% of phosphorylated peptides present consensus putative motifs for CK1, and that this peptides belong to specific mitotic sub-phases (Ly, Whigham et al. 2017). Together this data suggests that CK1 isoforms have important unexplored functions in mitosis.

1.2.3.5. CK1s in Cancer

Because CK1 proteins are involved in critical cellular processes, a strict regulation of their activity is needed in order to prevent the development of certain diseases. For instance, studies on the expression levels of CK1δ and CK1ε in young, healthy mice suggests that CK1 expression is strongly regulated, and different isoforms are expressed to different levels in distinct tissues (Utz, Hirner et al. 2010). The incidence of mutations in the coding sequence of CK1 isoforms or the improper regulation of their cellular activity have been linked to neurodegenerative disorders including Alzheimer disease (Flajolet, He et al. 2007, Perez, Gil et al. 2011, Adler, Mayne et al. 2019).

Moreover, it has been shown that both CK1δ and CK1ε expression appears to be up-regulated in some cancers and actively participate in the pathways regulating p53 stabilization (Huart, MacLaine et al. 2009, Inuzuka, Tseng et al. 2010). Taking on consideration the high relevance of CK1δ and CK1ε in genomic stability maintenance processes it seems obvious to consider that mutations leading to dysregulated activity of the CK1 family may lead to cancer development (Knippschild, Wolff et al. 2005). Loss of CK1α heterozygosity in p53 deficient gut leads to highly aggressive and invasive carcinoma pointing out this isoform as a potential tumor suppressor when p53 is lacking (Elyada, Pribluda et al. 2011). It has been shown that mutations in CK1ε frequently found in breast cancer lead to Wnt/β-catenin pathway function loss and concomitantly result in abnormal activation of the Wnt/Rac1/JNK and Wnt/Ca+ pathway, which generates an increment in cells migratory capacity and also decreased cell-adhesion (Foldynova-Trantirkova, Sekyrova et al. 2010). A mutation in the C-terminal domain of CK1δ has been reported to provide high oncogenic potential in ACPs (adenomatous colorectal polyps) by promoting adenomas development in the adjacent intestinal mucosa (Tsai, Woolf et al. 2007). Also, in BC (Breast carcinomas), CK1δ has been reported to present immunoreactivity changes correlated to the tumor differentiation degree; for instance immunohistochemistry of highly differentiated BC like low grade DCSI (ductal carcinoma *in situ*) show strong CK1δ staining while low differentiated cancers with low invasive capacity show reduced staining signals (Rosenberg, Cleveland et al. 2016).

In brief, there is a growing field of evidence pointing out the CK1 family as oncogenic drivers since their uncontrolled activity promotes genomic instability, proliferation and apoptotic processes inhibition. However it is not possible to deem them as oncogenes or tumor suppressors since their role in the malignancies progression is manifold and may strongly depend on the cellular context (Elyada, Pribluda et al. 2011).

1.2.3.6. CK1s and their substrates

Key regulatory proteins that participate in the control of the after mentioned biological processes have been identified as substrates targeted for phosphorylation by the CK1 isoforms (Knippschild, Gocht et al. 2005). The first attempts to identify specific characteristics shared by CK1 substrates pointed out the need of a priming phosphorylation event in the -3 position of the site pS/pT-X-X-S*/T*, it was later shown that the presence of a cluster of acidic residues located at the N-terminal side to the after mentioned site can effectively substitute for the priming phosphorylation event (Flotow and Roach 1991, Marin, Meggio et al. 1994). More recently, a non-canonical S-L-S motif with a parallel C-terminal cluster of acidic residues has been shown to be targeted by CK1 isoforms, although with less efficiency than the canonical phospho-primed motif (Marin, Bustos et al. 2003). In conjunction, this observations suggests that the CK1 family

can phosphorylate Ser/Thr residues even if they are not defined by a specific sequence motif, suggesting that the targeting of specific substrates is likely to be regulated by other factors, such as subcellular localization and substrate recruitment (Fulcher and Sapkota 2020). To date, the discovery and characterization of novel CK1 substrates is helping to broaden and deepen our knowledge on the previously reported functions for this kinase family, as well as opening new doors for unexplored cellular functions.

1.1.1 G0 phase and the Restriction Point

In multicellular living organisms, most cells that are terminally differentiated remain in a non-proliferative state (or quiescent state) known as G0; however, there are also some specialized cells that will continue to proliferate even well into adulthood. In both cases, the cells have committed to a specific cycle state were they will either exit the cell cycle and become quiescent (G0) or will start their own cell cycle (G1) in response to extracellular stimuli (Pardee 1989). Once the cell receives this extracellular signals to enter a new cycle of division (this transition is known as START in yeast and as the restriction point or "R" in mammalian cells) it won't be able to remain or eventually return to G1/G0, as cells that pass this restriction are committed to completion of the cell cycle and consequent division (Blagosklonny and Pardee 2002).

Originally, it was considered that once the R point is surpassed, any extracellular signals were no longer needed and the cell would be committed to enter the G1 phase and into a new cell cycle (Donjerkovic and Scott 2000). However, recent studies have shown that that instead of only being able to evaluate their mitogenic environment in the short window frame of time that the restriction point allows them, proliferating cells have the capacity of storing MAPK activity history in response to mitogenic stimuli and stress signals that are present throughout the whole life of a mother cell (Yang, Chung et al. 2017). In this manner, mother cells will transmit to the daughter cells mitogen-induced cyclin D1 mRNA and DNA damage-induced p53 protein, which in turn will induce variable expression of cyclin D1 and of p21 respectively and will determine in a great extent the future path of the daughter cells. Another important aspect to consider is that the molecular competition between stress and mitogenic signaling received by daughter cells also plays a key role in the cell cycle path decision-making (Yang, Chung et al. 2017). It has been proposed that protein synthesis rates function as a record system, given that the translation rate is strongly correlated with cell size and growth and it's directly regulated by extrinsic mitogenic stimuli that will influence the proliferation-quiescent behavior of daughter cells (Min, Rong et al. 2020).

One, if not the most important regulator of the G0 quiescent phase is TP53, a gene that transcribes for the renowned protein 53 (p53), the "guardian of the genome". P53 function is to regulate cell proliferation by preventing uncontrolled growth and division (Matlashewski, Lamb et al. 1984). P53, together with the Ras

(proto-oncogene) pathway are responsible for downregulating cyclin D1 and maintaining cells in G0; nevertheless, once mitogenic signals induce cyclin D1 production, Ras activity can be overcome (Peeper, Upton et al. 1997). Once stabilized, cyclin D1 can bind to CDK4 and CDK6, which in turn are activated by CAK (CDK-Activating kinase composed by CDK7-Cyclin H) (Makela, Tassan et al. 1994) and can move the cell pass through to the R point (Lolli and Johnson 2005). This process is carefully monitored by CKIs (CDK inhibitors), such as p21 or the Ink4 proteins (p16, p15, p18, p19) that are in charge of preventing unregulated CDK4/6-Cyclin D activity (Peter 1997). Other key regulators both during G0 and at the beginning of G1 are pocket proteins (pRb, p107 and p103) whose job is to bind and inhibit the expression of genes regulated by the E2F transcription regulators family (Helin, Harlow et al. 1993). Parallel to this, growth factors such as VEGF, PDGF, FGF and EGF to name a few, are also important extracellular signals that stimulate cells to past by the R point and to entry into the cell cycle (Blagosklonny and Pardee 2002).

1.1.2 G1 phase

The G1 phase is subdivided in three parts: Entry or Early-G1, Mid-G1 and Late-G1. During early G1, which we consider the beginning of the cycle, no CDKs-Cyclin complexes are active and its mainly characterized by the transcriptional activation of immediately early genes by mitogenic stimulation and activation of key early transduction pathways (Zetterberg, Larsson et al. 1995). In this sense, there are three main pathways involved in regulation of cyclin D promoter and its consequential expression: MAPK, PI3K/Akt and Wnt; other pathways include ER, NF-KB, JAK/STAT and Rac1/NADPH oxidase (Guo, Hao et al. 2011).

Depending on the cellular context, transcription factors E2F1 or E2F4 can activate cyclin D1 promoter, driving its accumulation through a positive feedback loop, aiding in the accumulation of Cyclin D, pushing progression trough G1 (Muller, Moroni et al. 1997). Rho/RAC1/Cdc42 signaling, which in principle induces changes in cytoskeletal conformation in response to mitogenic stimuli, can also promote early Cyclin D1 expression (Roovers and Assoian 2003). From the early stage to mid G1 phase, CDK4-Cyclin D and CDK6-Cylin D complexes hypophosphorylate pRb (Retinoblastoma protein) (Ho and Dowdy 2002). This hypophosphorylation allows pRb to associate with the transcription factors family E2F disabling them from activating transcription. Concomitantly, pRb phosphorylation causes it to dissociate from histone deacetylases, leading to derepression of the CCNE1 gene (Harbour, Luo et al. 1999), allowing for Cyclin E enrichment and its binding to CDK2.

Mid-G1 is marked by the conformation and activation of the CDK4/6-cyclin D complex thanks to sustained cyclin D accumulation induced by MAPK/ERK (Mitogen-activated protein kinase, originally called extracellular signal-regulated kinase) activity. MAPK/ERK is promoted by Rho kinase, who in turn

suppresses Rho/Cdc42 activity and who in turn its balanced out by MKP (Mitogen-activated protein kinase phosphatase) creating a flexibly balanced positive feedback loop. (Bhalla, Ram et al. 2002, Roovers and Assoian 2003).

G1 is considered in its late stage when pRb becomes hyperphosphorylated by active CDK2-Cyclin E, which causes E2F to dissociate from pRb, allowing the transcription factor to initiate transcription of the genes required for entry intro S phase (Bertoli, Skotheim et al. 2013). One of its targeted genes is Cyclin E, generating a positive feedback loop to aid in the CDK2-Cyclin E complex formation and activation, then the cell is considered to be in the G1/S transition (Ekholm, Zickert et al. 2001). Activation of the CDK2-Cyclin E complex on its Thr160 residue is performed by CAK (Larochelle, Pandur et al. 1998) and it can be dephosphorylated in the same residue by KAP phosphatase, rendering CDK2 inactive until it binds to its respective cyclin (Poon and Hunter 1995). CDK2-Cyclin E is inactivated by phosphorylation on Thr14/Tyr15 by Wee1/Mik1 related protein kinases, while dephosphorylation of the same residues by Cdc25A phosphatase activates the complex (Gu, Rosenblatt et al. 1992). In turn, Cdc25A is regulated on a transcriptional level in a positive manner by c-Myc in response to mitogenic signals or serum stimulation to lead cell cycle progression (Donjerkovic and Scott 2000) and negatively regulated by transcriptional inhibition from E2F4/p130 complex by recruiting histone deacetylase to Cdc25A promoter in response to TGF-β (Iavarone and Massague 1999). The KIP/CIP family members (p21, p27 and p57) of CKIs can also negatively regulate Cdc25A. In this late stage Cyclin D expression is sustained by PI3k/AKT pathway instead of MAPK/ERK (Marino, Acconcia et al. 2003).

During the after mentioned processes, CDC6 -a regulator of DNA replication- together with ORC (Origin recognition complex), Cdt1 (Chromatin licensing and DNA replication factor 1) and the heterohexameric MCM2-7 (minichromosome maintenance) complex, make up the pre-RC (pre-Replicative complex). CDC6 is recruited by ORC to the DNA origin sequence (rich in thymine) in an ATP dependent manner where it helps load two MCM2-7 complexes (DNA-Helicase) at each side of the replication origin for bidirectional replication (Speck, Chen et al. 2005); once MCM2-7 complexes are loaded, the rest of the after mentioned proteins become dispensable (Harvey and Newport 2003). During mid G1, CDC6 levels become highly enriched in the nucleus, helping with the conformation of the pre-RC at replication origins; however, they remain inactive because they depend on CDK2-Cyclin A activation trough phosphorylation (Petersen, Lukas et al. 1999).

1.1.3 S phase

The transition between G1 and S phase involves the conversion of pre-RCs into fully active replication forks; this involves unwinding of the DNA origin by the DNA replicative helicase (MCM2-7 complex), stabilization of the newly formed single-stranded DNA and loading of the replication machinery (Takeda and Dutta 2005). This processes depend on replication factors and CDK2-Cyclin A activity along with CDC7 (also known as DDK or ASK1/Dbf4 dependent kinase) (Kim, Yamada et al. 2003). The CDC7-ASK1/Dbf4 kinase is directly involved in the activation of chromosome replication, suggesting that it functions as a critical molecular switch for the start of S phase (Masai, Sato et al. 1999).

The complex CDK2-Cyclin E activity is at its peak during the G1/S transition, but as the cell fully enters S phase, cyclin E will be rapidly degraded (Hengstschlager, Braun et al. 1999). As S phase initiates, the SCF ubiquitin-protein ligase (Skp1/Cullin/F-box containing complex), targets CDK2 and GSK3β phosphorylated-Cyclin E for its ubiquitin-mediated degradation; SCF is responsible as well for the degradation of p27 and p21. This way the SCF complex will maintain the activities of CDK1 and CDK2 (in complex with Cyclin A) through the rest of the cell cycle by keeping the levels of this inhibitors down (Tsvetkov, Yeh et al. 1999, Bornstein, Bloom et al. 2003). Once CDK2 is free from Cyclin E, it can bind to Cyclin A; then Cdc25A will proceed to dephosphorylate the complex on its CDK2's Tyr-15 residue, consequently activating it (Blomberg and Hoffmann 1999). Cyclin A actively regulates multiple aspects of S phase, at first stance by driving phosphorylation of the pre-RC component CDC6, and components of the replication machinery like DNA pol λ (Cardoso, Leonhardt et al. 1993, Frouin, Toueille et al. 2005), CDC6 localization is nuclear during G1, but relocates to the cytoplasm during S phase after CDK2-Cyclin A2 activation to perform its duties (Petersen, Lukas et al. 1999).

DNA replication is an all-or-nothing process; once it starts, it will proceed to completion and once it's complete it won't occur again. The first step of this process is known as "Replication initiation". As mentioned before, the pre-RCs have been assembled during the G/S transition but remain stalled, this is where the Protein kinase CDC7 comes into action (Kim, Yamada et al. 2003). This cell division cycle protein is activated by the ASK protein (Known as Dbf4 in yeast) by binding into a complex who's main job is to activate/phosphorylate the MCM2-7 complexes (Sato, Arai et al. 1997). The loading of the MCM2-7 proteins onto replication origins is essential for replication fork firing, therefore it is also known as the RLF-M (Replication licensing Factor); as a consequence of replication, the MCM2-7 proteins are removed from the new duplex. This control mechanism ensures that no section of the genome will be replicated more than once by stopping the initiation of a new S phase round prior to mitosis (Blow and Hodgson 2002). This process is also known as the activation of Oris (DNA replication origins) and it's followed by the

loading and activation of Cdc45 in the Oris, also by action of the CDC7-Dbf4 complex during early S phase and in late origins during late S phase (Jares and Blow 2000). Cdc45 protein and GINS proteins-composed of Sid5 and Psf1-3 (Takayama, Kamimura et al. 2003)-work together to bind and activate the latent MCM2-7 helicase, creating the CMG (Cdc45/MCM2-7GINS) complex, where MCM2-7 proteins provide motor activity for unwinding the double helix DNA for replication and forming what is known as the replication fork (Petojevic, Pesavento et al. 2015). In this context Cdc45 is required for the recruitment of the replicative polymerases and will act as a physical link between initiation and elongation factors (Kukimoto, Igaki et al. 1999). After the CMG complex starts an initial origin unwinding event, the RPAs (Replication protein A) are in charge of binding the single stranded DNA to prevent the formation of unwanted hairpins (hydrogen bonds that bind single strand DNA in improper places) and to further stimulate origin unwinding (Walter and Newport 2000). As helicase unwinds the DNA, the DNA ahead is forced to rotate, which can result in super coiling which can eventually halt the replication fork by torsional resistance. To prevent this problem, Gyrase (a type of Topoisomerase) is in charge of alleviating this resistance by temporarily breaking the DNA strands, releasing the supercoil and immediately rejoining them (Wang 2002). This whole process is necessary for replicative polymerases recruitment, which is the final step for replication initiation (Jares and Blow 2000).

The next step is the formation of the initiation complex. In higher eukaryotes, three polymerases are essential for the replication process: DNA pol α (also known as Primase), DNA pol δ and DNA pol ε; all of them possess a conserved catalytic core but have specialized functions during elongation. After origin unwinding, DNA pol α (which is the only polymerase that can initiate synthesis *de novo* on the single stranded DNA) is recruited to synthesize a short RNA primer for the leading strand and several short RNA primers for the lagging strand (Sun, Shi et al. 2015). This primed template is needed by DNA pol δ and ε to bind the DNA strands and switch places with DNA pol α after primer synthesis; both DNA pol δ and ε poses proofreading exonuclease activity and perform at higher speed than DNA pol α. For the subsequent DNA processing and proper DNA binding, the DNA pols need to associate with the ring-shaped factor PCNA (Jonsson and Hubscher 1997). PCNA also requires the templated DNA so it can be positioned by the clamp loader known as RFC (ATPase similar to CDC6) to begin with the DNA synthesis (Ellison and Stillman 2001).

The conjuncture of all this molecular machinery is known as the eukaryotic replisome, and once is fully assembled, the cell can proceed with the processivity of the DNA; the standard replication speed is 1-2 kb per minute. DNA is read by the DNA polymerase in a 3’ to 5’ sense, which means that the new strand has to be synthesized in the 5’ to 3’ sense. The leading strand is continuously extended from the single primer

by DNA pol ε by adding the complementary nucleotides to the 3-OH' end. At the same time, DNA pol δ is responsible for the synthesis of the lagging strand replication, which has to be done in the opposite direction; the cell manages this by elongating the lagging strands trough discreet short pieces, known as Okazaki fragments (Okazaki, Okazaki et al. 1968). This is the reason why primase adds several primers to the lagging strand, so that each time helicase has opened enough length, the DNA pol δ binds to the primer with the help of the clamp complex and starts synthesizing the Okazaki fragments sending the fresh lagging duplex back towards the replication fork. When DNA pol δ reaches a new RNA primer, it disassociates and will bind again once helicase has unwound enough lagging strand (Takeda and Dutta 2005). The maturation of the Okazaki fragments is done by primer removal and nicks ligation as follows: RNAse H performs base pair excision through its 5' to 3' exonuclease activity to remove the left over unstable ribonucleotides in the lagging duplex, then DNA pol I replaces them with stable deoxynucleotides. After this DNA ligase connects each single gap that remains in the sugar-phosphate backbone between the lagging duplex and the Okazaki fragment through a phosphodiester bond. This whole mechanism is known as elongation and is how both the lagging and leading strands will be replicated in their totality (Takeda and Dutta 2005).

During the whole replication process, the histones, which are highly basic proteins that act as spools around which DNA strands wind and create the structural units known as nucleosomes, must be duplicated as well. During the G1/S phase transition the CDK2-Cyclin E complex phosphorylates a nuclear coactivator of histone transcription known as NPAT whose job is to recruit the Tip60 chromatin remodeling complex to promote transcription of histone genes (DeRan, Pulvino et al. 2008). As DNA is being actively replicated, histones are divided between the parent and daughter strands and the freshly synthesized histones are assembled in nucleosomes by the CAFs (chromatin assembly factors such as Asf1 and CAF-1) that actively travel along with the replication fork (Zhang, Shibahara et al. 2000). At the same time, replication fork progression depends on nucleosome assembly, potentially through a feedback loop mechanism where CAF-1 might signal to PCNA to unload from the new duplex upon nucleosome assembly (Groth, Corpet et al. 2007). Maintaining a proper Histone supply throughout the whole replication process is key in order to maintain proper fork speed and to avoid accumulation of DNA damage (Hoek and Stillman 2003, Gunesdogan, Jackle et al. 2014). This collaborative action between the DNA replisome and the CAFs is known as chromatin assembly (Alabert and Groth 2012). Immediately after replication and chromatin assembly, the cell has to re-establish its chromatin domains and epigenetic information; the PRC2 (Polycomb Repressive Complex 2) and other histone-modifying complexes can "copy" modifications present in old histones on the new histones (Ramachandran and Henikoff 2015).

Replication termination implicates fork convergence, synthesis completion, replisome disassembly and decatenation (Dewar and Walter 2017). As mentioned before DNA replication starts at multiple replication origin sequences, therefore replication forks encounter and terminate at many sites along the chromosome, this is known as convergence and is immediately followed by the disassembly of the replisome. The first step for the replisome disassembly is the removal of the CMG complex, this is performed by the SCF ubiquitin ligase by polyubiquitinating MCM2-7 causing the whole complex to be removed from the strand by VCP (Also known as ATPase p97) (Moreno, Bailey et al. 2014, Fullbright, Rycenga et al. 2016). It is believed that this polyubiquitination does not target the CMG complex for degradation, but that instead promotes its recycling. It is also important to point out that CMG will be unloaded only after the gap left between the lagging strand and the leading strand of a converging fork has been filled and ligated, suggesting that MCM2-7 ubiquitination will occur once the CMG complex finds and encircles double-stranded DNA (Dewar, Budzowska et al. 2015). It is possible that for the rest of the replisome and because the CMG complex has either direct or indirect contact with the proteins of the replication machinery, its unloading leads to passive disassociation of the complete replisome (Dewar, Budzowska et al. 2015). Proteins that do not interact with the CMG complex like PCNA, have to be removed in an independent manner; PCNA is unloaded by ELG1 (Also known as ATAD5) which also leads to the removal of the PCNA-interacting proteins such as DNA ligase and DNA pol δ (Kubota, Nishimura et al. 2013). The final step, named decatenation consists in the relief of the accumulated topological stress between the converging forks (Bermejo, Doksani et al. 2007). This can be achieved either by topoisomerase action ahead of the traveling fork or by coupling helicase activity with rotation of the whole fork relative to the unreplicated DNA (Schalbetter, Mansoubi et al. 2015). The latter method, relaxes the topological stress but at the expense of generating double-stranded intertwines behind the replication fork, which are deemed "precatenanes", this can be resolved by type II but not type I topoisomerases, and gaps are filled by extension of the leading strands (Bermejo, Lai et al. 2012).

The end of S phase and the S/G2 transition are marked by multiple positive feedback loops and specific transcriptional regulation that gradually increment CDK1 and PLK1 activities that will continue throughout G2 phase and culminate in enforced mitotic entry (Crncec and Hochegger 2019). At the end of S phase, once DNA replication has been successfully completed, a new cascade of transcription begins in response of activation of transcription factors such as NF-Y, FOXM1 and B-Myb (MYBL2) (Sadasivam, Duan et al. 2012). FOXM1 (Forkhead box protein M1) is a transcription factor that regulates de expression of a large group of G2/M-specific genes, such as PLK1, Cyclin B1, Nek2, SKP2 and CENPF; it also participates in the maintenance of genomic stability by aiding trough chromosomal segregation (Laoukili, Kooistra et al. 2005). FOXM1 accumulates upon entry into S phase (Major, Lepe et al. 2004) and it translocate to the

nucleus via the Raf/MEK/MAPK complex when it's Ser331 and Ser704 residues are phosphorylated, promoting its transcriptional activity (Ma, Tong et al. 2005). Eventually, MuvB and B-Myb will be required for the subsequent recruitment of FOXM1 to late gene promoters during G2 (Knight, Notaridou et al. 2009, Sadasivam, Duan et al. 2012).

During S phase, cyclin A localization is restricted to the nucleus by p21, however a recent study reported that during S/G2 transition, CDK2-Cyclin A2 complex re-localizes to the cytoplasm were it directly phosphorylates BORA initiating the characteristic activation of PLK1 during this transition. (Silva Cascales, Burdova et al. 2021). Further down on G2 the CDK2-Cyclin A2 complex will continue functioning as a trigger for mitotic kinase activation (Vigneron, Sundermann et al. 2018).

1.1.4 G2 phase

During G2 phase, Cyclin A2 is in charge of stimulating still on-going transcription and to inhibit degradation of key mitotic regulators in order to promote their accumulation (Lukas, Sorensen et al. 1999). At the same time that mitotic regulators enrich, Cyclin A dependent positive feedback loops promote CDK1 activation (Mitra and Enders 2004). It has been shown that Cyclin A depletion leads to G2 arrest probably due to errors in completing DNA replication lagging from S phase (Oakes, Wang et al. 2014) or by preventing proper PLK1 activation (Silva Cascales, Burdova et al. 2021). At this moment of G2 phase, CDK2-Cyclin A/E complexes will phosphorylate FOXM1 in its Thr600, Ser638, Thr611 and at Ser251 residues, this last one being critical for CDK1-Cyclin B1 subsequent targeted phosphorylation (Chen, Dominguez-Brauer et al. 2009). The phosphorylation at Thr596 by CDK1-Cyclin B1 recruits PLK1 to continue phosphorylating FOXM1 at its Ser715 and S724 residues, which will promote its transcriptional activity, recruiting the transcriptional co-activator CBP (p300/CREB binding protein) to enhance G2 specific transcription (Major, Lepe et al. 2004). FOXM1 is also essential during G2/M and mitotic progression by driving the transcription of cyclin B1, Cdc25B, PLK1 Aurora B, surviving and centromere proteins A/B (Krupczak-Hollis, Wang et al. 2004, Wang, Chen et al. 2005).

As previously mentioned, cyclin A depletion leads to G2 arrest and blocks mitotic entry, while depletion of Cyclin B1 does not block mitotic entry, but instead affects later on mitotic progression (Hegarat, Crncec et al. 2020). CDK1-Cyclin B1 complex activity is exclusive to the G2/M transition and checkpoint and is responsible for catalyzing entry into mitosis (Nurse 1990). After centrosomal separation, gradual accumulation of cyclin B increases the activity of CDK1 as cells prepare to enter mitosis (Lindqvist, van Zon et al. 2007). However, the CDK1-Cyclin B1 complex will remain inactive until inhibitory phosphorylation is removed; through a positive feedback loop, the CDK1-Cyclin B complex activates the

phosphatase Cdc25A which in reciprocity, activates the complex further by removal of phosphate groups on the Tyr15 and Thr14 from the activation site and deactivates the complex inhibitors responsible for this phosphorylations, known as Wee1 and Myt1 (Parker and Piwnica-Worms 1992, Mueller, Coleman et al. 1995). This loop is indirectly amplified by the complex formation and accumulation of the Aurora A kinase and its cofactor, BORA and in turn, this complex regulates the activation of PLK1 (Macurek, Lindqvist et al. 2008). Later in G2, the combined activities of CDK2-Cyclin A2 and CDK1-Cyclin B will generate massive modifications in BORA, protecting it from being targeted for degradation by the SCF complex and resulting in mitotic commitment (Vigneron, Sundermann et al. 2018, Silva Cascales, Burdova et al. 2021). This whole process will trigger the onset of prophase (Gavet and Pines 2010).

As previously mentioned, activated PLK1 will target Wee1 and Myt1 for phosphorylation, which will single it out for degradation through the $SCF^{-\beta\text{-}Trcp}$ complex (Nakajima, Toyoshima-Morimoto et al. 2003); at the same time, PLK1 activates/phosphorylates Cdc25B/C, feeding further in the CDK1 activation positive feedback loop (Lobjois, Froment et al. 2011). The end of the G2 phase and entry into mitosis occurs when a threshold level of activated CDK1-Cyclin B1 (also known as Maturation promoting factor or MPF) has been reached (Lindqvist, van Zon et al. 2007). Attenuated CDK2-Cyclin A2 and fully activated CDK1-Cyclin B1 complex (also referred to as MPF) trigger irreversible but crucial processes by phosphorylating a large number of substrates during the remains of G2 phase and early phases of mitosis (Holt, Tuch et al. 2009) to trigger centrosome duplication alongside the NEB (nuclear envelope breakdown) and chromosomal condensation, reversible disassembly of the Golgi ribbon into fragments to be split between future daughter cells, among other processes (Shorter and Warren 2002).

1.1.4.1 Centrosome maturation and duplication

Up to this point of this description of the cell cycle, we haven't discussed the cycle dynamics of the Centrosome, therefore it will be explained in detail before dwelling with the intricacies of the mitotic process. The cell enters G1 with only one centrosome composed of two centrioles and their pericentriolar material. One of the two centrioles is two cycles "older" than the other, which was generated on the previous cycle. During G1/S transition, the centriole pair splits, a process that is directly regulated by CDK2-Cyclin A/E activity and possibly by the SCF complex (Freed, Lacey et al. 1999). From each individual centriole a new one will grow in a perpendicular manner making the process semiconservative (Hinchcliffe, Li et al. 1999).

The pericentriolar material is also known as MTOCs (Microtubule Organizing Centers), it contains all the needed elements to nucleate and organize microtubules along with hundreds of other proteins (O'Connell,

Caron et al. 2001). This large plethora of proteins contained in the MTOCs must have specific interactions with the centrioles and with its functional components, however this interactions have not been characterized in their totality, nor has the structural core of the pericentrioles been fully described (Stearns 2001).

The earliest point of the cell cycle were two centrosomes can be found as individual bodies with their own pericentriolar material is when the cell is undergoing DNA replication, although it remains unclear if this happens during early or late S phase. At this point, the oldest centriole is marked by presenting distal appendages, by the presence of the cenexin protein (Lange and Gull 1995) and of ε-tubulin (Chang, Giddings et al. 2003) ; by the time that the cell reaches the G2/M transition, both centrosomes will have this characteristics. At the start of M phase, the amount of pericentriolar material on each duplicated centrosome increases side by side with the number of nucleated microtubules (Smith, Hegarat et al. 2011). During this whole process active CDK1 will depolymerize interphase astral MTs and MTs associated proteins, whose function in G2 was to inhibit centrosome separation (Crasta, Huang et al. 2006, Smith, Hegarat et al. 2011).

The last step of the centrosome cycle is separation. During prophase the two sister centrosomes will separate from each other as chromatin condenses at approximately one hour before the NEB (Nuclear envelope breakdown). The separation is propelled by microtubule motor-mediated sliding towards opposite poles of the cell aided by dynein (Whalley and Malliri 2015). The MT-sliding activity of Eg5 (Kinesin related motor protein) is crucial for this process, as it has been extensively shown that treatment of cells with Eg5 inhibitors like STLC (S-trityl-L-cysteine) produces monopolar spindles and arrest in mitosis (Mayer, Kapoor et al. 1999). It is believed that counteracting forces that oppose centrosome separation are crucial to achieve the proper force balance required for correct chromosome alignment (Woodcock, Rushton et al. 2010). Eg5 is positively regulated by CDK1 by regulating its localization trough phosphorylation/activation of Nek9, and by directly phosphorylating it on the Thr927 to stimulate MT-binding (Blangy, Lane et al. 1995). CDK1 also phosphorylates the GEF (guanine-nucleotide exchange factor) protein known as TIAM1 and its substrate RAC that localize to the spindle poles to create an inward force that helps stabilize and tighten the mitotic spindle (Woodcock, Rushton et al. 2010). CDK1 regulates proteins that both drive and oppose centrosome separation with the ultimate goal to achieve the perfect balance for correct chromosome alignment (Whalley and Malliri 2015). During mitosis, the two centrosomes define the poles of the mitotic spindle and will be segregated along with the chromatids at the end of cell division (Stearns 2001).

1.1.5 Mitosis

As described previously, mitosis initiation is triggered in an irreversible manner by the concomitant and culminating activation of CDK1-Cyclin B1 complex (Gautier, Norbury et al. 1988). When in mitosis, the cell objective is to equally distribute one of the centrosomes and half of the replicated genetic material between the two future daughter cells. Such an important task has to be accomplished with stringent fidelity, since failures in the process can lead to death in unicellular organisms and aneuploidy or polyploidy in multicellular organisms which is a huge aspect of cancerous progression (McIntosh 2016). Excessive cell division is an important aspect of malignancy in cancer, and on the other hand, insufficient or defective division may dwell down in conditions such as anemia. This relevant particularities of the mitotic process have tracked attention for deep and detailed study resulting in impressive advances in its understanding. However, a complete and detailed grasp of the mitotic process as a whole is currently in process (McIntosh 2016).

1.1.5.1 Prophase

The beginning of Prophase, the first step in mitosis is marked by very specific cellular morphological changes: At first glance, protein synthesis slows down but doesn't stop completely, maybe to allow for rapid re-start after division completion (Sivan, Kedersha et al. 2007). MTs and microfilaments lose their characteristically interphase stability and are dissolved by extensive phosphorylation (Maller 1986), stress fibers disappear but fibrous actin remains at the cell cortex and will be critical for the constriction ring formation during cytokinesis (Mitsushima, Aoki et al. 2010). Aside from this processes the most obvious change is the visible condensation of duplicated chromatin that occurs during Prophase. Chromosome compaction consists in the "packing" of the condensed chromatin loops in discrete individual bodies known as chromosomes (Kornberg 1977) with the help of crisscrossed strands of proteic fibers constituted by condensins and ATPases that have positive supercoiling activity, creating superhelical tension in the dsDNA (Kimura and Hirano 1997, Thadani, Uhlmann et al. 2012). Chromatin posttranslational modifications such as acetylated and/or phosphorylated histones, among other chromatin proteins aid in the compaction process, while at the same time shutting transcription down mainly because transcription factors are disassembled (Martinez-Balbas, Dey et al. 1995).

Chromatin condensation also marks the start of the process known as NEB (Nuclear Envelope Break-down) which takes place in late prophase, is characteristic of an "open mitosis" and can be completed within several minutes (Dultz, Zanin et al. 2008). The process starts with the dispersal of the NUPs (nucleoporins), lamins and intermediate filaments as a result of CDK1-Cyclin B1 directed phosphorylation. NUPs are soluble proteins that are the main components of the NPCs (Nuclear Pore Complexes) and are released to

the cytoplasm as stable subcomplexes (Terasaki, Campagnola et al. 2001). NUP98 has been reported to be a key phosphorylation target at the onset of this process; NUP53, the NUP107-160 complex and transmembrane NUPs NDC1, POM121 and GP210 are also phosphorylation targets during NEB onset, nevertheless the modulation mechanisms of this phosphorylations remains under intensive study (Eisenhardt, Redolfi et al. 2014, Weberruss and Antonin 2016). In the case of mammalian somatic cells, the NEB is supported by a mechanism that uses MTs pulling mechanical forces to tear further apart the holes left by the disassembly of the NPCs (Salina, Bodoor et al. 2002). The next step in nuclear disassembly is the lamina depolymerization (Gerace and Blobel 1980); phosphorylated A-type lamins are released into the nucleoplasm (Georgatos, Pyrpasopoulou et al. 1997) causing the proteins that conform the inner membrane of the nucleus to detach from the chromatin (Beaudouin, Gerlich et al. 2002). This whole chain of events is a result of the disruptive hyper-phosphorylation carried out by the CDK1-Cyclin B1 complex on the NE components, causing the retraction of the NE remains into the ER (Endoplasmic Reticulum) membrane system (Torvaldson, Kochin et al. 2015).

The ER undergoes complete structural re-organization during Prophase in conjunction with the NEB; The ER gets re-organized from its characteristic network of sheet-like cisternae and ribbon-like array into tubular structures (Lu, Ladinsky et al. 2009). Interestingly it has been shown in *Drosophila* embryos that this process is driven by a CDK1-Cyclin A directed phosphorylation of the ER complex and therefore is a hallmark process of early mitosis (Bergman, McLaurin et al. 2015). This tubular structures allow the ER to accumulate and align along the mitotic spindle as it forms itself and along the midbody/central spindle during late mitosis (Poteryaev, Squirrell et al. 2005).

In a similar manner during prophase, the Golgi apparatus has to be fragmented. The interphase Golgi goes from its characteristic flattened stacked cisternae morphology to VGMs (Vesiculated Golgi membranes) that can be found dispersed throughout the prophase cytoplasm (Seemann, Pypaert et al. 2002). The breakdown process starts with the Golgi structural protein GM130 being phosphorylated by the CDK1/Cyclin B complex at Ser-25; then as the cell enters telophase, GM130 is dephosphorylated by PP2A allowing its reassembly (Lowe, Gonatas et al. 2000). It has been reported that PLK3, a member of the Polo-like kinase family, localizes to the Golgi apparatus throughout interphase and mitosis, however said localization is lost when the Golgi is disrupted, either because of the activity of Golgi poisons (BFA) or by disruption of microtubule structures (Nocodazole) (Ruan, Wang et al. 2004). During cell cycle progression, PLK3 protein levels remain constant, however its kinase activity peaks during late S and G2, coinciding with the Golgi apparatus breakdown (Ouyang, Pan et al. 1997) PLK3 has been linked to actively participate during this process since it has been shown that an enhanced PLK3 kinase activity induces abnormal Golgi

fragmentation (Ruan, Wang et al. 2004). After fragmentation is completed, the VGMs become associated with the two maturing spindle poles and during anaphase, the vesicles move together with the sister chromatids and as the nuclear envelope reforms, the vesicles relax around the new nucleus and the centrosome (Seemann, Pypaert et al. 2002).

As we described previously, centrosome migration requires the help of dynein motor direction on MTs and as it turns out, this process helps accomplish the NEB by dynein-binding and colocalizing with proteins LIS1 and NDEL1 in the NE during prophase; the absence of this interaction delays entry into prometaphase (Hebbar, Mesngon et al. 2008). Prophase is considered finished when NEB is completed however, the mitotic spindle starts to form before this point is reached (Beaudouin, Gerlich et al. 2002). As mentioned before, duplicated centrosomes will physically separate and distance themselves from each other as chromatin condenses (Whalley and Malliri 2015). At this moment PLK1 can be localized to the centrosomes, where in conjunction with Aurora A are needed for proper maturation of centrosomes during prophase (Hannak, Kirkham et al. 2001); modifications by this enzymes promote γ-tubulin ring complexes formation which will nucleate the centrosome-associated MTs that will later on become the two distinct asters that will form the mitotic spindle (Haren, Stearns et al. 2009). The border between Prophase and Prometaphase is hard to delimitate since spindle formation will start at the time that chromosome condensation is finished (McIntosh 2016).

1.1.5.2 Prometaphase

The beautifully complex structure known as mitotic spindle becomes fully formed during prometaphase, in this phase the chromosomes are captured by the spindle by attaching to the structures known as kinetochores, one in each sister chromatid. Kinetochores are an impressive molecular machine composed of approximately 100 different proteins and complexes that have the ability to bind to specialized chromatin known as centromeres (Cheeseman 2014). Centromeric chromatin is composed at its core by 16 CENPs kinesins (Histone 3 variant centromere proteins, also known as CenH3) and it defines the localization of the core component CCAN (Constitutive Centromere associated network) (McAinsh and Meraldi 2011) present in centromeres during the entire cell cycle (Perpelescu and Fukagawa 2011). The CCAN serves as a physical platform were the KMN network assembles, being composed by the KNL1 (Kinetochore null protein 1), the MIS12 (4 subunit missegregation 12 complex) and the NDC80 (four subunit nuclear division cycle 80 complex) (Cheeseman, Chappie et al. 2006). This way the CCAN and the KMN network bind the kinetochore to the spindle MTs during prometaphase. The KMN network MT-binding is performed as described next: The NDC80 complex is a heterotetramer composed by NDC80 (known as HEC1 in humans), NUF2 (nuclear filamentous 2), SPC24 and SPC25 (Spindle pole component 24). SPC24-SPC25

heterodimers target the complex to the kinetochore and bind directly to the MIS12 complex (Petrovic, Pasqualato et al. 2010) while the NDC80-NUF2 heterodimer forms the calponin homology domain binding to MTs (Cheeseman, Chappie et al. 2006, Ciferri, Pasqualato et al. 2008).

Spindle MTs are dynamic and unstable by nature; frequently transitioning from growing to shortening and exceeding the rates of catastrophe by 10 times more than their interphase counterparts (Belmont, Hyman et al. 1990, Alberico, Zhu et al. 2016). According to the "Search and capture model" MTs continuously probe using diffusive rotations (Kalinina, Nandi et al. 2013) around the chromosome trying to find the kinetochores and once they finally do, they become stabilized by stable end-on attachments and removed from the dynamic pool (Kirschner and Mitchison 1986). In some instances, kinetochores attach to the end of the growing MT, but they bind more commonly with the MT wall (Magidson, O'Connell et al. 2011); this can lead to one kinetochore attaching to both spindle poles (merotelic connection) which will cause problems during segregation (Magidson, O'Connell et al. 2011). This can be solved by the fact that kinetochores are motile on the MTs that they bind. Kinesisn-5 and dynein (minus-end directed motor proteins) are attracted by their negatively charged end to the positively charged end of the growing spindle MT where they cluster, pulling the kinetochore and helping to position it properly (Heald, Tournebize et al. 1996). This whole process is aided by NUMA1 (Nuclear Mitotic Protein 1) binding to dynein and providing motor support for the establishment of the aspired bipolar array in metaphase (Chakravarty, Howard et al. 2004). It has been reported that MTs can also be nucleated from the kinetochore region and extend to interact with pole-nucleated MTs, enhancing the attachment (Kitamura, Tanaka et al. 2010).

When each opposite pole is correctly attached to each sister kinetochore, the chromosome is submitted to pulling force from each pole, putting its centromere under the tension necessary to promote attachment stability; MTs-kinetochore attachments that reach this point will persist, while those that lack this feature are unstable and tend to dissolve (Nicklas, Campbell et al. 1998). This process is known as EC (Error correction) and is the main mechanism by which proper spindle attachment occurs without the cell having to appeal immediately to checkpoint activation (Krenn and Musacchio 2015). As mentioned before, MTs-kinetochores interactions are highly dynamic, which helps when erroneous attachments occur and immediate destabilization is needed for proper correction. Aurora B is the main player in charge in this case localizing to the proximity of centromeres and kinetochores during prometaphase and is a component of the CPC (Chromosome Passenger Complex) (Adams, Maiato et al. 2001, Tanaka, Rachidi et al. 2002); The NDC80 complex is phosphorylated by Aurora B, reducing its affinity to MTs and promoting their detachment (DeLuca, Lens et al. 2011); it has been shown that PP1 (Protein Phosphatase 1) is responsible for counteracting this phosphorylations (Liu, Vleugel et al. 2010). This dynamic process will continue until

the proper tension is achieved and the kinetochore is physically "pulled away" from where Aurora B resides (Lampson and Cheeseman 2011).

The cell needs Cyclin A to be completely eradicated to be able to proceed through metaphase, as it has been reported that its permanence blocks entry into anaphase and subsequent mitotic phases (Su and Jaklevic 2001). During prometaphase to metaphase transition Cyclin A is targeted for degradation by the APC/C (anaphase-promoting complex APC/Cyclosome), a giant multi-subunit E3 ubiquitin-protein ligase that catalyzes the ubiquitination of many proteins through the 26S proteasome in an independent manner from the spindle assembly checkpoint (den Elzen and Pines 2001, Geley, Kramer et al. 2001). The APC/C is a machinery conserved from yeast to humans, relying in two independent cofactors to recognize specific targets at specific phases of the cell cycle, in the case of mitosis is Cdc20 for the metaphase to anaphase transition (Li, York et al. 2007) and Cdh1 during late mitosis but also in the G1/S transition where it prevents the accumulation of mitotic cyclins, stopping premature entry into S phase (Garcia-Higuera, Manchado et al. 2008).

1.1.5.3 Metaphase

Following complete spindle attachment, chromosomes commence their migration towards the middle of the rounded cell axis to align tightly in what is called the metaphase plate; this process is known as chromosome congression and it's the first step for the mitotic spindle to achieve the characteristic metaphase architecture where it aligns symmetrically achieving equal physical tension from each pole (Kapoor, Lampson et al. 2006).

The process of aligning the chromosomes on the same starting point minimizes the chances of chromosomes being left behind, although this process is still under investigation, there are two of the proposed mechanisms from which this can be achieved: The first proposed mechanism is called the "Polar ejection force" that states that as dynamical and unstable MTs grow, they push the prometaphase chromosomes towards the cell equator as a result; evidence of this can be the fact that chromosomal arms end up pushed away from the metaphase plate (Brouhard and Hunt 2005). The other mechanism is based on Kinesins-4 and -10 motor ability to walk over the MTs towards their positive ends while at the same time binding chromatin; it has been shown that independently knocking down each one of this kinesins does not impede proper metaphase alignment but that knocking down both of them at the same time does (Wandke, Barisic et al. 2012). Even after the chromosomes reach perfect metaphase alignment, chromatids cannot separate until the APC/C^{Cdc20} complex ubiquitinylates and marks Securin for degradation (the anaphase inhibitor protein) (Peters 2002). Securin is an inhibitor of Separase, a cysteine protease responsible of hydrolyzing

cohesin complexes (Holloway, Glotzer et al. 1993), therefore the degradation of Securin allows for the breakdown of the cohesin network responsible for linking the sister chromatids, permitting their proper separation (Peters 2006).

The metaphase spindle is a complex and fleeting state; even after chromosome congression is achieved, spindle MTs remain highly dynamic as those MTs that did not bind to kinetochores turn over with a half-life of ~30 seconds (Saxton, Stemple et al. 1984). At this point the end of metaphase is the moment when sister chromatids begin to segregate; the transition between metaphase to anaphase marks the point of no return as it implies the proteolysis of the mitotic regulators: Along with Securin, cyclin B1 is targeted for 26S-proteasome destruction by the APC/C ^{Cdc20} complex, leading to full CDK1 inactivation (den Elzen and Pines 2001, Geley, Kramer et al. 2001). Phosphatases then proceed to undo the characteristic phosphorylations of the mitotic state. It is assumed that until this moment the assembly of the APC/C^{Cdh1} complex (characteristic of G1 phase) is inhibited by Cdh1-CDK1-Cyclin B1-dependent phosphorylation to prevent its premature activation (Peters 2006). At this point, Cyclin B1 destruction can be delayed if the SAC (spindle assembly checkpoint) is activated and won't happen until proper formation and alignment of the metaphase plate. Only after the SAC is successfully overcome, the APC/C^{Cdc20} will trigger Cyclin B1 degradation, pushing the cell into anaphase (Clute and Pines 1999). For the case of cultured mammalian cells, there is an interval of ~20 min between the last chromosome attachment and the firing of anaphase (Rieder, Cole et al. 1995).

1.1.5.3.1 Mitotic Spindle orientation

Achieving a properly oriented cell division is pivotal in a wide range of contexts; for instance to produce healthy daughter cells, for maintaining tissue cohesiveness/homeostasis and during the whole process of embryonic development along with tissue differentiation (Kotak 2019, Lechler and Mapelli 2021). Proper orientation of the cell division is achieved by correctly positioning the mitotic spindle relative to a defined polarity axis (Lu and Johnston 2013). During metaphase, as polarized MTs connect to kinetochores to guide chromatids to the metaphase plate, the astral MTs protrude from the poles towards the opposite poles of the cell cortex; this will stabilize and position the whole mitotic spindle structure, and consequently will help the cell to achieve proper division orientation (Lechler and Mapelli 2021).

The $G\alpha_i$-LGN-NuMA complex along with the dynein-dynactin complex compose the basic molecular machinery in charge of attaching the astral MTs to the actomyosin cortex and generating the cortical force needed to pull and position the spindle (Zheng, Zhu et al. 2010). The GDP-loaded $G\alpha_i$ (α subunit of the three guanine nucleotide binding proteins) accumulates at the plasma membrane, concentrating in caveolin-

rich membrane blotches where it binds to LGN. This biding causes a conformational change that allows LGN to bind to the C-terminal domain of two NuMA (Nuclear mitotic apparatus) dimers. Simultaneously, NuMA interacts with dynein's light intermediate chain subunit through its N-terminal domain and LGN intercalates itself between dynein and dynactin, composing the LGN-NuMA-dynein cortical networks (Kotak, Busso et al. 2012). Further, it has been reported that NuMA is able to directly bind MTs plus ends (Seldin, Muroyama et al. 2016). The force needed for this system to position the spindle by pulling on the astral MTs is generated by ATP-dependent dynein; this is achieved thanks to dynein's capacity to perform retrograde movement towards MTs minus ends, therefore pulling the spindle poles towards the cell cortex (Laan, Pavin et al. 2012). Meanwhile, myosin physically links the astral MTs to the cortical actin cytoskeleton, cooperating with the dynein-dynactin network by providing additional pulling force by working alongside with the $G\alpha_i$-LGN-NuMA complex for spindle orientation (Woolner, O'Brien et al. 2008, Kwon, Bagonis et al. 2015). The actomyosin cortex provides a rigid scaffold that is able to withstand the traction forces exerted over the astral MTs by the MT motors (kinesin and dynein) that pull towards the spindle poles (Rizzelli, Malabarba et al. 2020).

The mitotic spindle orientation process is also aided by +TIPs (microtubule plus-end binding proteins) that serve as a cortical bait for the MTs to "capture" and gain stability; some of this proteins are members of the XMAP215/CLASP family (Slep 2010), EB1 (End-binding protein 1) (Rogers, Rogers et al. 2002). EB1 is capable of recognizing astral MTs plus ends (growing ends) helping CLASP1 and CLAPS2 to capture and stabilize them by linking them to the opposite cell cortex, this way stopping their constant depolymerization (Mimori-Kiyosue, Grigoriev et al. 2006). EB1 is also in charge of recruiting other +TIPs like the CLIP-170 that promotes MTs growth towards the cortex and regulates spindle orientation and (Miller, D'Silva et al. 2006) p150-dynactin, which is necessary for rotating the centrosome properly along the long axis of the cell, thus promoting proper spindle orientation (Skop and White 1998). EB1 has been reported to regulate the spindle orientation in cultured cells that have lost their tissue polarity by a MTs stabilizing mechanism downstream of β1-integrin mediated adhesion, helped by myosin-dependent remodeling of the actin cytoskeleton (Toyoshima and Nishida 2007). Concomitantly, guidance of microtubule assembly along the actin retraction fibers is mediated by the EB1/EB3 complex and is supported by MACF1 (microtubule-actin cross-linking factor 1) (Byers, Beggs et al. 1995).

As mentioned before, actin has a very well-studied scaffold function during cell round-up as part of the actomyosin ring, by controlling the generation of oriented force towards cell poles and by bearing said mechanical force (Blanchoin, Boujemaa-Paterski et al. 2014). Interestingly, a recent study performed in *Xenopus* embryonic epithelia has shown that mitotic actin filaments are also associated with spindle MTs

and present a coordinated assembly with physiological relevance (Dogterom and Koenderink 2019, Kita, Swider et al. 2019), and that *Xenopus* oocytes have been reported to nucleate actin filaments that apparently influence the anaphase spindle length (Woolner, O'Brien et al. 2008). This microfilaments may act as a structural scaffold during metaphase progression to enable chromosome segregation in the upcoming anaphase (Mogessie and Schuh 2017). Additionally, the novel discovery of centrosome's capability to nucleate actin in both interphase and mitotic cells, places centrosomes as the perfect command center for the crosstalk between MTs and actin microfilaments to take place (Farina, Gaillard et al. 2016, Farina, Ramkumar et al. 2019). During mitosis, this bursts in actin microfilaments are known as mitotic spindle actin clouds; being nucleated by the Arp2/3 complex present at the mitotic spindle-pole vicinity and localizing mainly in subcortical clusters or around the centrosomes, dissolving into the contractile ring in cytokinesis (Farina, Ramkumar et al. 2019). It is considered that their function is to dissuade the mechanical forces coming from the cortex resistance, possibly influencing mitotic spindle positioning and that preventing their nucleation leads to impaired mitotic spindle formation and can lead to severe mitotic defects (Plessner, Knerr et al. 2019). Apparently, the after mentioned actin structures have an uncharacterized function in mitotic spindle formation, with special relevance during metaphase congression, however the underlying mechanisms remain to be fully described along with the participation of unknown cross-linking proteins.

1.1.5.4 Anaphase

Anaphase is the period in mitosis when sister chromatids start to get pulled apart towards each opposite spindle pole until they get completely separated and become anaphase chromatids. This process is termed "Resolution of Sister Chromatids" and it requires the decatenation of centromeric chromatin by TOPOIIα; this topoisomerase needs to be sumoylated by RanBP2 in order for it to be recruited to the centromeres (Dawlaty, Malureanu et al. 2008). RanBP2 is an E3 SUMO-Protein Ligase that forms part of the NPCs during interphase and that if absent during anaphase, leads to formation of anaphase bridges and aneuploidy (Dawlaty, Malureanu et al. 2008).

Anaphase can be further subdivided in Anaphase A, where the distance between each chromatid and the spindle pole it faces gets decreased and Anaphase B, where said separation increases along with the distance between each spindle pole and the polymerization of the interpolar spindle takes place (Saxton and McIntosh 1987, Uhlmann 2001). Anaphase A starts when the KMTs (Kinetochore attached to MTs) begin shortening as a result of tubulin subunits loss at the kinetochores and at the spindle poles (Mitchison, Evans et al. 1986). The Kinesin-14 and Dynein present at the kinetochores participate in the shortening process by pulling the chromosomes as the KMTs they use as a bridge depolymerize; in the case of animal cells

this process is aided by the NuMA recruited during metaphase (Elting, Hueschen et al. 2014). During Anaphase A, the chromatids will reach the spindle poles and the KMTs will disappear. Studies analyzing the positions of non-KMTs positive ends have shown that during Anaphase B, this MTs slide past the kinetochores by continuing their nucleation and are aided by Kinesin-5 to form the interpolar spindle (Saxton and McIntosh 1987, Brust-Mascher and Scholey 2011). It has been shown in some specific types of cells (fungi and nematodes) that this MTs sliding serves as a break on the speed of the spindle elongation (Aist, Bayles et al. 1991). As previously described, the sliding force needed for the elongation comes from the dynein bound to each opposite pole of the cell cortex where the Astral MTs attach (Aist, Bayles et al. 1991). The elongated interpolar spindle will persist into telophase and cytokinesis; this will assure that the two sets of chromosomes have enough space between each other so cytokinesis can occur without crunching or damaging the traveling chromatids.

1.1.5.5 Spindle assembly checkpoint

The SAC (Spindle Assembly Checkpoint) is a signaling pathway that ensures correct chromosome segregation trough modulation of the mitotic master CDK1. Defects in SAC activity may result in unequal repartition of genetic information that if remained un-attended may facilitate accumulation of chromosomal aberrancies that can in turn lead to malignancies (Kops, Weaver et al. 2005). The spindle assembly checkpoint occurs during prometaphase. As described in detail previously, correct chromosome segregation depends on the establishment of proper binding and tension between chromosomes kinetochores and spindle microtubules, however when persistent issues arise that delay this process, the SAC becomes activated and arrests the cell in prometaphase until all chromosomes have properly attached to the spindle (Burke and Stukenberg 2008, Foley and Kapoor 2013).

In the SAC signaling pathway, the main components are the Ser/Thr kinases MPS1 (Monopolar spindle protein 1), BUB1 (Budding uninhibited by benzimidazole 1) and the non-kinase components MAD1 and MAD2 (Mitotic arrest deficient 1/2), BUB3 and BUBR1 (BUB-pseudo kinase related 1) (Kitagawa and Rose 1999). Throughout interphase and when the SAC is not activated, MAD1 and MAD2 are kept in the NPCs associated with their inhibitor p31 along with MPS1 (Iouk, Kerscher et al. 2002). Whether the NPCs shared localization and association with this proteins keeps the inactivated remains to be clarified.

The SAC catalyzes the formation of the MCC (Mitotic Checkpoint Complex) that captures CDC20 (Sudakin, Chan et al. 2001); BUBR1/MAD1/2 bind directly to CDC20 blocking access to the recognition sites inside the D-Box, disrupting its association with APC10. This promotes APC/C-dependent auto-ubiquitination of CDC20 stablishing prometaphase arrest by completely quenching the CDC20 pool (Foe, Foster et al. 2011). Studies in yeast showed a similar mechanism, where the putative proteins Mad and Bub,

function by sequestering Cdc20 (Peters 2002). In summary, this pathway delays segregation by preventing the APC/C from ubiquitinating Cyclin B1 and Securin trough inactivating its cofactor CDC20 (Hwang, Lau et al. 1998).

Kinetochores are essential for SAC activation; the KMN network constitutes the core MTs-binding machinery in eukaryotic chromosomes and it's in charge of relaying the MTs-binding status to the SAC, making it its main signaling activator (McAinsh and Meraldi 2011). KNL1, one of the main components of the KMN network in the kinetochore is targeted by MPS1 for phosphorylation, creating a docking motif for BUB1 and BUB3 binding (Cheeseman, Niessen et al. 2004). When BUB1 localizes to the kinetochore, it recruits the rest of the SAC components. Strikingly, it has been shown that phosphorylation on KNL1 carried out by MPS1 is also required for proper chromosomal alignment (Yamagishi, Yang et al. 2012).

Aurora A is required for SAC maintenance during prometaphase; it has been shown that its overexpressed is a hallmark of various cancers, as it is thought to permit SAC bypass (Hoar, Chakravarty et al. 2007). Under normal conditions, Aurora A phosphorylation of histone H3 variant CENP-A on its Ser7 residue is required for Aurora B recruitment at the kinetochore (Kunitoku, Sasayama et al. 2003); couple with this, Aurora A inhibition leads to spindle assembly defects, defective chromosome congression, premature entry into anaphase and loss of MAD2 from unattached kinetochores (Hoar, Chakravarty et al. 2007, Courtheoux, Diallo et al. 2018). Once all of the chromosome kinetochores have been properly attached to the mitotic spindle the MCC becomes disassembled and the SAC is turned off by, freeing and relieving CDC20 inhibition (Buffin, Lefebvre et al. 2005). This allows CDC20 to activate the APC/C as previously described and the cell continues with chromosome segregation and reaching anaphase (Foley and Kapoor 2013).

1.1.5.6 Telophase

As chromosomes reach each opposite cell pole, the new NE starts its reform and by the end of telophase, it will be completely reassembled. In order for this process to begin, the phosphorylation events that drove NPC disassembly during prophase have to be reverted. Having no traces of active CDK1, PP1 (Protein Phosphatase 1) with the help of specific targeting subunits, begins to massively dephosphorylate chromatin associated factors, Lamins, nucleoporins and NE membrane proteins allowing them to start the NE reassembly (Steen, Martins et al. 2000, Landsverk, Kirkhus et al. 2005, Vagnarelli, Hudson et al. 2006). First, NE reformation will take place around several pieces of compacted chromatin, the segregated chromosomes start the formation of this compact clusters by contracting their arms (axial shortening) next to the spindle poles, probably because of the renewed activity of condensins (Renshaw, Ward et al. 2010). This process is dependent on Aurora B inhibition by p97 (also known as Cdc48) and its subsequent

dissociation from chromatin effectuated by CUL3/KLH3/KLH9 (E3 ubiquitin ligase cullin 3 and adaptor proteins) (Hetzer, Meyer et al. 2001, Sumara, Quadroni et al. 2007).

The assembly of the new NE and NPCs depends on direct regulation by the small GTPase Ran. RanGTP (GTP-bound Ran) can be found enriched in the mitotic chromosomes thanks to the help of RCC1 (Ran guanine exchange factor 1) (Hetzer, Bilbao-Cortes et al. 2000). RanGTP will then bind to Importin-β1 and –β2 generating and allosteric conformational change that will cause them to release key NE and NPCs proteic components such as Lamin B, LBR (Lamin B receptor) and the NUPs (Harel, Chan et al. 2003, Walther, Askjaer et al. 2003). This displacement of Importins is the premise that guides both NE and NPC assembly, a process that was initiated in anaphase by the deposition on chromatin of prepores composed of the NUP107-160 complex (Sheehan, Mills et al. 1988, Walther, Alves et al. 2003). Targeting of the segregated mitotic ER tubules to the compacted chromatin regions where they will undergo massive reorganization over the chromatin surface, will give rise to the NE juxtaposed membranes (defined as INM-inner and ONM-outer nuclear membranes) (Anderson and Hetzer 2007). The nuclear lamina will attach to the inner membrane and associate to the decondensing chromatin after being dephosphorylated by PP1; in this sense the LBR provides essential chromatin docking sites for the starting sites of the new NE (Wilson and Newport 1988, Pyrpasopoulou, Meier et al. 1996). The DNA-binding inner nuclear membrane proteins that are located in the tips of the tubular ER have pivotal roles in establishing this chromatin–membrane contacts. Proteins like NDC1, POM121, NPC-associated SUN1 (SUN domain-containing protein 1) or the after mentioned NUP107-160 complex might mediate this interactions (Devos, Dokudovskaya et al. 2004). NE start to reform as discrete pieces when this proteins start to associate with chromosomes and lamins (Guttinger, Laurell et al. 2009). The conversion of the chromatin-associated ER tubules to the double NE membrane is controlled by the removal of ER-tubule-forming proteins like the Reticulon family proteins, Atlastins GTPases and Lunapark (Wang, Tukachinsky et al. 2016, Powers, Wang et al. 2017) (Anderson and Hetzer 2008).

The last step of the process is the closure of the NE which includes NPCs insertion in the area where the chromatin-associated prepores were established in anaphase by the NUP107-160 complex (Walther, Alves et al. 2003). But how does this assembly takes place? One of the proposed hypothesis is that the chromatin-associated prepores attract the membrane patches from aside, causing the membranes to encircle around it without having to fusion (Walther, Alves et al. 2003, Anderson and Hetzer 2007). Studies *in vitro* have reported that NE membrane-patch sealing is mediated by the SNARE protein receptor and the Atlastins in conjunction with the multiple interactions between the INM proteins with chromatin (Baur, Ramadan et al. 2007).

The successfully completed Telophase is marked by fully reassembled, transport-competent NPCs in the closed NE compartment with completely reconstituted the nuclear lamina, stablishing the interphase architecture of a defined nucleus, independent from the cytoplasm. By the end of the ER remodeling, it will acquire the flatten membrane-ribbon-like appearance extending from the NE to the periphery of the daughter cell (Anderson and Hetzer 2008). Chromatin decondensation will proceed throughout all telophase and by the end of it the nucleoli have become discernible, a hallmark that transcription has been re-started (Sheehan, Mills et al. 1988).

1.1.5.7 Cytokinesis

The process by which the mitotic cell is physically split in two is called Cytokinesis (Fededa and Gerlich 2012). The whole process and its culmination with daughter cell's abscission is coordinated with post mitotic NE assembly (Mackay, Makise et al. 2010). It is considered that cytokinesis begins in Anaphase B due to the formation of the interpolar spindle and because MTs stabilization and reorganization of the mitotic spindle can take place due to complete CDK1 inactivation. As described during Anaphase B, the formation of the interpolar spindle helps generate the space where the central spindle and later on the midbody will localize, providing the necessary MTs and the platform for abscission factors assembly (Glotzer 2009). The central spindle is built in part from overlapping MTs bundles that derive from the interpolar and *de novo* MTs that are nucleated during anaphase through the Augmin complex (Uehara, Nozawa et al. 2009, Uehara and Goshima 2010). When the nuclei of the daughter cells begin to reform, the Augmin complex starts to concentrate near the minus ends of the interpolar MTs, after they become detached from the poles. As a result, the freed γ-tubulin ring begins nucleating new MTs that become intertwined with the released interpolar MTs at the spindle midplane extending all the way to the cell cortex. A key component in this process is the PRC1 (MT bundling protein required for cytokinesis 1), a CPC factor that becomes activated during anaphase onset when CDK1-Cyclin B1 is quenched and that acts as a homodimer that binds selectively to the antiparallel MTs at the central spindle stabilizing them (Bieling, Telley et al. 2010, Subramanian, Wilson-Kubalek et al. 2010, Hu, Coughlin et al. 2011). This stable MTs are now able to bind the Tetrameric Centralspindlin Complex composed of a MKLP1 homodimer (Kinesin Motor Protein 1 and 2) and the Rho family GTPase MgcRacGAP (also known as CYK4) (Mishima, Kaitna et al. 2002, Pavicic-Kaltenbrunner, Mishima et al. 2007, Hutterer, Glotzer et al. 2009). MKLP1 phosphorylation by Aurora B releases it from inhibitory 14.3.3 binding proteins and promotes the formation of Centralspindlin clusters (Mendoza, Norden et al. 2009, Steigemann, Wurzenberger et al. 2009); Kinesin-6 will direct them to the MTs plus ends to accumulate at the central region where the Rho GTPase becomes active and initiate with the cell cleavage (Pavicic-Kaltenbrunner, Mishima et al. 2007, Hutterer, Glotzer et

al. 2009). PLK1 can be found at the central spindle after being targeted there by PRC1, where it participates in the division plane specification by phosphorylating MKLP2 (Neef, Preisinger et al. 2003) and CKY4 whose job is to bring ECT2 (Epithelial cell transforming 2) to activate RhoA helping stablish the area where the actomyosin contractile ring will be assembled (Yuce, Piekny et al. 2005, Wolfe, Takaki et al. 2009).

At the same moment that the Centralspindlin machinery is being assembled, the division plane where abscission will take place has to be established; how the mitotic spindle determines the positioning of the division plane has been extensively studied in a wide variety of model organisms and cell lines, therefore generating an intense debate due to controversial and conflicting results. Overall there are three possible mechanisms that orchestrate this process two of which are considered redundant that involve the astral MTs. The first hypothesis is known as "Astral stimulation hypothesis" that states that the astral MTs carry a furrow-inducing signal towards the cell cortex that derives from the spindle asters (Bringmann and Hyman 2005, Werner, Munro et al. 2007) and the second and redundant one, "the astral relaxation hypothesis" postulates that inhibition of the contraction of actin-myosin bundles exclusively near the spindle poles results in waves of contractile activity that concentrates at the central spindle, this way providing the necessary force for the actomyosin contraction (Fededa and Gerlich 2012). The third postulate is called "central spindle hypothesis"; it states that furrow induction originates at the central spindle because of the role it plays in the establishment of the division plane by concentrating and activating the cleavage machinery (Fededa and Gerlich 2012).

After the molecular machinery has been assembled at the division plane, the small GTPase RhoA stimulates the nucleation of unbranched actin filaments trough activation of Diaphanous-related formins (Castrillon and Wasserman 1994, Severson, Baillie et al. 2002) and by promoting myosin II activation trough phosphorylation of its light chain by the kinase ROCK (Matsumura 2005). This whole procedure is aided by Anillin, a scaffold protein that binds actin, myosin RhoA and CYK4 creating a link through which the equatorial signals will reach the central spindle (D'Avino, Takeda et al. 2008, Piekny and Glotzer 2008) and anchoring the actomyosin ring to the plasma membrane (Piekny and Maddox 2010). After actomyosin ring assembly, its physical contraction leads to the cytokinetic furrow ingression of the attached plasma membrane finally partitioning the cytoplasm of the two daughter cells. The force required for the contractile process is generated by motor protein myosin II; using the energy provided by ATP hydrolysis myosin II moves along the actin filaments gradually but efficiently constricting the cell membrane forming the cleavage furrow (Schroeder 1972, Egelhoff, Lee et al. 1993). This process also requires a supply of additional membrane components to compensate for the gradual increase of total cell surface; this involves targeted secretion of vesicles and specific lipids that travel along the MTs towards the cleavage furrow

(Bluemink and de Laat 1973, Skop, Bergmann et al. 2001, Albertson, Cao et al. 2008). The furrow ingresses until it reaches a diameter of 1-2 μm and remains there for 1 to 2 hours until abscission takes place (Steigemann and Gerlich 2009, Guizetti and Gerlich 2010). Immediately after complete furrow ingression, vesicles derived from Golgi and endosomes accumulate adjacent to the midbody, adding with the assembly of the new plasma membrane by fussing with it (Gromley, Yeaman et al. 2005, Schiel, Park et al. 2011). This striking and beautiful process is clearly visible through the light microscope.

Abscission consists in the removal of all the remaining cytoskeletal structures from the intercellular bridge along with a secondary ingression of the cell cortex involving 17 nm diameter helices filaments spawned trough the intercellular bridge and finally a fission of the plasma membrane (Steigemann and Gerlich 2009, Guizetti and Gerlich 2010). The incoming furrow bundles up the MTs of the interpolar spindle to form the intercellular bridge that contains the "midbody", an electron-dense matrix whose composition is not fully known, having ~100 proteins localizing there (Skop, Liu et al. 2004); this structure can persist like a pinched bundle for some time into the subsequent interphase. Ultimately the midbody is lost through a combination of proteolysis and completed cleavage along with the retraction and active removal of central spindle MTs (Byers and Abramson 1968). Disassembly of this structure is performed by the MTs-remodeler ATPase Spastin (Spastic paraplegia protein) (Roll-Mecak and Vale 2008, Connell, Lindon et al. 2009, Guizetti, Schermelleh et al. 2011). It is believed that high levels of polyglutamylation of the MTs attracts Spastin to the midbody (Lacroix, van Dijk et al. 2010). Following up comes Actin filament disassembly during late cytokinesis; this process depends on the PKCε-14-3-3 complex inactivating RhoA after furrow ingression is completed (Saurin, Durgan et al. 2008); the process is further controlled by Rab35 and its effector OCRL (Dambournet, Machicoane et al. 2011). Following successful abscission the midbody residues left behind (midbody derivatives) will have different fates depending on the cell type; it can either be excreted to the extracellular medium (Dambournet, Machicoane et al. 2011, Ettinger, Wilsch-Brauninger et al. 2011), degraded by autophagy (Pohl and Jentsch 2009, Kuo, Chen et al. 2011) or persist in the cytoplasm (Gromley, Yeaman et al. 2005, Ettinger, Wilsch-Brauninger et al. 2011).

Putting the cell cycle environment in context: As described previously, APC/C activation by phosphorylated Cdc20 depends on the positive feedback created by CDK1-Cyclin B1 peak performance, CDK1 inactivation leads to decreased activation of APC/C, by dissociation from Cdc20 (Kramer, Scheuringer et al. 2000). Cytokinesis is completed when the free APC/C can be activated by its other cofactor Cdh1, forming the APC/C^{Cdh1} complex that will proceed with Cdc20, Aurora B and PLK1 targeted degradation (Pfleger and Kirschner 2000, Stewart and Fang 2005). This way the end of cytokinesis is coordinated with the re-establishment of the interphase cellular environment, reestablishing the nuclear and

interphase cytoplasm environment with the disassembly of the spindle. The two disassembled spindle poles begin to function as centrosomes, initiating new interphase MTs nucleation to help establish the normal interphase cytoskeleton (Gupta, Mana-Capelli et al. 2013).

1.1.6 End of one cycle, start of the next one

As daughter cells have completed mitosis successfully and re-enter G1 phase, the APC/C^{Cdh1} will continue to target Skp2 and its cofactor Cks1 along with cyclin A and B for degradation, which will keep CDK1 and CDK2 activity null (Bashir, Dorrello et al. 2004). Because key components of the SCF ubiquitin ligase are being degraded, the CK1 inhibitors p21 and p27 come again into the picture and ensure permanence either on G0 or G1, before the young cell becomes stimulated and is ready to start with a new cycle. This scene however raises the question, how will CDK2 bind to Cyclin A and Cyclin E if APC is still targeting them well after mitosis is over? Here is where Emi1, a FBP (F-box protein) come into play; Emi1 transcription is induced by the previously described E2F transcription factors (which also induce Cyclins A, B and E transcription). When Emi1 accumulates, it inhibits APC/C^{Cdh1} in a non-proteolytic manner (Reimann, Gardner et al. 2001) and as a side effect it frees Skp2 and Cyclins A and B from APC/C^{Cdh1} ubiquitination-mediated degradation. In this scenario and in order to prevent premature push through G1, since CDK1's cyclins are being subtly transcribed and stabilized, a mechanism that keeps them at bay has to step up to the plate. As mentioned previously, in order for CDK1 to fully perform, it needs to be dephosphorylated by Cdc25A, however, in the context of G1/S and G2 phases, $SCF^{\beta\text{-}Trcp}$ degrades phosphorylated Cdc25A (Busino, Donzelli et al. 2003), therefore maintaining a timely balance between CDK2 activity and CDK1 ablation. Further on, CDK2 also aids in APC/C^{Cdh1} inactivation by phosphorylating its coactivator Cdh1, preventing the conformation of the fully functional cyclosome (Peters 2002).

1.1.7 Checkpoints for coordination and control of Cell cycle progression

Maintenance of a normal cell cycle ensures controlled proliferation and prevents the development of various diseases such as cancer. In order to maintain this control, the cell regulates its own cell cycle by activating mechanisms known as "Cell cycle checkpoints" (Bartek and Lukas 2007). Cell cycle checkpoints are specialized molecular pathways composing the cell's surveillance mechanisms that monitor proper progression of the cell cycle and that are in charge of detecting and correcting DNA insults (Bartek and Lukas 2007). Therefore, checkpoints overall function is the maintenance of genomic integrity. This is achieved by delaying or completely arresting the progression into the next phase of a cycle when damaged DNA is detected and by not allowing the cycle to continue until said damaged has been effectively corrected or mitigated until it the cell can deal with it (Kastan and Bartek 2004). Another crucial function of cell cycle checkpoints is to trigger processes like apoptosis or senescence, for instance if the cell has suffered

irreparable damage, if the cell's DNA damage response is ineffective or if proliferation is out of control, thus eliminating the threat this scenarios represent to an organism. On the other hand, accumulation of DNA damage without the proper activation of the specific checkpoints can lead to extensive genomic instability, resulting in small mutations or even chromosomal rearrangements that can lead to cell transformation and oncogenesis (Kastan and Bartek 2004, Medema and Macurek 2012). The cell cycle can potentially arrest at several stages, but overall, the timely responses can be classified in four major checkpoints: the G1 phase checkpoint, the S phase checkpoint, the G2/M transition checkpoint and the Spindle assembly checkpoint (previously explained in this work in the "Mitosis" subtheme) (Kastan and Bartek 2004, Aguilera and Gomez-Gonzalez 2008).

1.1.7.1 DNA Damage response as the main driver of checkpoint activation

The DNA Damage response is composed of a series of highly complex and specialized processes whose function is to detect a DNA lesion, identify its nature and activate the respective molecular pathway to repair it, while at the same time triggering cell cycle arrest (Bartek, Lukas et al. 2004, Aguilera and Gomez-Gonzalez 2008). This damage can be caused by endogenous agents such as replication stress and toxic by-products of the normal intracellular metabolism or by exogenous genotoxic agents such as ionizing radiation, UV light, exposure to free radicals or cancer-treatment drugs (Kastan and Bartek 2004). Nevertheless, regardless of the source of the DNA insult the DNA Damage response pathways will be activated; we will start by referencing DSBs repair (DNA Double strand breaks), the most serious DNA damage type.

The first step in the DDR process is detecting the presence of the damage, this is achieved through the recruitment of the MRN complex to the DNA lesions by RAD17 and γH2AX (Kinner, Wu et al. 2008, Bian, Meng et al. 2019). The MRN complex is a hetero-hexamer composed of two subunits of MRE11 (Meiotic recombination 11 homolog 1), two subunits of RAD50 (Double strand break repair protein) and two subunits of NBS1 (Nijmegen breakage syndrome protein 1) (Deshpande, Lee et al. 2017). Its known biochemical functions are: RAD50 ATP-dependent hydrolysis, DNA binding by multiple subunits, exonuclease/endonuclease activity and bridging the DNA molecules together (Hopfner, Craig et al. 2002). The MRN complex is relevant in the first stage response to DNA damage by acting as a flexible scaffold for DDR machinery recruitment and as a combined activator and regulator of the DSB signaling cascade (Williams, Lees-Miller et al. 2010). The MRN complex will also establish the pathway choice in DSB repair, the two major pathways are HR (Homologous recombination) and NHEJ (non-homologous end joining) (Hustedt and Durocher 2016). HR is error-free but requires resection and a sister chromatid to use as a recombination template, hence is favored during S and G2 (Li and Heyer 2008). Also, HR is the primary

mechanism (if not exclusively) for repair in the case of replication fork collapse caused by DSBs (Rothstein, Michel et al. 2000). On the other hand, NHEJ is error-prone but does not require a template and is incompatible with resection, which makes it functional throughout interphase and it has been shown to be activated by both the MRN complex and possibly in a specific manner by phospho-activated DNA-PK (Allen, Halbrook et al. 2003, Zhao, Kim et al. 2020). In the case of mammalian and yeast models, it has been reported that 25-50% of DSBs are repaired by NHEJ with high precision (Clikeman, Khalsa et al. 2001).

1.1.7.1.1 HR – Homologous recombination

The MRN complex licenses HR by starting the resection process through an endonuclease cut performed by MRE11 generating a 3' ssDNA overhang that blocks NHEJ from operating. This initial cut is followed by the bidirectional resection aided by EXO1 (exonuclease 1) and BLM (Bloom syndrome protein) therefore fully committing to HR (Shibata, Moiani et al. 2014). DNA-end resection establishes the DSBs repair pathway but also helps with degradation of stalled replication forks (Symington and Gautier 2011). BRCA1-CtIP mediate end-resection collaborates with the MRN complex to promote end resection and to trigger ATR signaling cascade (Sartori, Lukas et al. 2007). The resulting 3' ssDNA overhangs are quickly coated by RPA to protect them from nucleases (Chen, Lisby et al. 2013) and will later be replaced by Rad51 in a process mediated by PALB2-BRCA2 that are in turn recruited by BRCA1 (Sy, Huen et al. 2009). Rad51 is stabilized by BRCA1-BARD1 complex (Zhao, Steinfeld et al. 2017) and then, with the help of Rad54, Rad51 invades the homologous sequence, aligns the two homologous DNA overhangs and then its released from the ssDNA by Srs2 helicase, giving space for normal-base pairing between the invading and complementary strand and for subsequent DNA pol extension (Sung and Klein 2006). After extension is complete, the extended strand dissociates and anneals back with the non-invading strand (in the opposite side of the DSB), a process known as SDSA (synthesis-dependent strand annealing) (Helleday, Lo et al. 2007); on the other hand, both ends can invade each other, producing a double-Holliday structure and after resolution, will generate non-crossover or crossover recombinants; the remnants of ssDNA nicks and gaps are sealed by DNA pol and DNA ligase (Sung and Klein 2006).

1.1.7.1.2 NHEJ – Non-homologous end joining

NHEJ is considered to be the first line of response upon DNA damage; its first aim is to process the lesion as fast as possible to restore genomic continuity and to prevent further genomic instability, hence the fast response (30 min upon DNA insult) but low fidelity (Mao, Bozzella et al. 2008). Later on during following phases of the cell cycle (2-7 hours after DNA lesion occurred), homology-directed processes will restore the errors left behind by NHEJ (Asaad, Zeng et al. 2000, Mao, Bozzella et al. 2008). NHEJ can be

subdivided in the classical (C-NHEJ) and alternative (A-NHEJ) this last one being more active during S phase (Guirouilh-Barbat, Huck et al. 2008). The C-NHEJ goes as follows: After DBS recognition by Ku and subsequent recruitment of DNA-PK, DNA-PK phosphorylates itself (Thr-2609 and Thr-2647) and other targets such as RPA, the WRN helicase (with and without ATM absence) (Pichierri, Rosselli et al. 2003) and 53BP1, which recruits RIF1 to the DSB lesion to inhibit BRCA1 recruitment, thus promoting C-NHEJ and blocking HR (Zimmermann and de Lange 2014). Parallel, the MRN complex is also capable of firing NHEJ start by removing covalently bound proteins from DNA like the topoisomerase complex, this way facilitating the repair by NHEJ (Liao, Tammaro et al. 2016). The first step of NHEJ is "End processing"; NHEJ is ideal when repairing "clean" DSBs that present complementary overhangs (3' hydroxyl and 5' phosphate termini) such as those created by nucleases, however when said ends lack this complementary nature or present damaged bases, NHEJ appeals to "microhomology" to bind the few complementary bases and direct the repair (Davis, Chen et al. 2014). This process can lead to small insertions and deletions, hence the term "error-prone". The broken DNA strands get bridged and if needed, the ends get processed by the nuclease Artemis which will process DNA-ends and is specifically in charge of repairing DSBs induced by IR trough NHEJ (Jeggo and O'Neill 2002). Next Pol λ and Pol μ will fill in the gaps (Daley, Laan et al. 2005). Finally, XRCC4-DNA ligase IV complex seal the break through end ligation (Hentges, Ahnesorg et al. 2006), and the whole NHEJ machinery dissociates (Davis, Chen et al. 2014).

1.1.7.1.3 The ATM/ATR pathways roles during checkpoint activation

After assembly, the MRN complex will trigger the upstream activation of kinases ATM (Ataxia Telangiectasia mutated kinase), ATR (Ataxia Telangiectasia and Rad3-related kinase) (Blackford and Jackson 2017) (Awasthi, Foiani et al. 2015) while proteins Ku70 and Ku80 recruit and activate the other primary DDR player DNA-PK (DNA dependent protein kinase), depending on the nature of the lesion and the chosen repair pathway (Meek 2020). This upstream kinases belong to the phosphatidylinositol-3-OH kinase related family and present substantial overlapping similarities in their substrate specificity, nevertheless each one of this kinases also targets exclusive substrates (Bennetzen, Larsen et al. 2010). For instance the H2AX histone variant can be phosphorylated by ATM/ATR or DNA-PK on its Ser-139 residue producing the γH2AX, enhancing the DDR primary response (Burma, Chen et al. 2001, Cui, Yu et al. 2005).

Active ATM continues with γH2AX phosphorylation in the chromatin surrounding the DSB, which triggers the recruitment of the rest of the downstream participants for efficient DNA repair like TRIM49 (also RNF18), RNF168, HERC2, 53BP1 and BRCA1 (Bekker-Jensen and Mailand 2010) and also triggers

checkpoint activation (Medema and Macurek 2012). 53BP1 (TP53BP1 – Tumor suppressor p53 binding protein 1) is a key regulator of the DSB repair pathway favoring C-NHEJ; its accumulation depends on ATM/ATR through the recruitment of TRIM49 trough MDC1 binding to γH2AX (Schultz, Chehab et al. 2000). 53BP1 *foci* can be found still present in G1 phase cells that underwent replicative stress or DNA damage in the prior S phase (Lukas, Savic et al. 2011). C-NHEJ becomes defective in the absence of 53BP1 but not in the absence of γH2AX phosphorylation. However it has been shown that the MRN complex is considered to be an alternative 53BP1 recruiter, given the fact that a phospho-defective H2AX does no lead to defective 53BP1 *foci* formation (Yuan and Chen 2010).

For the checkpoint activation, the recruited and activated ATM phosphorylates Chk2 (Checkpoint kinase-2) at its Thr-68 residue, for instance in response to IR (ionizing radiation), which leads to stabilization of p53 promoting the transcription of the apoptotic genes Bax, Puma and Noxa (Ahn, Schwarz et al. 2000, Hirao, Kong et al. 2000). Apparently, Chk2 has specific regulating activity during apoptosis in response to DSB-creating agents, since UV-induced apoptosis does not involve Chk2 activation (Hirao, Kong et al. 2000), which is in good agreement with ATM specifically targeting Chk2 for activation (Jiang, Reinhardt et al. 2009). By contrast, in response to single stranded DNA lesions like resected DSBs or collapsed/stalled RF (Replication forks), RPA (replication protein-A) coats the single stranded DNA and participates in the recruitment and activation of ATR along with its cofactor ATRIP (Zou and Elledge 2003). Concomitantly, RPA binds Rad17 and recruits the ring-shaped trimeric complex 9-1-1 (Rad9-Hus1-Rad1) which is phosphorylated by ATR and in turn burst ATR activation trough TopBP1 and RHINO (Cotta-Ramusino, McDonald et al. 2011). Fully activated ATR can then phospho-activate Chk1 (Checkpoint kinase-1) at its Ser-317 and Ser-345 residues (Bartek and Lukas 2003), upon activation Chk1 is released from the chromatin and proceeds to establish the checkpoint response (Smits 2006). It has been observed that ATR can be activated in a secondary manner by the processing of DSBs by ATM (Sartori, Lukas et al. 2007).

The ATM pathway tends to be favored during S checkpoint, since it favors HR which is a more convenient repair strategy due to on-going replication. On the other hand, ATR activation favors C-NHEJ and A-NHEJ during G1 and G2 checkpoints since during this phases there is no easy access to a homologous strand for HR to take place (Iliakis, Wang et al. 2003). Additionally DNA-PK is capable of activating both NHEJ and HR to repair DSBs depending on the cell context (Budman and Chu 2005, Convery, Shin et al. 2005, Cui, Yu et al. 2005). In all cases, phospho-activation of RPA by DNA-PK, Chk1 by ATR and Chk2 by ATM will trigger cell cycle arrest by cascading the ablation of CDKs activity (Abraham 2001). CDKs activity is demolished by phosphorylation of Thr-14 and Tyr-15 performed by Wee1 and Myt1 kinases (Boutros, Lobjois et al. 2007). Contrary to this, CDKs can be re-activated by de-phosphorylation of the same residues

by action of the Cdc25 phosphatase family, driving forward the cell cycle progression (Rhind and Russell 2000). Therefore DNA damage response-induced cell-cycle arrest is also established by inhibiting one of the three (Cdc25A, B and C) phosphatases (Donzelli and Draetta 2003). For instance, upon DNA damage detection Cdc25A is phospho-inactivated in its Tyr-15 residue by Chk1 and targeted for proteasomal destruction (Mailand, Falck et al. 2000).

As previously described Cdc25B acts as a pioneer phosphatase that initiates a positive feedback loop that drives the G2/M transition (Lammer, Wagerer et al. 1998). Cdc25C sustains CDK1-Cyclin B1 activity during Mitosis when both of them are translocated inside the nucleus by PLK1 (Takizawa and Morgan 2000, Toyoshima-Morimoto, Taniguchi et al. 2002). After DNA damage detection, Cdc25B/C are phospho-inhibited by Chk1 or Chk2 at Ser-323 or Ser-216 respectively this way being inactivated by 14-3-3 phospho-affinity binding (Peng, Graves et al. 1997, Forrest and Gabrielli 2001). Meanwhile Cdc25A participates throughout the whole cell cycle by activating both CDK2-Cyclin E during S phase and CDK1-Cyclin B1 during the G2/M transition (Molinari, Mercurio et al. 2000). Upon genotoxic stress, Cdc25A is quickly targeted for proteasomal degradation through phosphorylation performed by either Chk1 or Chk2 (Mailand, Falck et al. 2000, Donzelli and Draetta 2003). This opens the field for Chk1 and Nek11 (Never in mitosis gene-A-related kinase 11) to phospho-inhibit CDK2 or CDK1 in their Tyr-15 substrate targeting them for $SCF^{\beta\text{-}Trcp}$ degradation, causing the activation of the G1 or the G2 checkpoint respectively (Mailand, Falck et al. 2000, Jin, Ang et al. 2008, Melixetian, Klein et al. 2009).

The DDR pathways need time to fully repair the DNA damage, therefore checkpoint activation needs to be maintained long enough for this to be fully accomplished (Medema and Macurek 2012). This means that DDR pathways are functionally connected with checkpoint activation and maintenance signaling. DNA damage can occur at any point during the cell cycle, therefore the checkpoint response aids by providing time for repair in the phase of the cell when the DNA insult occurred, propitiate a safe transition to a point where the damage can be repair optimally by allowing a partial processing and preventing a reaching a transition where the repair could be undermined (Iliakis, Wang et al. 2003). In the next sections a description of this processes will be provided.

1.1.7.2 G1 phase checkpoint

Upon DNA damage detection, p53 is the main driver of cell cycle arrest by transcriptionally activating the G1 checkpoint (Agami and Bernards 2000). In the case of DSBs detection during G1, activated DNA-PK phospho-inhibits HDM2 (Human double minute 2) in its Ser-17 residue to prevent it from stimulating p53 proteasomal degradation (Shangary and Wang 2008). Concomitantly, DNA-PK stabilizes p53 by inducing

a conformational change that protects it from HDM2 trough phosphorylating its Ser-15 and Ser37 residues (Shieh, Ikeda et al. 1997). This way p53 is able to induce p21 transcription that will block CDK2-Cyclin E, therefore establishing and maintaining the G1 checkpoint (Lukas, Bartkova et al. 2001). In this context but in an independent manner, both ATR and ATM can activate Chk1 or Chk2 respectively and phosphorylate HDM2 to reinforce the checkpoint establishment, phospho-stabilize p53, and further drive the G1 checkpoint establishment by blocking Cdc25A from dephospho-activating CDK4-Cyclin D1 (Bao, Tibbetts et al. 2001). Additionally, active p53 can drive MDM2 transcription, which generates a negative feedback through which p53 keeps itself in check; plus, subcellular localization of p53 and HDM2 appear to change in a dynamic manner, which provide additional regulatory levels of response (Melchionna, Chen et al. 2000, Lukas, Bartkova et al. 2001).

A similar process driven by Chk1 is believed to take place upon UV light irradiation (Mailand, Falck et al. 2000). Another mechanism leading to G1 checkpoint activation is GSK3-β mediated phosphorylation of cyclin D1 which leads to its degradation via the SCF-E3 ligase complex (Agami and Bernards 2000). This cyclin D1 destruction happens after IR exposure and is also mediated by ATM phospho-activation of FBXO31 (Santra, Wajapeyee et al. 2009). CDK2-Cyclin D1 complex disruption releases p21, which in turn will inhibit the CDK2-Cyclin E and CDK4-Cyclin D1 complexes preventing the cells from progressing through the G1/S transition (He, Siddik et al. 2005). Additionally, p38 might be involved in the G1 checkpoint establishment through phospho-activation the protein HuR at Thr-118, aiding with quick stabilization of p21-mRNA and its subsequent transcription (Lafarga, Cuadrado et al. 2009).

The G1 checkpoint can also be activated by external cues, independent of DNA damage, like the cell sensing the availability of nutrients and stored mitogenic history (Min, Rong et al. 2020). Anti-mitogens such as TGF-β (Transforming Growth Factor β), can cause G1 arrest by inhibiting Cdc25A transcription and activating the R point (Mukherjee, Winter et al. 2010). TGF-β signaling also activates the SMADs proteins, who in turn bind to transcription factors E2F4/5 to conform the Myc-repressor complex (Siegel and Massague 2003). In parallel SMADs can partner with the transcription factor Miz1 that activates the expression of p15 (of the Ink4 family) that will block the activity and conformation of the CDK4/6-Cyclin D1 complex, this arrest leads to accumulation of p21 and p27 (Shi and Massague 2003). GSK3-β can also be activated by growth factor withdrawal and similarly to its activation by DNA damage, will lead to Cyclin D targeted proteasomal degradation (Malumbres and Barbacid 2009). It has been shown that incapability to establish the G1 checkpoint is a landmark of a large subset of cancers, most probably because of the presence of mutations or loss of the TP53 gene, responsible for the expression of p53, the “guardian of the genome” (Powers, Pinto et al. 2020). Therefore, this cells have to rely on the activation of the G2 checkpoint

in order to survive through the activation of the ATR/Chk1, p38MAPK/MK2 and ATM/Chk2 (Reinhardt, Aslanian et al. 2007).

1.1.7.3 S phase checkpoint

The G1 checkpoint ultimate goal is to prevent the cell from entering S phase with severely damaged DNA, however when DNA damage takes place during DNA replication, the activation of the S phase checkpoint takes place (Lamb, Petit-Frere et al. 1989). The typical lesions that trigger the S phase checkpoint activation are IR-provoked DSBs and stalled replication forks (Cimprich 2007), or UV irradiation-caused pyrimidine dimers or photoproducts (Cadet, Grand et al. 2015). DNA breaks during S phase trigger the ATR/ATM-mediated activation of Chk1/Chk2 who will phosphorylate Cdc25A in its Ser-123 residue, targeting it for proteasomal degradation (Falck, Mailand et al. 2001, Kastan 2001) through the SCF complex (Busino, Donzelli et al. 2003); the loss of Cdc25A will keep both CDK2-Cyclin E/Cyclin A complexes in a phospho-inhibited state, thus establishing the S checkpoint arrest (Mailand, Falck et al. 2000, Xiao, Chen et al. 2003). Parallel to this process, it has been reported that ATM-dependent phosphorylation of several intermediates drives forward the S checkpoint. For instance, phospho-activation of NBS1 and MRE11 (components of the MRN complex) is required for proper S checkpoint execution (Lim, Kim et al. 2000, Goldberg, Stucki et al. 2003). MDC1, a BRCT-repeat containing protein is considered to be activated by ATM to recruit DDR machinery proteins to γH2AX sites (Stewart, Wang et al. 2003). BRCA1 targeted phosphorylation at its Ser-1387 by ATM is necessary for S checkpoint response, since it has been observed that if this site is mutated, BRCA1 is incapable of responding to IR induced damage (Xu, O'Donnell et al. 2002). On the other hand, the BRCA1-BARD1 complex is required for p53 stabilization upon IR trough ATM but not trough ATR response upon UV damage (Cortez, Wang et al. 1999, Fabbro, Savage et al. 2004).

As established before, HR is the go-to repair mechanism during S checkpoint. During HR repair, DNA-PK participates in the establishment of the S checkpoint by phosphorylating RPA32 in its Ser-4 and Ser-8 residues, which in turn causes growth arrest and delays progression into the G2/M transition (Liu, Opiyo et al. 2012). ATM activated Chk2 can also drive the S checkpoint by phosphorylating FOXM1 at Ser-361, leading to increased transcription of XRCC1 (Base excision repair factor X-ray cross-complementing group 1) and BRCA2 (Breast cancer associated gene 2) genes, proteins specifically required for DNA damage repair during DNA replication (Tan, Raychaudhuri et al. 2007).

1.1.7.4 G2/M checkpoint

The G2/M DNA damage checkpoint goal is to prevent cells presenting DNA lesions from entering mitosis at least until the most serious damage or staled replicative DNA has been successfully repaired (Nurse 1990). Under normal conditions, cells need the participation of the CDK1-Cyclin B1 complex to enter mitosis (Nigg 2001); however when cells are dealing with DNA lesions, CDK1-Cyclin B1 is inhibited through the phosphorylation of CDK1 in the T14/Y15 residues by the Wee1 and Myt1 kinases (Parker and Piwnica-Worms 1992). Normally, this inhibitory phosphorylations are removed by the phosphatase Cdc25C to trigger the onset of mitosis, so in order to prevent this from happening before the DNA damage is repaired, ATR/ inhibiting Cdc25C trough Chk1/Chk2 (O'Connell, Raleigh et al. 1997, Peng, Graves et al. 1997, Matsuoka, Huang et al. 1998), sequestering it in the cytoplasm via 14-3-3 proteins binding or by direct phosphatase activity inhibition (Furnari, Blasina et al. 1999, Lopez-Girona, Furnari et al. 1999). A parallel target for inhibition by Chk1 its Cdc25A and is considered to be determinant for proper G2 checkpoint response (Zhao, Watkins et al. 2002). Concomitantly, Chk1 phosphorylates Wee1 in its Ser-549 residue, promoting its binding to 14.3.3 protein enhancing the inhibitory activity of the kinase towards CDK1 (Lee, Kumagai et al. 2001) this way helping to consolidate the G2 checkpoint arrest state. Parallel to this, ATM/ATR inhibit PLK1, preventing it from activating Cdc25C and thus, delaying entry into mitosis (van Vugt, Smits et al. 2001, Elia, Cantley et al. 2003). PLK1 phosphorylation by ATM/ATR has been shown to be related to the DDR, plus it correlates with CDK1-Cyclin B1 downregulation and the G2 checkpoint establishment (Smits, Klompmaker et al. 2000). Additionally, it has been observed that the checkpoint protein CHFR drives PLK1 stabilization, delaying entry into mitosis upon mitotic stress (Scolnick and Halazonetis 2000, Kang, Chen et al. 2002). On the other hand, it has been reported that PLK3 is activated by ATM upon DNA damage detection; PLK3 phosphorylates Cdc25C in its Ser-216 which leads to its inactivation (Xie, Wu et al. 2001). Another strategy to regulate the G2 checkpoint maintenance is by abrogating CDK1 activity trough diminishing Cyclin B1 expression levels in response to IR and controlling its subcellular localization (Crawford and Piwnica-Worms 2001, Bulavin, Amundson et al. 2002). It has been shown in several cell lines that, upon DNA damage Cyclin B1 is sequestered in the cytoplasm by 14.3.3 binding, which in turn prevents Cyclin B1 to interact with its nuclear export factor exportin or CRM1 (Pines and Hunter 1994).

MAPK p38 and its downstream effector MK2 (MAPKAP kinase-2) play a crucial role establishing the G2 checkpoint by phosphorylating transcription factors like ATF2, MAC, MEF2 and p53, (Manke, Nguyen et al. 2005) for instance after UV exposure (She, Chen et al. 2000), heat or osmotic shock, response to cytokines and apoptosis or autophagy signals (Anerillas, Abdelmohsen et al. 2020). In this specific scenario, G2 checkpoint activation does not need p53 to be established but it does fully depend on the activity of the

p38MAPK/MK2 pathway for activation and maintenance (Reinhardt, Aslanian et al. 2007, Reinhardt, Hasskamp et al. 2010); this is achieved by ATM/ATR mediated activation of TAO (Thousand and one aminoacid protein kinases) that induce p38 activity trough MEK3 and MEK6 (Raman, Earnest et al. 2007). Even though p53 is not essential for a functional G2 checkpoint, it helps to sustain it through transcriptional repression of mitotic-inducing proteins like Cyclin B1, Cdc25B and PLK1 (McKenzie, King et al. 2010, Dalvai, Mondesert et al. 2011) and by inducing expression of its transcriptional target p21 (He, Siddik et al. 2005).

Once the DNA damage has been successfully repaired cells can begin to recover and prepare to exit the G2 checkpoint. This process starts with Wip1 (Wild-type p53-induced phosphatase) dephosphorylating the ubiquitin-ligase Mdm2 that targets p53 for proteasomal degradation and activates MdmX by dephosphorylating it in its Ser-402, allowing it to inhibit p53 transcriptional activity (Lu, Nannenga et al. 2005, Zhang, Lin et al. 2009). PLK1 is also an essential player during G2 checkpoint recovery, since it has been shown that its depletion completely abrogates cells ability to exit this checkpoint (van Vugt, Bras et al. 2004). Aurora A-activated PLK1 phospho-targets claspin and Wee1 for $SCF^{\beta\text{-}TrCP}$ proteasomal degradation, having CDK1 and CK2 aid with the phosphorylation process (Watanabe, Arai et al. 2005). Additionally, PLK1 can negatively regulate p53 by phospho-activating GTSE1 (G2 and S phase-expressed protein 1) which is a p53 negative regulator (Liu, Li et al. 2010). PLK1 also promotes the translocation of Cdc25B/C to the nucleus (Lobjois, Jullien et al. 2009), and inhibits Chk2 directly (van Vugt, Bras et al. 2004). Activated Cdc25B de-phosphorylates the CDK1-Cyclin B1 complex, inducing its translocation to the nucleus, while Cdc25C translocation to the nucleus enhances the re-activation loop, allowing the cell to progress from G2 to mitosis (van Vugt, Bras et al. 2004, Lindqvist, Kallstrom et al. 2005).

1.3. The Family with Sequence Similarity 110

Little is known about the three protein homologues that compose the Family with sequence similarity 110 (FAM110). This protein family was identified in a yeast two-hybrid screen when searching for CSPP (centrosome/spindle pole-associated protein) interacting proteins. The C20orf55 open reading frame was detected as a strong CSPP interactor through a β-Galactosidase assay and was further tested for colocalization with CSPP, which showed to be high (Hauge, Patzke et al. 2007). Through a homology search, it was found that C20orf55 belonged to a gene family consisting of three members, deemed FAM110A, FAM110B and FAM110C (as suggested by the HUGO Nomenclature Committee) that had not been yet described. The three members of the FAM110 family showed localization to centrosomes and spindle poles, while at the same time presenting specific characteristics of their own (Hauge, Patzke et al. 2007). For instance, it was reported that ectopic expression of FAM110B and FAM110C impaired the progression of the cell cycle, specifically in the G1 phase (Hauge, Patzke et al. 2007). Further, it was described that FAM110C overexpression caused microtubules aberrancies and in contrast, FAM110C depletion reduced integrin-mediated filopodia formation (Hauge, Fjelland et al. 2009); observations were also complemented with co-precipitation experiments that confirmed interaction of FAM110C with microtubules.

1.3.1. FAM110 homologues structure, regulation and localization

The three identified FAM110 homologues encode for proteins of 295 (FAM110A), 370 (FAM110B) and 321 (FAM110C) aminoacid residues. Their sequences present an apparently disordered pattern, with no previously described functional domain. A proline-rich stretch (aminoacids 161 – 182 in FAM110A) is present among all the three family members; additionally FAM110A has a unique proline-rich region ranging from aminoacids 136 – 146 (**Figure 4**). Species-specific homologues of the three human FAM110 members are found exclusively in vertebrates (Hauge, Patzke et al. 2007).

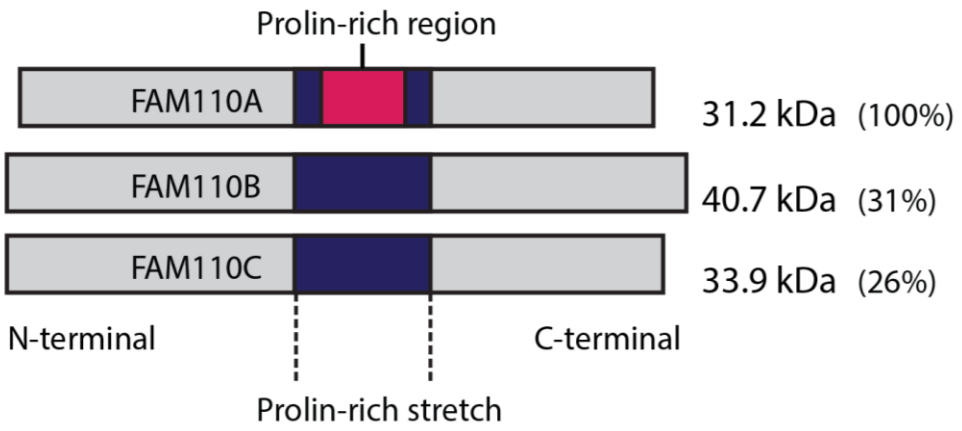

Figure 4. Protein architecture of the FAM110 homologues forms. Schematic diagram of the FAM110 homologues architecture; percentage values represent the sequence similarity of the complete sequence of each FAM110 isoform relative to the FAM110A sequence (Hauge, Patzke et al. 2007). A proline-rich stretch localized in the middle of the sequences is marked in blue, while a Proline-rich region, exclusive for the 110A homologue, is marked in pink.

In the study that first reported the existence of the FAM110 homologues, a cell cycle dependent expression, exclusively for FAM110A was described. By separating cells trough sorting in specific cell cycle phases (G1, S and G2/M) and extracting mRNA for RT-PCR and qPCR analysis, they observed that FAM110A expression levels increased in S and G2/M phases. This observation was compared to the levels present in asynchronic and G1 populations, indicating that FAM110A has a cell cycle-regulated expression pattern (Hauge, Patzke et al. 2007). The FAM110 family homologues were reported to localize to the centrosomes in interphase cells and to the mitotic spindle. FAM110A presents a diffuse cytoplasmic localization but it enriches at the centrosome during interphase; meanwhile during mitosis, its cytoplasmic localization remains while also enriching the spindle poles (Hauge, Patzke et al. 2007). Although the FAM110 homologues have several features in common, differences concerning cellular localization and their possible roles in cell cycle progression have been discussed. While FAM110A has been reported to have a cell cycle-regulated expression specifically increased in G2/M, it was observed that FAM110B and FAM110C induce G1 arrest when overexpressed (Hauge, Patzke et al. 2007). Additionally, FAM110A protein levels appear to have higher expression in endocrine tissue, gastrointestinal tract, testis, bone marrow and lymph node tissues; meanwhile FAM110A-mRNA presented the highest expression in skin tissue followed by the proximal digestive tract (esophagus and salivary glands) (Uhlen, Fagerberg et al. 2015).

1.3.2. FAM110 and cancer

The complete Family with sequence similarity 110 was shown to be aberrantly methylated in 241 breast cancer patients, marking a reduced time for distant metastasis occurrence (Hartmann, Spyratos et al. 2009); this observation was eventually reiterated by a following report were the same methylation status was observed in breast cancer cells (Locke and Clark 2012). In the specific case of FAM110A, it has been reported to be enriched in the adherent junctions colocalizing with E-cadherin and β-catenin which may suggest a relevant involvement during epithelial to mesenchymal transition during cancer pathogenesis development; additionally FAM110A has been observed to be normally expressed in primary PrCA (Prostate Cancer) but appeared to be significantly increased (1.5-fold) in prostate cancer metastasis (Tsuruta, Verhaegh et al. 2014). These results support the hypothesis that this unexplored family of small proteins play a role in cytoskeletal cellular functions and in cancer pathogenesis. In a study aimed to explore new molecular mechanisms involved in CRPC (Castration-resistant prostate cancer), authors analyzed a transcriptional data set of 329 cases of prostate cancer and obtained a list of potential gene products whose overexpression was driven by abnormal amplification. Through a first screen using a siRNA proliferation assay (short interfering RNA) FAM110B was identified among six recurring targets. They observed that FAM110B was able to regulate the AR (Androgen Receptor) signaling pathway in prostate cancer cells and vice versa; moreover, they observed that FAM110B depletion inhibited *in vitro* cell growth but that overexpression caused aneuploidy (Vainio, Wolf et al. 2012). Through a differential expression analysis in diverse tumor differentiation grades, FAM110B upregulation was reported to be negatively correlated with low survival time rates in patients with pancreatic adenocarcinoma and BRCA cancer (Huang, Guo et al. 2020); concomitantly it was observed that FAM110B expression levels gradually decreased in a parallel manner with tumor differentiation which means it may play a role during oncogenesis (Xi and Zhang 2018). In contrast with this, a very recent study using the Kaplan-Meyer survival analysis showed that FAM110B positive expression favored the median survival time in patients with NSCLC (Non-small cell lung cancer) in comparison to those with negative expression levels; Moreover they showed that FAM110B overexpression hampered several cancer cell lines invasion and proliferation while its depletion exerted the opposite effects in the same models. Interestingly this favorable FAM110B upregulation seemed to be linked to its capacity to stimulate β-catenin inhibitory phosphorylation, this way inactivating the Wnt/β-catenin pathway (Xie, Cai et al. 2020).

2. AIMS OF THE THESIS

The cell cycle is the sequence of events that a cell employs to duplicate its genome and divide it into two identical daughter cells. Polo-like kinases are major regulators of the cell cycle progression including promotion of the G2/M transition, formation of the mitotic spindle and the successful completion of cell division. The main member of this family, PLK1 has been deeply studied and its participation throughout mitosis and inhibition during checkpoint activation is well understood. In contrast, the closely related PLK3 has been reported to be activated upon checkpoint establishment, however the reported functions remain controversial. Here we propose to study the function of PLK3 in the cellular response to different kinds of stress and elucidate its protein partners. In parallel, we aim to identify potential new regulators of the cell cycle and mitosis by using gene expression profiling in human non-transformed cells. Resulting identified genes will be collated by analyzing published information about them and we will focus on pin-pointing genes that have not yet been characterized. The molecular mechanisms and underlying functions of a selected candidate gene will be investigated by a combination of immunofluorescence microscopy, live cell imaging and biochemical assays.

2.1 Aim 1. To identify function of PLK3 kinase in the cell cycle and DNA damage response.

(i) To pin point the role of PLK3 in the cellular response to stress.

(ii) To identify proteins that regulate PLK3 function through protein-protein interaction.

2.2 Aim 2. To identify and describe novel regulators of the cell cycle in mammalian cells.

(i) To identify novel genes that are differentially expressed during the cell cycle.

(ii) To describe the role of FAM110A during cell cycle progression and its function in mitosis.

(iii) To identify proteins that regulate FAM110A function through protein-protein interaction.

(iv) To identify the impact of casein kinase 1 on progression through mitosis.

3. MATERIALS AND METHODS

3.1 Antibodies and reagents

For the PLK3 focused goals, the primary antibodies used for Western blot analysis and Immunofluorescence assays are next listed: rabbit monoclonal to PLK3 (clone D14F12, Cell Signaling Technology, #4896); rabbit polyclonal to PLK3 (Novus Biologicals, Abingdon, UK, NBP23-2530); goat polyclonal to PLK3 (Bio-Rad, Hercules, CA, USA, VPA00063); rabbit polyclonal to PLK3 (Sigma-Aldrich, St. Louis, MO, USA, HPA060318); mouse monoclonal to PLK3 (clone B37-2, BD Pharmingen, San Jose, CA, USA, 556518); rabbit polyclonal to PLK3 (St. Johns Laboratory, London, UK, STJ93099); rabbit monoclonal Phospho-PLK1 (Thr210) Antibody (Cell Signaling Technology, Danvers, MA, USA #9062); -tubulin (Sigma-Aldrich); GM130, p38-pT180/pY182, cJun-pSer73, phospho-histone H2AX-Ser139 (referred to as -H2AX) and HIF1α (Cell Signaling Technology); PPP6R1, PPP6R2 and PPP6R3 (A300-968A, A300-970A, A300-972A, Bethyl Laboratories, Montgomery, TX, USA); 14-3-3, mouse monoclonal to PPP6C and TFIIH (Santa Cruz Biotechnology, Dallas, TX, USA); and rabbit polyclonal to PPP6C (Abcam, Cambridge, UK). HRP-conjugated secondary antibodies were from Bio-Rad, Alexa Fluor-conjugates from ThermoFisher Scientific (Waltham, MA, USA). Etoposide, leptomycin B and nocodazole were from Sigma-Aldrich, calyculin from Santa Cruz Biotechnology.

For the FAM110A focused goals, the primary antibodies used for Western blot analysis and Immunofluorescence assays are next listed: mouse monoclonal antibodies against FAM110A (clones F4 and B11, Santa Cruz Biotechnology), rabbit polyclonal against FAM110A (Novus Biotechnology), rabbit polyclonal against γ-Tubulin (Sigma Aldrich); mouse monoclonal against γ- tubulin (clone GTU-88, Sigma Aldrich); mouse monoclonal against α-Tubulin (Biorbyt); CSNK1E (clone A-6), CSNK1D (clone C8), CSNK1A (clone H7) from Santa Cruz, CSPP1 (Proteintech), β-actin (clone D6A8, Cell Signaling). HRP-conjugated secondary antibodies were from Bio-Rad, Alexa Fluor-conjugates from ThermoFisher Scientific (Waltham, MA, USA). Small molecule inhibitors BI2536, MLN8054, RO3306, and PF-670462 were dissolved in DMSO and were from MedChemExpress.

3.2 Generated constructs

pcDNA4/TO/PLK3-myc construct was obtained from Abgent. DNA fragment coding for EGFP was cloned in-frame into HindIII-EcoRI sites of pcDNA4/TO/PLK3-myc-His. Alternatively, fragment carrying PLK3 was sub-cloned into pEGFP-C2 (Clontech, Mountain View, CA, USA). PLK3-H590A-K592M, PLK3-K91R, PLK3-T219A, and PLK3-T219D mutants were generated by site-directed mutagenesis. To generate EGFP-PLK3-DPBD mutant lacking the C-terminal PBD domain, we PCR amplified the fragment

corresponding to residues 1–465 of PLK3 and ligated it into pcDNA4/TO/EGFP-myc backbone using Gibson assembly. All constructs were validated by sequencing. This constructs were used to generate the stable cell lines used in this work and for the transient transfection for Immunoprecipitation assays.

pFucci-S/G2/M Green-Hyg and pFucci-G1 Orange expressing hGeminin (1-110) and hCdt1 (30-120) fragments fused with fluorescent reporters in order to generate a cell line stably expressing the FUCCI indicator. Plasmids were obtained from MBL International (Sakaue-Sawano, Kurokawa et al. 2008). pCMV6-FAM110A-Myc DDK carrying the coding sequence for mouse FAM110A (NM_028666) was ordered from Origene. DNA fragment coding for FAM110A was subcloned into pEGFP-C1 backbone using Gibson assembly. Site-directed mutagenesis of the pEGFP-FAM110A was performed as described previously (Zheng, Baumann et al. 2004). Numbering of the putative phosphorylation sites corresponds to sequence of the human FAM110A (NP_001035812). pEGFP-FAM110A-ΔC was generated by opening pEGFP-FAM110A with PstI and blunting with Klenow fragment. pEGFP-FAM110A-C was generated by ligation of the PstI/BamHI fragment of FAM110A (corresponding to amino acids 185-296) to pEGFP-C1. To generate pEGFP-FAM110A-N (corresponding to amino acids 1-136), the HindIII/BamHI fragment was removed from pEGFP-FAM110A, the plasmid was blunted with Klenow and re-ligated. All constructs were validated by sequencing. This constructs were used to generate the stable cell lines used in this work and for the transient transfection for Immunoprecipitation assays.

3.3 Cells

Human hTERT-immortalized RPE1 cells, HEK-293 cells, U2OS cells and HeLa cells were obtained from ATCC and were grown in DMEM supplemented with 6% FBS (Gibco, Waltham, MA, USA) and Penicillin/Streptomycin antibiotics. Cells were regularly tested for mycoplasma infection using MycoAlert kit (Lonza, Basel, Switzerland).

3.3.1 CRISPR-Cas9 PLK3 knock out cell lines generation

To generate PLK3 knock out cell line, RPE cells grown at 6-well plate were transfected with synthetic sgRNA (CRISPRevolution sgRNA EZ Kit; Synthego, Menlo Park, CA, USA) and recombinant EnGen Spy Cas9 NLS (New England Biolabs, Ipswich, MA, USA) using CRISPRMAX reagent (ThermoFisher Scientific). Two independent targeting sequences in exon 2 of human PLK3 were UGUCAGUGGCCUCGUAGCAG and GGGCUUCGCCCGCUGCUACG. Three days after transfection, single cells were seeded on 96-well plates and individual clones were expanded. Genomic DNA was isolated from individual clones and the fragment corresponding to DNA from intron 1 to exon 3 was amplified by PCR, sequenced and analyzed by TIDE software (Desktop Genetics, Cambridge, MA, USA).

For selected clones, PCR fragments were inserted into pcr2.1-TOPO plasmid, and plasmid DNA from 10 bacterial colonies was sequenced to confirm individual alleles of PLK3. The following two independent clones were selected for further functional testing: RPE-PLK3-KO clone cr1.2 carries a single nucleotide insertion in the target site and a 54 bp deletion at intron/exon2 transition; RPE-PLK3-KO clone cr2.3 is a homozygote carrying a single nucleotide insertion within the target sequence in exon 2. Loss of PLK3 expression in the knock-out cells was further validated by immunoblotting.

3.3.2 EGFP-PLK3 stable ectopic expression cell lines generation

To generate the EGFP-PLK3 stable cell lines, HEK293 cells were transiently transfected with pcDNA4/TO/EGFP-PLK3-myc plasmid; after 48 hours of transfection, cells were treated with zeocin for 3 weeks. Formed colonies were harvested and sorted for GFP positivity as a polyclonal stable cell line; EGFP stable cell line was taken as control for selection and future experiments.

3.3.3 hTERT- immortalized RPE1 cell line and EGFP-FAM110A variants cell lines generation

Human hTERT-immortalized RPE1 cells (here referred to as RPE) were obtained from ATCC and were grown in DMEM supplemented with 6 % FBS (Gibco,Waltham, MA, USA) and Penicillin and Streptomycin antibiotics. U2OS stable cell line expressing Tubulin-mCherry-H2B-GFP were reported previously (Tanenbaum, Macurek et al. 2008). Cells were regularly tested for mycoplasma infection using MycoAlert kit (Lonza, Basel, Switzerland). To generate RPE cells stably expressing the FUCCI indicator, we transfected RPE cells with pFucci-S/G2/M Green-Hyg plasmid, cultivated in media supplemented with hygromycin for 2 weeks and selected cells expressing the reporter using Influx cell sorter (BD Biosciences) (Macurek, Benada et al. 2013). Subsequently, we transfected these cells with pFucci-G1 Orange plasmid, cultivated them for 2 weeks in media with geneticin, sorted single cells expressing the G1 reporter using Influx cell sorter (BD Biosciences) and expanded individual cell clones. The resulting RPE-FUCCI cells were tested for expression of both components of the FUCCI indicator by flow cytometry. To generate the RPE stable cell line expressing EGFP-FAM110A-WT, cells were transfected with the linearized pEGFP-FAM110A plasmid, incubated with the transfection cocktails for 4 hours and then supplemented with fresh media. After 48 hours of transfection, the cells were submitted to selection with Geneticin for 3 weeks. Formed colonies were harvested and sorted for GFP positivity as a polyclonal stable cell line; EGFP stable cell line was taken as control for selection and future experiments. Transfection of plasmid DNA was performed using Lipofectamine 2000 (Thermo Scientific) or by polyethylenimine.

3.3.4 EGFP-FAM110A (and variations) stable ectopic expression cell lines generation

To generate the EGFP-FAM110A-WT and variants stable cell lines, RPE cells were transiently transfected with pEGFP-FAM110A-flag and variants plasmids; after 48 hours of transfection, cells were treated with geneticin for 2 weeks. Formed colonies were harvested and sorted for GFP positivity as a polyclonal stable cell line; EGFP stable cell line was taken as control for selection and future experiments.

3.4 siRNA knock-down assays

To perform knock down assays, 200 000 cells were seeded per well in 6 well-plates. They were incubated for 12 hours before attempting knock down. Controls were cells that received non-coding siRNA cocktails alongside treated cells. RPE and HeLa parental cells were transfected with Silencer Select siRNA oligonucleotides at final concentration 5 nM using RNAiMAX (Thermo Scientific) has transfection agent (old media was replaced with fresh media before adding the transfection cocktails). After 24 hours of incubation with the complexes, cells were split and incubated for 24 hours more. Cells were collected after 48 hours of initial transfection, fractionated for total protein lyse in SB Buffer and/or fixed in 70% EtOH or 4% PFA for future FACS preparation. Targeting sequences for PLK3 are: GGCUUUGGGUAUCAACUGU for siRNA PLK3-I and GCAUCAAGCAGGUUCACUA for PLK3 siRNA-II. Targeting sequences for PLK1, PP6C, PPP6R1 and PPP6R3 are: UCAUAUUCGACUUUGGUUGCC for siRNA PLK1, AUCUUUCAUCACAACGUCCUC for siRNA PP6C, UUGCGGUUGACGACCUUGCAC for siRNA SAPS1 and UUAGGUGUCCCAUGUAACCAT for siRNA SAPS3. Targeting sequences for FAM110A are: CAAUACAAGGUUUUUGACA for siRNA FAM110A#4, GGCUCCACCCUGUUGUGAA for siRNA FAM110A#5. Targeting sequences for FAM110B and CSPP1 are: CCUGGGAAUGGAAAACUUU for siRNA FAM110B and UCAAUGUCUAGUCCUUUCCAT for siRNA CSPP1. Targeting sequences for CK1δ and CK1ε are: AUUUCUUCUCGCUAAUCCTT for siRNA CSNK1D and UAUGUUGAGAAUUCGGAGGGA for siRNA CSNK1E. Cells were collected 48 h after transfection.

3.5 Stress induction assays

For the stress induction assays, 200 000 cells were seeded per well in 6 well-plates. They were incubated for 12 hours before starting each treatment. Controls were cells that received no treatment alongside treated cells. To induce DNA Damage by UVC radiation, cells were exposed to 10 and 20 J/m2 in a Bio Rad Gs Gene Linker UV Chamber® (Gentile, Latonen et al. 2003). First, culture media was aspirated and cells were washed once with 1X PBS. Cells were submitted to the UV light immediately after PBS wash was removed; afterwards, warm media was provided and cells were incubated for 30 minutes in normal conditions before total cell lysates were collected in SB Buffer. To submit cell to hyperosmotic shock,

normal media was replaced with media supplemented with 350 mM NaCl or 480 mM mannitol (Wang, Dai et al. 2011). For hypotonic shock induction, normal media was replaced with media diluted 1:1 with water. Cells were incubated for 40 min under this conditions. For the hypoxia-response assay, the normal media was replaced with media supplemented with 150–300 μM CoCl2 (hypoxia-mimic agent) and incubated for 12 hours (Wang, Gao et al. 2008). Total cell lysates were collected in SB. For the ionizing radiation assays cells were exposed to 3 Gy using an X-RAD 225XL Biological Irradiator (Precision; Cu filter 0.5 mm). Total cell lysates were collected after 1 hour and 8 hours of exposure.

3.6 Cell sorting, RNA isolation and BeadChip hybridization

Asynchronously growing RPE-FUCCI cells were collected by trypsinization and RFP+/GFP- (corresponding to G1 cells) and RFP-/GFP+5 (corresponding to G2 cells) populations (approx. 0.5 x 10_6 cells) were sorted using Influx cell sorter into RNAlater Stabilization Solution (Thermo Scientific). Total asynchronic population was collected as control. RNA was isolated by RNeasy Mini Kit (Qiagen) and its quality was verified by Qubit Fluorometer (Thermo Scientific). RNA was transcribed to cDNA by Illumina TotalPrep RNA Amplification Kit, hybridized to Illumina HumanHT-12_v4 Expression BeadChip and scanned using BeadStation 500 (Illumina). Four biological replicates were processed in parallel on one BeadChip. Fold change in gene expression and statistical significance were calculated by limma software package (Ritchie, Phipson et al. 2015).

3.7 Quantitative Real-Time Polymerase Chain Reaction (qRT-PCR)

RPE parental cells were transfected with siPLK3-I, siPLK3-II and control. After 48 hours of siRNA transfection cells were collected and total RNA was isolated using RNeasy Mini Kit (Quiagen, Hilden, Germany). cDNA was synthesized from 3 μg total RNAs using random hexamer and RevertAid H Minus Reverse Transcriptase (ThermoFisher Scientific). Real-time quantitative PCR was performed on LightCycler 480 Instrument II (Roche, Basel, Switzerland) using LightCycler 480 SYBR Green I Master (Roche) and the following primers: PLK3-forward TGAGGACGCTGACAACATCTAC, PLK3-reverse CAGGTAGTAGCGCACTTCTGG, ATP5B-forward TGAAGAA-GCTGTGGCAAAAGC, and ATP5B-reverse GAAGCTTTTTGGGTTAGGGGC. Relative amount of PLK3 mRNA is presented as the ratio to ATP5B mRNA. RNA was isolated from RFP+/GFP-(corresponding to G1 cells), RFP-/GFP+ (corresponding to G2 cells) and RFP+/GFP+ (corresponding to S cells) RNeasy Mini Kit (Qiagen). cDNA was synthetized using 0.5 μg RNA, random hexamer, and RevertAid H Minus Reverse Transcriptase (Thermo Scientific). RT-qPCR was performed using LightCycler 480 SYBR Green I Master mix (Roche) using following cycle conditions: initial denaturation 95°C for 7 min, followed by 45 cycles of denaturation

95°C for 15 s, annealing 60°C for 15 seconds and extension 72°C for 15 seconds. Ct values were determined using LigtCycler480 software. Data are presented as the ratio of the tested mRNA to GAPDH mRNA.

3.8 Cell synchronization

RPE cells were synchronized in G0 by growing to confluency, then cells were split to fresh medium supplemented with 2 mM thymidine and incubated for 36 hours (Benada, Burdova et al. 2015). After two washes in PBS, cells were released to fresh medium and were collected at 2 hours intervals. After 4 hours from thymidine release, nocodazole (100 ng/ml) was added to the media to arrest cells in prometaphase. All cells were collected by trypsinization, spinned down and fractionated as follows: 1/10 of the sample was separated and fixed in 70% ice-cold Ethanol, stored at -20 °C for subsequent staining FACS and 9/10s were immediately lysed with SB buffer and boiled for 5 minutes. Alternatively, nocodazole-arrested cells were collected by mitotic shake off at 16 h after release form thymidine block and submitted to the same sample preparation treatment.

3.9 Flow cytometry (FACS)

The cells that were fixed with 70 % ice-cold EtOH as described before, were spinned down to remove supernatant and then permeabilized with 0.5 % Triton X-100 for 15 minutes at room temperature and blocked with 1 % BSA for 30 min. Subsequently, cells were incubated with pMPM-Cy5 conjugated antibody (Cell Signaling, 1:500) for 1 hour at room temperature, washed once with 1X PBS and resuspended in 1X PBS supplemented with DAPI (5 µg/ml). FACS analysis was performed using LSR II (BD Bioscience) and the obtained data was analyzed using the FlowJo.10 software (Tree Star, BD). Single cells were gated using SSC and FSC, DNA content was determine using DAPI and mitotic cells were quantified using the Cy5 channel.

3.10 Cell fractionation

RPE cells fractionation was performed as previously described (Xu and Stern 2003, Macurek, Lindqvist et al. 2010). Soluble cytosolic fraction was obtained by incubating cells in buffer A (10 mM HEPES pH 7.9, 10 mM KCl, 1.5 mM $MgCl_2$, 0.34 M sucrose, 10% glycerol, 1 mM DTT, 0.05% Triton X100 and protease inhibitor cocktail) at 4 °C for 10 minutes and spin down at 1500X g for 2 minutes. Pelleted nuclei were further extracted with an equal amount of buffer B (10 mM HEPES pH 7.9, 3 mM EDTA, 0.2 mM EGTA, 1 mM DTT) and spin down at 2000X *g* for 2 minutes yielding a soluble nuclear fraction. Insoluble chromatin was washed with buffer B and resuspended in SDS sample buffer.

3.11 Immunofluorescence

Cells grown on coverslips were fixed with 4% PFA for 20 min at room temperature, washed once with 1X PBS and permeabilized with 0.5% Triton X-100 for 15 min. Cells were further incubated with ice-cold methanol for 5 min and blocked with 3% BSA-1X PBS for 30 min. Coverslips were incubated with primary antibodies for 3 hours at room temperature inside a wet chamber. After washing 3 times with 1X PBS, cells were incubated with AlexaFluor-conjugated antibody for 1 hour at room temperature. Coverslips were subsequently washed 3 times with 1X PBS, incubated with DAPI (0.1 µg/ml) for 5 min at room temperature, washed once with distilled water and mounted on microscopy glass slides using VectaShield as mounting media. Imaging was performed using Leica Sp8 confocal microscope equipped with HC PL APO 63x/1.40 oil objective (NA 1.40). Images were analyzed and processed using LAS AF Lite software (Leica, Wetzlar, Germany).

For the induction of DNA damage response experiment, a previously described protocol was implemented (Burdova, Storchova et al. 2019); cells exposed to ionizing radiation were fixed with 4% PFA for 15 minutes, permeabilized with 0.5% Triton X-100, and probed with antibody against H2AX (Cell Signaling Technology). Images were acquired using Olympus ScanR system equipped with 40X/NA 1.3 objective (Olympus, Tokio, JApan). Number H2AX-positive foci per nucleus was determined using spot detection module. More than 300 nuclei were quantified per condition.

Cells grown on coverslips were fixed with 4 % PFA for 20 min at room temperature, washed once with 1X PBS and permeabilized with 0.5% Triton X-100 for 15 min. Alternatively, cells were incubated with ice-cold methanol for 5 min and blocked in 3 % BSA dissolved in 1X PBS for 30 min. Coverslips were incubated with primary antibodies for 3 hours at room temperature inside a wet chamber. After washing with 3 times with 1X PBS, cells were incubated with AlexaFluor-conjugated antibody for 1 hour at room temperature. Coverslips were subsequently washed 3 times in PBS, incubated with DAPI for 5 min at room temperature, washed once with distilled water and mounted on microscopy glass slides using VectaShield as mounting media. Imaging was performed using Leica Sp8 confocal microscope equipped with HC PL APO 63x/1.40 oil objective (NA 1.40). Images were analyzed and processed using the LAS AF Lite software (Leica, Wetzlar, Germany). For the mitotic spindle orientation (angle quantification) assay, cells were grown on fibronectin-coated coverslips and were fixed 48 h after transfection with indicated siRNAs and stained for γ-tubulin. Metaphase cells were imaged by Leica SP8 confocal microscope at 0.5 µm z-stacks with a 5.00 zoom value. Angle of the mitotic spindle relative to the growth surface was calculated from the linear distance between the spindle poles and the relative height distance (number of z-stacks) of both spindle poles as previously described (Toyoshima and Nishida 2007).

For the actin dynamics measurement, cells that had undergone 48 hours after respective siRNA transfection and seeded on coverslips were incubated for 18 hours with STLC to arrest in prometaphase and generate monopolar mitotic spindles. Cells were then forced out of mitosis by supplementing them with 20 μM RO3306 and incubated for the stipulated time points (Farina, Ramkumar et al. 2019)). Cells were then pre-extracted for 60 sec and fixed with 4% PFA for 20 min. For actin filament staining, cells were permeabilized with 0.5% Triton X-100 for 15 min and blocked with 3% BSA-1X PBS for 30 min. Coverslips were incubated with primary antibody against γ-tubulin (mouse-monoclonal) for 3 hours at room temperature inside a wet chamber. After washing 3 times with 1X PBS, cells were incubated with Alexa-647-mouse secondary antibody for 1 hour at room temperature. Coverslips were subsequently washed 3 times with 1X PBS and incubated with Alexa-568-phalloidin (200 nM) for 20 min and washed once with 1X PBS. Lastly, chromatin was labelled with DAPI (0.1 μg/ml) for 10 min at room temperature, washed once with 1X PBS and mounted on microscopy glass slides using VectaShield as mounting media. Coverslips were sealed using clear nail polish and the tops were washed with distilled water to retrieve salt residues. Fixed cell images were acquired using a Leica Sp8 confocal microscope equipped with HC PL APO 63x/1.40 oil objective (NA 1.40). Images were analyzed and processed using LAS AF Lite software (Leica, Wetzlar, Germany).

3.12 Time-lapse microscopy

U2OS-H2B-GFP/Tub-mCherry cells, parental RPE or RPE cells stably expressing EGFP-FAM110A variants were transfected with control or specific siRNA oligonucleotides as described above and after 24 hours of transfection, seeded into Lab-TekII coverglass chambers (Thermo Scientific). After 32 hours post transfection, subconfluent cells were imaged every 5 minutes for up to 24 hours using Leica DMI6000 microscope equipped with N PLAN 40x/0.55 CORR DRY objective inside a 37°C, 5% CO2 environmental chamber. Films were analyzed using LAS AF Lite software (Leica). Division kinetics was determined manually by counting each 5 min interval from the nuclear envelope breakdown to metaphase-to-anaphase transition. In total, 100 individual cells were quantified per condition in three independent experiments.

3.13 Spindle angle orientation measurement

To analyze orientation of the cell division, we measured the angle between the long axis determined in the interphase cell just before mitotic entry and the division axis determined in anaphase as described previously (He, Kannan et al. 2017, Fulcher, He et al. 2019). Cells in which longitudinal axis was not apparent at G2/M transition were excluded from the analysis. Cell division was considered mis-oriented when the angle exceeded 15°. In total, 30 individual cells were quantified per condition in three independent experiments

3.14 Actin dynamics measurement

After 48 hours of respective siRNA transfection, cells grown on coverslips were incubated for 18 hours with STLC to arrest in prometaphase and generate monopolar mitotic spindles. Cells were then forced out of mitosis by supplementing them with 20 μM RO3306 and incubated for the stipulated time points (Farina, Ramkumar et al. 2019). Cells were then pre-extracted for 60 sec and fixed with 4% PFA for 20 min. For actin filament staining, cells were permeabilized with 0.5% Triton X-100 for 15 min and blocked with 3% BSA-1X PBS for 30 min. Coverslips were incubated with primary antibody against γ-tubulin (mouse-monoclonal) for 3 hours at room temperature inside a wet chamber. After washing 3 times with 1X PBS, cells were incubated with Alexa-647-mouse secondary antibody for 1 hour at room temperature. Coverslips were subsequently washed 3 times with 1X PBS and incubated with Alexa-568-phalloidin (200 nM) for 20 min and washed once with 1X PBS. Lastly, chromatin was labelled with DAPI (0.1 μg/ml) for 10 min at room temperature, washed once with 1X PBS and mounted on microscopy glass slides using VectaShield as mounting media. Coverslips were sealed using clear nail polish and the tops were washed with distilled water to retrieve salt residues. Fixed cell images were acquired using a Leica Sp8 confocal microscope equipped with HC PL APO 63x/1.40 oil objective (NA 1.40). Images were analyzed and processed using LAS AF Lite software (Leica, Wetzlar, Germany).

3.15 Immunoprecipitation and mass spectrometry

HEK293 cells stably expressing EGFP or EGFP-PLK3 were extracted in CO-IP buffer (20 mM HEPES pH 7.5, 10% glycerol, 150 mM NaCl, 0.5% NP40) supplemented with cOmplete protease and PhosSTOP phosphatase inhibitors (Sigma) and sonicated during 20 seconds for 3 rounds; samples were kept on ice at all times. Cell extracts were cleared by centrifugation at 15,000 rpm for 10 min at 4 ◦C. Supernatants were recovered and fractionated as follows: 1/10 of the sample was taken as "Input" and 9/10s were subsequently given the GFP-Trap beads (Chromotek, Planegg, Germany); beads were activated by washing for 3 times with ice cold non-supplemented CO-IP buffer. Cell lysates containing the GFP-Trap beads were incubated for 3 hours at 4 ◦C with constant rotation. After incubation time was completed, GFP-Trap beads were spin down and the supernatant was removed; beads were washed three times in ice-cold CO-IP buffer. Bound proteins were eluted from beads by adding Laemli buffer and boiling the samples for 5 min. Input and CO-IP samples were analyzed in the same gel by immunoblotting. Alternatively, bound proteins were analyzed by mass spectrometry using Orbitrap Fusion (Thermo Scientific). Proteins bound to EGFP-PLK3 that were enriched compared to the empty EGFP control in at least two out of three independent experiments were considered as potential interactors and were validated by immunoprecipitation followed by immunoblotting. For *in vitro* kinase assay, wild-type or mutant EGFP-PLK3 was immunoprecipitated using GFP Trap, washed three times in CO-IP buffer and incubated with

casein in kinase buffer (10mM HEPES pH7.4, 5mM $MgCl_2$, 2mM EGTA, 1mM DTT, 2.5mM β-glycerolphosphate, 100 µM ATP and 5 µ Ci ^{32}P-γ-ATP) for 20 minutes at 30 °C. Proteins were separated using SDS-PAGE, and phosphorylation was visualized by autoradiography.

RPE cells stably expressing EGFP or EGFP-FAM110A were grown in the presence of nocodazole for 12 hours to enrich the mitotic population, mitotic cells were collected by mitotic shake off and extracted in CO-IP buffer (20 mM HEPES pH 7.5, 10 % glycerol, 150 mM NaCl, 0.5 % NP40) supplemented with cOmplete protease and PhosSTOP phosphatase inhibitors (Sigma) and sonicated for 20 seconds for 3 times, samples were kept on ice at all times. Cell extracts were cleared by centrifugation at 15 000 rpm for 10 minutes at 4°C. Supernatants were recovered and fractionated as follows: 1/10 of the sample was taken as "Input" and 9/10s were subsequently given the GFP-Trap beads (Chromotek, Planegg, Germany); beads were activated by washing for 3 times with ice cold non-supplemented CO-IP buffer. Cell lysates containing the GFP-Trap beads were incubated for 3 hours at 4 °C with constant rotation. After incubation time was completed, GFP-Trap beads were spin down and the supernatant was removed; beads were washed three times in ice-cold CO-IP buffer. Bound proteins were eluted from beads by adding Laemli buffer and boiling the samples for 5 min. Input and CO-IP samples were analyzed in the same gel by immunoblotting. Alternatively, bound proteins were analyzed by mass spectrometry using Orbitrap Fusion instrument (Thermo Scientific) and MaxQuant software. Three biological replicates were analyzed by mass spectrometry and median peptide intensities were compared. Statistical significance was calculated using Student's T-test. Alternatively, cell extracts from EGFP-FAM110A cells were incubated with 2 µg of mouse IgG, CSNK1E or CSNK1D antibodies (all Santa Cruz) for 2 hours at 4 °C with constant rotation. After primary incubation was completed, bound proteins were immobilized by adding Protein A/G UltraLink beads (Pierce) to the cell extract and incubated for 3 hours at 4 °C with constant rotation. Beads were spinned down and washed 3 times with ice-cold non-supplemented CO-IP Buffer. Bound proteins were eluted from beads by adding Laemli buffer and boiling the samples for 5 min. Input and CO-IP samples were analyzed in the same gel by immunoblotting. Where indicated, cell extracts were prepared in RIPA buffer (25 mM Tris pH 7.6, 150 mM NaCl, 1.0 % NP40, 1.0 % sodium deoxycholate, and 0.1 % SDS) to reduce background binding in immunoprecipitation.

3.16 *In vitro* phosphatase assay

For the *in vitro* phosphatase assay, cells were synchronized in G2 or in mitosis by overnight treatment with RO3306 or nocodazole respectively. Cells were extracted using RIPA buffer, sonicated for 20 seconds on ice and spun down for 10 minutes at 4°C. Endogenous FAM110A was immunoprecipitated from cell extracts using rabbit polyclonal antibody (2 µg/reaction, Novus Biotechnologies) and immobilized by

incubation on pA/G beads for 2 hours at 4 °C with constant rotation. After washing four times in 1X PBS, beads were incubated with mock or λ-phosphatase (800 U/reaction, Santa Cruz) at 20°C for 30 minutes. Reaction was stopped by addition of 4x Laemli buffer and mobility of FAM110A was evaluated by immunoblotting.

3.17 *In vitro* kinase assay

Wild-type or mutant EGFP-FAM110A or EGFP alone was immunoprecipitated from transiently transfected HEK293 cells using GFP-Trap beads and the CO-IP buffer supplemented as described above, but in this specific case, the CO-IP buffer contained a 1 M NaCl concentration. Beads were washed three times in the CO-IP buffer containing high salt, then once in ice-cold 1X PBS and finally, bound proteins were eluted by 2 M glycine, immediately neutralized and stored at -80°C. Purified proteins were checked by immunoblotting for the absence of co-purified protein kinases CDK1 and CK1. Purified proteins were incubated with 100 ng of GST-tagged CSNK1D (Sigma) in kinase buffer (10 mM HEPES pH 7.5, 2.5 mM β-glycerolphosphate, 1 mM EDTA, 4 mM MgCl2 and 100 μM ATP) for 20 min at 30°C. Where indicated, kinase buffer was supplemented with 5 μCi of gamma-32P-ATP. Reaction was stopped by mixing with 4X Laemli buffer and boiling the samples for 5 minutes. Samples were analyzed by immunoblotting.

3.18 Statistical analysis

For Western blots quantification, signal intensity of the bands from 3 biological replicates (n = 3) was calculated using gel analysis plug-in in ImageJ. After background subtraction, signal was normalized to the corresponding loading control and to non-treated condition. Statistical significance was evaluated using two-tailed unpaired t-test or by ANOVA test in GraphPad Prism version 5.0 (GraphPad Software). Experiments were performed at least three times unless stated otherwise. Values in bar graphs are presented as mean ± SD. Statistical significance was evaluated using Student's two-tailed unpaired t-test or by ANOVA test in GraphPad Prism version 5.0 (GraphPad Software) and p values ≤ 0.05 were considered significant (* $p<0.05$, ** $p<0.005$, *** $p<0.001$, **** $p<0.0001$).

3.19 Data availability

The complete data set from expression profiling of RPE-FUCCI cells was deposited in ArrayExpress database (https://www.ebi.ac.uk/arrayexpress/experiments/E-MTAB-9626/) under accession number E-MTAB-9626. Data is currently available to the general public.

4. RESULTS

4.1 Aim 1

4.1.1 PLK3 localizes to plasma membrane, Golgi and Centrosome

PLK3 subcellular localization has been a subject of contention. Some studies have reported that PLK3 can be localized to the Golgi apparatus (Ruan, Wang et al. 2004, Xie, Wang et al. 2004), enriching in the plasma membrane (Holtrich, Wolf et al. 2000) and even inside the nucleus and nucleolus (Zimmerman and Erikson 2007, Wang, Gao et al. 2008). Nonetheless, some of this studies relied on non-validated PLK3 antibodies, therefore we decided to first address the veracity of the existing published data in order to stablish a grounded starting point for our study. We started by screening all commercially available PLK3 antibodies by testing them through immunoblotting and immunofluorescence. By implementing siRNA knock down of PLK3 in RPEs parental cells, we observed that the PLK3 antibodies corresponding to BioRAD, Novus Biologicals, Sigma and BD Pharmingen, had unspecific reactivity (Fig. A). The only antibody that managed to recognize endogenous PLK3 was the rabbit monoclonal antibody (clone FD4F12) from Cell Signaling Biotechnology. This antibody recognized three bands, the slowest migrating one (80 - 90 kDa) was determined as unspecific since the other two that migrated faster (65 – 75 kDa) disappeared after treatment with two independent siRNAs specifically designed to target and knock-down PLK3 (**Figure 5-A**). In another independent experiment, using one of this siRNAs against PLK3 and one against PLK1 and probing with the Cell Signaling PLK3 antibody, we confirmed that the two observed bands between 65 to 75 kDa disappeared but were not affected by the knock down of PLK3's homolog, PLK1 (**Figure 5-B**).

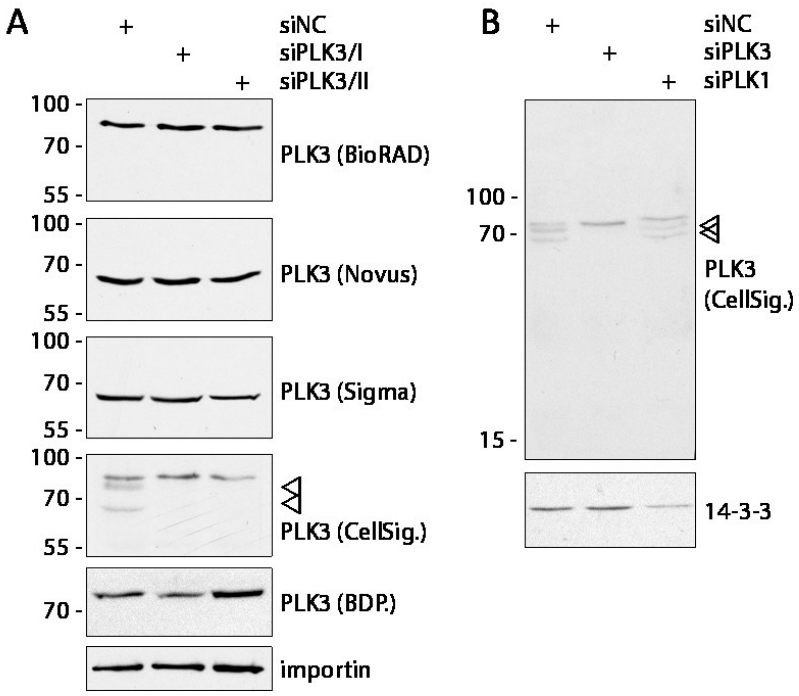

Figure 5. PLK3 commercial antibodies specificity testing in Western Blot. A. RPE cells transfected with non-targeting control siRNA or two siRNAs targeting PLK3. After 28 h, whole cell lysates were separated by SDS-PAGE and probed with indicated antibodies. Numbers indicate mobility in kDa. Position of PLK3 is indicated by arrowheads. Importin was used as loading control. **B.** RPE cells were transfected with non-targeting control siRNA or siRNA to PLK3 or PLK1. Whole cell lysates were probed with rabbit monoclonal PLK3 antibody (Cell Signaling). Protein 14.3.3 was used as loading control. The position of PLK3 is indicated by arrowheads.

Then, we proceeded to test the detection capacity of this antibodies trough IF; unfortunately, none of the after mentioned antibodies managed to recognize endogenous PLK3 successfully trough immunofluorescence assays. Because of this issue, we decided to generate a stable cell line using HEK293 cells that would express an ectopic PLK3 tagged with EGFP. The PLK3 localization pattern in the stable cell line was also contrasted with the one observed in transiently transfected parental RPE cells. In both instances, EGFP-PLK3 was observed enriched in the plasma membrane, partially colocalizing with GM130 at the Golgi apparatus, and in the centrosome, which was delimitated by probing for γ-tubulin (**Figure 6**). The observed PLK3 intracellular pattern showed enrichment in the plasma membrane, localization in the centrosome and in punctual areas of the Golgi apparatus, partially confirming some of the previously reported data (Holtrich, Wolf et al. 2000, Xie, Wang et al. 2004, Zimmerman and Erikson 2007, Wang, Gao et al. 2008).

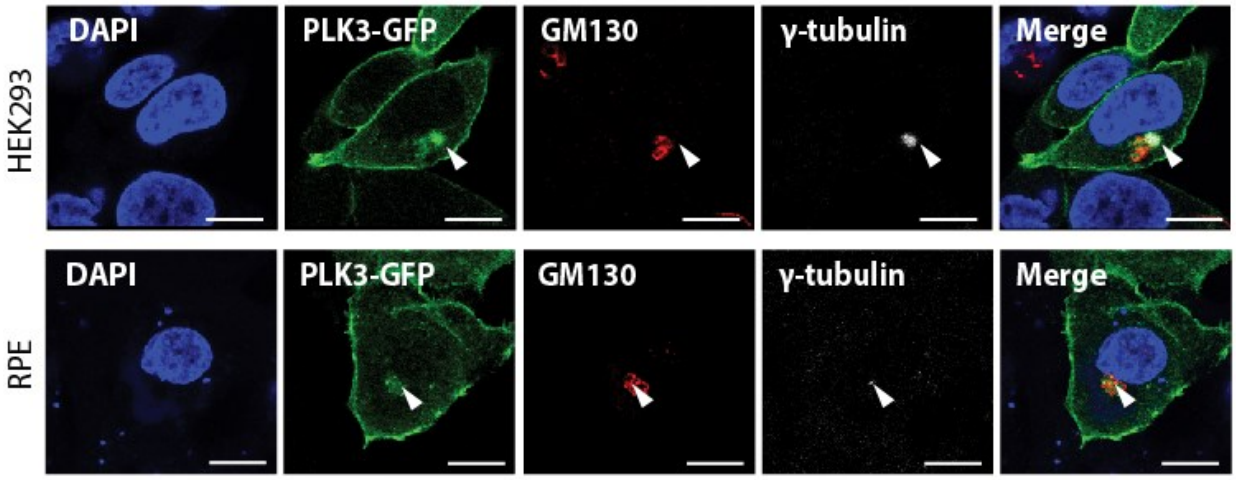

Figure 6. PLK3 localizes at plasma membrane and Golgi apparatus. On the top panel, we show HEK293 cells stably expressing EGFP-PLK3. This cells were grown on coverslips, fixed and probed with antibodies against GM130 as Golgi marker and against γ-tubulin as centrosome marker and imaged by confocal microscopy. On the bottom panel RPE cells were transiently transfected with EGFP-PLK3, grown on coverslips, fixed and probed with the after mentioned antibodies. Arrow heads indicate the position of the centrosome. Bar indicates 5 µm.

We also tested the reactivity of the mentioned PLK3 antibodies by immunofluorescence in the EGFP-PLK3 cell line; probing with the rabbit monoclonal antibody from Cell Signaling showed a perfectly overlapping signal with the overexpressed PLK3 and presented no apparent sign of cross-reactivity. This suggested that this antibody can recognize and is specific for PLK3 but that its titer may be too low for detection of the endogenous protein (**Figure 7-first vertical panel**). In the case of the St. John laboratory PLK3 antibody, we observed that while it successfully stained the enriched ectopic EGFP-PLK3 in the centrosomal vicinity, it also presented an unspecific signal in the nucleus (**Figure 7-last vertical panel**), a localization that has been reported in the past for PLK3 (Zimmerman and Erikson 2007, Wang, Dai et al. 2014) but where the antibodies used were not validated. Finally, the rest of the listed PLK3 antibodies (Novus, Sigma and BD Pharmingen) failed to recognize even the overexpressed EGFP-PLK3 (**Figure 7-three vertical panels in the middle**).

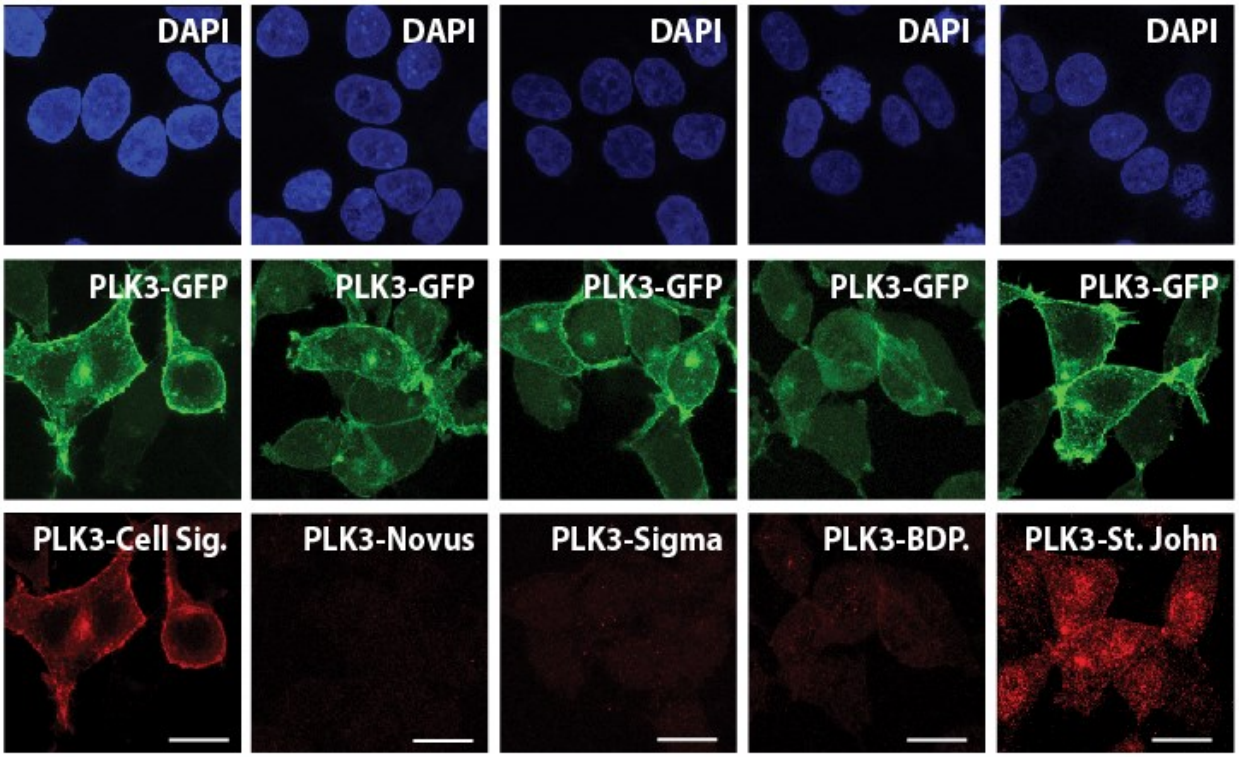

Figure 7. PLK3 commercial antibodies testing in EGFP-PLK3 Stable cell line. The HEK293-EGFP-PLK3 Stable cell line was fixed and probed with the indicated PLK3 commercially available antibodies. Bar indicates 5 µm.

We then decided to test the titer of the after mentioned antibodies trough WB using the EGFP-PLK3 stable cell line. We proceeded then to obtain total protein lysates from a control EGFP stable cell line that was generated side-by-side with the EGFP-PLK3 stable cell line, and of the HEK293 parental cells. We observed that the majority of the antibodies failed to recognize the endogenous and ectopic EGFP-PLK3 (BD Pharmigen, Novus, Sigma) and two of them showed high cross-reactivity (BioRad and St. Jhons). On the other hand and as we expected, the Cell Signaling antibody presented high affinity to the EGFP-PLK3 ectopic protein and lacked cross reaction bands, this in contrast with the St. Jhons antibody, which also recognized the ectopic EGFP-PLK3 but presented multiple cross reactivity bands (**Figure 8**).

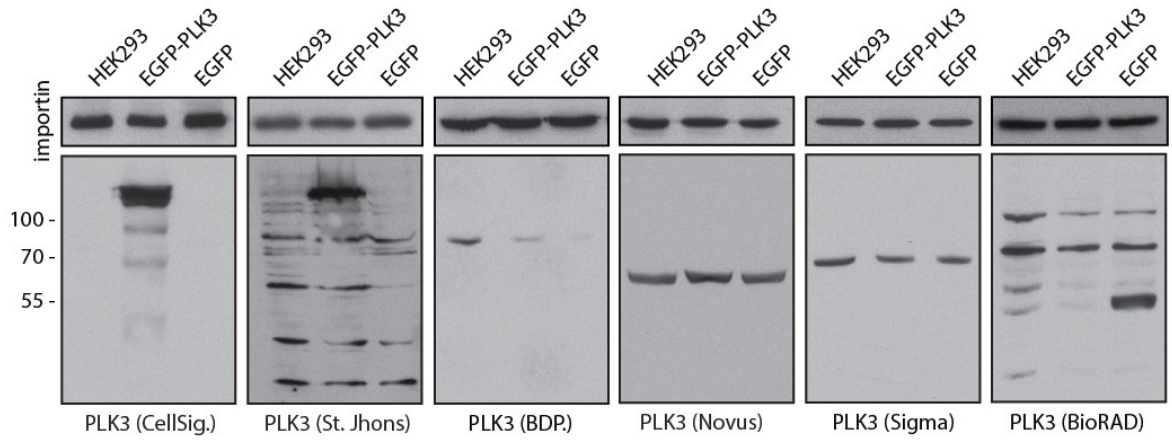

Figure 8. Analysis of commercial antibodies capacity to recognize overexpressed PLK3. Cell lysates from HEK293, HEK293-EGFP-PLK3 and HEK293-EGFP were probed with indicated antibodies by immunoblotting. Note that only PLK3 antibodies from Cell Signaling and St. Johns recognized the ectopic EGFP-PLK3. Antibody from St. Johns presented high cross-reactivity. Numbers indicate mobility in kDa.

Due to the fact that the majority of the commercially available antibodies showed poor performance and that our experimental observations on PLK3 intracellular localization were conflicting with the data previously published, we decided to test PLK3 localization dynamics and response to genotoxic stress (**Figure 9**). PLK3 has been reported to be localizing in discrete nuclear inclusions inside nucleoli under non-stressed conditions and throughout several cell lines (HeLa, MCF10A, RPEm T98G and 293T cells) (Zimmerman and Erikson 2007); because we failed to observed said reported localization, we took in the possibility that shuttling between the cytoplasm and the nucleus by PLK3 under specific conditions might be the case, as it was reported for its murine homolog Fnk (FGF-inducible kinase) (Alberts and Winkles 2004). To test this we submitted the EGFP-PLK3 stable cell line to leptomycin B (LMB) plus proteasome inhibitor MG132 treatment to stop protein export dynamics dependent on CRM1 function. Our results did not show any accumulation of EGFP-PLK3 in the nucleus suggesting that, opposite to the homolog Fnk, human PLK3 is not constantly shuttling between the nuclear and cytosolic compartments. Next, we submitted the EGFP-PLK3 stable cell line to UV light irradiation to test PLK3 response upon DNA damage (**Figure 9-B**). As opposed to what has been previously reported, we did not observe accumulation of EGFP-PLK3 in the nucleus neither in non-stressed conditions nor after exposure of cells to UV light (Zimmerman and Erikson 2007, Wang, Dai et al. 2014).

Fractionation assays performed in RPEs showed that PLK3 localizes principally in the Triton X100 soluble fraction where cytosolic proteins are contained, meanwhile PLK3 was not detected in the chromatin fraction (**Figure 9-C**). This observations correspond with a recently reported function of membrane-associated PLK3 during Fas-L-mediated cell death and with other reports implicating PLK3 in Golgi apparatus integrity (Xie, Wang et al. 2004, Helmke, Raab et al. 2016).

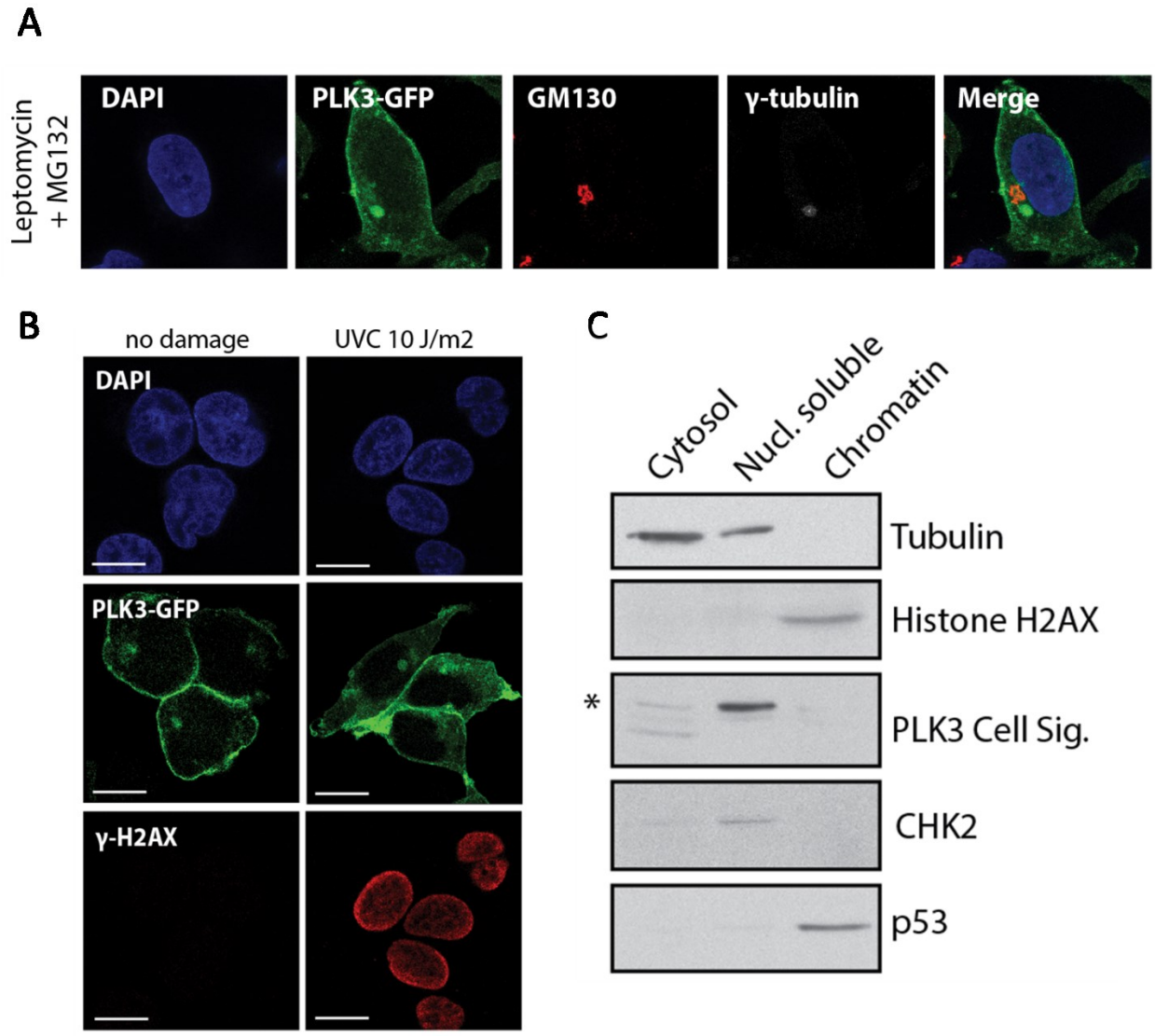

Figure 9. PLK3 localization in response to genotoxic stress. A. HEK293-EGFP-PLK3 Stable cell line was treated with Leptomycin and proteasomal inhibitor MG132 for 3 h. fixed and imaged using confocal microscopy. Bar indicates 5 µm. **B.** HEK293-EGFP-PLK3 Stable cell line was fixed 2 h after exposure to mock or UVC and imaged using confocal microscopy. **C.** Cytosolic, nuclear soluble and chromatin fractions of RPE cells were probed with indicated antibodies. Tubulin was used as a marker for the cytosolic fraction, CHK2 for the nuclear soluble fraction and histone H2AX for chromatin. Asterisk indicates non-specific band of PLK3 antibody.

Next, we wanted to study EGFP-PLK3 distribution and behavior throughout the cell cycle. We observed that PLK3 expression levels were comparable starting from G1 phase to Mitosis (**Figure 10-A**), contrary to what was previously described (Alberts and Winkles 2004). PLK3 localization to the plasma membrane was showed to be constant through all the phases of mitosis and also enriching spindle poles during mitosis (**Figure 10-B**) (Jiang, Wang et al. 2006).

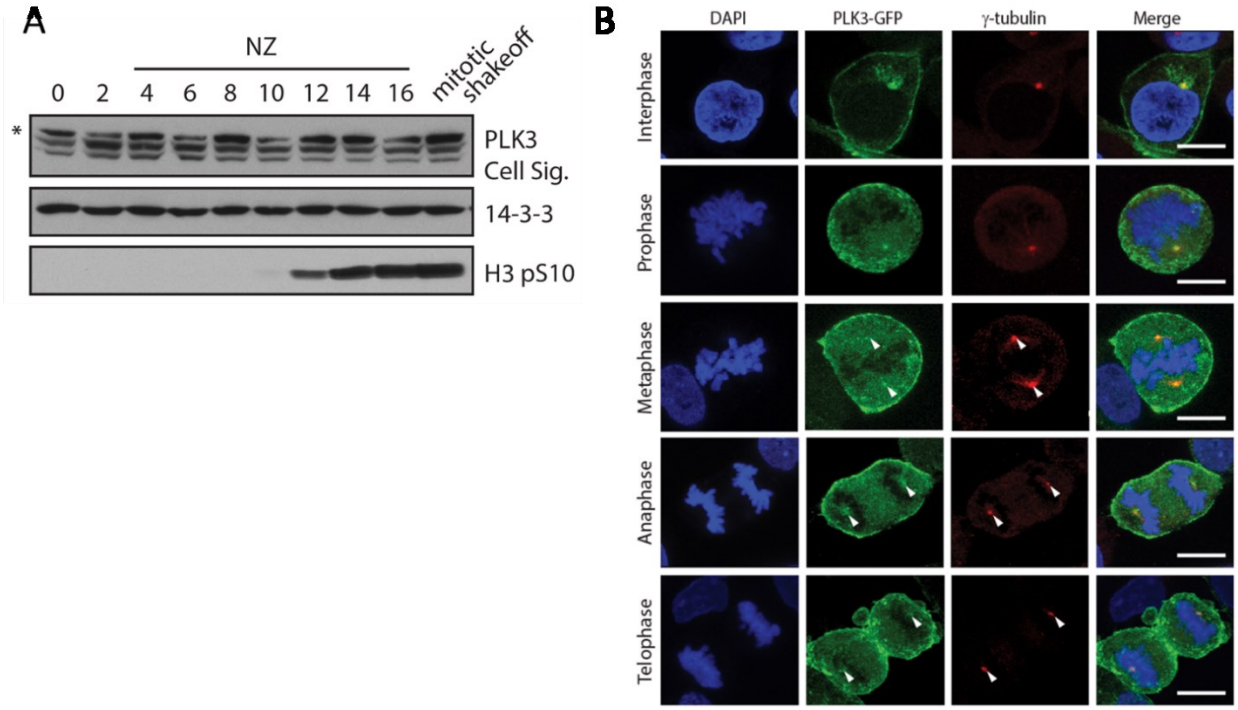

Figure 10. Distribution of EGFP-PLK3 during the cell cycle. A. Stable HEK293-EGFP-PLK3 cells were synchronized at G1/S transition with a thymidine block for 36 hours. After incubation time, cells were washed twice with PBS and released to fresh media. After 4 hours of release, Nocodazole was added to stop cell cycle progression at prometaphase. Cells were collected at 2 hours intervals. Last sample presented in the gel was collected by mitotic shake-off to obtain an exclusive mitotic population. Histone H3-pS10 was used as a marker for mitotic cells. Asterisks indicate the non-specific reactivity bands. **B.** Stable HEK293-EGFP-PLK3 cells were fixed, stained for γ-tubulin and analyzed by confocal microscopy. Shown are maximal projections of representative cells in interphase and throughout mitosis phases. Bar indicate 10 µm.

4.1.2 PLK3 is disposable for cell response to genotoxic stress and osmotic stress

In the light of our previously described observations, we wished to reassess PLK3 relevance over various cellular functions attributed to it. For this purpose we generated a stable Knock-out PLK3 cell line in the human diploid RPE cells using CRISPR/Cas9-mediated gene editing. Through genomic DNA sequencing we confirmed the successful targeting of both alleles in the exon 2 of PLK3 (**Figure 11-A**) and subsequently the absence of PLK3 protein expression by immunoblotting with the functional PLK3 antibody from Cell Signaling and also with the rest of the after mentioned antibodies (**Figure 11-B, C**).

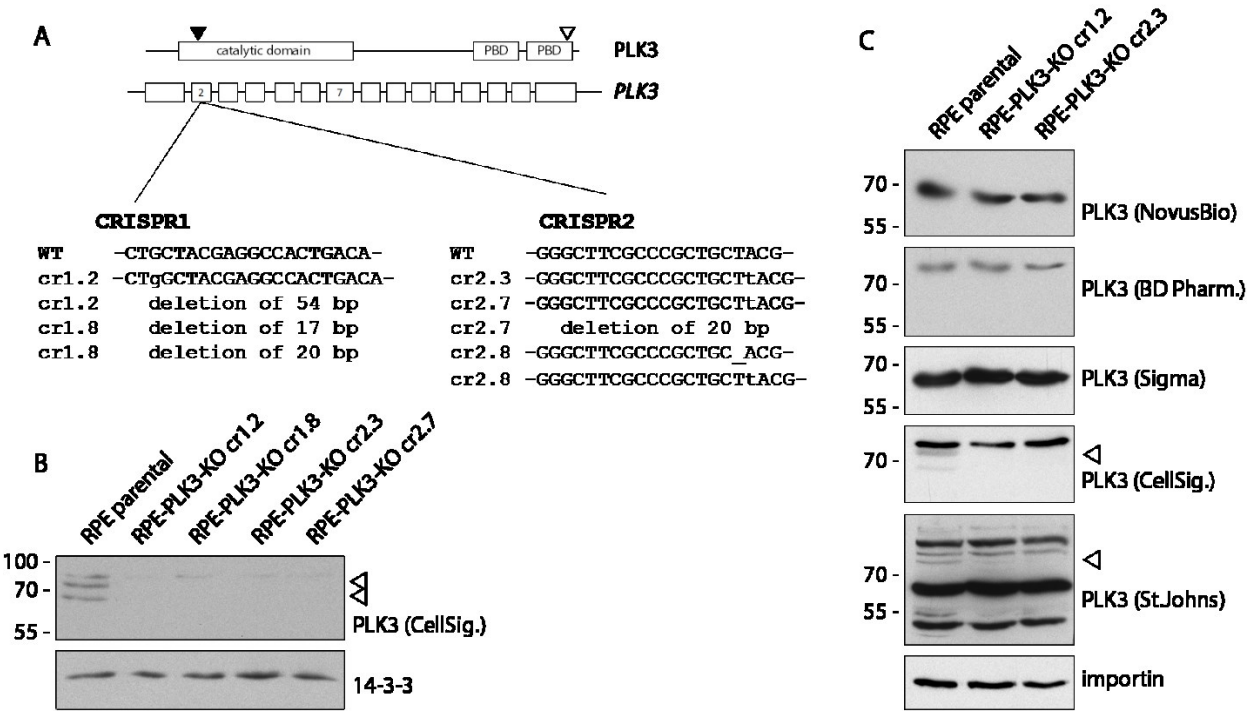

Figure 11. Generation of RPE-PLK3 knock out cell lines. A. Schematic diagram of CRISPR/Cas9-mediated targeting of human PLK3 and of domain organization of PLK3 protein. Black arrowhead indicates the position of the key ATP-binding Lysine 91 in the catalytic C-terminal domain. Empty arrowheads indicates the position of the epitope of the PLK3 antibody from Cell Signaling. Fragments of the genomic DNA from selected clones were PCR amplified and analyzed by sequencing. **B.** Parental RPE and selected clones of RPE-PLK3-KO cells were analyzed by immunoblotting using rabbit monoclonal PLK3 antibody (Cell Signaling). **C.** Parental RPE and two independent clones RP-PLK3-KO cells were probed with indicated antibodies. The position of PLK3 is being indicated by an empty arrowhead. Please pay careful attention to the missing band corresponding to PLK3 in staining with St Johns antibody and the high level of cross reactivity bands.

After confirmation that the RPE-PLK3-KO cells were lacking PLK3 and were functional, we submitted this cells alongside the parental RPE cells to various forms of stress and probed their ability to trigger the respective downstream signaling response. This assays were also implemented in parental RPE cells that had underwent PLK3 depletion through two independent siRNAs; this was done with the intention to collate

the results in the RPE-PLK3-KO cell lines with a temporal PLK3-KD in case of the activation of genetic compensatory mechanisms in our Knock-out model (El-Brolosy and Stainier 2017).

As the first stress response assay, cells were exposed to different intensities of UVC light (10 or 20 J/m^2), incubated for 30 min and analyzed by immunoblotting (**Figure 12**). Exposure of cells to UVC led to the increment of YH2AX as a result of DNA crosslinks generation and activation of NER (Oh, Bustin et al. 2011) and phosphorylation of c-JUN (by JNK) in its pS73 residue to protect cells from UV-induced apoptosis (Wisdom, Johnson et al. 1999). Notably, we did not observe any impairment in the activation of this pathways when comparing visually between parental and KO cell lines (**Figure 12-A**) and neither trough immunoblot intensity quantification (**Figure 12-B**). Concomitantly, PLK3 depletion through siRNA presented the same after mentioned lack of impairment (**Figure 12-C, D**) (Wang, Dai et al. 2007).

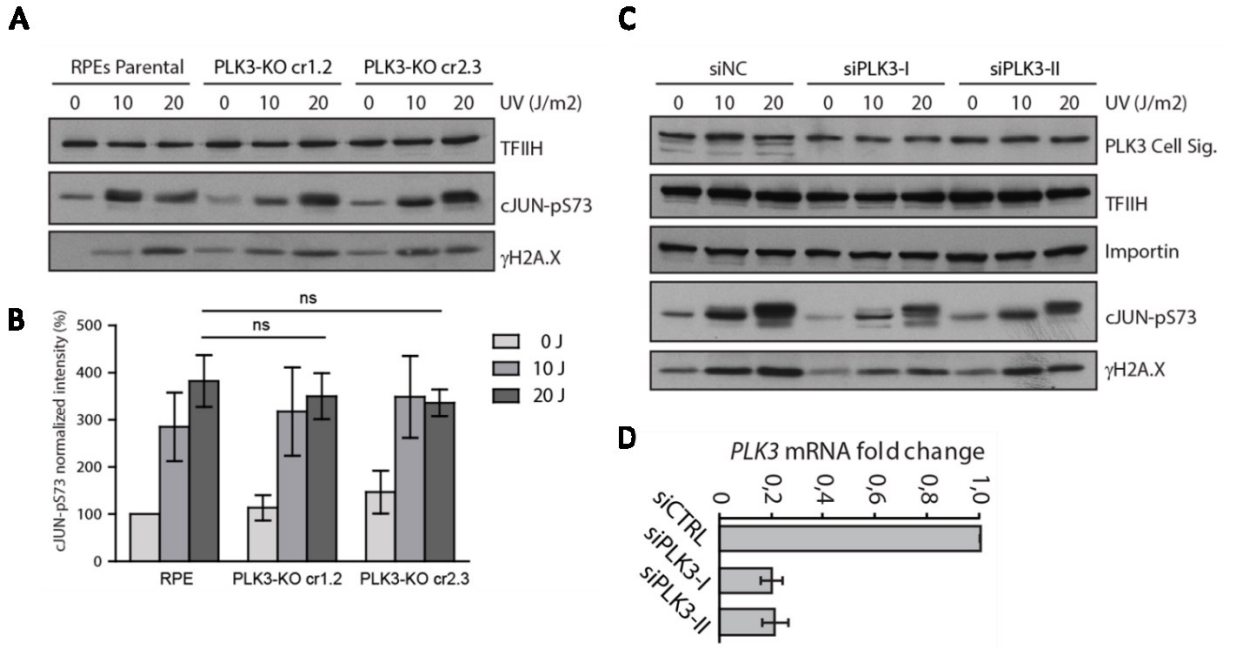

Figure 12. Loss of PLK3 does not affect cell response to DNA damage generated by UV irradiation. A. Parental RPE cells or the RPE-PLK3-KO stable cell lines were exposed to UVC irradiation, collected after 30 min and total cell lysates were harvested (n=3). A representative immunoblot is shown; antibody against cJUN-pS73 was used to measure the DNA damage response dynamics when WT-PLK3 was present or absent in the system. Concomitantly, probing for YH2AX was used as an additional DNA damage marker and TFIIH was used as loading control. **B.** Bar graph shows the immunoblot quantification of the cJUN-pS73 activation after treatment time points. Values were normalized to control (non-irradiated) treatment in the Parental RPE cells. Statistical significance was analyzed by two-tailed Student's T-test. Bars indicate median ±SD. **C.** Parental RPE cells were trasnfected with control or two various PLK3 siRNAs and were treated in the same manner as cell lines shown in panel A; total cell lysates were harvested (n=2) and analyzed by immunoblotting. **D.** Quantification and validation of PLK3 knock down trough siRNA by using RT-qPCR. PLK3 mRNA levels were normalized to ATP5B.

Next, cells were submitted to hypertonic or hypotonic osmotic stress for 40 min and analyzed by immunoblotting (**Figure 13**). Phosphorylation of c-JUN (by JNK) in its pS73 residue alongside p38 in its pT180/pY182 residues was used to detect osmotic stress-induced pathways activation (Sheikh-Hamad and Gustin 2004). Similar to the case of UVC irradiation, we did not observe a decrease in the level of c-JUN activation neither in the PLK3-KO cell lines nor in the PLK3 depleted cells (**Figure 13-A-C**); both experimental observations suggest that, upon DNA Damage insults PLK3 is not involved in c-JUN regulation as it was previously reported (Wang, Dai et al. 2011, Wang, Payton et al. 2011).

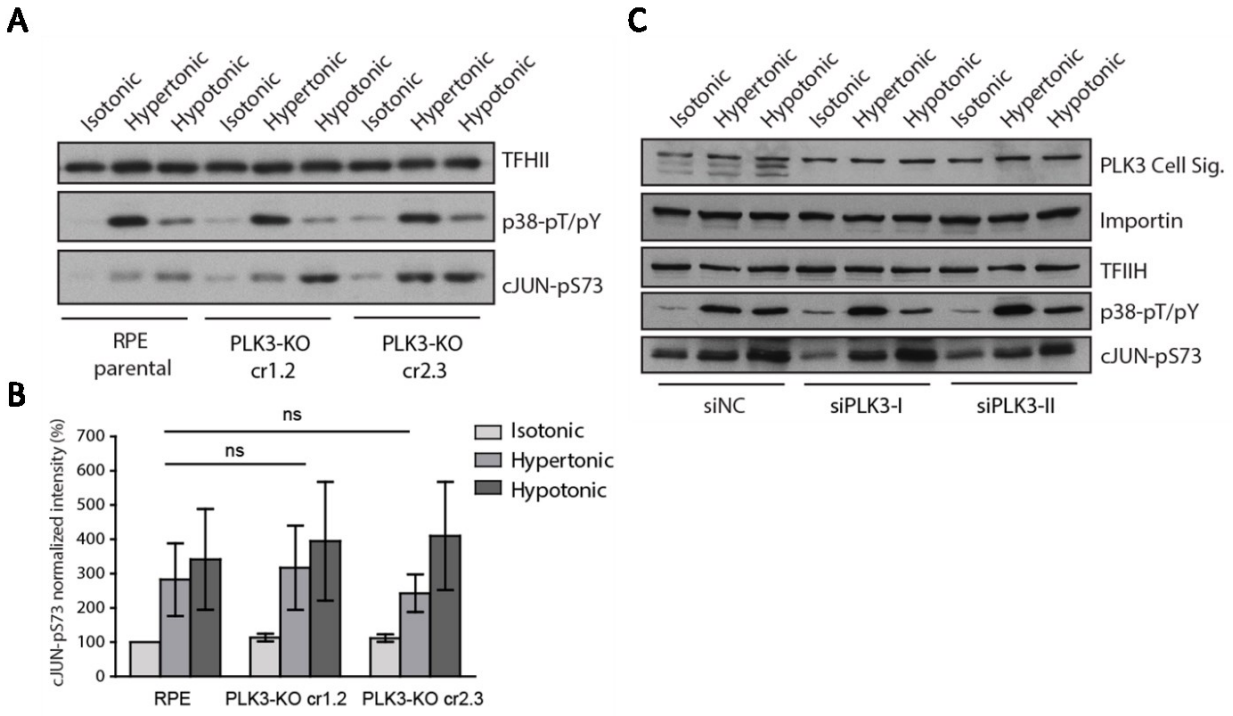

Figure 13. Loss of PLK3 does not affect cell response to Osmotic stress. A. Parental RPE cells or the RPE-PLK3-KO stable cell lines were submitted to either hypotonic or hypertonic shock for 40 min; total cell lysates were harvested (n=3). A representative immunoblot is shown. Antibody against the active form of p38-pT180/pY182 was used to detect the activation of the adaptive osmotic stress response. Concomitantly, cJUN-pS73 probing was used to measure immediate cell stress response and TFIIH was used as loading control. **B.** Bar graph shows the immunoblot quantification of the cJUN-pS73 activation after treatment time points. Values were normalized to control (isotonic) treatment in the Parental RPE cells. Statistical significance was analyzed by two-tailed Student's T-test. Bars indicate median ±SD. **C.** Parental RPE cells were trasnfected with control or two various PLK3 siRNAs and were treated in the same manner as cell lines shown in panel A; total cell lysates were harvested (n=2) and analyzed by immunoblotting.

With the objective of analyzing the role of PLK3 during cellular response to hypoxia cells were treated with cobalt chloride ($CoCl_2$), a hypoxia-mimicking agent in two different concentrations. The assay was implemented in the PLK3-KO cell lines and in the RPE and HeLa parental cell lines after siRNA mediated PLK3 depletion (**Figure 14**). We observed similar HIF-1α induced levels after immunoblot quantification (**Figure 14-B**) and in the parental cell lines, suggesting that PLK3 does not inhibit HIF-1α stabilization in human cells as it was previously reported (Yang, Bai et al. 2008).

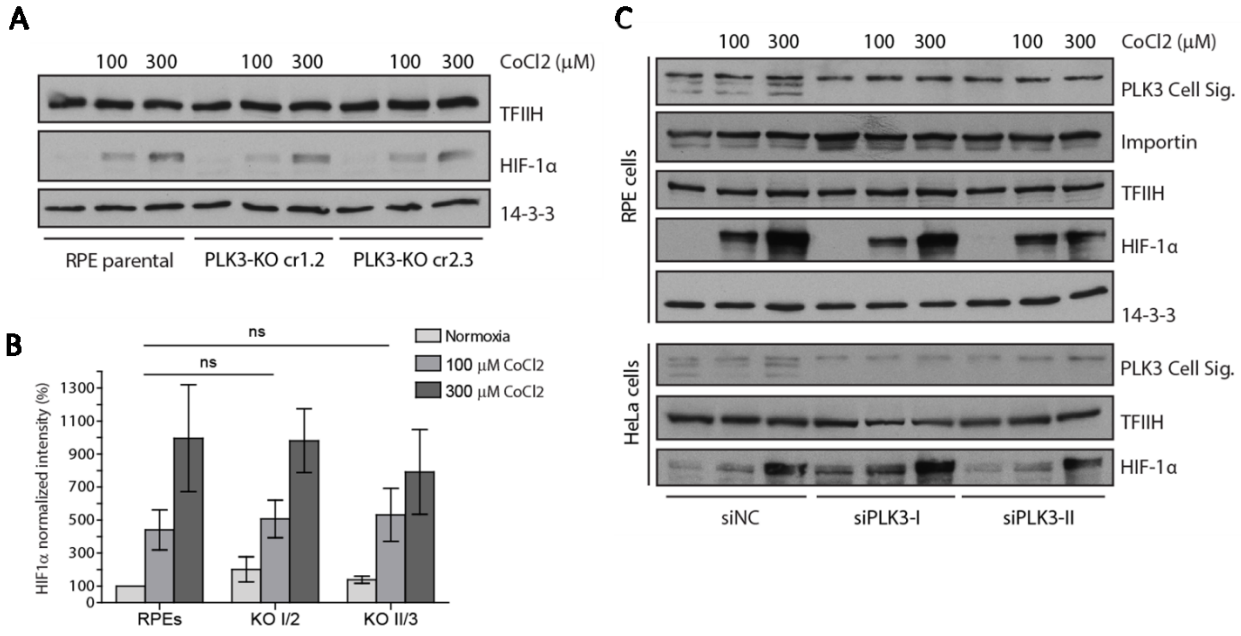

Figure 14. **Loss of PLK3 does not affect cell response to hypoxia. A.** Parental RPE cells or the RPE-PLK3-KO stable cell lines were submitted to hypoxia-mimicking conditions by media supplementation with $CoCl_2$ (100 – 300 μM); cells were collected after 24 hours and total cell lysates were harvested (n=3). A representative immunoblot is shown. Antibody against HIF-1α was used to detect the stabilized protein and thus, the activation of the hypoxia response pathway. TFIIH and Pan14.3.3 probing were used as loading controls. **B.** Bar graph shows the immunoblot quantification of the HIF-1α stabilization after treatment. Values were normalized to control (Normoxia) treatment in the Parental RPE cells. Statistical significance was analyzed by two-tailed Student's T-test. Bars indicate median ±SD. **C.** Parental RPE cells were trasnfected with control or two various PLK3 siRNAs and were treated in the same manner as cell lines shown in panel A; total cell lysates were harvested (n=2) and analyzed by immunoblotting.

Finally, for DNA Damage response evaluation, we performed quantification of YH2AX nuclear foci formation after exposure of the PLK3-KO cell lines to IR (ionizing radiation) (**Figure 15**). As expected after IR exposure, an increase in the number of nuclear foci of the RPE parental cells at the early 1 hour time point was observed, followed by a decrease at the later 8 hours' time point corresponding to DNA damage repair activity (Burdova, Storchova et al. 2019). After 8 hours of irradiation it was possible to detect induction of p21, a well-known p53 target and cell cycle mediator (Marino, Acconcia et al. 2003). Nevertheless, recurrence and disappearance of the YH2AX nuclear foci was not significantly different than in the PLK3-KO cell lines (**Figure 15-A**). Parallel to this, total cell lysates were analyzed by immunoblot to observe the activation of the ATM-CHK2 pathway (**Figure 15-B**). In comparison to RPE parental cells, PLK3-KO cell lines did not present any difference in the levels of phosphorylated CHK2 at the T68 residue, neither for KAP1 at S824 and S473. In the same manner, RPE parental cells that were temporarily depleted of PLK3 were subjected to the same IR treatment, presenting no significant differences in DDR between PLK3 depleted and control RPE cells (**Figure 15-C**).

Together this observations suggest that loss of PLK3 does not affect the ATM-CHK2 activation pathway (Ziv, Bielopolski et al. 2006, Kleiblova, Stolarova et al. 2019). In consonance with the results obtained in the PLK3-KO cells, RPE parental cells that were submitted to the same ionizing radiation treatment but after PLK3 depletion trough siRNA showed no impairment in the DNA damage response activation (**Figure 15-C**). Based on this observations, we concluded that, even in the absence of PLK3 cells are able to activate ATM, arrest in the cell cycle checkpoint and repair DNA with comparable dynamics as cells with full functional PLK3 expression.

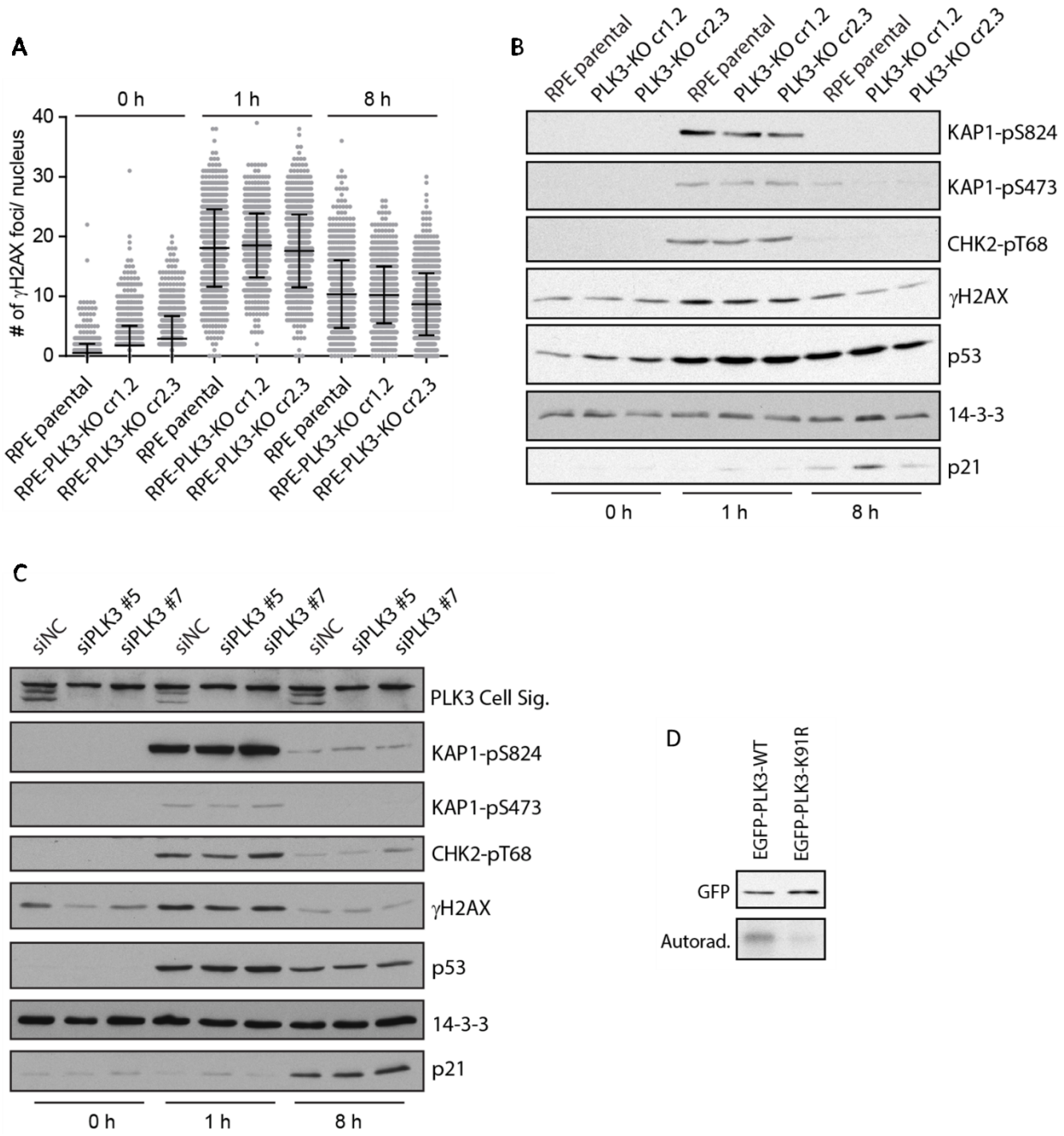

Figure 15. Loss of PLK3 does not affect stress cell response to ionizing radiation. A. Parental RPE or RPE-PLK3-KO cells were exposed to 3 Gy of ionizing radiation and fixed after 1 and 8 hours' time points. Number of YH2AX positive foci per nucleus were quantified trough ScanR microscopy (n=3). Statistical significance was analyzed by two-tailed Student's T-test. Bars indicate median ±SD. **B.** Parental RPE pr RPE-PLK3-KO cells were treated as in A and whole cell lysates were analyzed by immunoblotting (n=2). **C.** Praental RPE cells were transfected with control or two various PLK3 siRNAs and were treated as in A and whole cell lysates were aalyzed by immunoblotting (n=2). **D.** Parental RPE cells were transfected with the wild-type PLK3 or kinase-dead K91R mutant; PLK3 was isolated by GFP trap and incubated with casein in kinase buffer supplemented with radioactive ATP. Phsophorylation of casein was detecetd by autoradiography.

As opposed to PLK1, a sensitive kinase that is immediately deactivated upon genotoxic stress, PLK3 has been reported to be robustly activated upon various forms of stress (van Vugt, Smits et al. 2001, Bahassi el, Conn et al. 2002).To test this premises, we performed an *in vitro* kinase assay employing casein as a target substrate and EGFP-PLK3 purified from cells previously exposed to various forms of stress (**Figure 16**). At first instance we tested the ability of the purified EGFP-PLK3 and observed that the wild-type but not the kinase-dead PLK3-K91R mutant managed to efficiently phosphorylate casein *in vitro* (**Figure 15-D**). We employed the same process of purification for EGFP-PLK3 after submitting the cells to a variety of cellular stressors. The resulting purified EGFP-PLK3 was then tested for degree of activation (**Figure 16-A**). Upon immunoblotting signal quantification, it was very interesting to see that there was no significant change in PLK3 activity upon exposure of cells to UVC, treatment with etoposide, $CoCl_2$ or exposure mannitol as an osmotic stress agent (**Figure 16-B**). Taken together, this results compile good evidence to support our premise that enzymatic activity of PLK3 is not responding nor activated upon different types of stress and it confirms our finding that PLK3 is disposable for genotoxic and osmotic stress cellular response.

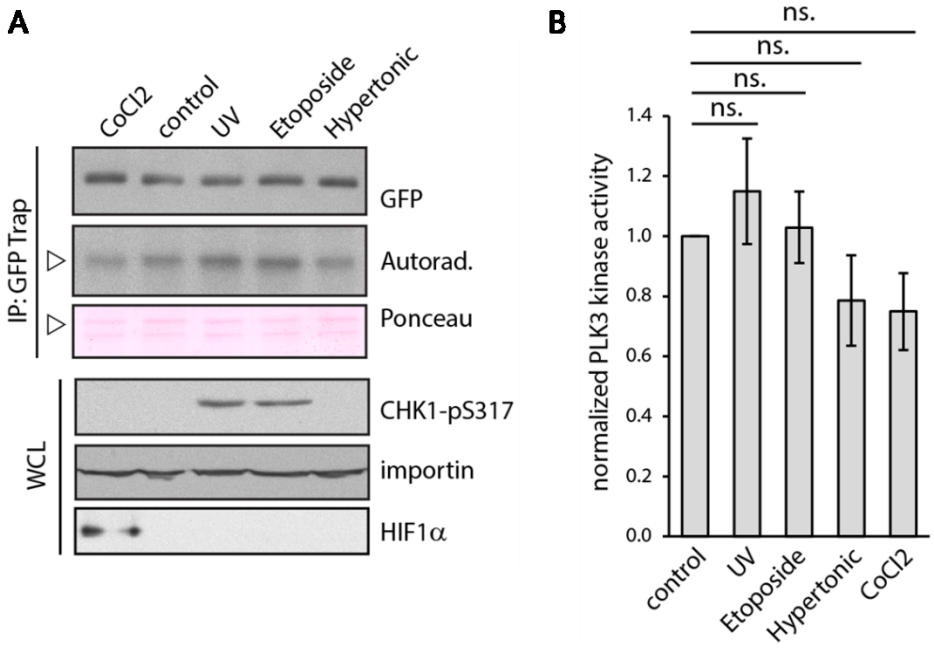

Figure 16. Assessment of PLK3 kinase activity upon treatment with various types of stress. A. Cells were exposed to various forms of stress including treatment with CoCl2 (200 μM, 12 h), exposure to UV (10 J/m2), etoposide (4 μM, 1 h), hypertonic media (480 μM mannitol) or left untreated as control. EGFP-PLK3 was isolated using GFP trap and kinase assay was performed as in Figure 11D. Induction of stress pathways was analyzed by immunoblotting of cell extracts, probing for HIF-1α and CHK1-pS317. Empty arrowheads indicate identical position on the electrophoretic gel. **B.** Quantification of the kinase assay performed in (A) Signal was normalized to the non-treated control (n=3). Statistical significance was analyzed by two-tailed Student's T-test. Bars indicate median ±SD.

4.1.3 PLK3 interacts with PP6 Phosphatase through the PBD domain

The next step was searching for PLK3 functional modulators through protein-protein interactions; for this purpose we immunoprecipitated EGFP-PLK3 from the stable cell line generated in HEK293 and identified co-immunoprecipitated proteins through mass spectrometry. Those protein hits that were enriched in complex with EGFP-PLK3 in comparison to the EGFP control for at least two out of three independent experiments were considered as potential interactors (**Table 1**). Amid other proteins, four components of a serine/threonine-protein phosphatase 6 were identified highly enriched in complex with EGFP-PLK3. These included the regulatory subunits PPP6R1, PP6R3 and ANKRD28 plus the catalytic subunit PPP6C.

Table 1. Mass spectrometry analysis of purified EGFP-PLK3. Soluble fraction of total cell extracts from the HEK293-EGFP-PLK3 and HEK293-EGFP stable cell lines were incubated with GFP-trap beads, washed three times and submitted to mass Spectrometry analysis for bound proteins identification. Three biological replicates were performed. Numbers in the first column indicate the average log difference between EGFP-PLK3 and EGFP samples.

Avg. log difference	Gene	Protein name
13.32	PLK3	Serine/threonine-protein kinase PLK3
8.77	VPRBP	Protein VPRBP (DDB1 – and CUL4-associated factor 1)
8.11	ANXA6	Annexin A6
6.97	ANKRD28	Serine/threonine-protein phosphatase 6 regulatory Ankyrin repeat subunit A
6.90	RPL34	60S ribosomal protein L34
6.40	PPP6R1	Serine/threonine-protein phosphatase 6 regulatory subunit 1
6.39	MOV10	Putative helicase MOV-10
6.39	VDAC3	Voltage-dependent anion-selective channel protein 3
6.36	HNRNPDL	Heterogeneous nuclear ribonucleoprotein D-like
6.25	ACTG1	Actin, cytoplasmic 2
6.10	EBNA1BP2	Probable rRNA-processing protein EBP2
6.01	BRIX1	Ribosome biogenesis protein BRX1 homolog
5.87	STAU1	Double-stranded RNA-binding protein Staufen homolog 1
5.76	MVB12B	Multivesicular body subunit 12B
5.68	MARCKSL1	MARCKS-related protein (MARCKS-like protein 1)
5.66	RPL37A	60S ribosomal protein L37a
5.65	TMED2	Transmembrane emp24 domain-containing protein 2
5.62	ANK3	Ankyrin-3
5.60	NDUFA13	NADH dehydrogenase 1 alpha subcomplex subunit 3
5.55	PPP6R3	Serine/threonine-protein phosphatase 6 regulatory subunit 3
…		
4.36	PPP6C	Serine/threonine-protein phosphatase 6 catalytic subunit

Following this interesting result, we performed immunoprecipitation using the EGFP and EGFP-PLK3 stable cell lines in order to confirm the interaction with the after mentioned complex *in vivo* (**Figure 17**). Our results confirmed that PLK3 interaction with the endogenous PPP6C as well with its regulatory subunits PPP6R1 and PPP6R3 was specific, since interaction with PPP6R2 deemed to be null (**Figure 17-A**). After confirming that PLK3 exists in complex with PP6 and its regulatory subunits, we opted to map said interaction. Through a series of immunoprecipitation assays we managed to pin point that interaction with the PP6 complex was mediated through the PBD domain since the EGFP-PLK3-ΔPBD mutant (lacking the PBD domain) failed to pull down the PP6 complex (**Figure 17**). In a similar manner, the EGFP-PLK3-H590A-K592M mutant, predicted to be the site of interaction inside the PBD domain also impaired the interaction with PP6 and its subunits, marking the PBD domain as necessary for interaction with the PP6 holoenzyme (**Figure 17-B**) (Elia, Rellos et al. 2003). Interestingly, PP6 subunits were recently identified in a complex with PLK1, marking the possibility that interaction with PP6 might be conserved among the polo-like kinase family (Kettenbach, Schlosser et al. 2018).

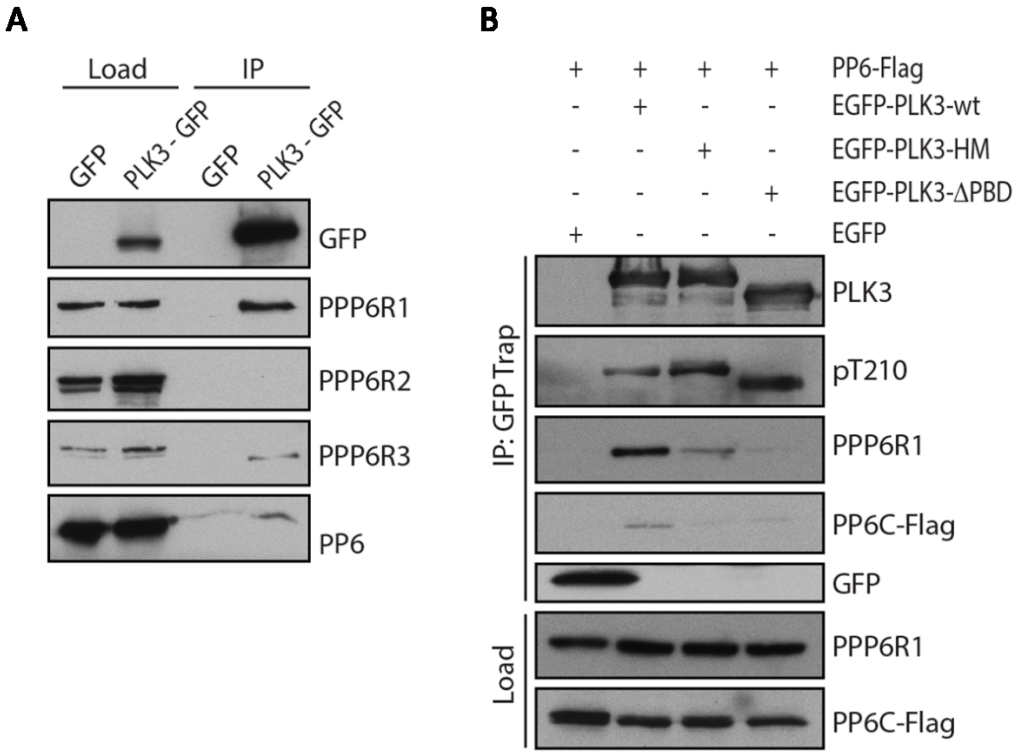

Figure 17. Mass spectrometry results verification trough EGFP-PLK3 immunoprecipitation. **A.** EGFP or EGFP-PLK3 was immunoprecipitated using GFP-trap beads from cell extracts obtained from the asynchronic growing stable cell lines, Bound proteins were analyzed by immunoblotting (n=3). Representative blot is shown. **B.** Cell extracts obtained from HEK293 cells transiently transfected with EGFP-PLK3, EGFP-PLK3-ΔPBD or EGFP-PLK3-H590A-K592M (referred to as PLK3-HM) were incubated with GFP-Trap beads and bound proteins were analyzed by immunoblotting.

Subsequent to this observations we wished to study the subcellular distribution of PLK3 and its possible colocalization with the PP6 complex. For this purpose we performed siRNA mediated depletion of PP6, PPP6R1 and PPP6R3 and analyzed the KD efficiency and the intracellular localization (**Figure 18**). Trough immunofluorescence assays and confocal imaging we observed colocalization between EGFP-PLK3 and endogenous PP6C at the centrosome (**Figure 18-A**). Antibody against PPP6R3 showed a strong nuclear staining and a partial colocalization with γ-tubulin and EGFP-PLK3 at the centrosome. Knock-down assays also helped us validate the specificity of the antibodies employed (**Figure 18-B**).

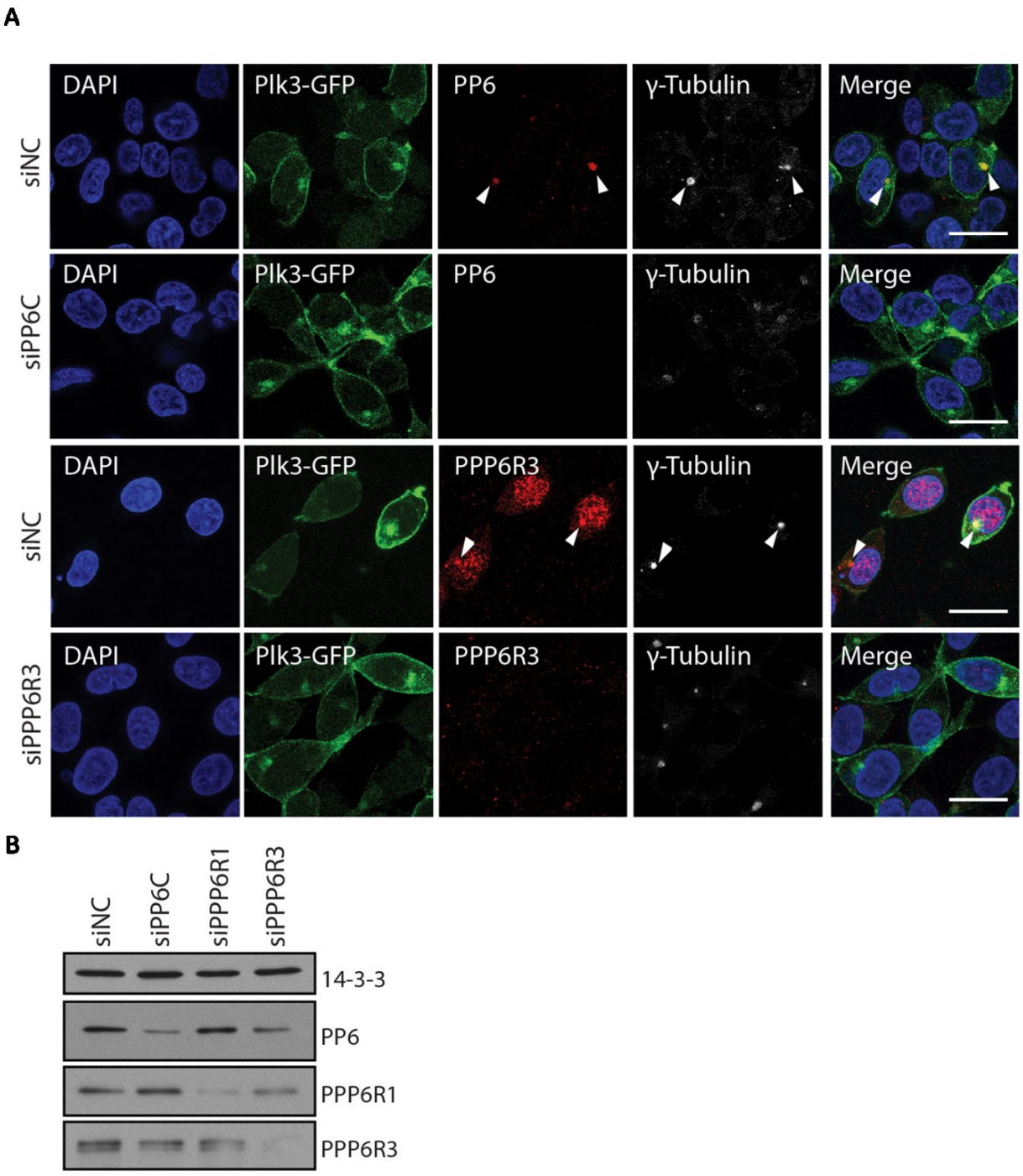

Figure 18. Intracellular localization of PLK3 and confirmed interactors. A. The EGFP-PLK3 stable cell line was transfected with control siRNA, siRNA against PP6C (upper panel) and siRNA against PPP6R3 (bottom panel). 48 hours after transfection, cells were fixed, probed for PP6C and PPP6R3 respectively and γ-Tubulin in both instances. Imaging was performed using confocal microscopy. Arrowheads indicate the position of the centrosome. Bar indicates 20 μm. **B.** Representative WB of the knock-down efficiency validation from panels in (A).

4.1.4 PLK3 is phosphorylated in the T-Loop but this does not affect its kinase activity

PLK1 has been shown to be activated by phosphorylation of the T210 residue in its T-loop by Aurora-A kinase during the G2/M and throughout mitosis (Chan, Santamaria et al. 2008, Macurek, Lindqvist et al. 2008). Because the T-loops of PLK1 and PLK3 present a high percentage of homology, we fathomed the possibility of PLK3 being modified trough phosphorylation in the same manner, since PLK3 presents a similar phosphorylatable motif (T219) (**Figure 19-A**). Through immunoprecipitation of EGFP-PLK3-WT and EGFP-PLK3-T219A mutant and by probing with an antibody directed against PLK1-pT210 we confirmed that PLK1-pT210 antibody is able to specifically recognize phosphorylated PLK3-pT219 (**Figure 19-B**). To understand further the nature of this phosphorylation we treated the stable EGFP-PLK3 cell line to a broad spectrum phosphatase inhibitor known as calyculin and immunoprecipitated EGFP-PLK3 to enrich the protein for PLK1-pT210 probing trough immunoblotting (**Figure 19-C**). While we observed that untreated cells presented a mild PLK3 phosphorylation, those treated with calyculin showed a massive increase in the level of PLK3 phosphorylation at T219, which leads us to consider that phosphorylation of this site is being constantly removed by an opposing phosphatase (Swingle, Ni et al. 2007). As we have shown with our previous described data, we considered PP6 to be a promising candidate for this ordeal. To test this, we performed co-transfections in the EGFP-PLK3 stable cell line using a plasmid expressing PP6C and PPP6R1 both tagged with FLAG and immunoprecipitated EGFP-PLK3. We observed that, effectively, PP6 counteracted PLK3 phosphorylation in its T219 residue and that said dephosphorylation was enhanced when both PLK3 and PP6 where in complex with the regulatory subunit PPP6R3 (**Figure 19-D**). This result is in concordance with the observation that EGFP-PLK3-ΔPBD showed higher levels of phosphorylation in the T-loop compared to the wild type PLK3 (**Figure 17-B**).

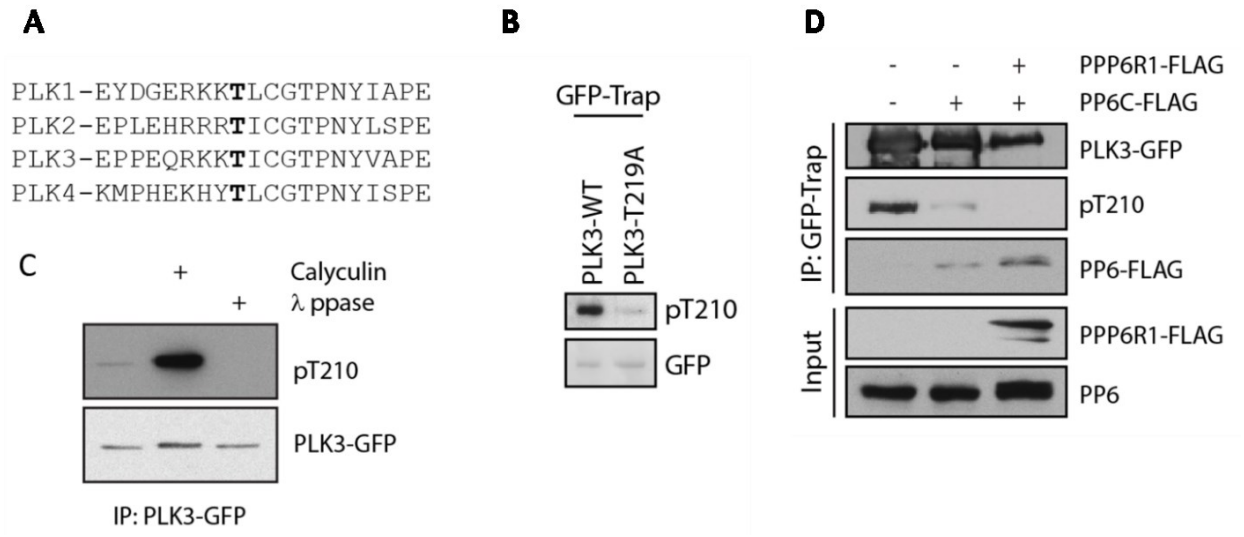

Figure 19. PLK3's T-Loop is targeted for phosphorylation in the same manner as PLK1. A. Analysis of the T-Loop sequence in four members of the Polo-like family. The T-Loop sequences appear to be highly conserved; Threonine residues corresponding to the T210 in PLK1 and to T219 in PLK3 are shown in bold. **B.** EGFP-PLK3-WT and EGFP-PLK3-T219A were immunoprecipitated from transiently transfected cells using GFP-Trap beads. Immunoblots were probed using a specific antibody against pT210-PLK1 and against GFP. **C.** EGFP-PLK3 was isolated from transiently transfected HEK293 cells that were previously treated with mock or calyculin using GFP-Trap beads. Isolated EGFP-PLK3 was incubated in presence of lambda phosphatase for 20 min. All samples were probed with pT210-PLK1 antibody. **D.** EGFP-PLK3 stable cell line was transfected with PP6C and/or PP6R1, cell lysates were obtained and EGFP-PLK3 was immunoprecipitated using GFP-Trap beads. Level of PLK3 phosphorylation was evaluated by immunoblotting with the pT210-PLK1 specific antibody.

Interestingly, we noted that siRNA mediated depletion of endogenous PP6 increased the T219 phosphorylation signal, indicating that PP6 phosphatase controls PLK3 phosphorylation levels in cells (**Figure 20-A**). By employing an *in vitro* kinase assay, we tested the contribution of the pT219 modification in the T-loop over PLK3 activation. We found that EGFP-PLK3-WT was able to efficiently phosphorylate casein, opposite to the kinase-dead mutant EGFP-PLK3-K91R, however the activation of the EGFP-PLK3PT219 and the phosphorylation mimicking mutant EGFP-PLK3-T219D were the same as for the activity of the wild-type PLK3 (**Figure 20-C**). Concomitantly, we noted that neither depletion of PP6 nor treatment of cells with calyculin affected the activity of PLK3 (**Figure 20-A**). Finally, we performed co-immunoprecipitation of EGFP-PLK3 with PP6C-FLAG and its regulatory subunit PPP6R1-FLAG and used them to perform an *in vitro* kinase assay (**Figure 20-D**). Results showed that EGFP-PLK3 co-precipitation in complex with the PP6 holoenzyme did not affect the kinase activity of PLK3. Based on this data, we conclude that PLK3 activation does not require phosphorylation of the T-loop at the T219 residue and that PP6 phosphatase does not control the PLK3 activity levels in cells.

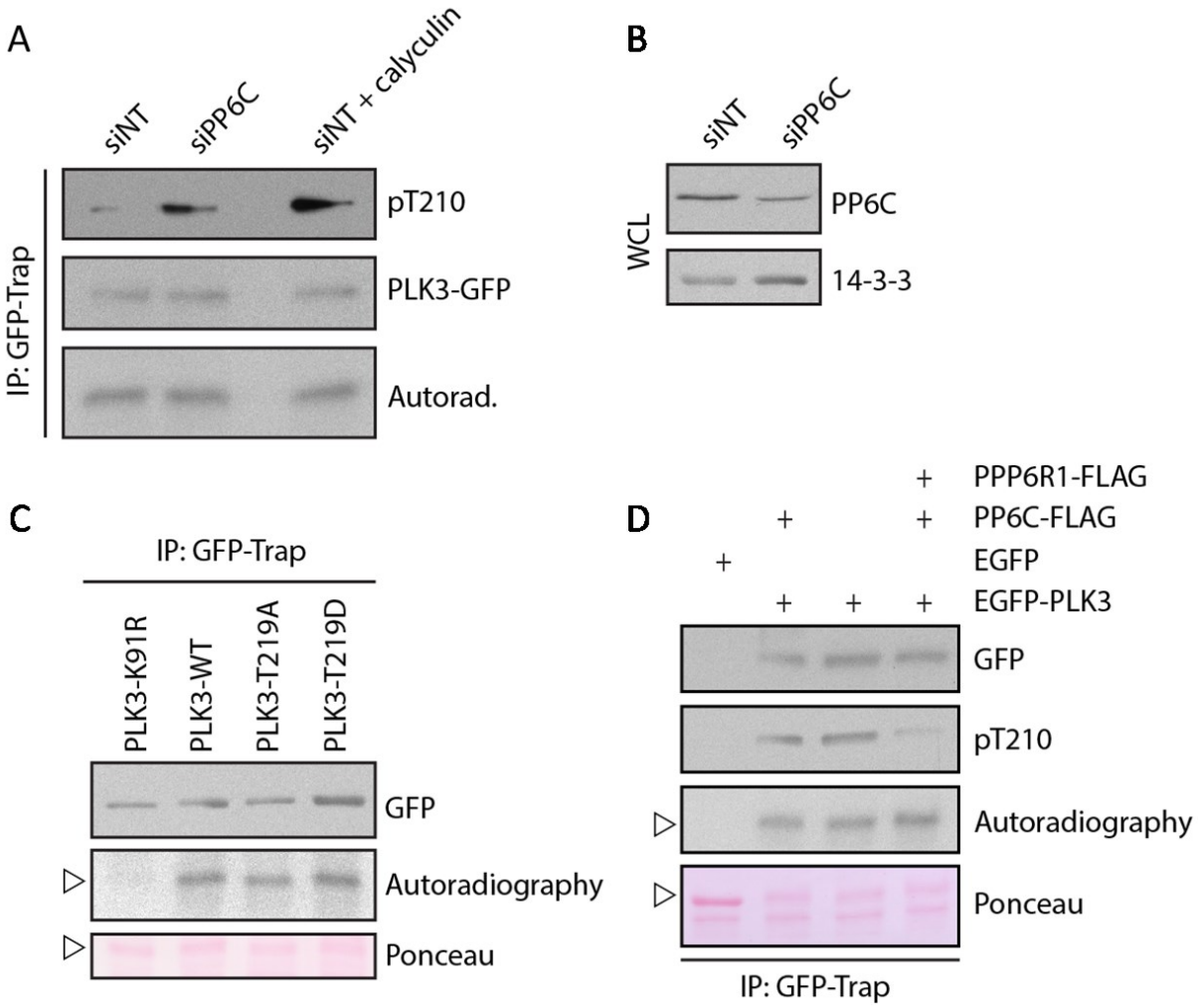

Figure 20. PP6 dephosphorylates PLK3. A. EGFP-PLK3 Stable cell line was transfected with control siRNA or siRNA against PP6. After 48 hours, cells were treated with calyculin for 20 min right before total cell lysate extraction. EGFP-PLK3 was immunoprecipitated using GFP-Trap beads. PLK3's phosphorylation level was evaluated by immunoblotting using the pT210-PLK1 specific antibody. PLK3's kinase activity was measured by incubating the isolated EGFP-PLK3 with casein and ^{32}P-γ-ATP for 20 min at 30 °C. Phosphorylation levels after the assay were detected by autoradiography; EGFP-PLK3 presence was determined by probing with GFP antibody. **B.** Representative Immunoblot of PP6 knock-down efficacy. **C.** Kinase assay was performed as in A (n=2). PLK3's kinase activity was measured by incubating the isolated EGFP-PLK3 with casein and ^{32}P-γ-ATP for 20 min at 30 °C. Phosphorylation levels after the assay were detected by autoradiography; EGFP-PLK3 presence was determined by probing with GFP antibody. Arrowheads indicate casein's position on the electrophoretic gel. **D.** HEK293 cells were co-transfected with EGFP as control and EGFP-PLK3 plus PP6C-FLAG and/or PPP6R1-FLAG constructs. Kinase assay was performed as in A. PLK3 phosphorylation levels were evaluated by probing with the pT210-PLK1 specific antibody and phosphorylation of the casein by autoradiography (n=2). Arrowheads indicate casein's position on the electrophoretic gel.

4.2 Aim 2

4.2.1 Screen for G2/M expressed genes in human non-transformed RPE-FUCCI cells

The premise of this project consisted in identifying novel or poorly described genes that are involved in cell cycle control and regulation by comparing gene expression trough out the different cell cycle phases using non-transformed human cells, having a particular interest on the G2/M transition. Inhibitor-reliant synchronization techniques have been the to-go strategy implemented to study periodically expressed genes in individual phases of the cell cycle, both in normal and cancer human cell lines (Chaudhry, Chodosh et al. 2002). Unfortunately, chemical cell cycle synchronization is not optimal for this purpose/ since it generates a substantial level of cellular stress having a significant impact over what would be considered canonical gene expression, meaning under no external stimuli or stress influence (Cooper and Shedden 2003, Grant, Brooks et al. 2013). In order to avoid generating alterations in the overall normal gene expression fluctuations during each phase of the cell cycle we generated a human hTERT-immortalized RPE cells that stably expressed the fluorescent ubiquitination-based cell-cycle indicator (FUCCI) (Sakaue-Sawano, Kurokawa et al. 2008, Sakaue-Sawano, Yo et al. 2017). This RPE-FUCCI cell line permitted us to identify the G1 (RFP positive), G2/M (GFP positive) and S (double positive) populations in asynchronic cultured cells (**Figure 21-A**). Next, asynchronic RPE-FUCCI cells populations were separated by FACS-sorting in the G1 (RFP+) and G2 (GFP+) populations (**Figure 21-B**).

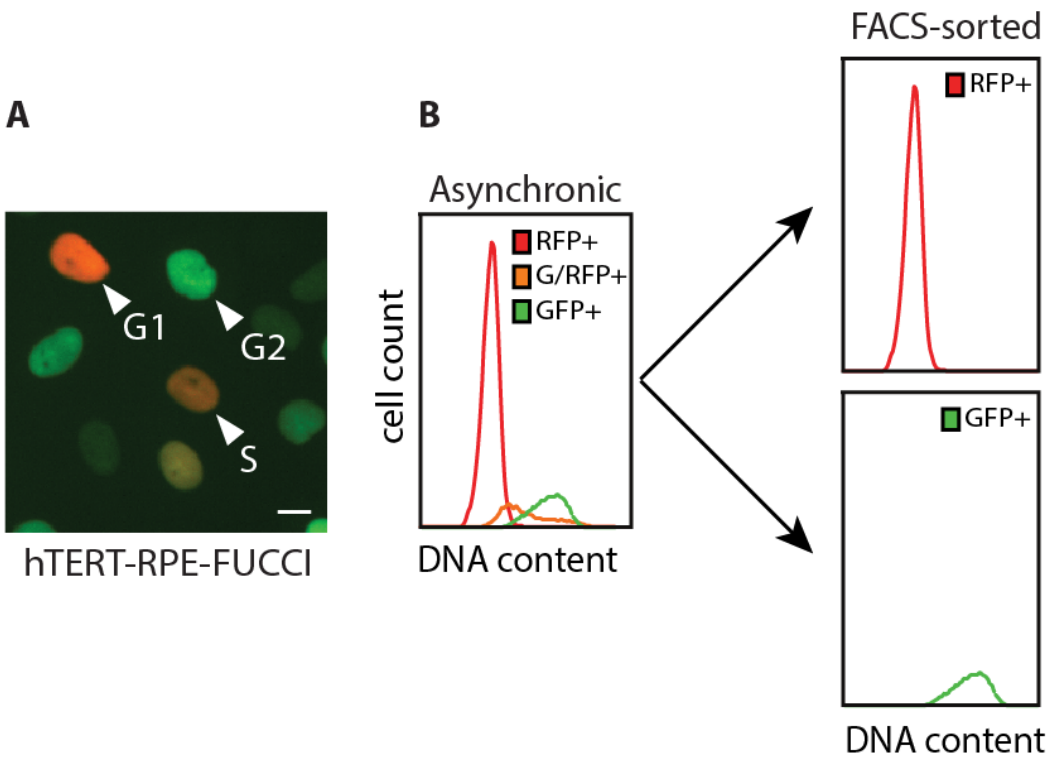

Figure 21. Screen for cell cycle regulated genes using RPE-FUCCI cells. A. Representative image of asynchronic FUCCI cells imaged by immunofluorescence microscopy; arrows and legends pin point the specific color for each cell cycle phase. Scale bar indicates 10 μm. **B.** Schematic of flow cytometry sorting of RFP+ and GFP+ cells from asynchronously growing RPE-FUCCI cells. DAPI was used to probe for DNA content.

This sorted populations were used to perform gene expression profiling by Expression BeadChip (Illumina) to measure the activity (expression levels) of hundreds of genes depending the cell cycle phase; fold change expression was focused on hits enriched in G2 phase (**Figure 22**). Enrichment of CCNE1 (Cyclin E) mRNA in the G1 (RFP+) and asynchronic populations contrasted with CCNA2 (Cyclin A) mRNA and CCNB1 (Cyclin B1) mRNA along with Fos transcription factors (FOS) mRNA levels in G2 cells confirmed the efficacy of the sorting procedure (Pines and Hunter 1989, Pagano, Pepperkok et al. 1992, Baldin, Lukas et al. 1993, Ohtsubo, Theodoras et al. 1995, Hyun, Becam et al. 2006).

The G2 sorted population showed high enrichment of canonical mitotic operators involved in mitotic entry, organization of the mitotic spindle and sister chromatids segregation such as: Mitotic kinases Mps1 (MPS1/TTK), PLK1 (PLK1), Aurora A (AURKA) and CENP proteins (INCENP); Kinetochore proteins like kinetochore complex component Ndc80 (NDC80) and Kinetochore protein Nuf2 (NUF2); Centromeric histone associated proteins like the CENPs CENPA, CENPF, INCENP); MTs motor proteins from the Kinesin proteins superfamily (KIF2C, KIF14, KIF18A) and components of the APC/C like the Ubiquitin conjugation enzyme E2 C (UBE2C) (Lindqvist, Rodriguez-Bravo et al. 2009, Hara and Fukagawa 2018, Srivastava, Zasadzinska et al. 2018). Along with the after mentioned canonical gene expression profiles, 701 significantly upregulated transcripts were identified as differentially expressed between G2 and G1 populations ($q < 0.05$, fold change >2) (**Figure 22**). A group of this transcripts was selected for further analysis. Among the identified upregulated genes we found ubiquitin modifying enzymes (NEURL1b, TRAIP, DCAF15), DNA or histone associated proteins (PIF1, BRD8, RAD51AP) and genes with unknown function (FAM72D, FAM110A, LAS2, GAS2L3).

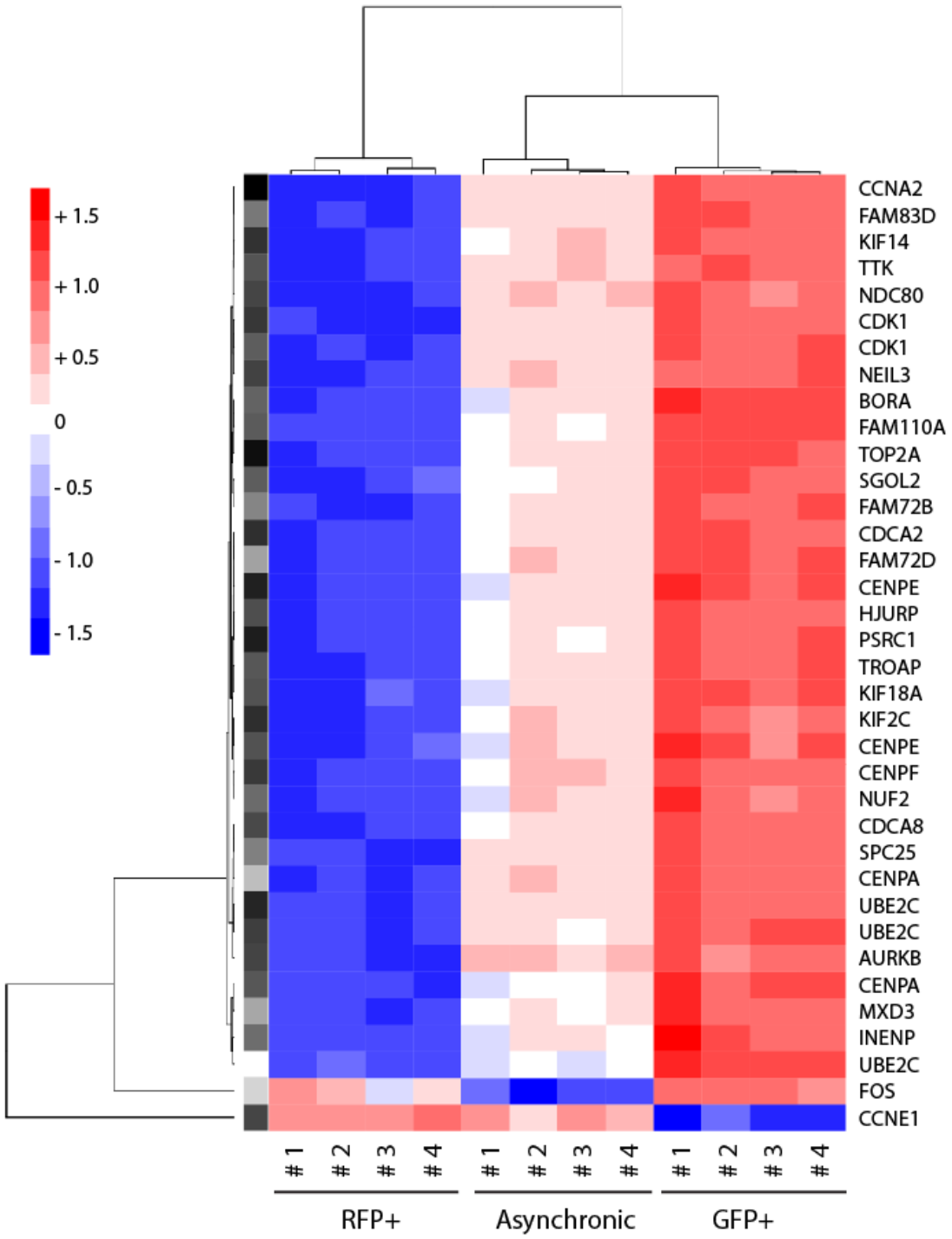

Figure 22. Heat map of gene expression profiling score map obtained by Expression BeadChip (Illumina). RNA was isolated from asynchronic RPE-FUCCI cells, RFP+ (G1 phase) and GFP+ (G2 phase) cells and analyzed using Illumina HumanHT-12 v4 Expression BeadChip (n=4). Shown are 36 transcripts with fold change expression > 8 between G2 and G1 cells q>0.05. Color scale of the row Z score is shown on the left.

In order to confirm the differential expression pattern of selected transcripts, GFP positive, RFP positive and double positive populations were used to extract total mRNA for quantitative real-time PCR analysis (**Figure 23**). This assay confirmed the expected expression pattern of the after mentioned known genes involved in the cell cycle control. In accordance with the expression profiling result, we found significant enrichment of Cyclin E in G1 and S phase followed by a sharp decline in G2 (Ohtsubo, Theodoras et al. 1995); on the contrary Cyclin A2 mRNA levels were low during G1 increasing gradually trough S phase and peaking during G2/M transition (Pagano, Pepperkok et al. 1992).

One of the selected transcripts for quantification was DNA helicase PIF1, which presented a clear upregulation during G2 as it has been shown that it participates in DNA replication termination and that it associates to telomeres in a cell cycle-specific manner (Budd, Reis et al. 2006). The Neuralized member NEURL1b (also known as NEUR2), an E3 ubiquitin ligase that targets the PDE9A phosphodiesterase, an important secondary messenger in several physiological and pathological processes (Taal, Tuvikene et al. 2019) and CKAP2 (Cytoskeleton-associated protein 2) that is found associated to MTs during late G2 and that is targeted by the APC/C^{Cdh1} during mitotic exit (Seki and Fang 2007), presented a similar expression pattern as PIF1. Family 110 member A presented a similar expression trend as Cyclin A2; low levels during G1 that seemed to double during S phase and increase 3 times in the G2/M transition according to the previously reported cell cycle-dependent expression pattern (Hauge, Patzke et al. 2007).

FAM72D was recently reported as part of the FOXM1 transcription factor network, participating in cell proliferation control and survival (Chatonnet, Pignarre et al. 2020). FAM72D presented a similar expression pattern as FAM110A, although its upregulation was 10 times higher in G2 than in G1. CDCA2 (Cell division cycle associated 2 also known as PPP1 regulatory subunit 81) is a subunit responsible for targeting PP1 to chromatin during anaphase (Liu, Vleugel et al. 2010) was also one of the observed hits, alongside G2E3, an E3 ubiquitin ligase considered essential during embryogenesis and the DNA damage response (Brooks, Banerjee et al. 2007, Brooks, Helton et al. 2008). This hits behaved in a similar manner, showing gradual increase in expression trough S phase towards G2 phase.

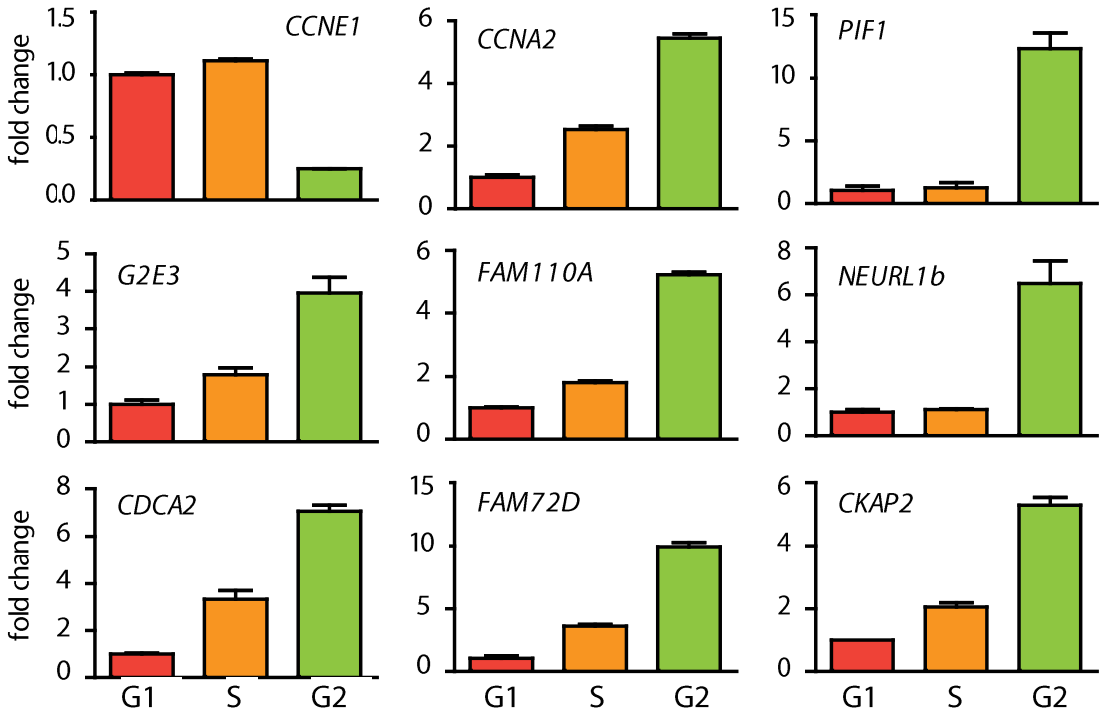

Figure 23. Confirmation of differential expression of the selected transcripts by QRT-PCR. RFP+ (G1 phase), GFP+ (G2 phase), and GFP+/RFP+ (S phase) RPE-FUCCI cells were sorted by flow cytometry, RNA was extracted and analyzed using qRT-PCR (n=3). Expression is normalized to GAPDH mRNA. Bars show mean ±SD.

Based on the commercially available tools, we proceeded to test several of the mentioned candidate genes that are highly expressed in G2 but have so far not been implicated in the cell cycle control or their role in cell cycle is not well explored. We observed that the small protein known as FAM110A (Family with sequence similarity 110 member A) showed interesting attributes, so we selected it for further analysis.

4.2.2 FAM110A antibody validation

In order to validate and asses the degree of specificity of three commercially available antibodies against FAM110A, we performed a siRNA-mediated depletion of this hit in parental RPE cells. First, we addressed the specificity through WB. The visible decrease of the detected bands validated the functionality and specificity for WB detection. Another aspect of our interest in testing FAM110A knockdown was to detect any possible effect over the normal progression of the parental RPEs cell cycle; therefore we immunoblotted with the mitotic marker Phospho-Ser10 modification in Histone3. We observed a slight visible increment in the band when cells were partially depleted of FAM110A, which could signal an enrichment and therefore delay in the mitotic population (**Figure 24**).

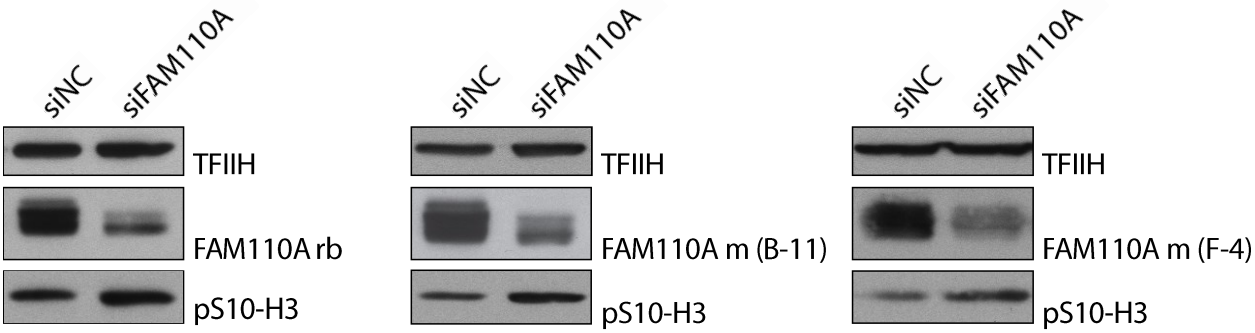

Figure 24. FAM110A commercial antibodies validation trough WB. RPE cells were transfected with control of FAM110A siRNA, whole cell lysates were prepared after 48h and indicated antibodies were tested by immunoblotting.

Following with the antibodies functionality test, we performed IF staining for detection of endogenous FAM110A in control cells and compare it to FAM110A depleted cells (**Figure 25-A**). We observed an interesting enrichment of the protein in the spindle poles and in the proximal mitotic spindle microtubules in the control metaphase cells. FAM110A signal intensity quantification of enriched signal in the centrosomes showed a significant reduction after FAM110A KD (**Figure 25-B**). In contrast, a persistent nuclear signal could be observed in the interphase cells even after siRNA KD, suggesting that the antibody presents non-specific binding capacity and therefore we deemed the nuclear localization as antibody cross-reactivity (**Figure 25**, **Figure 26**).The observed intracellular localization of FAM110A was in accordance with what was previously reported in transiently transfected HEK293 cells both in mitotic and interphase cells (Hauge, Patzke et al. 2007).

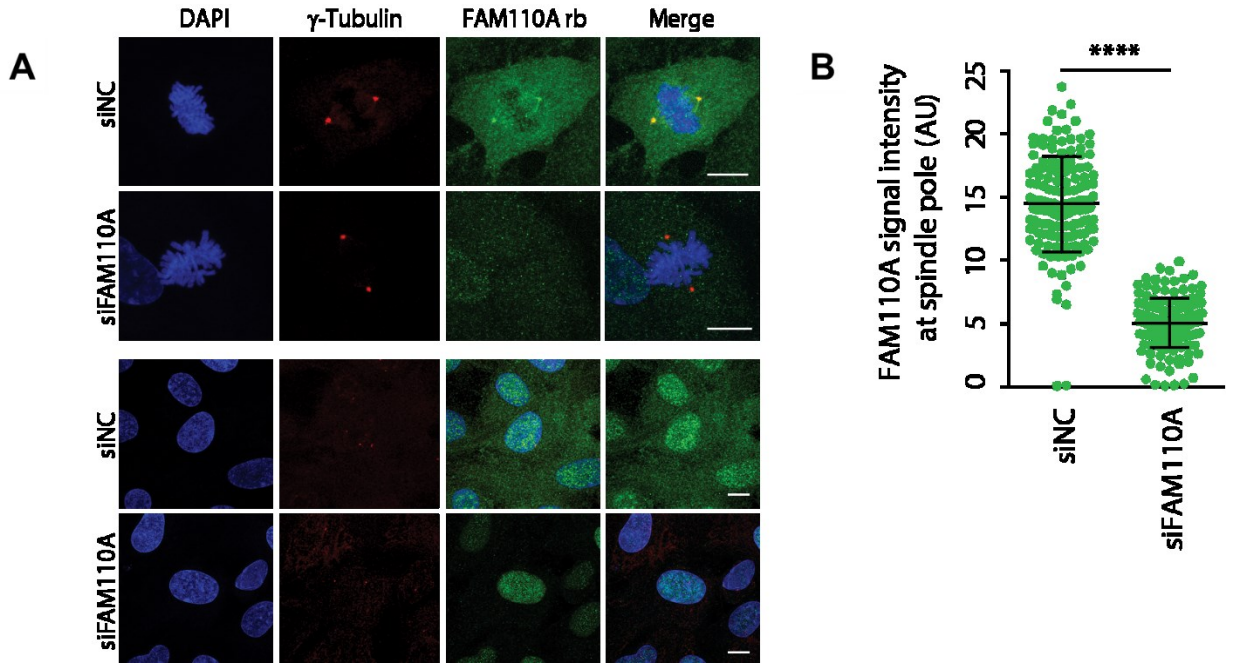

Figure 25. FAM110A endogenous localization validation trough immunofluorescence in RPE cell line. A. RPE cells transfected with control of FAM110A siRNA were fixed with 4% PFA, probed with rabbit polyclonal antibody against FAM110A and mouse monoclonal γ-tubulin, and were analyzed by confocal microscopy. First two panels show maximal projection of representative mitotic (metaphase) cells while lower panels show interphase cells. Scale bars indicate 10 µm. **B.** FAM110A spindle pole intensity quantification in control and siFAM110A treated RPE cells from (E). Signal intensity of the rabbit polyclonal antibody to FAM110A was determined in regions positive for γ-tubulin, Each dot represents a single spindle pole. Bars show median ±SD. Significance was evaluated by a t-test (n=3), (****p<0.0001).

Endogenous immunofluorescence staining using the validated rabbit polyclonal antibody in the U2Os cell line showed an enriched signal in the centrosome and a diffused cytosolic distribution in interphase cells that also disappeared after siRNA KD. The localization in the spindle poles and the proximal spindle microtubules previously observed was also noted (**Figure 26-A**). A similar but weaker signal was detected using the mouse monoclonal mouse antibody clone B11 from Santa Cruz, maybe do to the previously discussed inability of the antibody to recognize the phosphorylated epitope (**Figure 26-B**). This helped us to confirm in another cell line and with two different antibodies the specificity of the e observed intracellular localization of FAM110A.

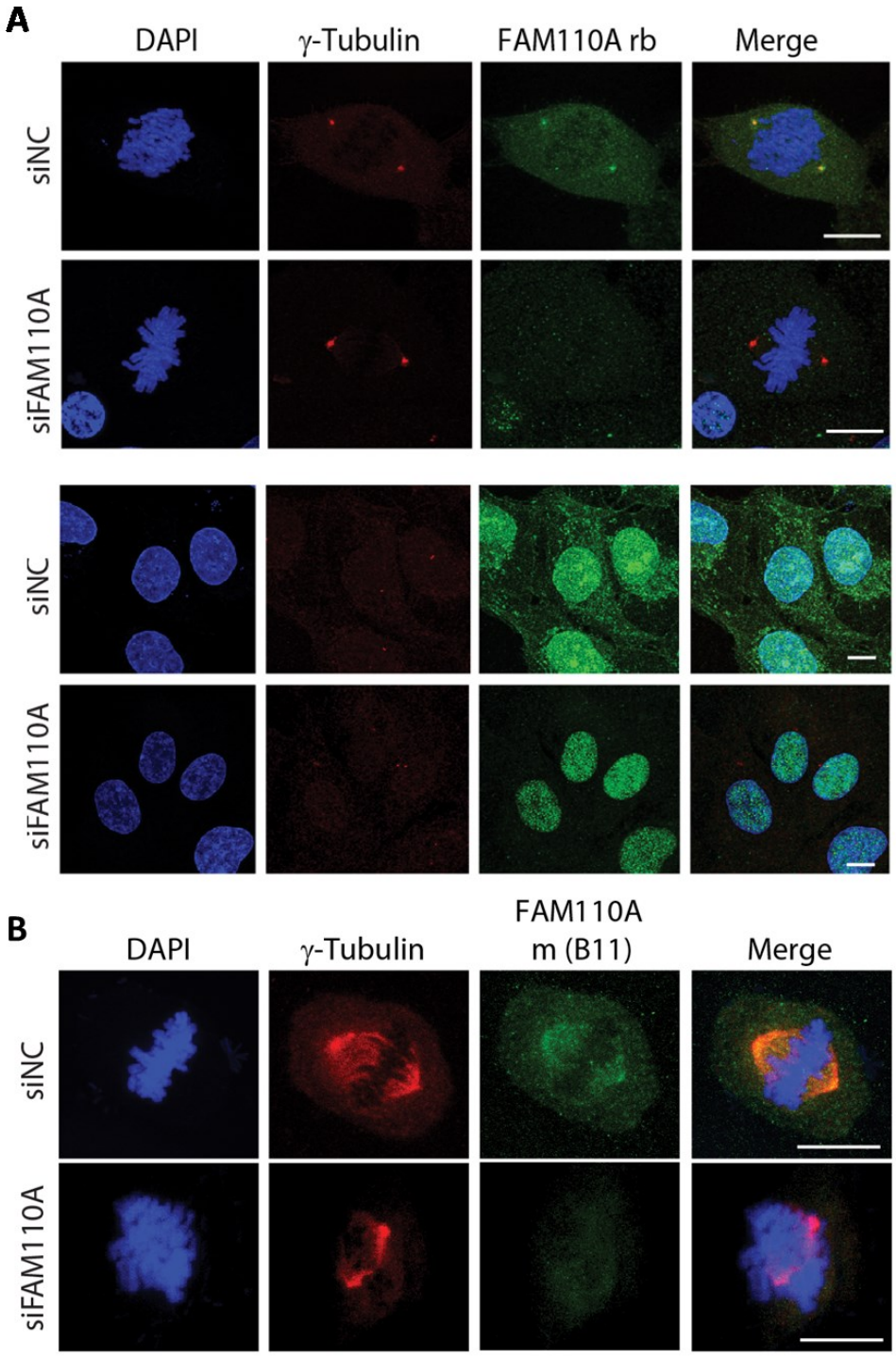

Figure 26. FAM110A endogenous localization validation trough immunofluorescence in U2Os cell line. A. U2Os cells transfected with control of FAM110A siRNA were fixed with 4% PFA, probed with rabbit polyclonal antibody against FAM110A and mouse monoclonal γ-tubulin. First two panels show maximal projection of representative mitotic (metaphase) cells while lower panels show interphase cells. **B.** The same U2Os transfected cells were probed using the Clone B11 mouse polyclonal antibody against FAM110A and monoclonal γ-tubulin; all samples were analyzed by confocal microscopy. Scale bars indicate 10 µm.

4.2.3 FAM110A is highly expressed in G2 and localizes at mitotic spindle during mitosis

As after mentioned, during the antibody testing we observed that FAM110A specific intracellular localization appeared to be in the spindle poles and proximal mitotic spindle in two independent cell lines, we decided to further down explore its distribution throughout mitosis in RPE cells. Starting from prometaphase cells, we observed the presence of FAM110A in the already duplicated centrosomes, localization that was maintained as mitosis progressed through metaphase and anaphase and also a slight decoration of the plasma membrane could be discerned. During telophase an enrichment in the constriction ring was visible (**Figure 27**).

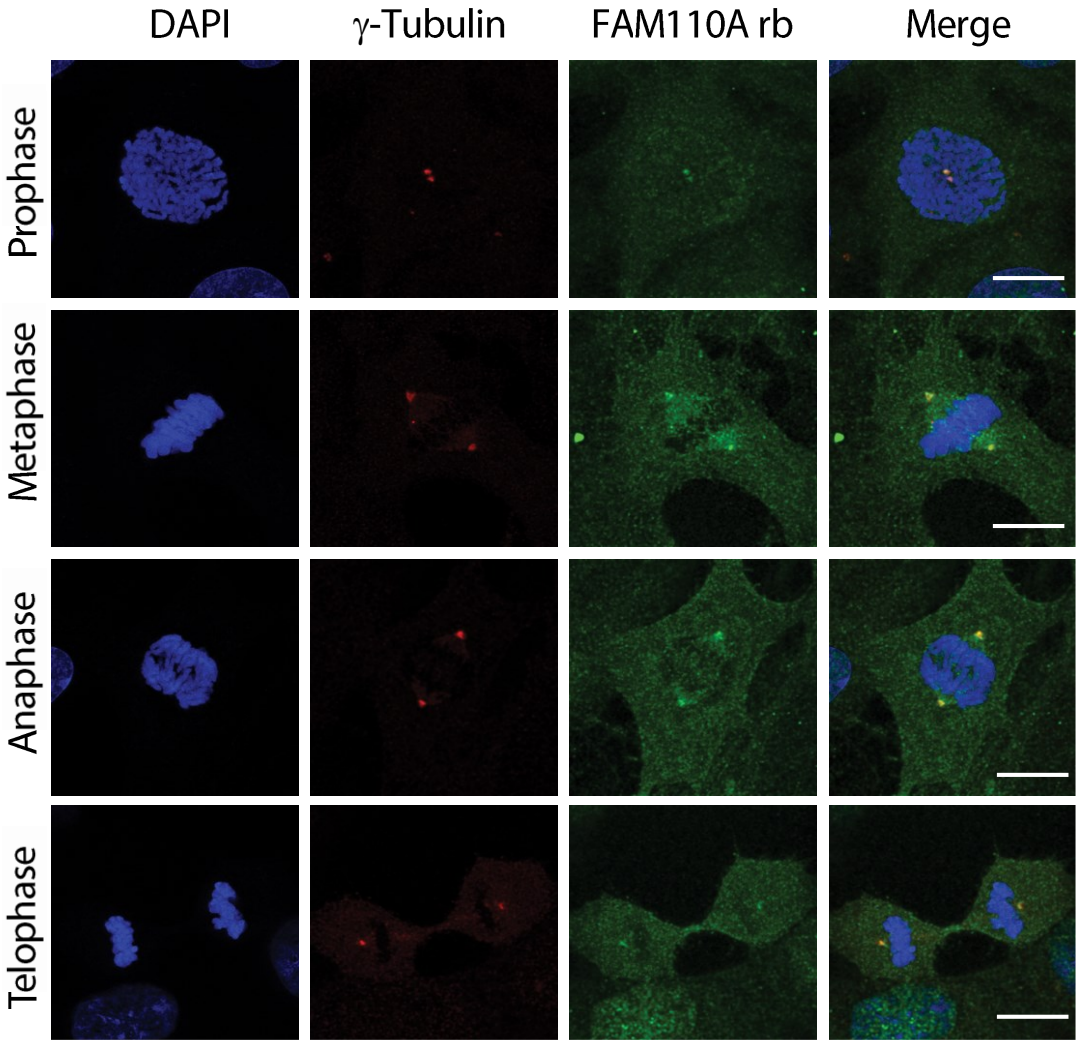

Figure 27. FAM110A localizes to the mitotic spindle during mitosis. Asynchronously growing RPE cells were fixed and probed with the rabbit polyclonal antibody to FAM110A. Shown are representative images of cells in mitotic phases. Individual z-stacks were de-convoluted using Huygens Deconvolution Software, processed sequentially and are presented as maximum projections. Scale bars indicate 10 μm.

To complement the expression analysis performed in the asynchronic FUCCI cells, we deemed necessary to establish FAM110A's expression pattern throughout the cell cycle; for this we performed a single thymidine block to synchronize parental RPE cells at the G1/S transition. After 36 hours of arrest, cells were troughly washed and released in fresh media and time points were taken every 2 hours after release. After 4 hours of thymidine release Nocodazole was added to the media to stop the cells at prometaphase, avoiding this way for fast cells to start a new cycle and ensuring that populations would be phase specific; cell samples were also analyzed through FACS (**Figure 28-A**). Trough Western Blot band intensity quantification we observed that FAM110A was expressed at basal levels in G1/S-arrested cells and that its total expression increased as cells progressed through S and G2 phase, reaching its highest expression rate during G2/M transition and mitosis (**Figure 28-B**).

Interestingly, as the cells progressed synchronized through the cell cycle and FAM110A expression levels increased, FAM110A seemed to slow down its migration trough the SDS-PAGE, culminating in the slowest band when the cell population was exclusively mitotic. In contrast, this mobility shift did not happen when cells were arrested in G2 and mitotic entry was prevented. During this experiments it was very interesting to observe that the FAM110A-Clone B11 antibody (Santa Cruz Biotechnology) failed to recognize the slower migrating bands trough immunoblotting which suggest that it's only capable of recognizing the non-phosphorylated epitope of the protein (**Figure 28-A**). By contrast, by releasing a mitotic population from Nocodazole arrest and analyzing the mobility behavior of FAM110A it was clearly visible that the shift present in the mitotic cells disappeared (**Figure 28-C**). We hypothesized this mobility shift could be due to extensive post-translational modifications of FAM110A, mainly phosphorylation. To test this we immunoprecipitated endogenous FAM110A from G2 and Mitosis arrested cells and supplemented them with lambda phosphatase. By analyzing the treated Mitotic immunoprecipitated FAM110A using the non-treated G2 and M samples as mobility shift references, it was possible to observe that after the lambda phosphatase treatment, the mobility shift partially decreased, indicating that the post-translational modification responsible for it is phosphorylation, although other types of modifications cannot be discarded (**Figure 28-D**).

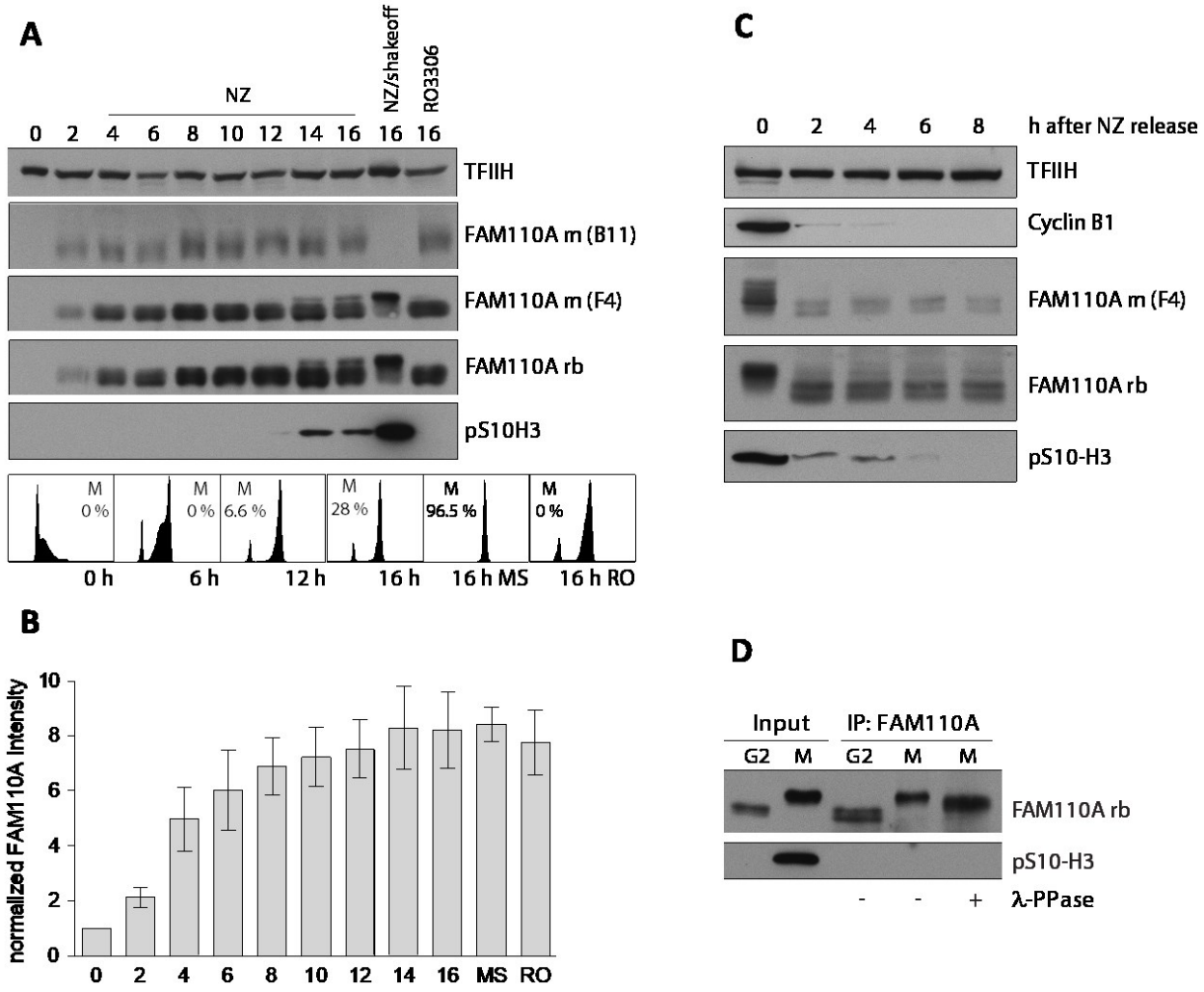

Figure 28. FAM110A expression is upregulated during G2 phase and is post-translationally modified during mitosis. A. RPE cells were released for indicated times from a thymidine block (2 mM) and collected cells were analyzed by immunoblotting and FACS. Nocodazole was added after 4 h to arrest cells in mitosis. Alternatively, RO3306 inhibitor was added to prevent mitotic entry. Where indicated sample was collected by mitotic shake-off (MS) to obtain pure mitotic population. Samples were analyzed by immunoblotting (upper panel). In parallel, cell cycle progression was followed by flow cytometry using DAPI and MPM2 staining. Representative histogram plot is shown, M indicates percentage of mitotic cells. **B.** Signal of the rabbit FAM110A antibody was quantified in three independent replicates and normalized to the loading and to the thymidine arrested sample. Bars show median ±SD. **C.** RPE cells were arrested in mitosis by Nocodazole, collected by mitotic shake-off and released to fresh media for indicated times to allow mitotic exit. Loss of p10-H3 signal was used as marker of mitotic exit. **D.** Immunoblotting of RPE cells arrested with RO3306 (G2) or with Nocodazole (M) were extracted and endogenous FAM110A was immunoprecipitated using rabbit polyclonal antibody immobilized on pA/G beads. Beads were incubated with mock or with lambda phosphatase for 20 min at 30 °C.

We decided to test if this pattern of expression was extended among other cell lines by comparing total protein lysates of G1, G2, Mitotic and RO3306 arrested populations in RPE, U2Os and HeLa (**Figure 29-A, C**). In all the mentioned cell lines FAM110A presented a similar enrichment from G1 to G2, showing a fold change of ~7 in RPEs and of ~8 in U2Os ($p<0.001$ and $p<0.005$, respectively); a very similar value of that observed in RO3306 arrested populations; the mitotic populations showed a slight increase in the FAM110A enrichment relative to G2 but was not statistically significant (p = ns and p = ns, respectively) (**Figure 29-B**).

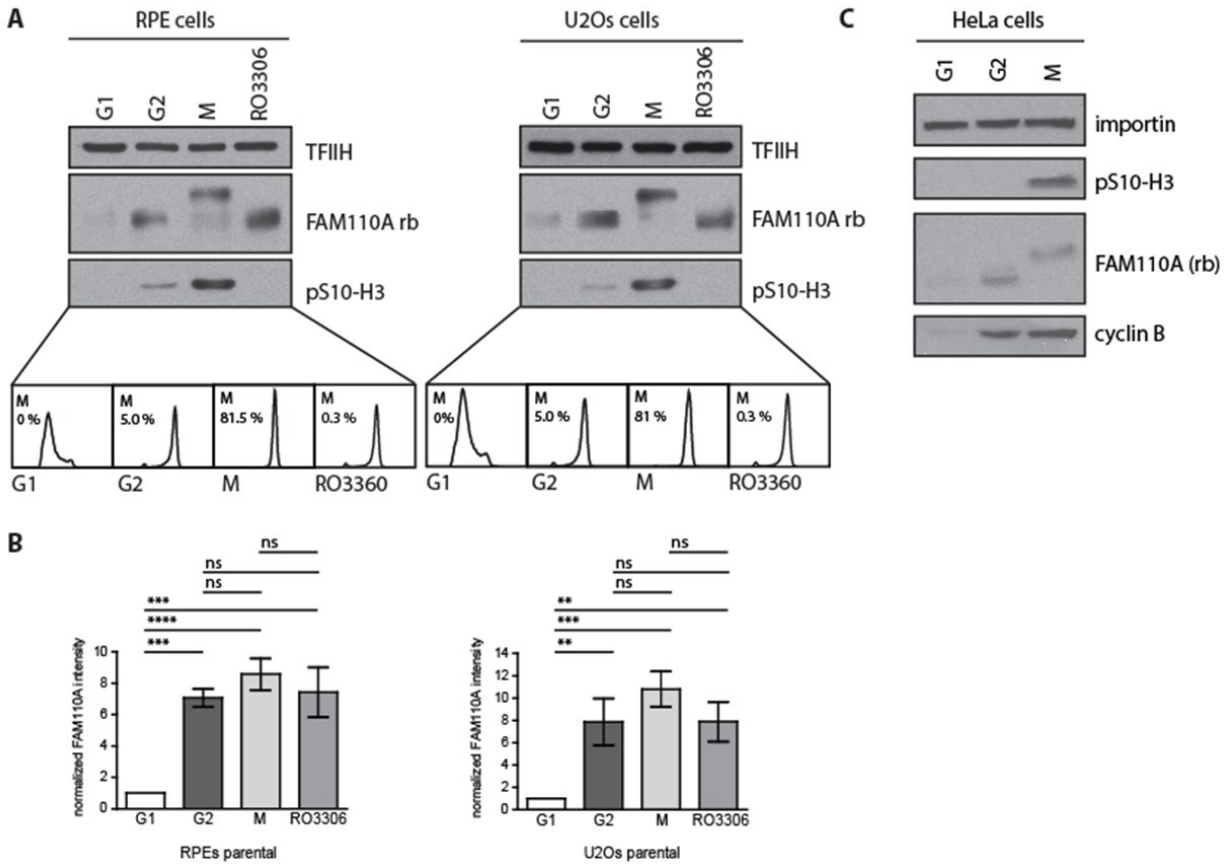

Figure 29. FAM110A expression profile analysis and comparison between the RPE, U2Os and HeLa cell lines. Representative blots and corresponding FACS data comparing FAM110A expression levels in G1 (thymidine arrested), G2 (8 hours after thymidine release), M (Nocodazole arrested) and G2 (RO3306 arrested). **B.** Signal of the rabbit FAM110A antibody was quantified in three independent replicates and normalized to the loading and to the G1 thymidine arrested sample. Bars show median ±SD, significance was evaluated by ANOVA (n=3), **p<0.005, ***p<0.001, ****p<0.0001. **C.** HeLa cells were treated in the same manner as RPE and U2Os' Cyclin B was used as an additional marker for G2 and prometaphase populations. Enrichment of p10-H3 signal was used as marker of mitosis.

So far, our results in FAM110A endogenous localization, along with its cell cycle-specific expression pattern and clear extensive post-translational modifications during mitosis led us to wonder what could be FAM110A role in mitosis. For this matter we decided to study in more detail the FAM110A depletion phenotype during the cell cycle and also focusing specially in mitotic progression.

4.2.4 Depletion of FAM110A slows down mitotic progression and leads to mitotic defects

In order to study FAM110A function in the cell cycle we used siRNA mediated depletion of this protein to analyze the consequent effects in the cell cycle profile using FACS by comparing the population distributions between control and treated cells. We found that depletion using two independent siRNA sequences generated a slight enrichment in the mitotic population (more specifically a 70% increase). Parallel to this, KD of the homologue FAM110B and CSPP1 was also carried out (**Figure 30-A**). Mitotic populations were quantified and our results showed that the apparent mitotic delay was exclusive for FAM110A KD suggesting that FAM110A might have specific functions during mitotic progression and that KD of the other two proteins had no direct effect in the mitotic population (**Figure 30-B**). The mitotic population enrichment after FAM110A KD was also detected trough immunoblotting with the mitotic marker Phospho-Ser10 modification in Histone3 (**Figure 30-C**).

Although FAM110A was initially identified as a putative binding partner of the centrosome/microtubule associated protein CSPP1, their biochemical interaction *in vivo* has never been described. Even though the FAM110 and CSPP1 proteins have been shown to share certain features, like their subcellular localization, vertebrate-restricted expression, cell cycle-dependent expression levels (for the case of FAM110A and CSPP1) and induction of G1 arrest when overexpressed (for the FAM110B-C homologues and CSPP1) (Patzke, Stokke et al. 2006, Hauge, Patzke et al. 2007) we failed to see any direct link between FAM110A hypothesized mitotic function and CSPP1 (**Figure 30-B**).

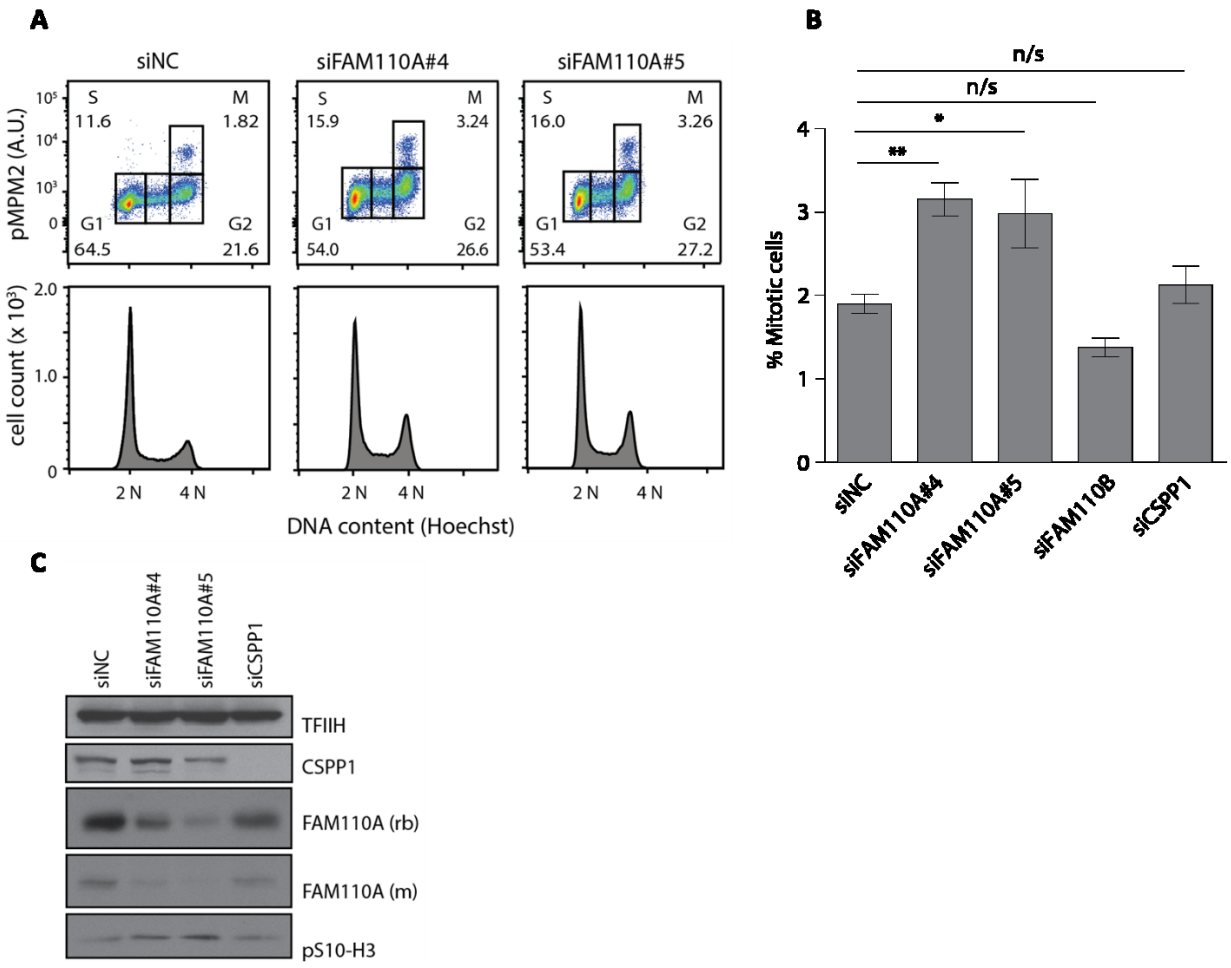

Figure 30. Depletion of FAM110A impairs progression through mitosis. A. RPE cells transfected with control or FAM110A siRNA were fixed, stained with MPM2 antibody (marker of mitosis) and DAPI, and were analyzed by flow cytometry. Representative panels are shown gating for each cell cycle phase. **B.** Quantification of the mitotic index from three independent experiments in the A-panel set-up, shown is median ±SD (n=3); statistical significance was determined by ANOVA (* $p<0.05$, ** $p<0.005$). **C.** Representative Immunoblot analysis of total RPE lysates after control, FAM110A, FAM110B and CSPP1 siRNA treatment.

With the objective of validating the mitotic delay phenotype we observed in the parental RPE cell line through a rescue experiment, we generated a stable cell line in this same cells using a selection plasmid that would ectopically expressed the WT FAM110A tagged with EGFP. We performed siRNA mediated KD of endogenous FAM110A using this stable cell line (**Figure 31-A**) and through FACS analysis we detected that the ectopic expression of EGFP-FAM110A prevented the enrichment of the mitotic population (**Figure 31-B**). Further, by employing confocal microscopy in this EGFP-FAM110A stable cell line we observed a comparable intracellular localization throughout mitosis as the endogenous FAM110A and that the enrichment in the plasma membrane outline was also present (**Figure 31-C**). It was previously reported that

ectopic expression of the FAM110C homologue triggered impairment of cell morphology and caused microtubule bundle formation (Hauge, Patzke et al. 2007), however in our FAM110A-EGFP stable cell line no apparent morphology problems occurred, neither in cell morphology nor in the organization of the mitotic spindles, indicating that this mild expression is well tolerated by the RPE cells.

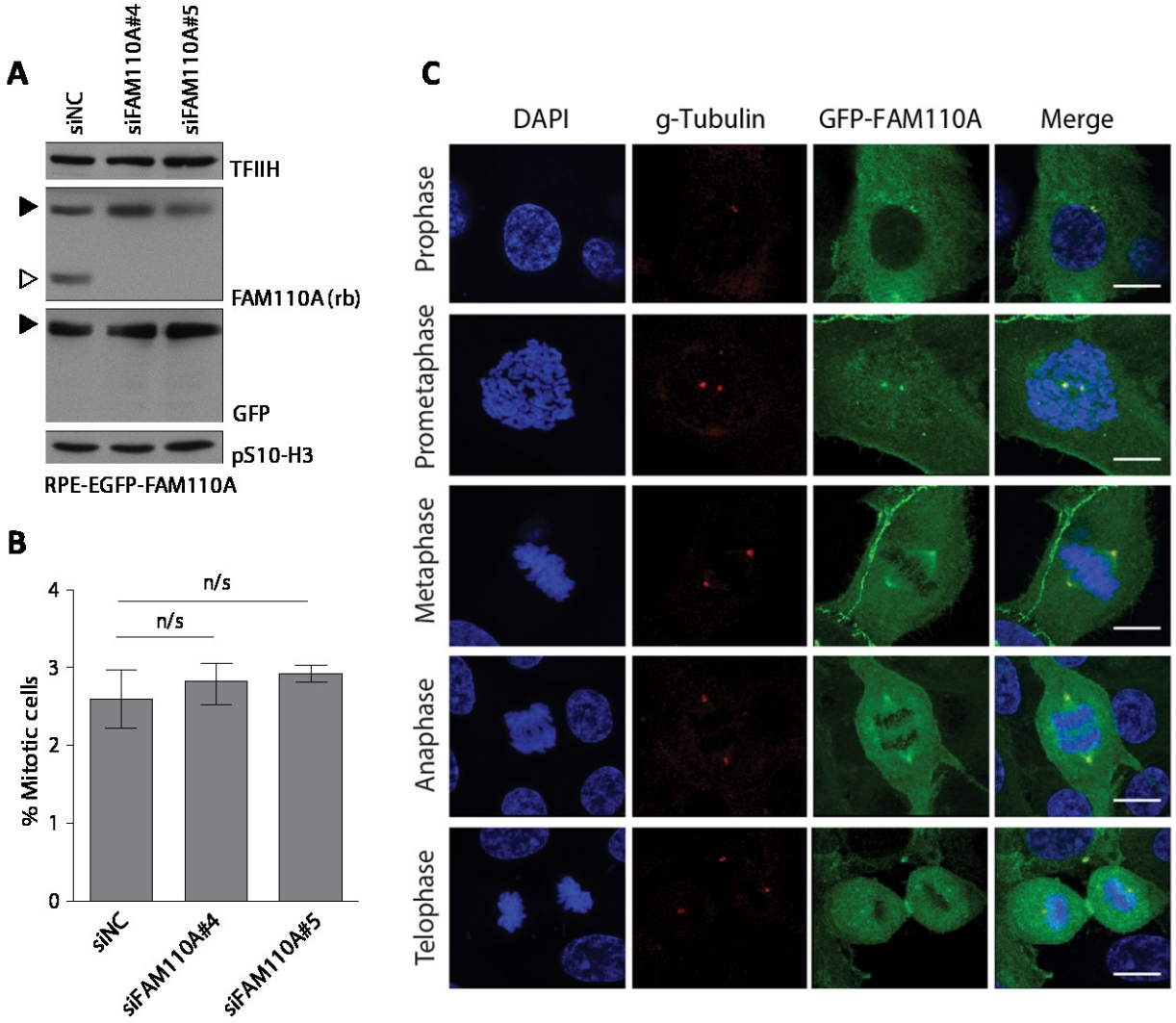

Figure 31. Ectopic expression of GFP tagged FAM110A rescues mitotic delay and localices to mitotic spindle poles and plasma membrane. A. RPE cells stably expressing mouse EGFP-FAM110A were transfected with control or two various FAM110A siRNAs and whole cell lysates were analyzed by immunoblotting with indicated antibodies; empty arrowhead indicates position of the endogenus FAM110A, filled arrowhead the EGFP-FAM110A. **B.** mitotic index was determined by flow cytometry. Statistical significance was evaluated by ANOVA (n=3). Bars indicate median ±SD. **C.** RPE cells stably transfected with EGFP-FAM110A were fixed, probed with a mouse monoclonal antibody against γ-tubulin and analyzed by confocal microscopy. Shown are representative images of cells in various phases of mitosis. Scale bars indicate 10 µm.

With the intention to elucidate the nature of the observed mitotic delay phenotype in FAM110A depleted cells, we decided to carry out a mitotic defect scoring using control and siRNA treated cells for microscopy analysis. We concluded that depletion of FAM110A significantly increased the recurrence of aberrant chromosomal alignment and multipolar spindles, specifically during metaphase (**Figure 32-A**). The most common aberrancies observed were lagged chromosomes that failed to attach to the mitotic microtubules and where left out of the mitotic plate and loosely attached chromosomes (**Figure 32-B**). In this same FAM110A depleted cells, we also observed frequent lagging or broken chromosomes during anaphase (**Figure 32-C, D**).

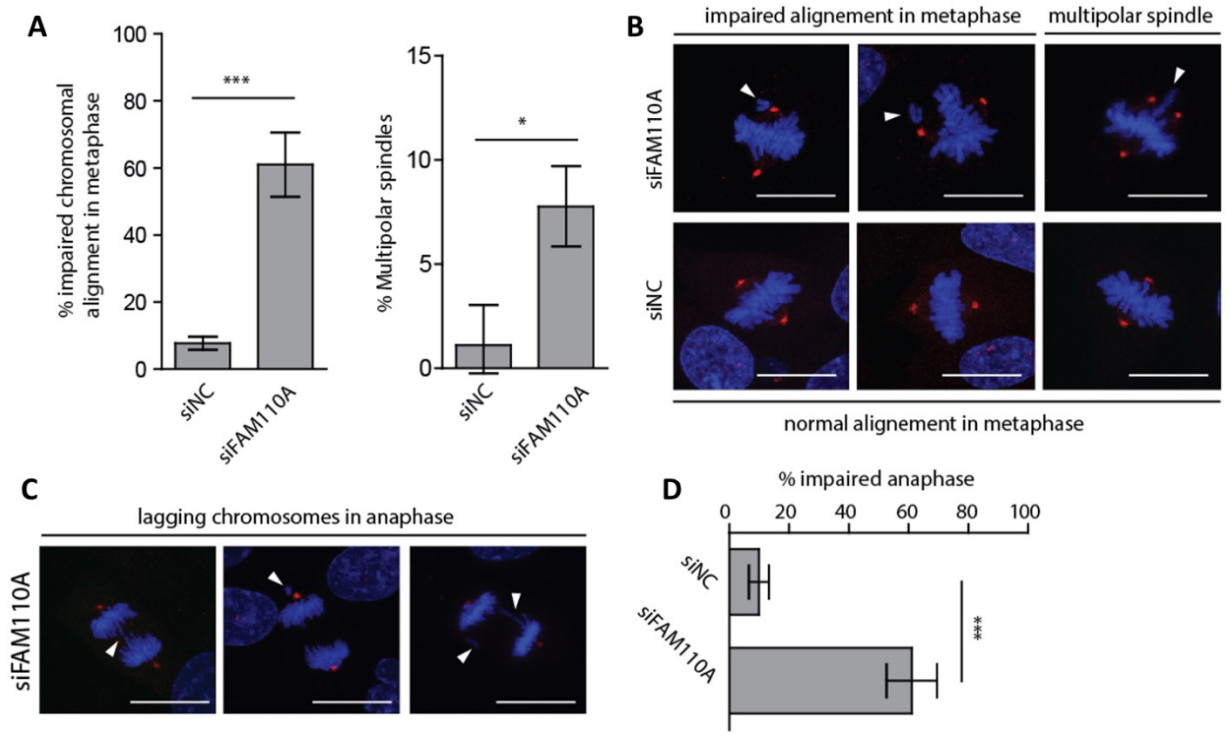

Figure 32. FAM110A depletion causes impaired chromosomal alignment. **A**. RPE cells transfected with control or FAM110A siRNA were grown for 48 h and treated with MG132 (10 µM) for 30 min prior fixation to trap mitotic cells in metaphase. Impaired chromosomal alignment and multipolar spindles were scored and representative images are shown. Scale bars indicate 20 µm arrowheads point to misaligned chromosomes. 30 metaphases were evaluated per condition (n=3). Bars indicate median ±SD. Statistical significance was determined by two-tailed Student's T-test, (*** $p<0.001$, *$p<0.05$). **B.** Representative panels of impaired chromosomal alignment in metaphase and multipolar spindle after control or FAM110A siRNA treatment. **C.** Representative panels of lagging chromosomes during anaphase after FAM110A depletion. **D.** Quantification of lagging chromosomes in anaphase cells from (C). More than 30 anaphases were evaluated per condition (n=3). Representative images of abnormal anaphase are shown, scale bars indicate 20 µm, arrowheads point to incorrectly segregating chromosomes. Statistical significance was determined by two-tailed Student's T-test. Bars indicate median ±SD (*** $p<0.001$).

In order to be able to describe with more detail the metaphase misalignment phenotype caused by loss of FAM110A, we performed live imaging in asynchronously growing U2Os-H2B-GFP cells. We measured the time from nuclear envelope breakdown (NEB) to the metaphase to anaphase transition (MAT) and compared between the control cells or FAM110A depleted cells (**Figure 33-A, B, D**). We observed that FAM110A depletion significantly increased the required time needed for initiation of anaphase. During the analysis, we observed that a fraction of cells with depleted FAM110A that failed to segregate the chromosomes died during the experiment or progressed to the G1 presenting a severely impaired nuclear organization (**Figure 33-C, D**). Based on this data we conclude that FAM110A depletion extends the time that cells spend in mitosis, specifically in metaphase, most probably because of defects in mitotic spindle organization that lead to impaired chromosomal alignment.

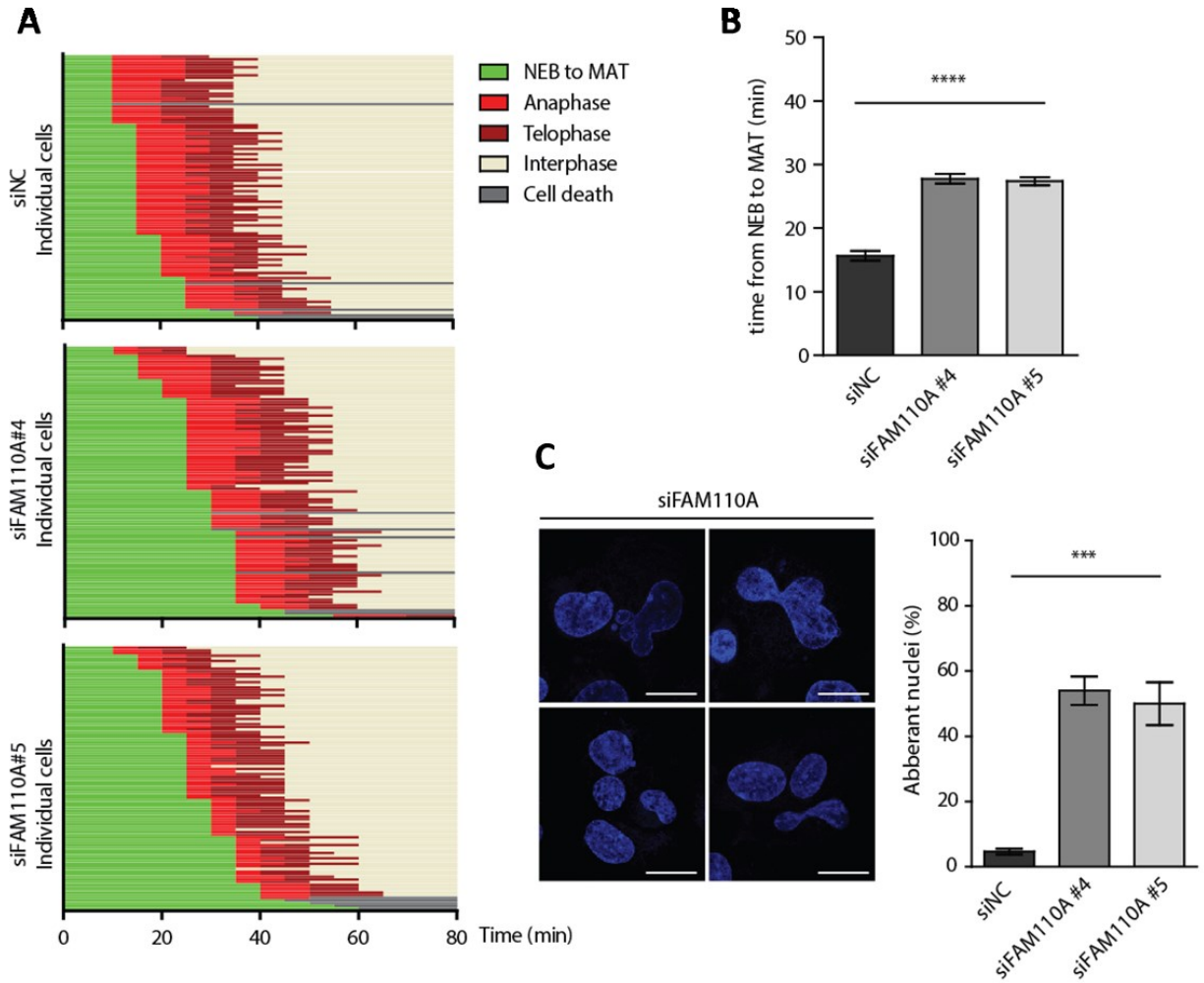

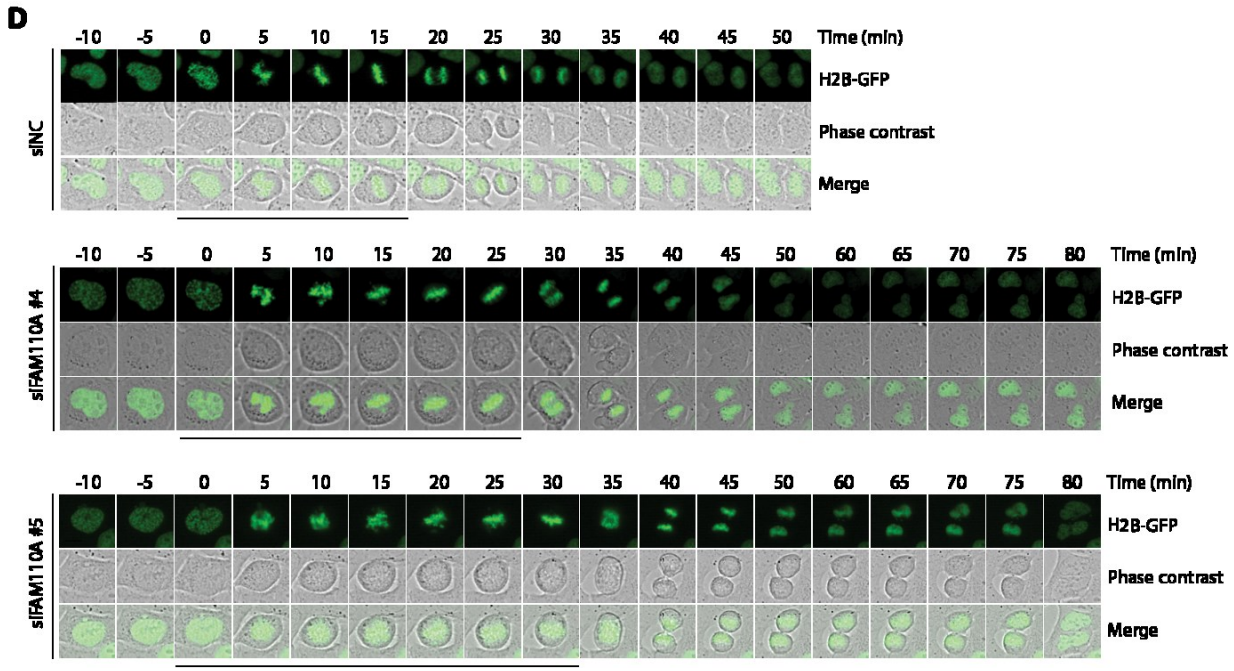

Figure 33. FAM110A depletion increases metaphase length and causes segregation problems. A. Progression through mitosis was categorized in cells from (A) (100/condition) as follows: nuclear envelope breakdown to the metaphase-to-anaphase transition (MAT), anaphase, telophase and interphase. Data from one of three experiments are shown, each bar indicates one cell. Cells that died during imaging are shown in grey. **B.** Time from the nuclear envelope breakdown to MAT was quantified from (A). Shown is median ±SD (n=3). Statistical significance was determined by ANOVA (**** $p<0.0001$). **C.** Abnormal nuclear organization was scored in cells from (A) that completed cell division. Representative images of aberrant nuclei are shown. Scale bar indicates 15 µm. Plotted is percentage of cells with aberrant nuclei. Shown is median ±SD (n=3). Statistical significance was determined by ANOVA (***$p<0.001$). **D.** Representative sequential panels of U2Os cells stably expressing H2B-EGFP treated with control or two different FAM110A siRNAs and after 48 h (n=3). Cells were filmed in 5 min intervals; the bellow line marks the panels corresponding to the beginning of NEB (0 min) to the MAT.

4.2.5 FAM110A interacts with cytoskeletal-related proteins and two casein kinase 1 isoforms during mitosis.

In order to unravel the mechanism by which FAM110A might influence mitotic progression, the first step was to identify its potential interactors during mitosis by mass spectrometry analysis. For this purpose, cell extracts from the control EGFP and the EGFP-FAM110A stable cell lines that where enriched in mitosis using Nocodazole were obtained. Using GFP-trap beads, control EGFP and EGFP- FAM110A were immunoprecipitated along with their interacting proteins and their identities were elucidated through mass spectrometry (**Table 2**). The obtained results showed an interesting list of cytoskeleton-related proteins, with actin showing the highest fold change score and α/β-catenin as some of the strongest hits suggesting that FAM110A might be associated with the actin cytoskeleton and to cell adhesion complexes. This proteomic analysis also showed that the genes TUBB8 and TUB1AC (coding for β-tubulin and α-tubulin

respectively) were also significantly enriched in complex with EGFP-FAM110A during mitosis, although their enrichment was considerably lower than that of actin, possibly due to the depolymerizing effect that Nocodazole has on microtubules.

Table 2. Mass spectrometry analysis of purified EGFP-FAM110A from a mitotic arrested cell population. Cells extracts from RPE cells table expressing EGFP or EGFP-FAM110A arrested in mitosis by Nocodazole were incubated with GFP trap. Bound proteins were analyzed by mass spectrometry. Shown are top ten proteins that were significantly enriched in EGFP-FAM110A complex compared to EGFP in three independent experiments Number indicates the fold change interaction compared to the control.

Protein ID	Gene	Protein	Fold change
Q9BQ89	FAM110A	Protein FAM110A	671
P68133	ACTA1	Actin	216
P49674	CSNK1E	Casein kinase I isoform epsilon	96
P35221	CTNNA1	Catenin alpha-1	80
Q13813	SPTAN1	Spectrin alpha chain, non-erythrocytic 1	43
P35222	CTNNB1	Catenin beta-1	42
Q13049	TRIM32	E2 ubiquitin-protein ligase TRIM32	41
P62258	YWHAE	14-3-3 protein epsilon	41
O43707	ACTN4	Alpha-actinin-4	40
P48730	CSNK1D	Casein kinase I isoform delta	23
	…	…	
Q3ZCM7	TUBB8	Tubulin beta-8	9
Q9BQE3	TUBA1C	Tubulin alpha-1C	7

Aside from the cytoskeletal related-proteins, the Casein kinase isoforms epsilon (CSNK1E or CK1ε) and delta (CSNK1D or CK1δ) where detected as mitotic EGFP-FAM110A interactors. Next, we performed immunoprecipitation assays using asynchronic or mitotic populations of the same cell lines using the after mentioned setup, and validated the proteomic analysis results (**Figure 34-A**). The results showed that CK1ε and CK1δ but not CK1α are able to interact with FAM110A throughout the whole cell cycle but that said interaction increases substantially during mitosis. Interestingly, the interaction with actin appeared to be exclusive for mitosis, unlike the case of α-catenin which presented a similar interaction pattern like the CK1 isoforms. Conversely, immunoprecipitation of endogenous CK1ε and CK1δ in the EGFP-FAM110A stable cell line confirmed the interaction, showing the strongest interaction during mitosis (**Figure 34-B**).

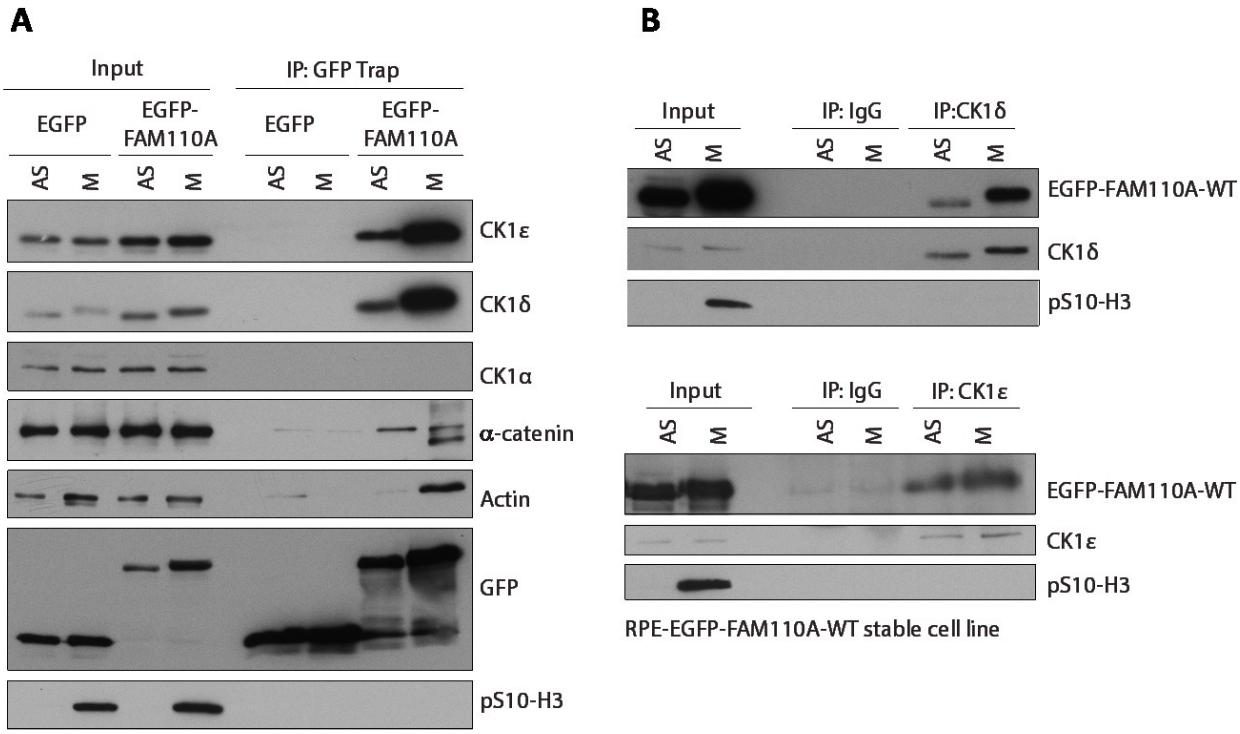

Figure 34. Immunoprecipitation assays to confirm FAM110A binding interaction with CK1 isoforms. A. Cell extracts from asynchronously growing or mitotic RPE-EGFP or RPE-EGFP-FAM110A cells were incubated with GFP Trap and bound proteins were analyzed by immunoblotting. Antibody against PS10-H3 was used as a marker of mitosis. **B.** Cell extracts from asynchronously growing or mitotic RPE-GFP-FAM110A cells were incubated with CSNK1D (upper panel) and CSNK1E (lower panel) antibody or control IgG and then immobilized on protein A/G beads. Bound proteins were probed with antibody against GFP or CK1δ. Staining for pS10-H3 was used as marker of the mitotic population.

Next, we aimed to map the interaction between EGFP-FAM110A and the endogenous CK1ε and δ isoforms by generating a series of truncated mutants and punctual aminoacid mutations of the WT-FAM110A sequence (**Figure 35-A**). The first part of the immunoprecipitations aimed to establish the regions responsible for actin, tubulin and CK1 isoforms binding, therefore focusing on truncated mutants (**Figure 35-B**). Interestingly, deletion of the C-terminal part of FAM110A prevented its binding to tubulin and to the CK1ε and δ isoforms and concomitantly, the deletion of the rest of FAM110A aside from the C-terminal domain was sufficient to maintain this interaction.

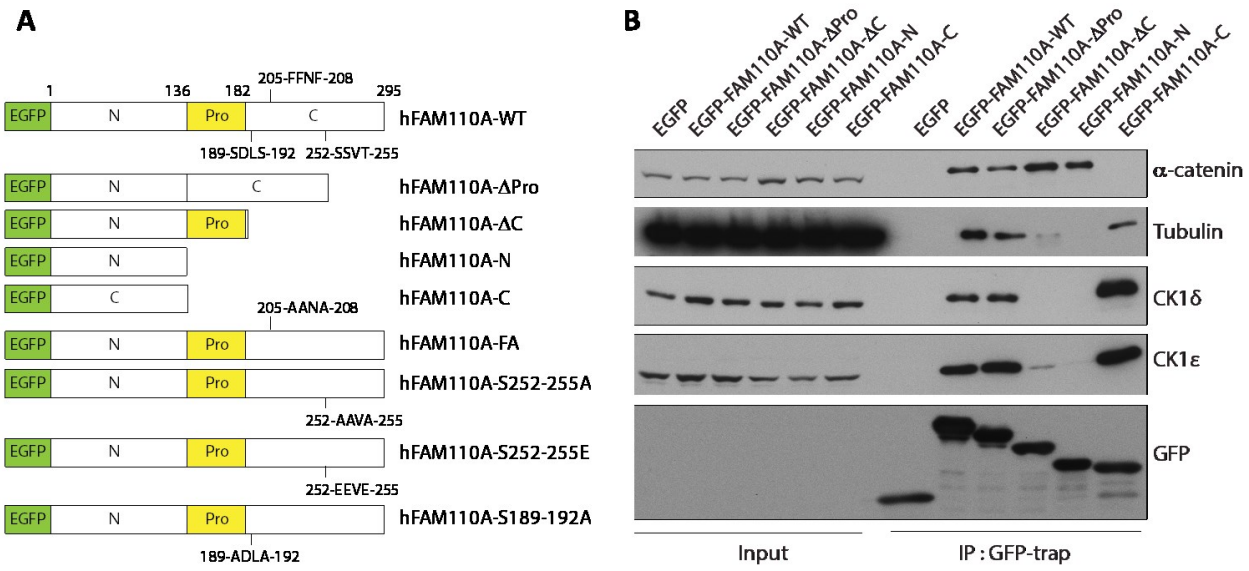

Figure 35. Mapping of FAM110A interactions trough truncation mutants by immunoprecipitation assays. A. Scheme of the EGFP-FAM110A mutant constructs used for tubulin and CK1 isoforms interaction mapping. Numbering is based on human FAM110A. N, C and Pro represent N-terminal, C-terminal and Pro rich domains, respectively. **B.** HEK293 cells were transfected with indicated constructs and after 48 h they were lysed in RIPA buffer. Cell extracts were immunoprecipitated with GFP Trap and probed by immunoblotting (n=2).

Contrariwise, actin and the α/β-catenin isoforms showed an opposite binding behavior to the one previously described (**Figure 36-A**), being able to bind to the mutants presenting exclusively the N terminal domain but failing to bind when only the C terminal domain was present. In the case of the ΔPro mutant (lacking the Proline-rich stretch) pull down of all reported interactions proved comparable to that of the WT-FAM110A. By analyzing FAM110A aminoacid sequence we identified a short peptide sequence (F-X-X-X-F) resembling a reported consensus docking motif for CK1 within the C-terminal domain (Okamura, Garcia-Rodriguez et al. 2004, Fulcher, Bozatzi et al. 2018). Based on this, we hypothesized that performing punctual mutagenesis of the F205, F206 and F208 residues (that we deemed corresponded to this consensus docking motif) to alanines would impair the interaction of EGFP-FAM110A with the CK1 isoforms (**Figure 36-B**). Through immunoprecipitation we confirmed that indeed, FAM110A presented the CK1 docking motif detected in its C-terminal domain and that it is the region responsible for binding to CK1 isoforms. Through this experiments we concluded that FAM110A binding to tubulin and actin is mediated by opposite regions in the protein and that CK1 binding depends on the presence of the after mentioned consensus docking motif.

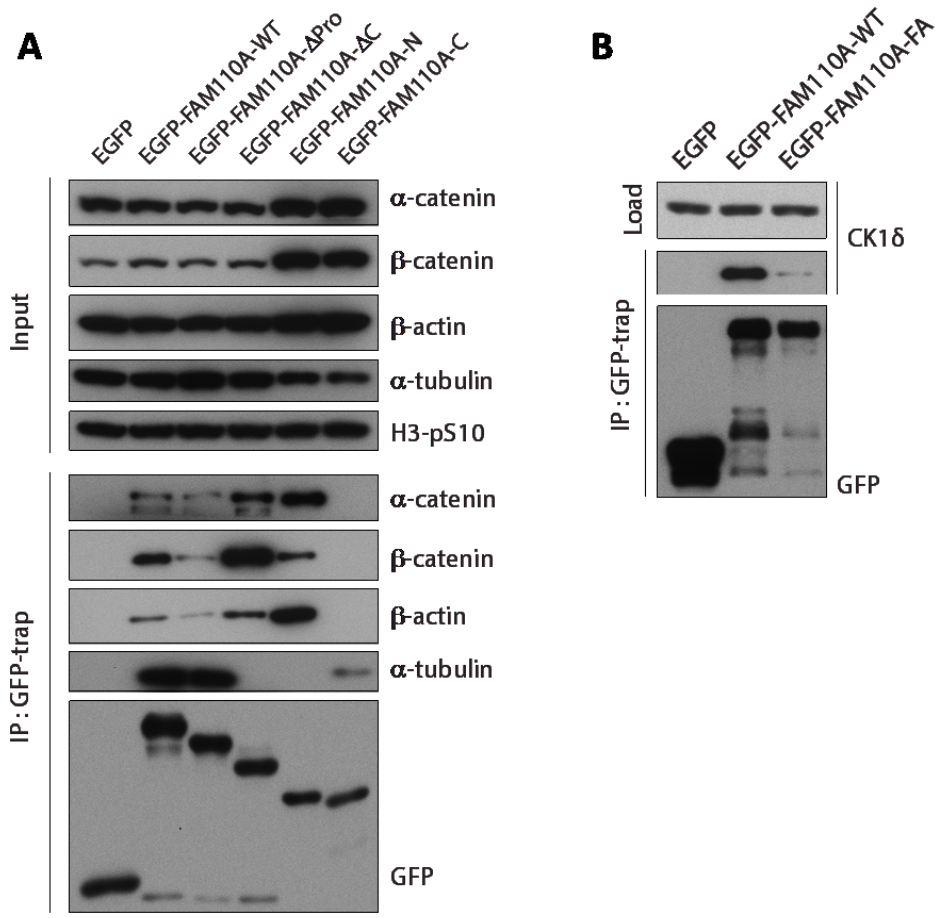

Figure 36. Mapping of FAM110A interactions trough truncations and point mutations by immunoprecipitation assays. A. HEK293 Cells were transfected with indicated constructs, synchronized in mitosis by Nocodazole and were lysed in IP buffer 48 h after transfection. Cell extracts were immunoprecipitated with GFP Trap and probed by immunoblotting. **B.** HEK293 cells were transfected with EGFP, EGFP-FAM110A-WT and EGFP-FAM110A-FA. Cell extracts were immunoprecipitated with GFP-Trap and binding of CK1 was determined by immunoblotting (n=3).

4.2.6 C-terminal domain of FAM110A is phosphorylated by CK1 in mitosis

As we have stated before, FAM110A appears to undergo extensive post-translational modifications, showing a clear decrease in its migration speed when the cell enters mitosis. We also previously showed that one of this modifications is phosphorylation. In order to identify protein kinases that could be responsible for directly phosphorylating FAM110A during mitosis we treated RPE cells that were arrested in mitosis with selective small-molecule inhibitors with specificity against the main known protein kinases that are active during the G2 and M phases of the cell cycle. We tested the effect of this inhibitors over FAM110A trough WB to visualize any effect over its electrophoretic mobility (**Figure 37-A**). One of the selected inhibitors, BI2536 increased the mobility of Cdc27 due to its specific inhibition of PLK1 (Kraft, Herzog et al. 2003, Lenart, Petronczki et al. 2007) while the Aurora A inhibitor MLN8054 prevented its auto phosphorylation at the T288 residue (Manfredi, Ecsedy et al. 2007) thus showing that inhibition of this kinases was successful. However, both instances failed to have any effect over FAM110A mobility, therefore discarding FAM110A as potential substrate of this kinases. On the contrary, treatment with the CDK1 inhibitor RO3306 resulted in the loss of the mobility shift of FAM110A, suggesting that CDK1 might phosphorylate FAM110A during mitosis. Following with this possibility, by performing a kinase assay we found that CDK1/Cyclin B phosphorylates FAM110A *in vitro* (**Figure 38-B**), however it is important to take note that RO3306 treatment forces cells out of mitosis and that this effect could be directly responsible for the loss of FAM110A phosphorylation.

Taking in account our previous observations, we decided to test if quenching CK1ε and δ activity using the PF670462 inhibitor had an effect over FAM110A mobility shift in mitosis. In fact we observed that the mobility shift was reduced after treatment without inducing mitotic exit both in RPE (**Figure 37-A**) and U2Os cells (**Figure 37-C**) allowing at the same time for FAM110A detection with the B11 monoclonal antibody, consistent with its dephosphorylation. Cyclin B1 was employed as a marker of mitotic permanence. With the intention of validating the after described observations after the inhibitors treatment, we performed siRNA mediated depletion of the CK1ε and CK1δ isoforms and enriched the mitotic population by treating with Nocodazole (**Figure 37-B**). By analyzing the mobility shift of FAM110A trough WB we observed that depletion if CK1δ but not of CK1ε impaired partially the mobility shift. This result indicated that in fact, CK1 is responsible for FAM110A phosphorylation in mitosis, specifically by the δ isoform and that the ε isoform might perform redundant functions over it.

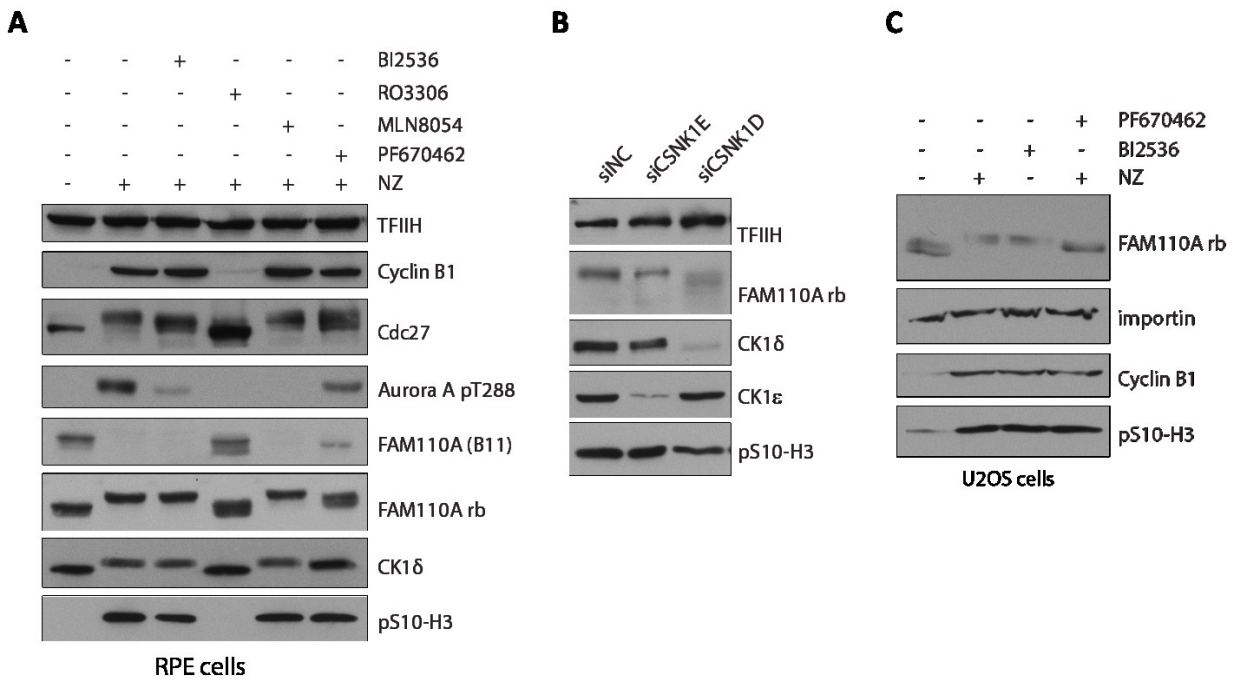

Figure 37. C-terminal domain of FAM110A is phosphorylated by CK1 in mitosis. A. RPE cells arrested in mitosis by Nocodazole (Z) were treated with DMSO, PLK1 inhibitor B12536 (100 nM), Aurora-A inhibitor MNL8054 (0.25 μM) CDK1 inhibitor RO3306 (20 nM) or CK1 inhibitor PF670462 (1 μM) for 60 min, collected and analyzed by immunoblotting with indicated antibodies. Asynchronously growing RPE cells are shown for comparison (first line, non-treated). Staining for H3-PS10 served as a marker for mitosis (n=3). **B.** RPE cells were transfected with control. CSNK1D or CSNK1E siRNA and Nocodazole was added 12 h before collecting the cells by mitotic shake-off. Whole cell lysates probed with indicated antibodies. **C.** U2Os cells were trapped in mitosis by overnight treatment with Nocodazole or PLK1 inhibitor BI2536 (100 nM) and collected by mitotic shake-off. Part of the Nocodazole arrested cells was further treated with CK1 inhibitor PF670462 (1 μM) for 60 min. Whole cell lysates were probed with indicated antibodies. Staining for pS10-H3 served as a marker of mitosis.

To confirm the ability of CK1δ to phosphorylate FAM110A in the specified regions responsible for their binding, we used purified EGFP-FAM110A-WT along with the ΔC and ΔPro mutants to perform a kinase assay (**Figure 38-C**). We found an induction of a similar mobility shift in the WT and ΔPro but not in the ΔC mutant showing that while CDK1 phosphorylates the N-terminal domain of FAM110A, CK1δ does it in the C-terminal domain (**Figure 38-A, B**). Through this results we concluded that CK1 interacts and phosphorylates FAM110A in its C-terminal domain during mitosis even though FAM110A's aminoacid sequence lacks the canonical consensus phosphorylation motifs for CK1δ. Nevertheless, data obtained from the PhosphoSitePlus database showed two phosphorylated regions within human FAM110A C-terminal domain, specifically the S189-192 and S252-255 residues that could correspond to non-canonical phosphorylation motifs for CK1 (Flotow, Graves et al. 1990, Hornbeck, Zhang et al. 2015). By generating stable cell lines expressing this two mutants, we observed that out of the two motifs, only S252-255 substitution to alanines affected FAM110A mobility in mitosis while S189-192 substitution had no apparent

effect over it (**Figure 39-A**). Concomitantly with this, incubation of purified EGFP-FAM110A-S252-255 with active CK1δ in presence of hot ATP showed to have a reduced mobility shift as well as less ATP incorporation compared to the WT variant (**Figure 38-D**), although the observed incomplete reduction of the phosphate incorporation in the in vitro assay might mean that additional residues are phosphorylated by CK1 in FAM110A C-terminal domain.

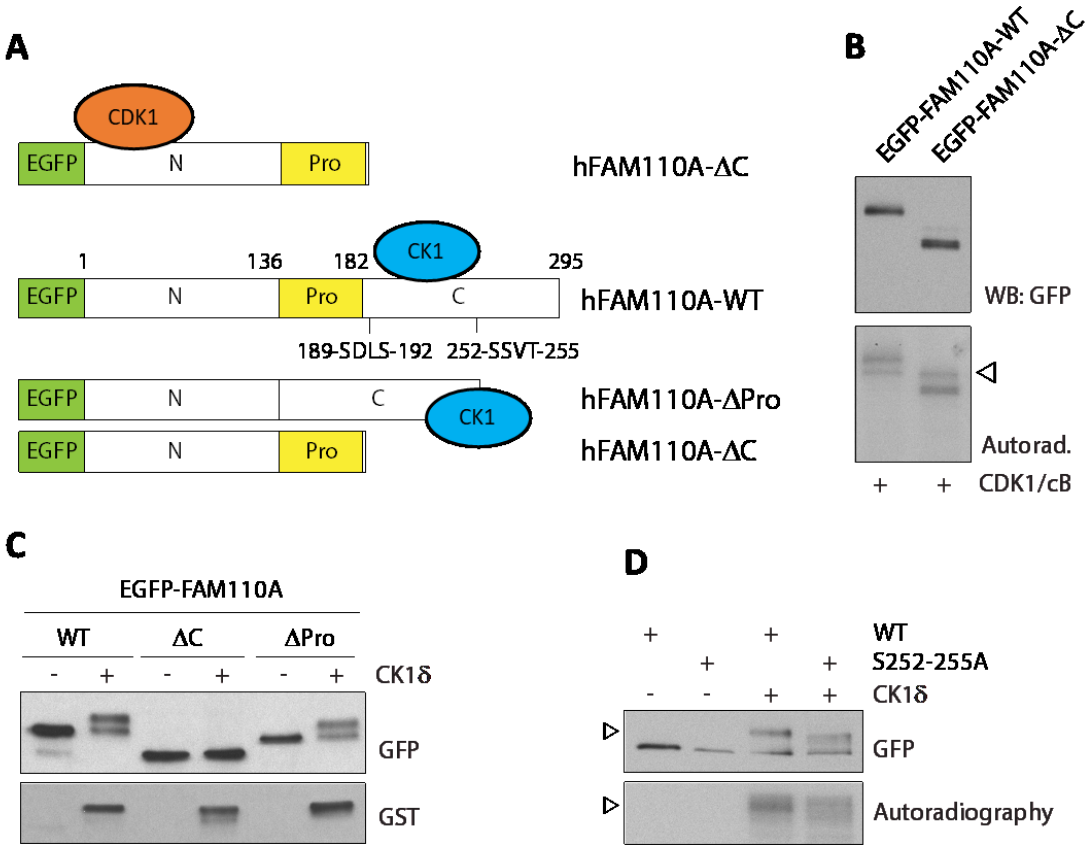

Figure 38. Mapping FAM110A interaction with CDK1 and CK1 A. Diagrams of truncated mutants used to map interaction with CDK1 and CK1, the two Kinases identified interacting with FAM110A. **B.** Isolated EGFP-FAM110A-WT or ΔC proteins were incubated with active CDK1/GST-cyclin B1 in a kinase buffer containing 32P-γATP for 20 min at 30°C. Phosphorylation was detected by autoradiography and position of FAM110A by immunoblotting. Empty arrowhead indicates position of CDK1. Mobility of the proteins was analyzed by immunoblotting (n=2). **C.** EGFP-FAM110A-WT, -ΔPro or -ΔC proteins isolated from transfected HEK293 cells using GFP-trap were incubated with mock or with active GST-CK1δ for 20 min at 30°C. Mobility of the proteins was analyzed by immunoblotting (n=2). **D.** Isolates EGFP-FAM110A –WT or -S252-255A proteins were incubated with mock or with active GST-CK1δ in the presence of 32P-γATP for 30 min at 30°C. Phosphorylation of the substrate was detected by a mobility shift in immunoblotting with anti-GFP antibody or by autoradiography. Empty arrowhead indicated the same position on SDS-PAGE gel.

A non-canonical motif sequence (K/R-X-K/R-X-X-S/T) has been reported to be phosphorylated by CK1δ in several sulfatides and cholesterol-3-sulfate binding proteins (Kawakami, Suzuki et al. 2008) There are 3 putative sites in FAM110A that resemble this non-canonical motif. This observation may suggest that CK1δ is capable of phosphorylating Ser/Thr residues that lack any specific sequence motif (Fulcher and Sapkota 2020), and that in the case of FAM110A could be regulated by other factors, such as its subcellular distribution, previous priming phosphorylations and even the stage of the cell cycle. Altogether this results confirm that CK1 phosphorylates FAM110A during mitosis, specifically in the S252-255 cluster.

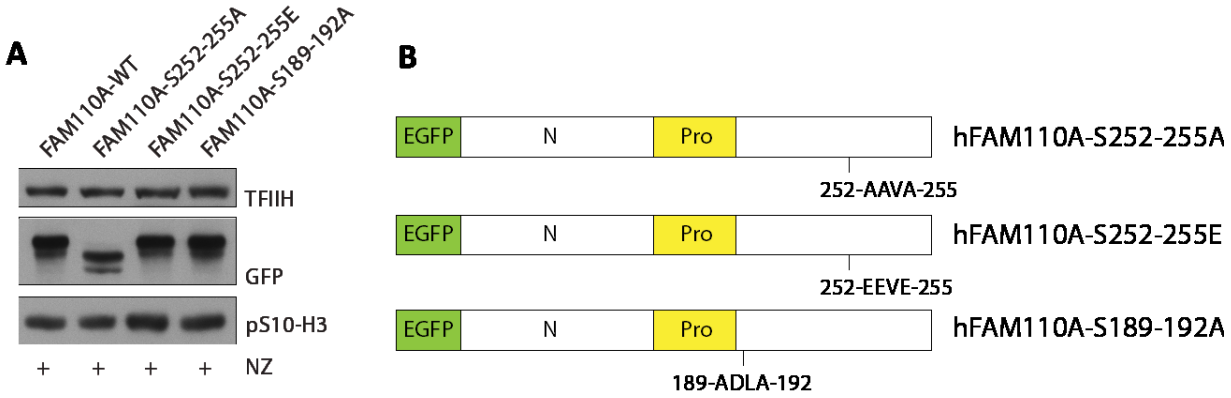

Figure 39. Phosphorylation of key aminoacids (S252-255A) contained within de C-terminal domain of FAM110A is performed by CK1 in mitosis. A. Cells stably expressing EGFP-FAM110A-WT or the listed mutants were arrested in mitosis by Nocodazole and collected by mitotic shake-off. Whole cell lysates were analyzed by immunoblotting (8% SDS-PAGE). **B.** Diagrams of point mutations generated in FAM110A sequence; Serine residues S252, S253 and S255 were mutated to alanines, making this motif non-CK1 phosphorylatable (top panel).This same Serine residues were mutated to glutamic acid, which mimics the phosphorylation (middle panel). Serine residues S189 and S192 were also mutated to alanines, as this were also hipothesized to be targeted by CK1 (bottom panel).

4.2.7 Phosphorylation of FAM110A by CK1 controls its function in mitosis

In order to uncover the functions of FAM110A along with CK1 during mitosis, the next step was to compare the impact of their depletion and inhibition over mitotic progression. For this we employed a U2OS stable cell line expressing an EGFP tagged H2B making it an excellent tool for mitosis live imagining without the need of live DNA staining. U2OS-H2B-EGFP were depleted of FAM110A and CK1 activity was inhibited with PF670462; we observed that CK1 inhibition extended the duration of mitosis and caused metaphase misalignment along with segregation errors in a similar manner than that of FAM110A depletion (**Figure 40-A, B**).

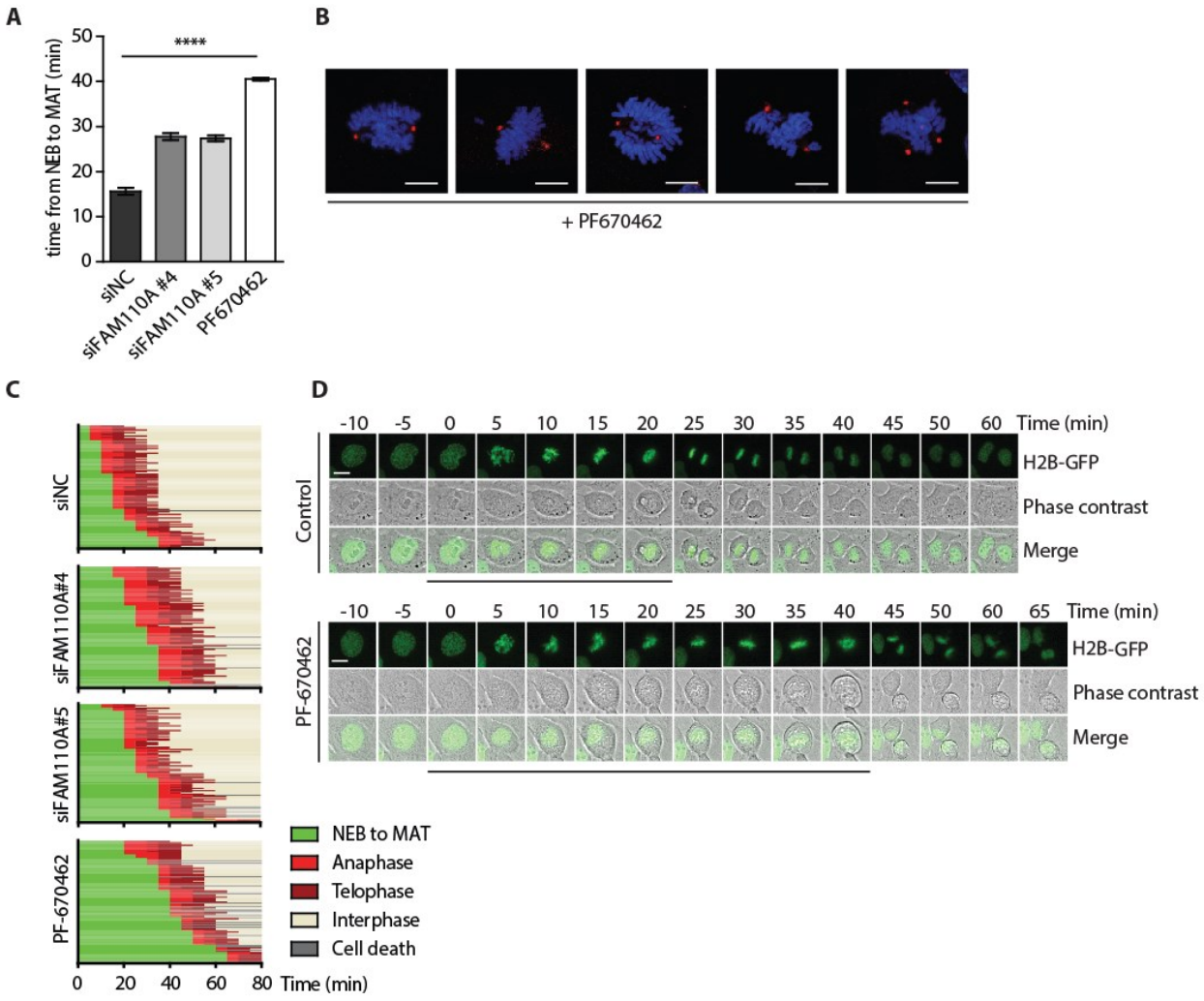

Figure 40. Metaphase delay phenotype caused by FAM110A KD and CK1 inhibition in U2OS-H2B-EGFP cell line. A. U2OS-H2B-EGFP cells were transfected with indicated siRNAs for 48 h or were treated with PF670462 for 12 h and filmed in 5 min intervals for 24 h. time from nuclear envelope breakdown to MAT was quantified in 100 cells. Shown is mean of the medians ±SD (n=3). Statistical significance was determined by ANOVA (**** $p<0.0001$). **B.** Representative panels of impaired chromosomal alignment in metaphase and multipolar spindle after PF670462 treatment. **C.** Progression through mitosis was

categorized in cells from (A) (100/condition) as follows: nuclear envelope breakdown to the metaphase-to-anaphase transition (MAT), anaphase, telophase and interphase. Data from one of three experiments is shown, each bar indicates one cell. Cells that died during imaging are shown in grey. **D.** Representative sequential panels of U2OS-H2B-EGFP cells treated with control or with the PF670462 inhibitor (n=3). Cells were filmed in 5 min intervals; the bellow line marks the panels corresponding to the beginning of NEB (0 min) to the MAT.

In accordance with this results, we noted that extended mitosis was also observed after siRNA mediated depletion of CK1δ and CK1ε in an individual manner, suggesting that both isoforms are involved in mitotic progression regulation (**Figure 41-A, B**).

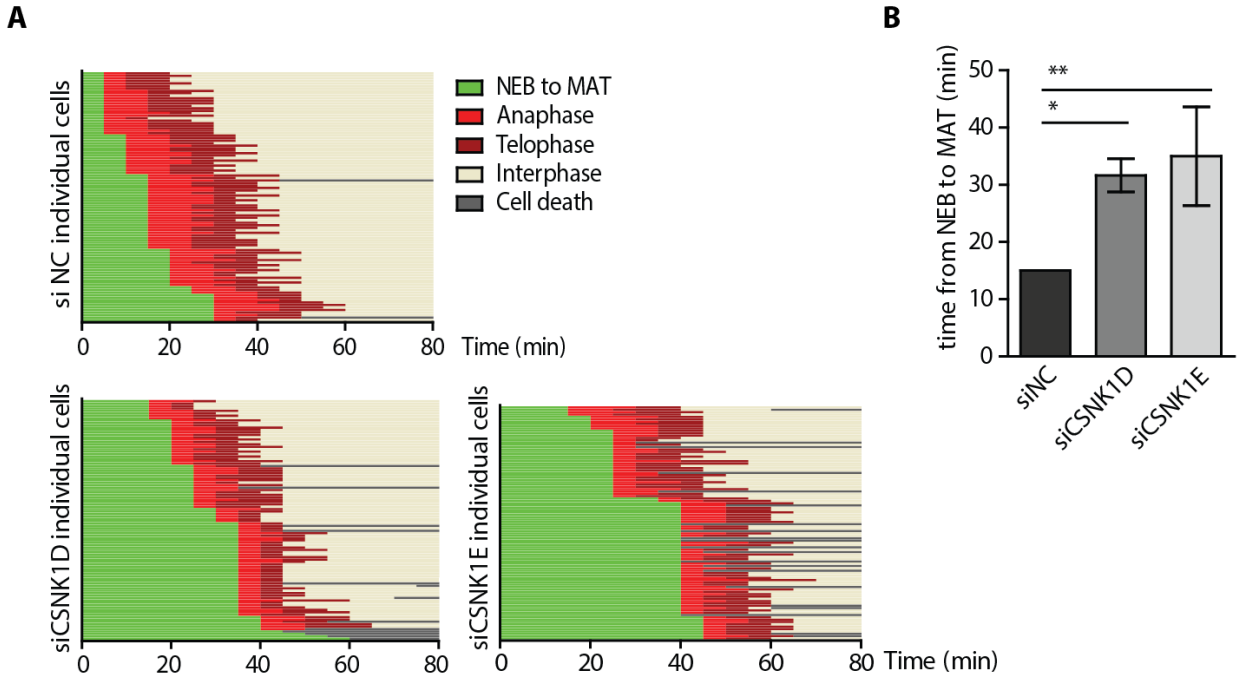

Figure 41. Metaphase delay phenotype caused by CK1δ and CK1ε isoforms KD in U2OS-H2B-EGFP cell line. A. U2OS-H2B-EGFP cells were transfected with control, CK1δ or CK1ε siRNA; after 48 h of transfection, cells were filmed in 5 min intervals for 24 h. Time from NEB to MAT was quantified in 100 cells, shown are plots from one of the three replicates. **B.** Quantification of cells in (A). Shown is mean of the medians ± SD. Statistical significance was determined by ANOVA (n=3).

Encouraged by this observations we decided to test if the CK1-mediated phosphorylation of FAM110A modulates its function during mitosis. In order to accomplish this we generated a series of cell lines that would express the mutant variants (truncations and point mutations) of the FAM110A sequence and assayed their ability to prevent the effects generated by the loss of endogenous FAM110A.

In the first instance, NEB to MAT transition timing was measured as described previously and the mitotic index was measured by flow cytometry (**Figure 42**). This assays revealed that when endogenous FAM110A was depleted and contrary to the RPE parental cell line, cells expressing the ectopic EGFP-FAM110A-WT did not enrich the mitotic population and managed to progress through mitosis with normal speed. In a comparable manner ectopic EGFP-FAM110A-ΔPro mutant rescued the depletion phenotype too, which suggests that the proline-rich stretch is disposable for FAM110A mitotic function (**Figure 42-A, C**). In comparison, ectopic expression of either FAM110A-ΔC, FAM110A-FA or FAM110A-S252-255 mutants showed a significantly increased mitotic population and NEB to MAT delay, comparable to that observed in the RPE parental cell line.

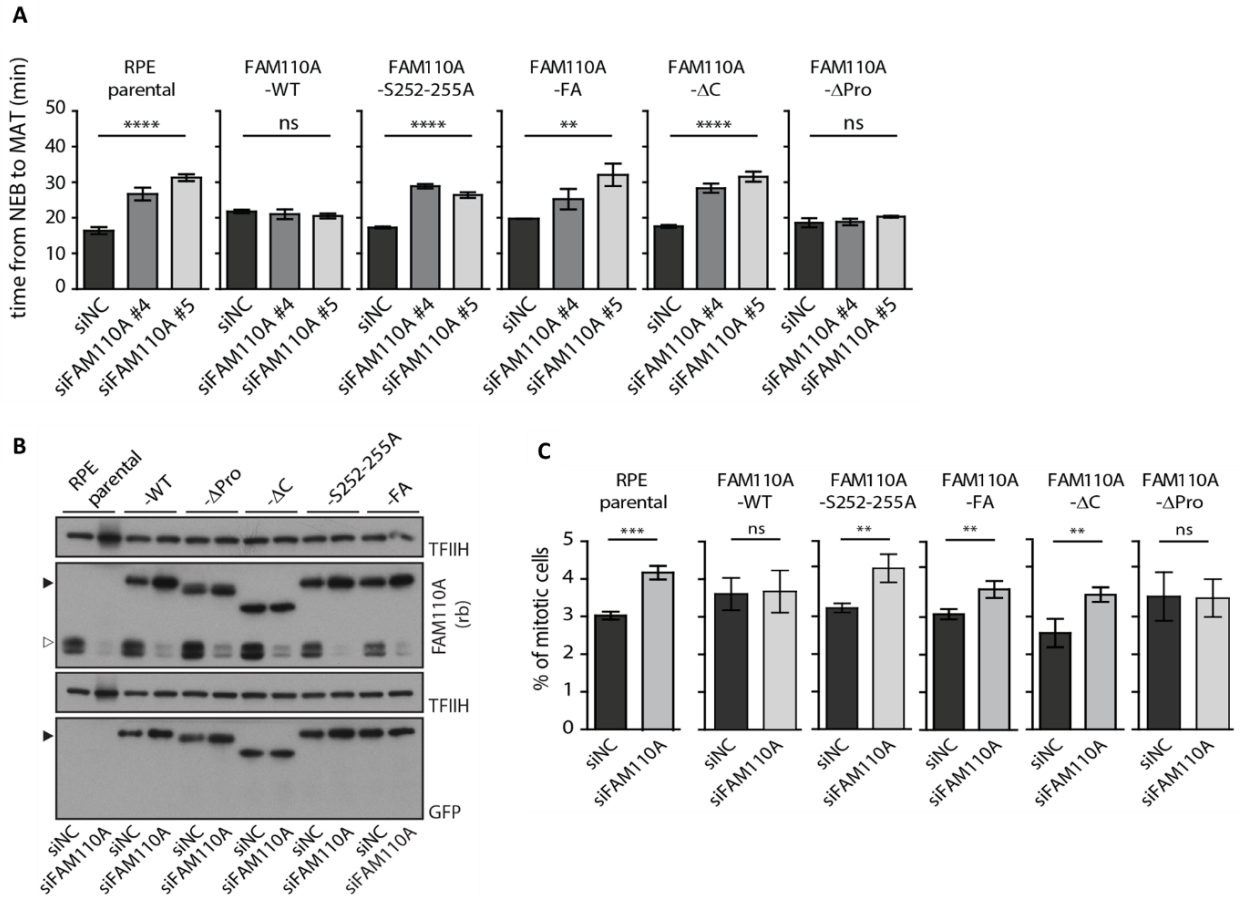

Figure 42. Metaphase delay phenotype caused by FAM110A KD in FAM110A variants stable cell lines. A. RPE parental cells or RPE cells stably expressing the wild-type or indicated mutant EGFP-FAM110A variants were transfected with control (siNC) or two various FAM110A siRNAs and were analyzed by time-lapse microscopy. Plotted are means of the medians of the time from NEB to MAT ±SD. A hundred cells were quantified per condition (n=3). Statistical significance was determined by ANOVA (**** $p<0.0001$, ** $p<0.005$). **B.** Representative Immunoblot analysis of samples from (A). Full arrow indicates migration of the EGFP-FAM110A-WT and other variants, empty arrow indicates endogenous FAM110A. Staining for TFIIH was used as a loading control. **C.** Quantification of the mitotic index from three independent experiments in the A-panel set-up, shown is median ±SD (n=3); statistical significance was determined by ANOVA (** $p<0.005$, *** $p<0.001$).

In the second instance we tested the same FAM110A variants for metaphase chromosomal alignment rescue after endogenous FAM110A and CK1δ siRNA mediated depletion or by CK1 isoforms inhibition (**Figure 43-A, C**). Our results showed that EGFP-FAM110A-WT rescued the metaphase misalignment but failed to rescue the same phenotype but caused by CK1δ depletion; concomitantly, the EGFP-FAM110A-S252-255A mutant failed to rescue the metaphase alignment issues both upon depletion of FAM110A and CK1δ as well as by PF670642 treatment. Contrariwise, we noted that the phosphorylation-mimicking mutant EGFP-FAM110A-S252-255E rescued the metaphase misalignment phenotype in both instances of siRNA mediated depletion of FAM110A and CK1δ and after the PF670642 inhibitor treatment (**Figure 43-A, C**). Upon this observations we concluded that CK1δ controls FAM110A mitotic function by phosphorylating the S252-255 cluster present in its C-terminal domain.

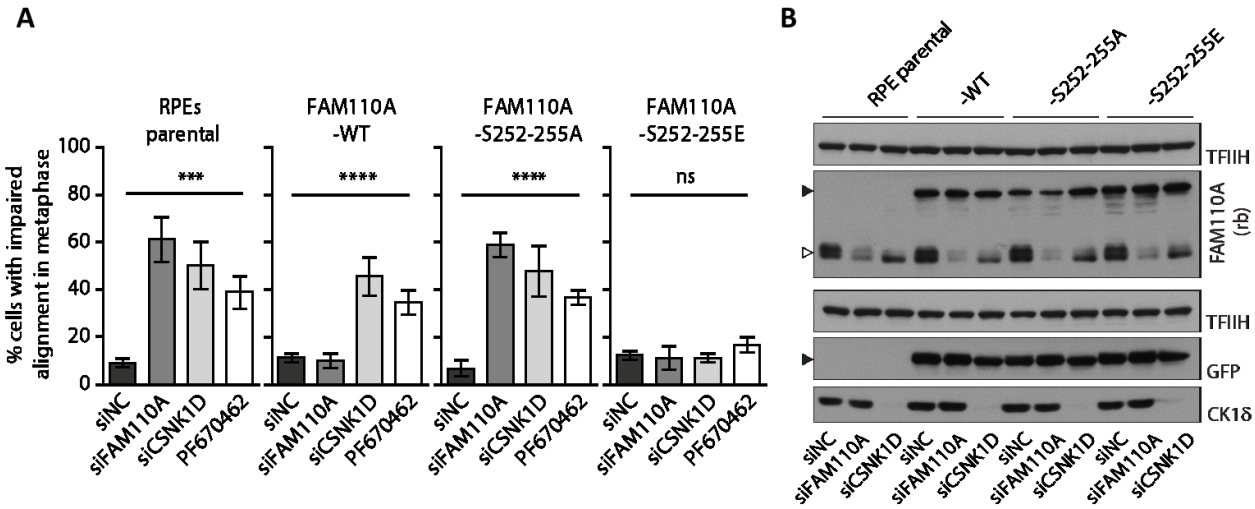

Figure 43. FAM110A-S252-255E rescues chromosome misalignment and disrupted mitotic spindle positioning caused by FAM110A KD and CK1 KD or inhibition. A. RPE parental cells or RPE cells stably expressing indicated EGFP-FAM110A variants transfected with control (siNC), FAM110A or CSNK1D siRNA and grown for 48 h. Alternatively, cells were incubated with PF670462 for the last 12 h. Cells were treated with MG132 for 30 min prior fixation. Impaired chromosomal alignment was scored in >30 metaphase cell per condition. Error bars indicate median ±SD. Statistical significance was determined by ANOVA (n=3) (**** $p<0.0001$, *** $p<0.001$). **B.** Representative Immunoblot analysis of samples from (A and B). Full arrow indicates migration of the EGFP-FAM110A-WT and other variants, empty arrow indicates endogenous FAM110A. Staining for TFIIH was used as a loading control.

Recently a mitotic function has been adjudicated to the CK1 isoforms, specifically involving them in the establishment of the mitotic spindle (Brockman, Gross et al. 1992, Panbianco, Weinkove et al. 2008, Fulcher, He et al. 2019). Originally, it was considered that the longest axis of a cell acted as a determinant for the placement of the spindle axis according to Hertwig's rule, postulated all the way back to 1884 (Rizzelli, Malabarba et al. 2020). However, state-of the art studies have demonstrated the importance of cell anisotropy as a major predictor for mitotic spindle alignment. Moderately anisotropic cells obey Hertwig's rule only partially while symmetrically elongated cells oblige their division along their longest axis; meanwhile, tension and mechanical cell shape deformation represent relevant factors influencing spindle placement as well (van Leen, di Pietro et al. 2020). Taking this into consideration, we wished to investigate the possibility that CK1δ performs specific functions in mitosis through its phosphorylation of FAM110A we employed our U2OS-H2B-GFP cell line to measure the nuclear division axis relative to the longitudinal axis of the cell (**Figure 44-A, C**). We excluded cells that showed a marked anisotropic morphology and focused on cells that presented a clear elongated shape; we observed that control cells did follow Hertwig's rule, while the cells treated with PF670462 or depleted of FAM110A and CK1δ presented an increased angle (>15°) between the long axis and the division axis (**Figure 44-B**) (Tame, Raaijmakers et al. 2016, Fulcher, He et al. 2019). In a similar manner, by analyzing the cell division orientation in the EGFP-FAM110A stable cell line variants, we observed that EGFP-FAM110A-ΔC, EGFP-FAM110A-FA and EGFP-FAM110A-S253-255A failed to rescue the phenotype while EGFP-FAM110A-WT and EGFP-FAM110A-ΔPro rescued it (**Figure 44-D**).

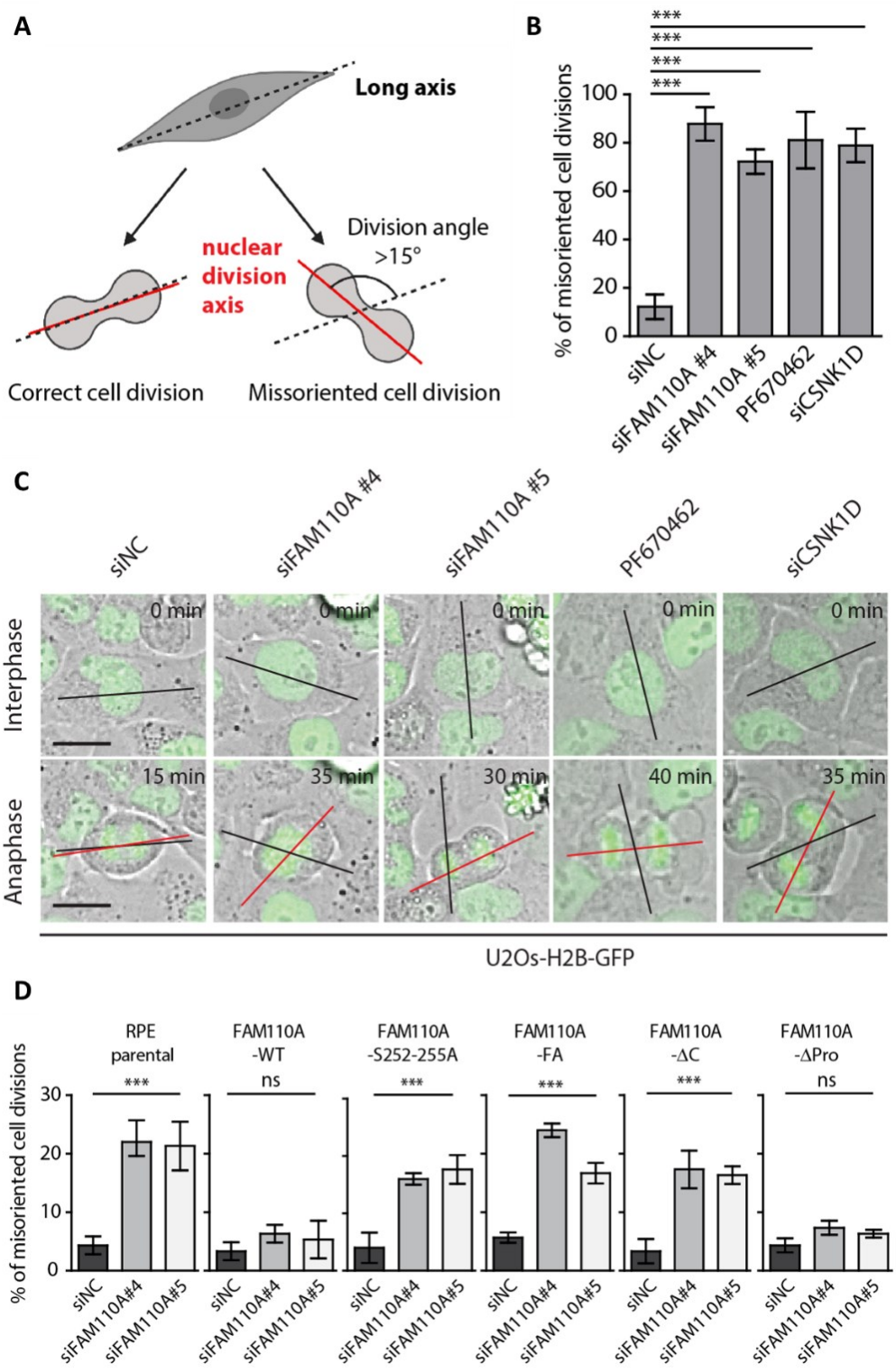

Figure 44. FAM110A and CK1 control the axis of cell division. A. Diagram depicting evaluation of the cell division orientation criteria **B.** Quantification of (C). Angle between the long cellular axis and nuclear division axis was determined from the time-lapse films. Plotted is the percentage of cells exhibiting miss oriented cell division with the angle exceeding ±15°. Thirty cells were quantified per condition (n=3) Statistical significance was determined by ANOVA. Bars indicate median ±SD (*** p>0.001). **C.**

U2OS-H2B-EGFP cells were transfected with control, CK1δ, or two various FAM110A siRNAs and were analyzed by time-lapse microscopy. Alternatively, cells were treated with CK1 inhibitor PF670462 (1 μM) overnight. Angle between the long axis (black line) of each individual cell and axis of the nuclear division in anaphase (red line) was measured. Representative images of interphase cells just before mitotic entry and of anaphase cells are shown. Scale bars indicate 15 μm. **D.** Parental RPE cells or EGFP-FAM110A stable cell line variants that were transfected with control (siNC) or with two different FAM110A siRNAs were filmed and percentage of ells in three independent experiments. Statistical significance was determined by ANOVA. Bars indicate median ±SD (*** $p<0.001$).

To ascertain whether the observed cell division disorientation was a consequence of spindle positioning impairment, we proceeded to measure the angle between the spindle axis and the growth axis as (Toyoshima and Nishida 2007) (**Figure 45-B**). We employed the U2OS-H2B-EGFP cell line by growing them in fibronectin-coated coverslips, depleting them from FAM110A and CK1δ or by inhibiting CK1 activity with PF670462. We detected an increase in the spindle angle after all the treatments (**Figure 45-A**). By employing the EGFP-FAM110A stable cell line variants used in the metaphase misalignment rescue assay but this time to measure their spindle angle degree, we found that after endogenous FAM110A depletion, EGFP-FAM110A-WT and EGFP-FAM110A-ΔPro fully rescued the increased spindle angle (**Figure 45-C, D**). On the other hand the EGFP-FAM110A-ΔC, EGFP-FAM110A-FA and EGFP-FAM110A-S253-255A stable cell lines failed to re-establish the proper spindle positioning angle (**Figure 45-E**). Based in this observation, we pondered the possibility of CK1δ controlling the mitotic spindle orientation through FAM110A phosphorylation. On first instance we noted that EGFP-FAM110A-WT successfully rescued spindle angle after FAM110A depletion but failed to do so when CK1δ was depleted or the CK1 isoforms were inhibited. Interestingly, we found that the EGFP-FAM110A-S252-255E cell line that mimics a phosphorylated FAM110A had a normal spindle angle both after depletion of CK1δ or after inhibition of the CK1 isoforms (**Figure 45-E**). Based on this exciting observations, we concluded that FAM110A interacts with and it's phosphorylated by CK1δ, and that said interaction is needed for key mitotic processes, such as correct chromosomal alignment during metaphase, thus allowing a correct positioning of the mitotic spindle which in turn permits correct segregation of sister chromatids.

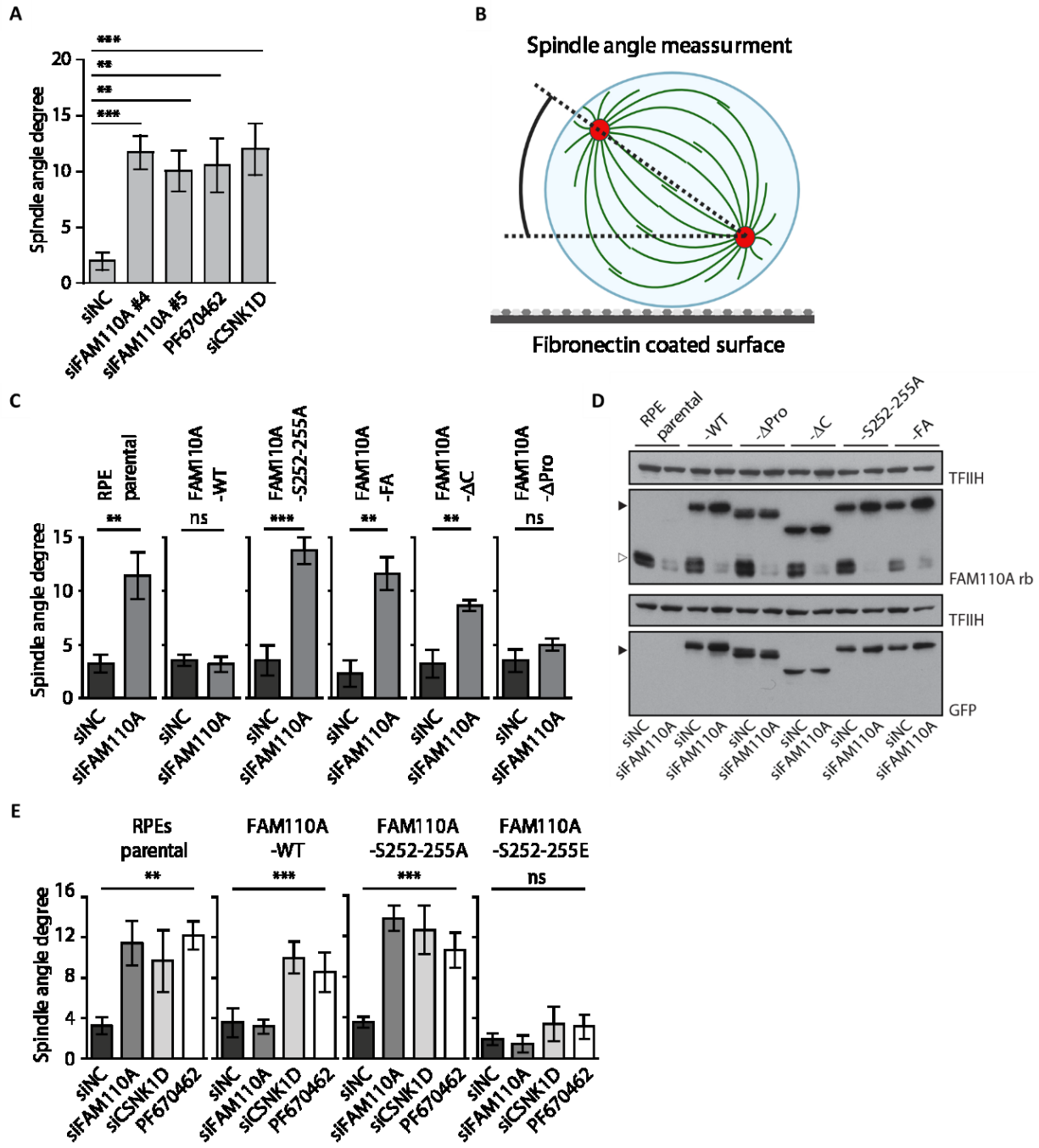

Figure 45. FAM110A and CK1 independent KD or inhibition indirectly cause disruptions in correct mitotic spindle positioning. A. RPE cells transfected with control, CK1δ, or two various FAM110A siRNAs and cells treated with PF670462 were fixed after 48 h stained for γ-tubulin and metaphase cells were imaged by confocal microscopy (Z-stacks 0.5 µm). Plotted is a mean of medians of the spindle angle degree determined by the elevation of the spindle axis and growth axis parallel to surface. A total of 30 cells were quantified per condition. Statistical significance was determined by one-way ANOVA (n=3). Bars indicate median ±SD (*** p<0.001, ** p<0.005). Diagram depicts the spindle angle measurement. **B**. Diagram that exemplifies how the spindle angle degree was measured. **C.** RPE parental cells or RPE cells stably expressing the wild-type or indicated mutant EGFP-FAM110A variants were transfected with control or two various FAM110A siRNAs, fixed after 48 h and stained for γ-tubulin.

Metaphase cells were imaged by confocal microscopy (z-stacks 0.5 μm) and spindle angle between the spindle axis and growth axis was determined. Plotted is a mean of medians from three repeats where 30 cells were imaged for each condition. Error bars indicate median ±SD. Statistical significance was determined by (ANOVA) (n=3) (*** $p>0.001$, ** $p<0.005$). **D.** Representative Immunoblot analysis of samples from (A). Full arrow indicates migration of the EGFP-FAM110A-WT and other variants, empty arrow indicates endogenous FAM110A. Staining for TFIIH was used as a loading control. **E.** RPE cells or RPE cells stably expressing the wild type FAM110A, -252-255A or -252-255E mutants were transfected with control, FAM110A or CSNK1D siRNAs. In parallel, cells were treated with PF670462 (1 μM) for 12 h.

After obtaining this interesting information on FAM110A function in the mitotic spindle alongside CK1δ, we wished to investigate if there might be a connection between the observed metaphase misalignment and spindle orientation defect upon FAM110A depletion or phosphorylation obstruction. A recent report on the LGN protein (also known as GPSM2), a motif protein that interacts with dynein during spindle positioning in metaphase, showed to be displaced if chromosomes get in close proximity to the plasma membrane during metaphase (Kiyomitsu and Cheeseman 2012). When performing depletion of endogenous FAM110A on the HeLa-LGN-GFP cell line, we noted that metaphase cells treated with control siRNA presented a normal metaphase alignment and symmetrical distribution of GFP tagged LGN (**Figure 46-A**), while the ones treated with siRNA against FAM110A showed displacement of GFP-LGN signal when misaligned chromosomes where in proximity to the plasma membrane (**Figure 46-B**). Altogether this results imply that the impaired spindle orientation observed in FAM110A-depleted cells might by a secondary effect, consequence of the misaligned chromosomes triggering LGN displacement.

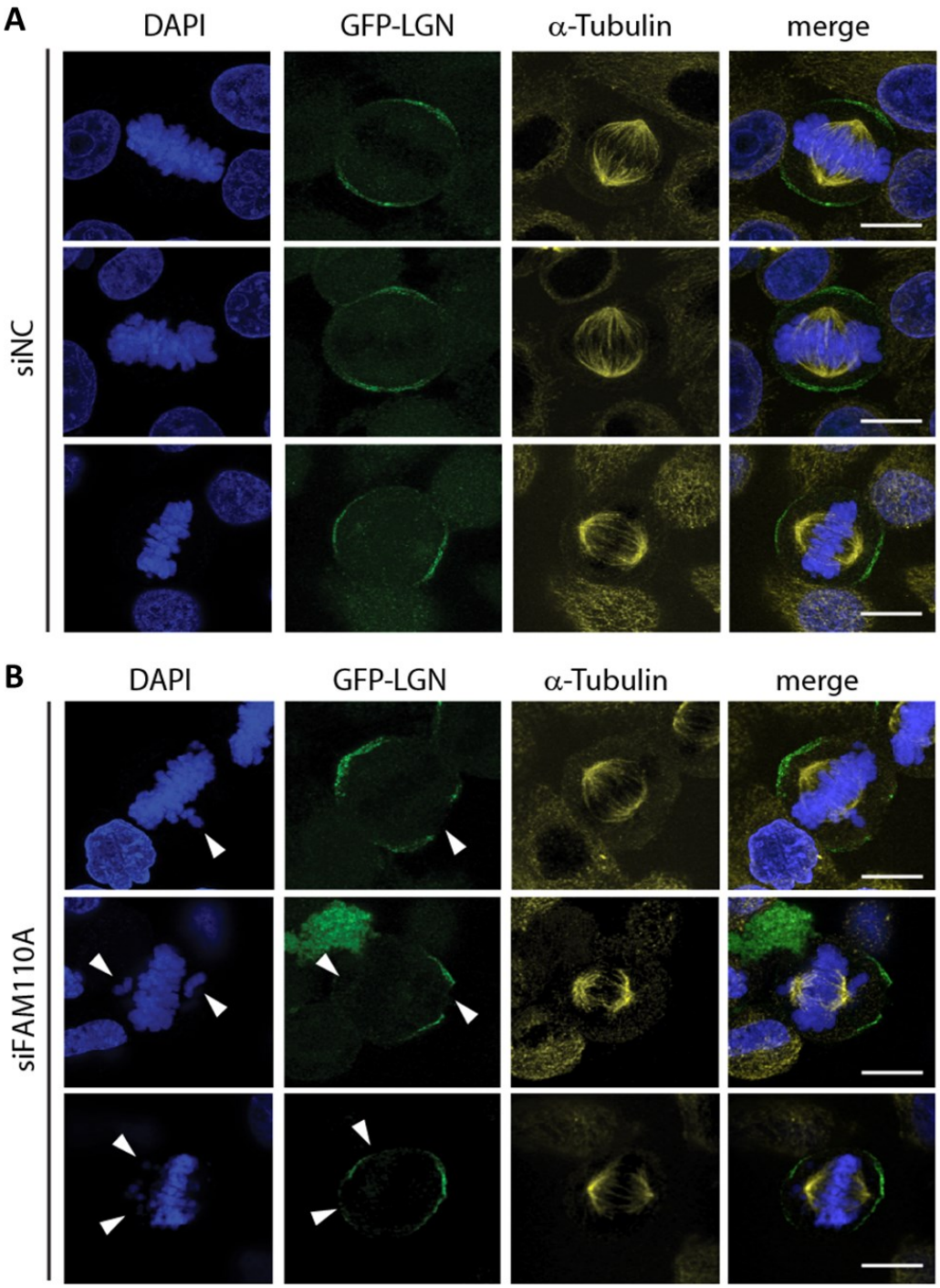

Figure 46. FAM110A and CK1 control the axis of the cell division. A. HeLa cells stably expressing GFP-LGN were transfected with control siRNA. **B.** HeLa cells stably expressing GFP-LGN were transfected with FAM110A siRNA, fixed after 48 h and imaged by confocal microscopy. Shown are maximal projections of de-convoluted z-stack images from representative metaphase cells. Arrowheads show regions with a low level of GFP-LGN. Scale bars indicate 10 µm.

4.2.8 CK1-dependent phosphorylation of FAM110A promotes its interaction with mitotic spindle

So far, our results have shown that FAM110A is phosphorylated in the C-terminal domain by CK1 and that said C-terminal domain is responsible for tubulin binding (**Figure 35-B**). Parting from this premise we hypothesized that interaction and phosphorylation of FAM110A by CK1δ or both CK1 isoforms could control its ability to localize to the mitotic spindle trough tubulin interaction. In agreement with this we found that depletion of CK1δ trough siRNA prevented endogenous FAM110A to localize to the spindle poles (**Figure 47-A, B**). Interestingly, treating the cells with the CK1 inhibitor PF670462 reduced further endogenous FAM110A enrichment in the spindle poles, presenting the possibility of a combined inhibition of CK1δ and CK1ε effect. It was also possible to observe metaphase impairment after CK1 depletion or inhibition (**Figure 47-A**).

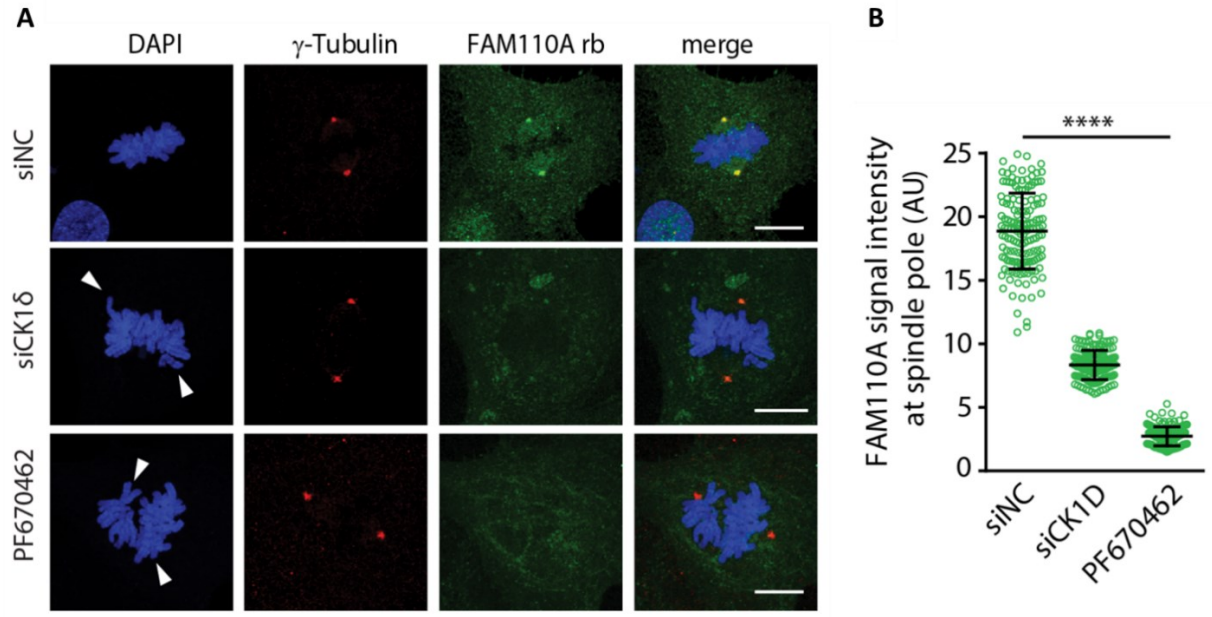

Figure 47. CK1 knock-down or inhibition prevents FAM110A localization to the mitotic spindle. A. RPE parental cells were transfected with control siRNA or CSNK1D siRNA or were treated with PF670462. MG132 inhibitor was added for 30 min prior fixation. Cells were probed with rabbit polyclonal to FAM110A and mouse monoclonal to γ-tubulin. Representative images are shown, scale bars indicate 10 µm. **B.** Quantification of (A). Plotted is median FAM110A endogenous intensity at spindle poles positive for γ-tubulin ±SD. Each dot represents a single pole. Statistical significance was determined by ANOVA (n=3) (**** $p<0.0001$).

Next, we wished to elucidate the intracellular localization of our previously analyzed EGFP-FAM110A variants. By performing confocal microscopy on the EGFP-FAM110A-WT and the truncated and point mutated variant cell lines we managed to observe their intracellular behavior, presenting a pattern that seemed to coincide with their CK1 interaction capacity (**Figure 48-A**). With the intention to assert this first

hand observation, we performed signal intensity quantification at the spindle poles (**Figure 48-B**). As expected, EGFP-FAM110A-WT enriched at the mitotic spindle poles. It was interesting to see that the EGFP-FAM110A-C fragment presented a comparable enrichment at the poles, indicating that the C-terminal domain of the protein is enough to promote its binding to microtubules. On the contrary, the CK1-binding deficient EGFP-FAM110A-FA mutant bestowed low spindle pole enrichment. This observation was concomitant to that of the truncated variant EGFP-FAM110A-ΔC, which presented the same low enrichment due to its lack of CK1 binding domain. Along this line it was very interesting to see that the spindle pole enrichment of the EGFP-FAM110A-S252-255A mutant was also significantly reduced, although in a lesser manner that the -FA and -ΔC mutant. However the phosphorylation mimicking mutant EGFP-FAM110A-S252-255E presented a comparable enrichment in the spindle poles such as the –WT variant.

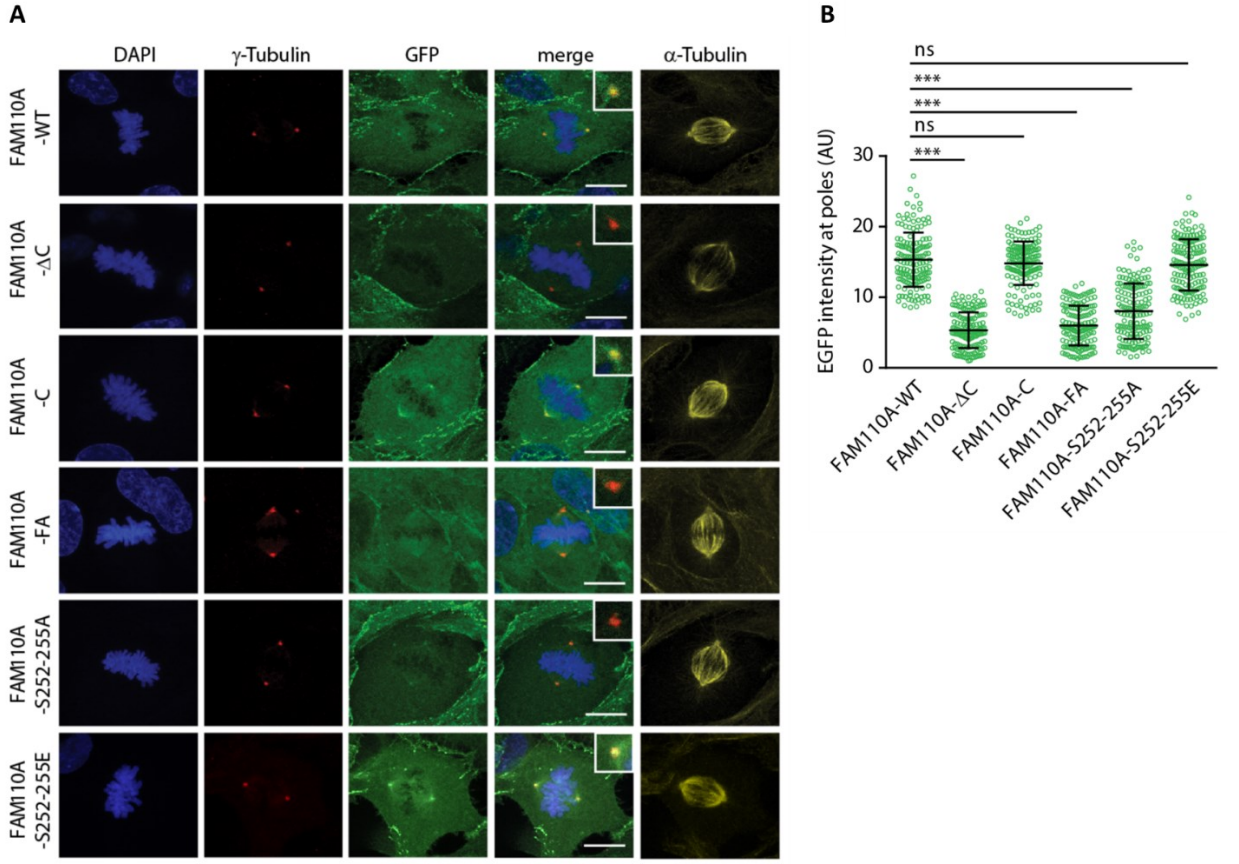

Figure 48. CK1-dependent phosphorylation of FAM110A promotes its interaction with mitotic spindle. A. Cells expressing the wild-type or mutant EGFP-FAM110A were fixed and stained for γ-tubulin and α-tubulin and analyzed by confocal microscopy (z-stack 0.16 μm). Representative images of maximal projections of the metaphase cells are shown. Scale bars indicate 10 μm. Merged images show signal of DAPI, γ-tubulin and EGFP. Insets show a single Z plane at the spindle pole. **B.** Quantification of (A). Plotted is median EGFP intensity at spindle poles positive for γ-tubulin ± SD. Each dot represents a single spindle pole. Statistical significance was determined by ANOVA (n=3) (*** $p<0.001$).

As mentioned before, the localization patterns of this stable cell lines matched with the CK1 binding capacity we have been discussing in an intensive manner trough out this work. Therefore the next step was to establish if the CK1 phosphorylation-targeted S252-255 motif had an essential role in FAM110A intracellular localization and function. For this purpose the EGFP-FAM110A-WT and the EGFP-FAM110A-S252-255E stable cell lines were treated with the PF670462 inhibitor and imaged trough confocal microscopy for visual assessment and intensity quantification (**Figure 49-A, B**). We observed that treatment of cells with the CK1 inhibitor PF670462 prevented EGFP-FAM110A-WT to properly localize to the spindle poles and that on the contrary, PF670462 treatment did not affect localization of the phosphorylation mimicking mutant EGFP-FAM110A-S253-255E. Following trough, we tested the impact of CK1-dependent phosphorylation of FAM110A over its capacity to bind with tubulin trough an immunoprecipitation assay (**Figure 49-C**). The obtained data showed that CK1-inhibition prevented the interaction between the ectopic EGFP-FAM110A-WT and tubulin; meanwhile this inhibition did not affect EGFP-FAM110A-S252-255E capacity to bind to tubulin. Added to this, EGFP-FAM110A-S252-255A failed to interact with tubulin, even in non-CK1-inhibited conditions. Altogether, this results helped us to conclude that CK1-mediated phosphorylation of the S252-255 residues is key for FAM110A interaction with the mitotic spindle, however we do not discard the possibility that additional phosphorylation sites might be also key regulators of FAM110A interaction with the mitotic spindle microtubules.

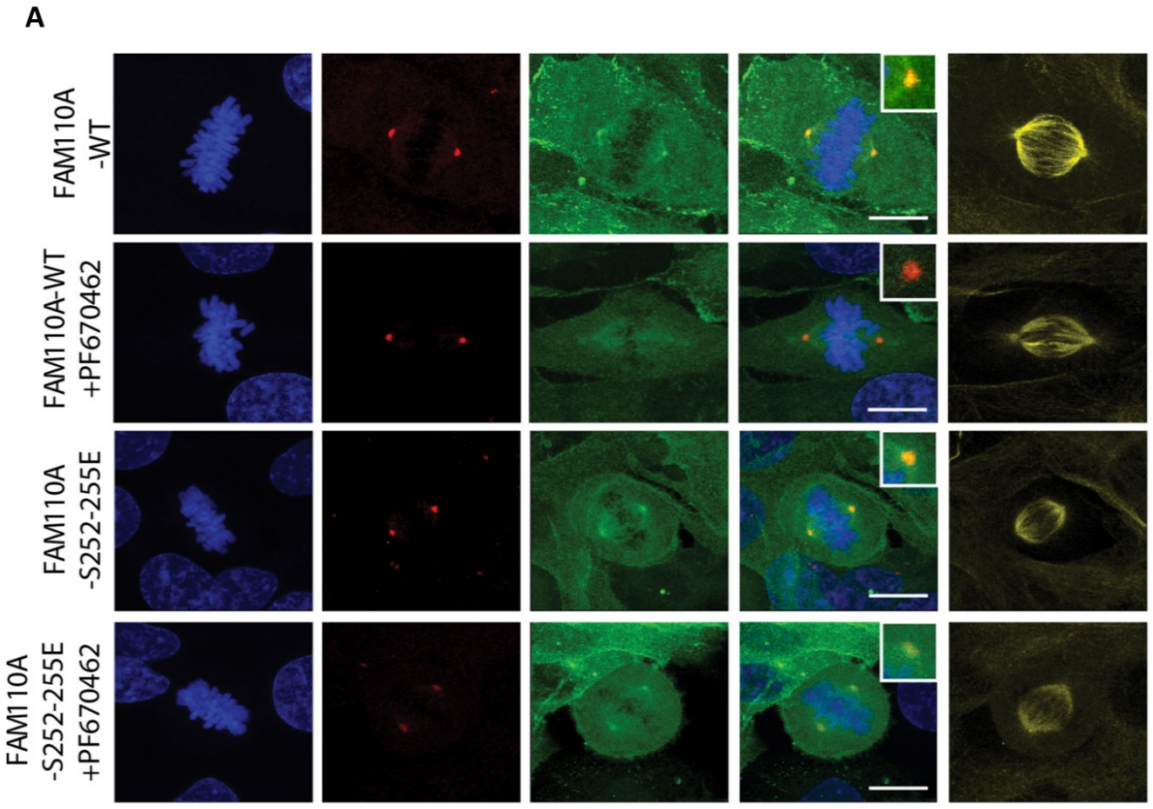

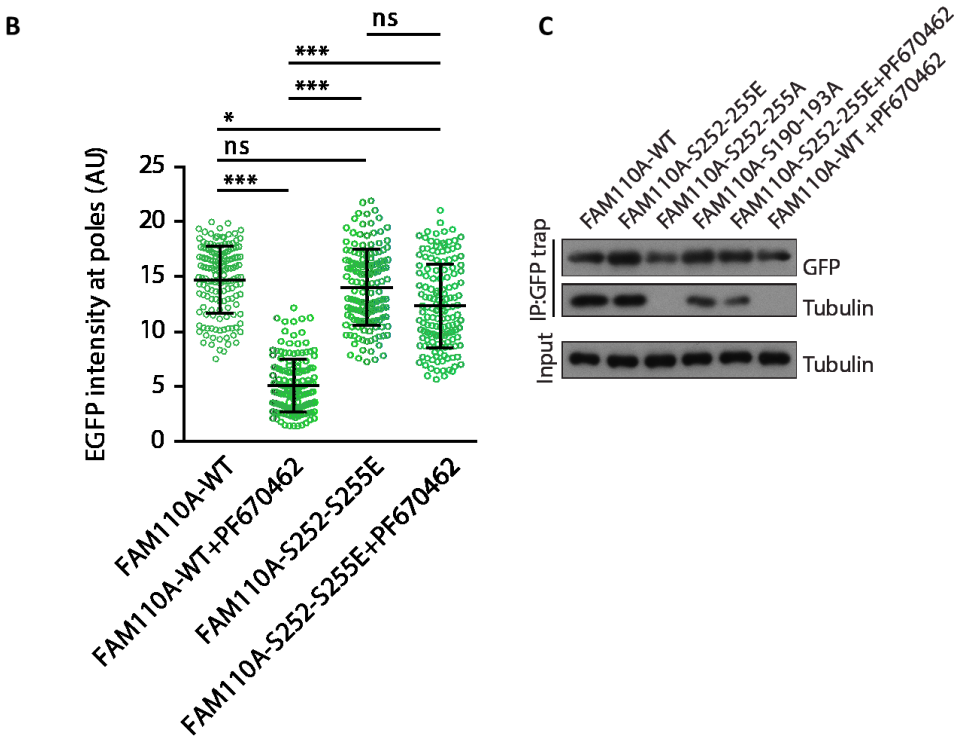

Figure 49. CK1-dependent phosphorylation in the 252-255 serine-motif is key for its localization to mitotic spindle and it's binding with tubulin. A. RPEs cells expressing the wild-type FAM110A or FAM110A-S252-255E mutant were treated with DMSO or with PF670462 for 6 h and were stained and images as in (Fig.22 A). **B.** Quantification of (A). Plotted is median EGFP intensity at spindle poles positive for γ-tubulin ± SD/ Each dot represent a single spindle pole. Statistical significance was determined by ANOVA (n=3) (*** $p<0.001$, * $p<0.05$). **C.** HEK293 cells transfected with indicated constructs were treated or not with PF670462 for 6 h. Pull down from cell extracts was performed using GFP trap and binding of tubulin was determined by immunoblotting (n=2).

Next, we wished to investigate FAM110A's previously observed ability to bind with actin. At first instance we tested if the FAM110A-252-255A or the FAM110A-FA mutants had any effect over the interaction with actin; we confirmed that this mutants impaired tubulin interaction but had no effect over actin interaction (**Figure 50**). Concomitantly, the interaction pattern was conserved for the other FAM110A interactors: α/β-catenin and α-actinin (**Figure 50**). Based on this observations we concluded that actin binding is entirely regulated through the N-terminal domain of FAM110A (**Figure 36**).

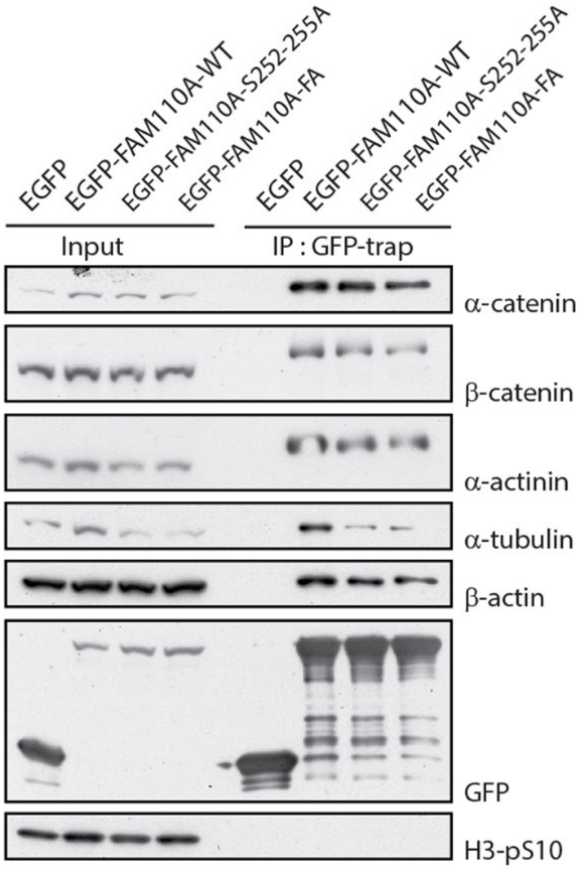

Figure 50. Assessment of point mutations (-S252-255 and -FA) effect on actin binding through immunoprecipitation assay. HEK293 cells were transfected with EGFP, EGFP-FAM110A-WT, EGFP-FAM110A-S252-255A and EGFP-FAM110A-FA. Cell extracts were immunoprecipitated with GFP Trap and binding of interactors was determined by immunoblotting (n=3).

Previously we observed that Tubulin binding pattern was opposite to that of Actin, having the C-terminal domain binding Tubulin and the N-terminal domain binding Actin (**Figure 36**). So in order to understand in more detail the interaction of FAM110A with Actin we generated new truncation mutants in the N-terminal domain to map the actin-binding site. The first mutant lacks aminoacids ranging from sites 1 to 136 (Δ1-136), the next truncations lacked the 1-43 residues (Δ1-43) and the 1-8 residues (Δ1-8); all of the mutants still contained the Proline rich region (**Figure 51-A**).

By implementing immunoprecipitation assays we observed that the Δ1-136 and Δ1-43 mutants failed to interact with actin but the Δ1-8 mutant had no issues binding to it; interestingly the α/β-catenin and α-actinin followed the same binding trend as actin while all of the mutants bound tubulin normally (**Figure 51-B**).

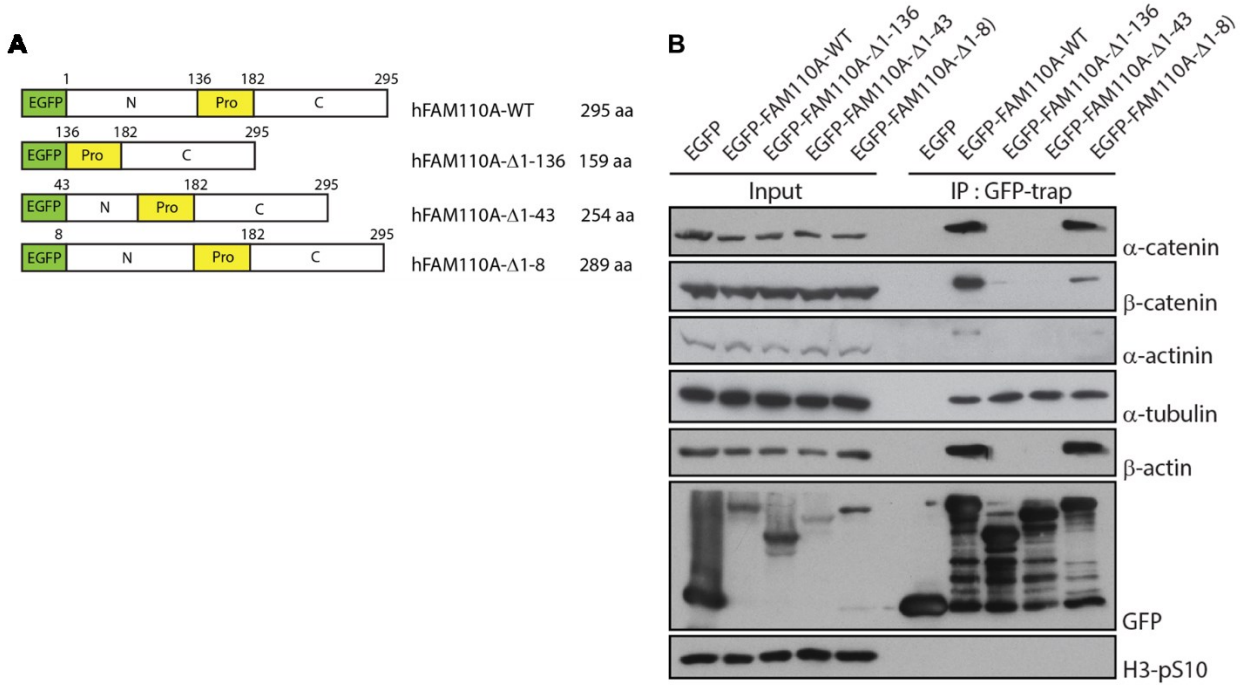

Figure 51. Mapping of FAM110A acting binding site through truncation mutants by immunoprecipitation assays. A. Schematic representation of the EGFP-FAM110A mutant constructs used for actin binding site mapping. Numbering is based in human FAM110A. "N", "C" and "Pro" represent N-terminal, C-terminal and Proline rich domains respectively. **B.** HEK293 cells were transiently transfected with indicated constructs and after 36 hours were arrested in mitosis with NDZ. 12 hours later cells were lysed in CO-IP buffer. Cell extracts were immunoprecipitated with GFP-trap (ChromoTek) and probed by immunoblotting; (n=3).

By analyzing the predicted protein structure of FAM110A, we observed that the N-terminal region contained a predicted α-helix structure ranging from the residues Lys-39 to the Glu-65 (**Figure 52-A**). Mutant Δ1-136 failed to bind actin since it lacks the complete N-terminal domain, and Δ1-43 mutant failed to bind to it probably because the after mentioned α-helix structure is lacking 4 residues that might be important for proper protein folding (**Figure 52**).

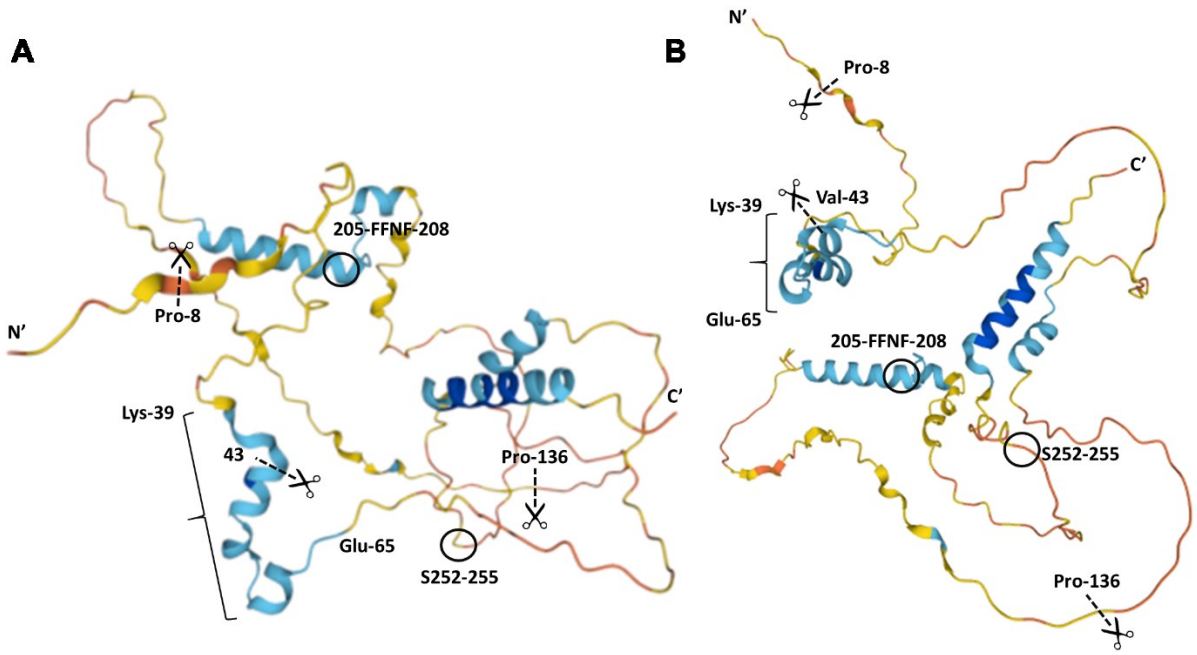

Figure 52. FAM110A predicted protein structure (AlphaFold). A. FAM110A predicted protein structure observed from its left side. Pointed lines with scissors show the places where the mutants were cut. Residues Lys-39 to Glu-65 composed a predicted α-helix that could be a putative binding site for actin. **B.** FAM110A predicted protein structure observed from bellow.

After analyzing the actin-binding capacity of this mutants through immunoprecipitation we asked if impairment of FAM110A's ability to bind actin could affect its intracellular localization. In order to answer this we used RPE cells to generate stable cell lines with the FAM110A-Δ1-136 and FAM110A-Δ1-8 and used them alongside the FAM110A-WT stable cell line to perform immunofluorescence assays in metaphase cells (**Figure 53-first panel**). It was possible to observe an enrichment of FAM110A-WT in the plasma membrane and stress fibers that appear to overlap partially with the signal from the phalloidin-labelled actin in the actomyosin ring. For the FAM110A-Δ1-136 and FAM110A-Δ1-8 mutant stable cell lines it was possible to see a clear mitotic spindle localization in both cases which coincides with the ability of both mutants to bind tubulin; however in the case of the FAM110A-Δ1-136 mutant the enrichment in the plasma membrane was lost, we attribute this to the fact that this mutant is incapable of binding actin (**Figure 53-second panel**).

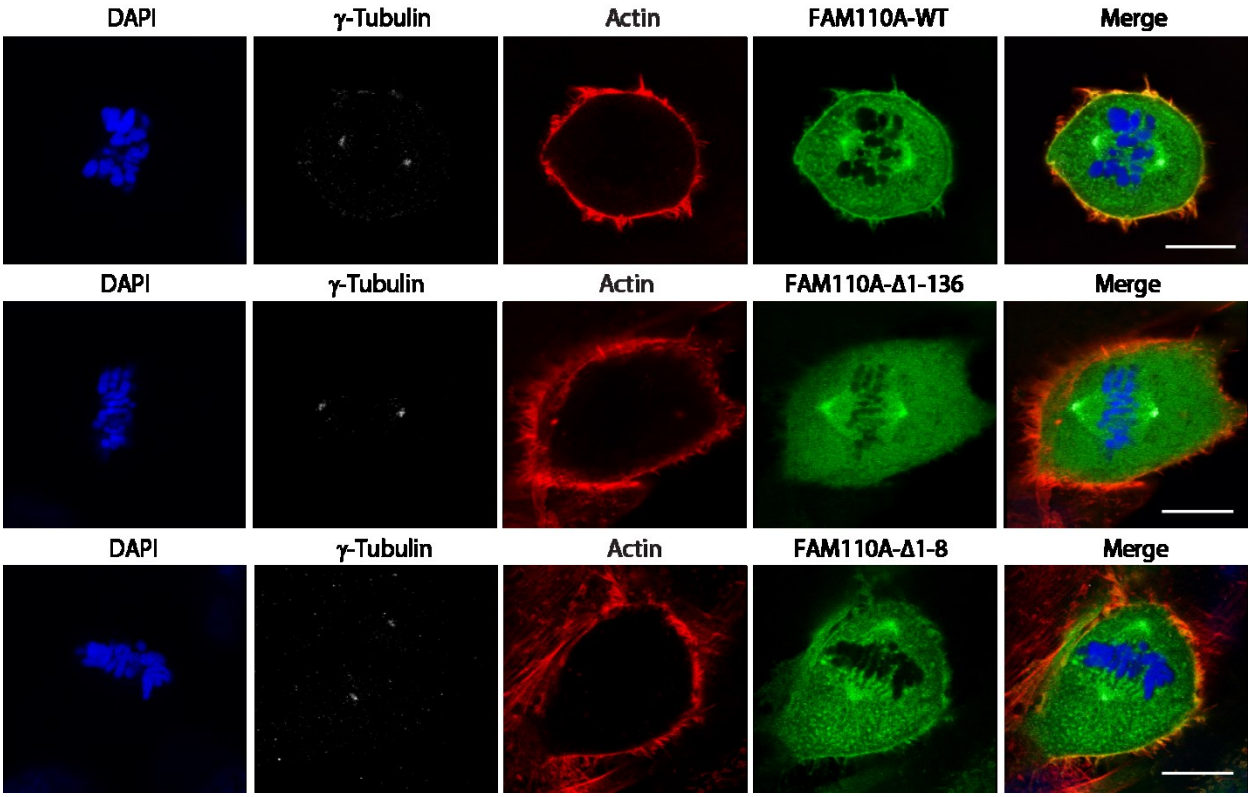

Figure 53. EGFP-FAM110A-WT localizes to mitotic spindle and to the plasma membrane; the N-terminal domain of FAM110A is disposable for localization to the mitotic spindle but needed for plasma membrane localization enrichment. FAM110A-WT, FAM110AΔ1-136 and FAM110AΔ1-8 (EGFP) stable cell lines were fixed, probed with a mouse monoclonal antibody for γ-tubulin detection (grey) and probed with phalloidin-568 for actin detection (red). Shown are single stacks of representative metaphase cells. Scale bars indicate 10 µm.

Previously we observed that FAM110A binds to actin exclusively during mitosis (**Figure 34-A**), therefore we decided to investigate if this interaction could have any relevancy in the metaphase misalignment phenotype we reported previously. For this purpose we used the after mentioned cell lines to knock down FAM110A through siRNA and analyzed the metaphase alignment phenotype (**Figure 54-AError! Reference source not found.**). After 48 hours of transfection, cells were treated with MG132 inhibitor to generate a tight metaphase plate and the misaligned chromosomes where scored. A total of 30 cells per cell line, per condition where counted. We observed that both WT and -Δ1-8 rescued the chromosomal misalignment observed in the EGFP cells and that the -Δ1-136 stable cell line showed significantly more misalignment metaphases. This led us to believe that FAM110A actin-binding is relevant during metaphase and that it's mitotic function it's not exclusive to tubulin binding. We also analyzed the effects of FAM110A depletion in this cell lines through FACS and observed a mitotic population enrichment following the same trend as the metaphase misalignment prevalence (**Figure 54-B**).

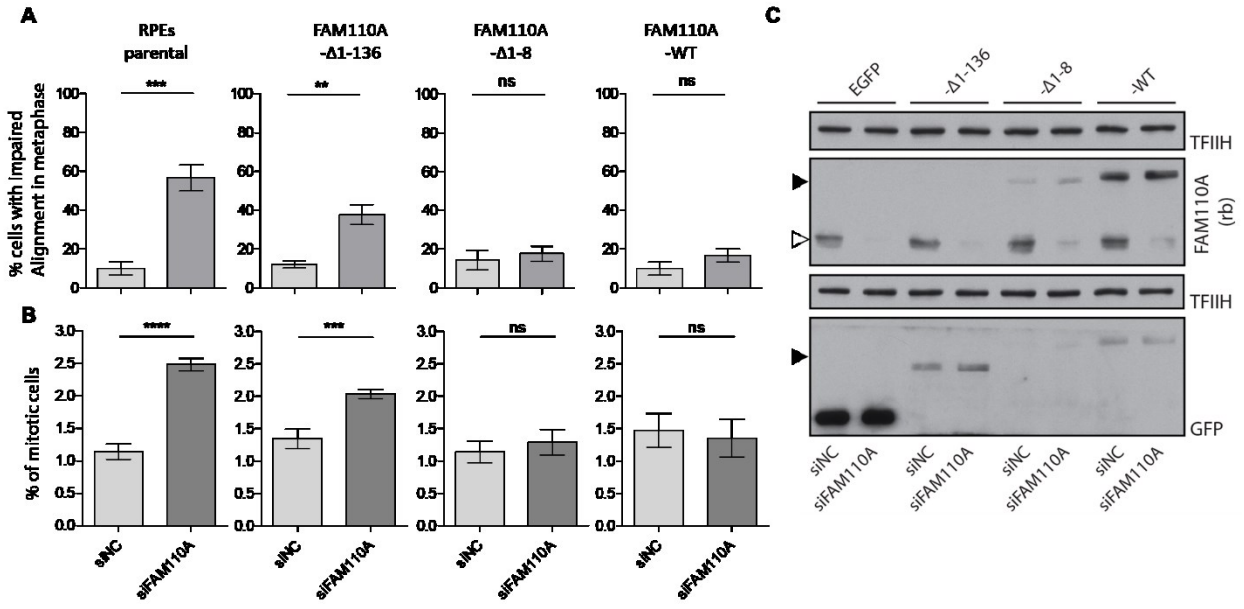

Figure 54. Metaphase misalignment phenotype and mitotic delay caused by FAM110A KD in FAM110A stable cell lines expressing acting-binding deficient variant (Δ1-136) and small deletion (Δ1-8). A. RPE parental cells or RPE cells stably expressing indicated EGFP-FAM110A variants transfected with control or FAM110A siRNA and grown for 48 h. Cells were treated with MG132 for 30 min prior fixation. Impaired chromosomal alignment was scored in >30 metaphase cell per condition. Bars indicate median ±SD. Statistical significance was determined by two-tailed Student's T-test (n=3) (** $p<0.005$, *** $p<0.001$). **B.** Quantification of the mitotic index from cells collected from the same group of experiments; cells were probed for pS10-H3 and consequently with Alexa-647 (n=3). Statistical significance was determined by two-tailed Student's T-test. Bars indicate median ±SD (**** $p<0.0001$, *** $p<0.001$). **C.** Representative Immunoblot analysis of samples from (A), note that the FAM110A rb antibody was unable to detect mutant Δ1-136, most probably due to loss of the recognition epitope. Full arrow indicates migration of the EGFP-FAM110A-WT and other variants, empty arrow indicates endogenous FAM110A. Staining for TFIIH was used as a loading control.

Finally, we wished to address the relevancy of FAM110A's ability to bind to Tubulin and actin at the same time in the mitotic context. Farina and collaborators showed that during the metaphase to anaphase transition, actin is nucleated from the centrosomes reaching its enrichment peak in early anaphase which is accompanied by reduction in microtubules density (Farina, Ramkumar et al. 2019). This cross-talk between the microtubules and the actin microfilaments is currently a hot topic in the cytoskeleton dynamics field (Dogterom and Koenderink 2019, Rizzelli, Malabarba et al. 2020), and new proteins that act as intermediaries in this cross-talk are currently being described. Since FAM110A localizes to the centrosomes and interacts with both actin and tubulin during mitosis, we decided to replicate Farinas approach to measure if FAM110A might be involved in the actin-tubulin cross-talk during mitotic progression. For this, we employed RPE cells to knock-down FAM110A, arrested them with STLC overnight, generating monopolar spindles and prometaphase arrest (Skoufias, DeBonis et al. 2006). By consequently

supplementing with RO3306 to inhibit the CDK1/Cyclin B1 complex, cells were forced to progress out of mitosis, triggering centrosomal actin nucleation (**Figure 55**) (Farina, Ramkumar et al. 2019). Cells were imaged through confocal microscopy and subsequently actin intensity was measured at the starting point (0 min) and at the last point (10 min) of RO3306 supplementation (**Figure 55-B**). We observed the enrichment of the actin nucleation in a ring that surrounds the centrosomes when control cells reached 10 min after forced mitotic exit and surprisingly we observed that FAM110A depletion hampered actin enrichment in comparison to control's 10 min time point (**Figure 55-C**).

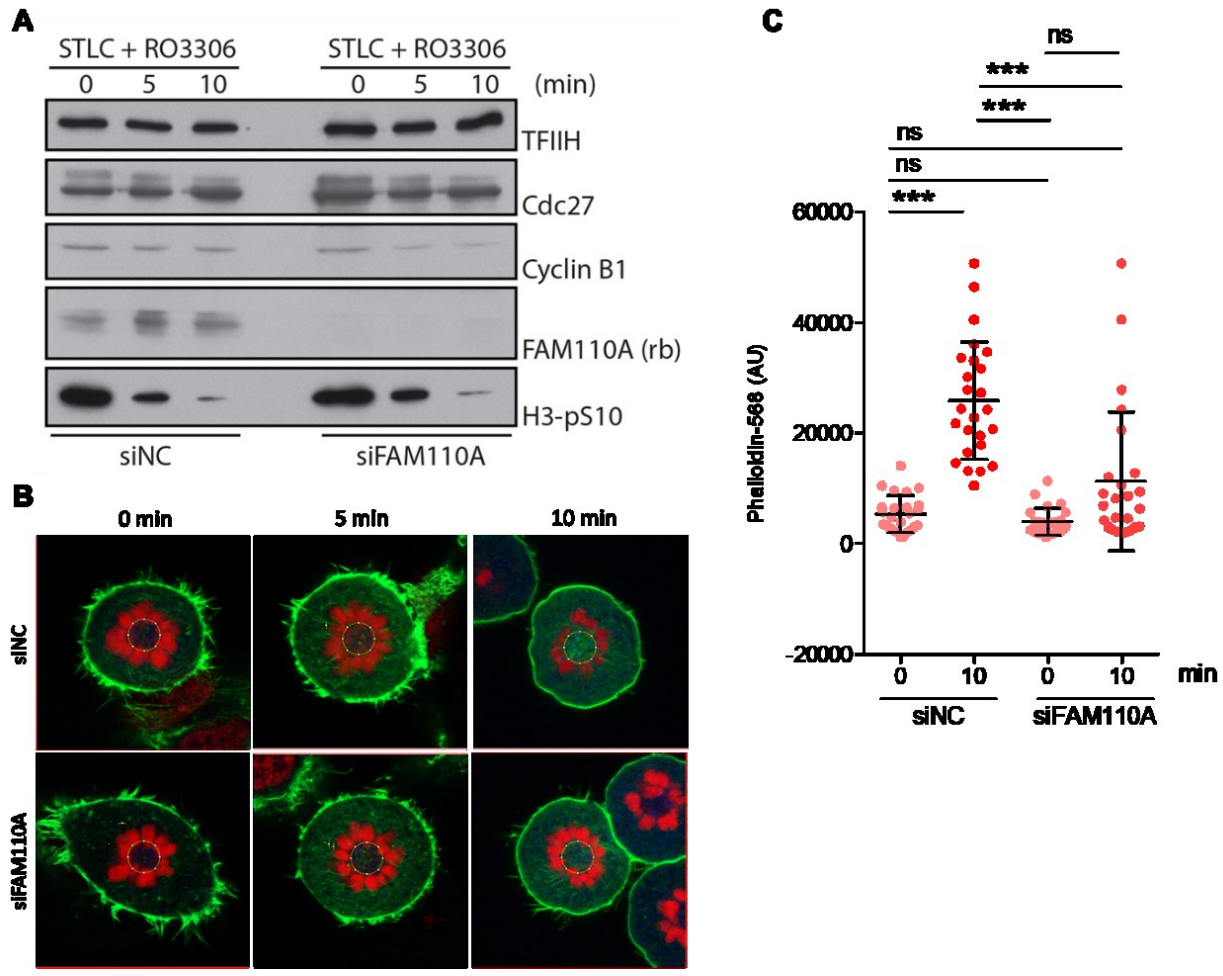

Figure 55. FAM110A depletion impairs centrosomal actin enrichment. RPE parental cells where transfected with control or FAM110A siRNA and after 24 hours re-seeded in coverslips. After 12 hours cells attached to coverslips were treated with STLC for 12 hours; STLC arrested cells were then treated with RO3306 (20 μM) for the annotated time points (0, 5 and 10 minutes) (Farina, Ramkumar et al. 2019). **A.** Representative Immunoblot to assess the efficacy of FAM110A KD and the cell cycle status of the cells. **B.** Immediately after treatment, cells were pre-extracted and fixed. Cells were then stained with phalloidin for actin labeling (green) and with DAPI from chromatin labeling (red). **C.** Quantification of actin enrichment around monopolar centrosomes. Bars indicate median ±SD. Statistical significance was determined by ANOVA (n=3) (*** $p<0.001$).

Taken together, these results paved a path to an interesting plethora of possibilities regarding FAM110A's molecular functions during cytoskeletal dynamics during mitosis. Excitingly, it was possible to observe that FAM110A loss hindered the enrichment of actin surrounding the centrosome, which might give us a clue on why the lack of actin binding produces misaligned metaphases in a similar manner as the lack of tubulin binding does (**Figure 32**Figure 30, **Figure 55**). Future research will help us establish the molecular basis of the effect of FAM110A depletion over the centrosomal actin dynamics.

5. DISCUSSION

In this work, we planned to study molecular mechanisms underlying transitions between individual phases of the cell cycle with a special focus on activation of the cell cycle checkpoints upon various forms of stress. In the first part of this study, we took a candidate approach and focused on PLK3 that was previously implicated in checkpoint control but its functions still remained controversial. By combining targeted gene editing technologies and biochemical assays we established that PLK3 was not involved in the cell response to three different cellular-stress contexts, specifically DNA damage, hypoxia and osmotic stress. The discrepancy between our findings and previous reports could be explained by lack of specificity of the tools (including antibodies and shRNA) that were not properly validated in the previous studies. We have demonstrated that some of the previously used reagents show a cross reactivity with non-specific protein targets and therefore we challenge the former conclusions on the role of PLK3 in cellular stress response. We confirmed the localization of PLK3 to the Golgi apparatus and plasma membrane that could suggest a novel function during Golgi dynamics and death response but since this reached beyond our research interests we did not follow this possibility in detail.

For the second part of this work, we performed a cell cycle-phase focused transcriptomic analysis using diploid-non transformed human RPE-FUCCI cells. We employed a non-stress-triggering sorting approach that allowed us to observe cell cycle-mediated transcription without the need of cell arrest or synchronization. Through this strategy we obtained an informative cell cycle-dependent transcription profile that might prove to be a valuable source of information for the study of cell cycle genetic expression regulation in unperturbed, normal cells. We identified a total of 701 transcripts that presented a differential expression pattern between the G1 and G2 phases. Overall our results showed high correlation with a current study that reported a differential gene expression pattern across cell cycle using non-transformed RPE cells and by basing the sorting parameters trough live-DNA staining, sorted phase specific populations for total RNA extraction and pair-end total RNA sequencing to validate their observations (Van Rechem, Ji et al. 2020). Our results showed to be in accordance with the extensively-described functions of cell-cycle control genes and in addition, we managed to pin-point several new genes, highly expressed specifically during the G2 phase of which their function remained elusive. Among this genes with unbeknownst function we had FAM83D, FAM72D and FAM110A. During the time the experimental work of this study was in process, a novel FAM83D function was published, adjudicating it a mitotic spindle positioning function (Fulcher, He et al. 2019) and coinciding with our observations of its cell cycle expression profile.

5.1. PLK3 role in cell cycle progression and DNA damage response

As the first aim of this work, we wanted to identify PLK3 kinase function during cell cycle progression and during cell cycle checkpoint activation. PLK3 has been reported to be an IEG (Immediate early gene) (Donohue, Alberts et al. 1995, Holtrich, Wolf et al. 2000) being rapidly activated upon a wide variety of stimuli that can lead to DDR activation (Bahassi el, Myer et al. 2006). In contrast, PLK1 function has been reported to be inhibited upon DNA damage detection, marking opposing activities of this two PLKs and evidencing the complexity of their specific cell cycle functions. At first instance PLK3 subcellular localization has been a matter of constant debate, it has been reported to enrich nucleoli (Zimmerman and Erikson 2007), to localize to the cytoplasm and translocate to the nucleus upon catalytic domain activation (Alberts and Winkles 2004), to localize to the Golgi apparatus and centrosome (Ruan, Wang et al. 2004) and to enrich the plasma membrane (Helmke, Raab et al. 2016). Due to the lack of immunofluorescent-working antibodies we generated a cell line stably expressing EGFP-PLK3 to study its intracellular localization. In our stable cell line, we observed enrichment of EGFP-PLK3 at the plasma membrane, which coincides with a report of PLK3 being activated upon interaction with CD95 during FasL (Fas ligand) apoptosis induction (Helmke, Raab et al. 2016). We also observed that PLK3 localized in the centrosome and Golgi apparatus confirming the observations of previous reports about this specific localization (Xie, Wang et al. 2004, Sadasivam, Duan et al. 2012). However, ectopically expressed PLK3 did not translocated to the nucleus upon genotoxic stress. Concomitantly, our cell cycle analysis showed that PLK3 protein levels remain constant throughout the cell cycle progression and are not boosted upon stress stimulation.

By performing an extensive reviewing of PLK3 published literature, we noted that preceding PLK3 studies relied mainly on purifying the endogenous PLK3 by immunoprecipitation with a polyclonal antibody whose specificity was never validated (Wang, Gao et al. 2008, Wang, Payton et al. 2011, Wang, Dai et al. 2014). Unfortunately, the employed antibody reported in this studies was discontinued, therefore it was not possible to validate it by ourselves. Nevertheless, we tested several commercially available antibodies the majority of which, lacked specificity or completely lacked sensitivity to detected endogenous PLK3. The only antibody that proved useful for western blotting of endogenous protein was from the brand Cell Signaling, but it lacked immunofluorescence capacity. The rest of the antibodies presented poor affinity to ectopically expressed PLK3 along with high cross-reactivity in western blots and a non-specific nuclear staining in the case of immunofluorescence. Seeing the antibodies poor performance, we strongly believe that previous reported data involving PLK3 during the stress and DNA damage response should be taken in consideration with healthy skepticism, as the veracity of the reported data may be affected by low specificity of the primary antibodies employed.

Next, we aimed to pin point the role of PLK3 in the stress cellular response. We generated two independent PLK3 Knock-out cell lines in the hTERT immortalized human RPE cells using CRISPR/Cas9-mediated gene editing targeting two different regions inside the critical ATP-binding cluster inside the catalytic domain. After validation, this cell lines were then submitted to several types of DNA insults and stress-inducing agents. The two independent RPE-PLK3-KO clones did not present any difference in HIF-1α stabilization during hypoxia-mimicking conditions, in phosphorylation of C-Jun after exposure of cells to UVC irradiation and in activation of the DNA damage response after exposure of cells to ionizing radiation. It is important to state that we corroborated our observations by depleting PLK3 in parental non-transformed RPE cells and in transformed HeLa and U2Os cell lines. With the intention to contrast this data, we purified EGFP-PLK3 from cells that were exposed to the after mentioned stress-inducing treatments and employed it to perform kinase assays using casein as a substrate and as a way to measure the level of PLK3 kinase activity; our results showed that there was no significant increase in PLK3 activity after the stress treatments. To amplify the specificity of this kinase assay we tested the EGFP-PLK3 side by side with the kinase dead mutant EGFP-PLK3-K91R. In conjunction, our data shows that PLK3 is disposable during cell response to hypoxia, osmotic stress or different types of DNA damage (Ionizing radiation and UVC exposure). Therefore we concluded that contrary to what was previously reported, PLK3 is irresponsive to cellular stress.

Another important goal was to identify proteins that regulate PLK3 function through protein-protein interaction. PLK3 presents a conserved Thr-219 residue (homologous to PLK1 Thr-210) reported to be the key aminoacid for PLK1 activation (Macurek, Lindqvist et al. 2008), therefore we decided to explore the functional relevance of this modification in PLK3. Indeed, we observed that PLK3 is post-translationally modified in this residue and that the nature of the modification was phosphorylation. Further we identified PP6 (Protein Phosphatase 6) holoenzyme to be in charge of continuously dephosphorylating PLK3. PP6 has been reported to regulate ASK3 (also known as MAP3K15) kinase by inactivating it through de-phosphorylation, this way promoting cell survival upon hyperosmotic stress (Watanabe, Umeda et al. 2018). Based on this observation we decided to test if PLK3 response to osmotic stress was modulated by PP6 however, after implementing both hypertonic and hypotonic conditions we observed that neither PLK3 activation (by assessing the phosphorylation status of Thr-219) nor interaction with PP6 where significantly affected. Further we did not detect any effect over PLK3 activity after PP6 depletion, inhibition or overexpression. Finally we observed that the T219D phospho-mimic mutant and the non-phosphorylatable T219A enzymatic activities turned out to be comparable to the one showed by PLK3-WT which leads us to believe that PLK3 regulation mechanism is distinct to PLK1's and may need additional modifications that control its physiological functions.

Following with the previously described enrichment in the plasma membrane, centrosomes and Golgi apparatus that we observed in our cell line stably expressing EGFP-PLK3, we extrapolate that PLK3 physiological relevance resides in its potential impact on cell-to-cell adhesion, membrane receptors interaction and regulation of Golgi-related intracellular trafficking processes that in turn have been reported to be functionally regulated by PP6 (Bhandari, Zhang et al. 2013, Ohama, Wang et al. 2013). Remarkably, PLK3 kinase function is activated upon interaction with death receptor CD95 and other DISC components via a novel PLK activation mechanism (Helmke, Raab et al. 2016), which coincides with our observations that PLK3 does not follow the same activation mechanism as PLK1. Upon said activation, PLK3's capacity to phosphorylate pro-caspase 8 on its Thr-273 residue and stimulate its apoptotic function represents a novel extrinsic apoptotic pathway directly regulated by kinase-active PLK3 (Helmke, Raab et al. 2016). PLK3 upregulation and pro-caspase 8 Thr-273 phosphorylation status correlates with higher survival rates in cancer patients, marking PLK3 as an interesting target through which the extrinsic death pathway can be activated in tumors that present high expression levels of this PLK. Unfortunately, due to RPE cultured cells innate resistance to FasL stimulation (Kaestel, Madsen et al. 2001) we were unable to validate this interesting function in our system.

Finally, recent reports have shown that upon PLK3 downregulation, prostate cancer exhibits reduced proliferation and metastasis which highlights it as a potential as a tumor suppressor (Lin, Bai et al. 2019); contrastingly PLK3 overexpression induces apoptosis and suppresses cell proliferation by cytokinesis interference (Conn, Hennigan et al. 2000). In specific contexts PLK3 expression is elevated in breast and ovarian cancers and downregulated in head, neck, lung and liver cancers suggesting that PLK3's expression status varies depending on cancer type (Deng, Lu et al. 2021). Due to this variability the use of PLK3 expression as a prognostic marker depends on the tumor type, nevertheless it could prove to be an interesting therapeutical target to induce apoptosis in cancer cells (Lin, Bai et al. 2019, Ou, Sun et al. 2019, Babagana, Kichina et al. 2020). Phosphoproteomic studies can be an interesting tool to identify novel PLK3 substrates, helping to describe in more detail its role during cell cycle progression and carcinogenesis.

5.2. FAM110A as a novel CK1 substrate during mitotic progression

We followed with investigating the cell cycle function of the previously reported but uncharacterized protein FAM110A (Hauge, Patzke et al. 2007). We found that FAM110A localized to the centrosome and diffusely in the cytoplasm in interphase cells, but that once the cell entered mitosis and progressed to metaphase, FAM110A enriched at the poles of mitotic spindles and at the proximal spindle microtubules colocalizing with CSPP1 and γ-tubulin. Further down in telophase, FAM110A was found localizing to the cleavage furrow. FAM110A depletion assays performed trough siRNA caused cells to accumulate in mitosis, with an important percentage of this cells (~60%) presenting chromosomal alignment aberrations and spindle organization defects; interestingly this aberrant mitotic phenotype proved to be rescued by ectopic expression of EGFP-FAM110A-WT. Further, live cell imagining showed that FAM110A KD caused mitotic progression to slow down, particularly by delaying the metaphase-to-anaphase transition. Interestingly, it has been reported that prometaphase-metaphase lengthening, even if the chromosomal segregation was correct, may induce a cell cycle arrest in the following G1 phase of the daughter cells (Uetake and Sluder 2010), suggesting that this delay in mitosis causes stress accumulation, even if the delay is only transient. Coupled with this observations, by analyzing the cell division behavior and mitotic spindle orientation of FAM110A depleted cells, it was possible to detect an impairment of the correct cell division axis set up along with a faulty spindle orientation establishment.

Analysis of FAM110A cell-cycle expression profile trough SDS-PAGE showed that during mitosis FAM110A underwent massive post-translational modifications. Based on this observations we employed siRNA and small-molecule inhibitors assays to establish that CDK1 and CK1 are the kinases responsible for an important wedge of the post-translational phosphorylation observed in FAM110A during mitosis. Trough *in vitro* kinase assays, CDK1 proved to be responsible for phosphorylating the N-terminal domain of FAM110A, while CK1 showed to phosphorylate the C-terminal domain. Along this line, CK1 was identified in complex with FAM110A through mass spectrometry analysis and immunoprecipitation assays; it was clear that this interaction incremented during mitosis when comparing it to the interphase interaction. FAM110A domain mapping trough protein truncations and immunoprecipitations revealed that FAM110A C-terminal domain mediates its interaction with CK1 through a hypothesized residue sequence (F-X-X-X-F) that resembled a reported consensus docking motif. This was further proved by the inability of the corresponding EGFP-FAM110A-FA mutant to bind with CK1. Subsequently we implemented site-directed mutagenesis of the S252-255 residues that we identified as potential CK1 phosphorylation substrates to test their functional relevancy. Interestingly we observed that the -FA mutant deficient in CK1 binding and the –S252-255A mutant deficient in CK1 phosphorylation failed to counteract the depletion of endogenous FAM110A during chromosomal misalignment and mitotic progression delay rescue experiments. We

would like to emphasize that additional residues within the C-terminal domain might also be targeted for phosphorylation by the CK1 isoforms. Following with the mitotic defects analysis, we found that inhibition of the CK1 isoforms or depletion of CK1δ generated a similar spindle positioning defect of that caused by FAM110A siRNA-mediated KD. This turned out to be very interesting as the previously mentioned FAM83D study reported that the CK1α isoform is targeted to the mitotic spindle through its interaction with FAM83D where they aid during proper spindle positioning (Fulcher, He et al. 2019). Our data helps us support the premise that other CK1 isoforms also contribute to the organization of the mitotic spindle.

In order to elucidate the role of FAM110A during mitosis and to determine if said role was dependent on its interaction with CK1 and its consequent phosphorylation, we obtained data that showed a similar incapability of between EGFP-FAM110A-WT and the –FA and -S252-255A mutants to rescue the mitotic spindle positioning defect generated by CK1δ depletion or by CK1 isoforms inhibition. On top of this, by submitting the phosphorylation mimicking EGFP-FAM110A-S252-255E mutant to the after mentioned phenotype rescue assays, we found that it was able to prevent the chromosomal misalignment and spindle misorientation that otherwise the EGFP-FAM110A-WT and the –FA and -S252-255A mutants were incapable to rescue. Altogether this results suggest that FAM110A is a highly relevant substrate of CK1δ during mitosis. Based on this results, we propose that CK1δ controls proper chromosomal alignment during metaphase by directly targeting the FAM110A-S252-255 residues for phosphorylation, this way promoting its interaction with the mitotic spindle microtubules. We consider that the observed displacement of GFP-LGN generated by the proximity of misaligned chromosomes as a result of FAM110A depletion, is responsible at least partially, of the resulting spindle positioning defects. The mentioned putative contribution could be similar as the previously reported for CLIP-170 or CENP-E depletion (Tame, Raaijmakers et al. 2016). Interestingly, mitotic spindle positioning defects have been reported to be prevalent in mice-tumors, (Fleming, Temchin et al. 2009) which puts in context the importance of impaired spindle orientation during oncogenic progression. Paired to this, the CK1 family has been reported to have relevant functions during mitotic progression (Knippschild, Gocht et al. 2005). For instance the CK1α isoform was reported to localize to the centrosome during interphase and to MTs asters and kinetochores during chromosome segregation (Brockman, Gross et al. 1992, Stoter, Bamberger et al. 2005). More recently it was reported to be targeted to the spindle poles by the spindle protein CHICA (also known as FAM83D), where it participates in the mitotic spindle proper positioning process (Fulcher, He et al. 2019). The CK1 family has also been linked to cancer progression due to disruption of their regulatory activities in the Wnt/β-catenin pathway, leading to defects on cell-to-cell adhesion and dysregulated migration.
Further we decided to address the functional nature of FAM110A's ability to bind actin and its mitotic relevance. "Spindle actin" has been reported to participate during metaphase, specifically during meiosis

(metaphase II) in several species of mammalian eggs including humans. Spindle actin function proved to be essential for chromosomal congression and segregation by stabilizing kinetochore-fibers (MT bundles that align and segregate the chromosomes) (Mogessie and Schuh 2017). We have observed the dynamic formation of said spindle actin fibers in RPE cells arrested with STLC and forced out of mitosis by RO3306 addition (Farina, Ramkumar et al. 2019) and analyzed the effects of FAM110A's loss in said process. An interesting observation is that depletion of FAM110A does not affect the formation and functionality neither of the mitotic spindle nor of the astral microtubules. The actomyosin ring presented a normal shape even after depletion of FAM110A and CK1δ, however centrosomal actin filaments nucleation seemed to be either slowed down or impaired. This suggests that the issues caused by FAM110A depletion like the metaphase misalignment and NEB to MAT delay could be caused by the lack of FAM110A possible bridging or "gluing" function between spindle actin and spindle MTs.

Backed up by the present data, we have demonstrated that FAM110A is a mitotic substrate targeted for phosphorylation by CK1δ, where it's needed for chromosome congression and that this process is also aided by FAM110A's ability to bind actin. We observed that the actin-binding deficient mutant FAM110A-Δ1-135 showed a similar metaphase phenotype misalignment than FAM110A-depleted RPE cells. One exiting possibility could be that FAM110A works as a bridge trough which spindle microtubules might interact with the actin cytoskeleton, as it has been recently reported that during early anaphase actin transiently accumulates around the spindle poles, proposing a new centrosomal function both as actin and microtubule organization centers (Farina, Ramkumar et al. 2019). On another perspective, the cortical actin cytoskeleton has been directly linked to mitotic spindle morphogenesis and at the same time unexpected mitotic spindle functions are being granted to the actin filaments (Kunda, Pelling et al. 2008, Mogessie and Schuh 2017, Plessner, Knerr et al. 2019). Both of this premises turn out to be very interesting as we have reported in this study that FAM110A localizes to the spindle poles throughout mitosis and that mass spectrometry analysis along with immunoprecipitation assays show an interaction with tubulin and actin during mitosis. Our results showed that the C-terminal domain of FAM110A was sufficient to bind to spindle microtubules and to pull down tubulin; on the other hand it turned to be disposable for actin binding (binding that showed to happen exclusively in mitosis). Taken together, these observations tell us that FAM110A interaction with actin and tubulin is mediated through the opposing terminal domains of the protein, marking this small protein as a possible emissary during spindle MTs and mitotic Actin filaments crosstalk dynamic.

Following through, the results of the mass-spec analysis performed on purified mitotic FAM110A showed interaction with α-actinin and with the α/β-catenin isoforms, known cytoskeletal-related proteins (Perez-Moreno, Jamora et al. 2003). Let's put the functional relevance of this interactions in context: Metaphase cells maintain contact to their substrate trough *mitotic focal adhesion complexes* (Taneja, Fenix et al. 2016) formed by FAK (focal adhesion kinase), that promotes the recruitment of talin (Lawson, Lim et al. 2012) and paxillin to the retraction fibers, where they bind to the cytoplasmic tail of the β1-integrin subunit (transmembrane receptor protein), linking the extracellular matrix to the actin contractile machinery (Kanchanawong, Shtengel et al. 2010). The contraction machinery is composed of actin retraction fibers that bind to β1-integrin subunits trough talin and tensin, while vinculin reinforces the tension (Garcin and Straube 2019). In this context, paxillin is phosphorylated by FAK and will work as a messenger activating several signaling pathways that promote cell migration (Lopez-Colome, Lee-Rivera et al. 2017). Myosin and α-actinin are in charge of inter-connecting the actin retraction fibers in proximity if the mitotic focal adhesion complexes (Blanchard, Ohanian et al. 1989); α-actinin dimers bind to actin microfilaments in an anti-parallel manner, crosslinking two microfilaments through the opposite ends of their dumbbell shape (Murphy and Young 2015). Therefore we consider the possibility that FAM110A interaction with the α-actinin and α/β-catenin isoforms might be happening in the mitotic focal adhesion complexes and that FAM110A might help bridge and anchor the focal machinery to the mitotic actin filaments. Interestingly, abnormal α and β-catenin staining has been detected in crypts of tumors from APC mutant mice, suggesting a possible role for this proteins in spindle orientation (Fleming, Temchin et al. 2009). Concomitantly, α/β-catenin isoforms link the actin microfilaments attached to afadin-bound LGN to the transmembrane E-cadherin, a protein that has been reported to participate in control of cell polarity and migration. This interesting interactors' pin-point a plausible role for FAM110A and its homologs 110B and 110C in other cytoskeletal related processes that have potential relevance in cell transformation susceptibility.

Currently, there is robust evidence that shows a direct association between mitotic spindle misorientation with tumor formation, metastasis and developmental pathologies (Lu and Johnston 2013). The FAM110 family downregulation has been linked to carcinogenic events, mainly related to metastasis proneness and loss of cell-to-cell adhesion (Xi and Zhang 2018, Huang, Guo et al. 2020) due to faulty or unstable focal adhesion machinery. In this context, FAM110A's relevance in metaphase alignment and spindle positioning proves to be relevant for instance, during early carcinogenic events when spindle misorientation may contribute to the loss of normal tissue organization and early tumor formation (Fleming, Temchin et al. 2009) and later on during the detachment of malignant cells that can lead to metastasis.

6. CONCLUSION

6.1. Aim 1. To identify function of PLK3 kinase in the cell cycle and DNA damage response.

By employing CRISPR-Cas9-mediated gene editing, we knocked-out PLK3 in non-transformed RPE cells and tested for impairment of the stress response and for DNA damage dynamics changes. By performing mass spectrometry of purified EGFP-PLK3 we aimed to identify protein interactors that could modulate the function of PLK3. The results obtained during my PhD studies show that PLK3 is disposable during cellular stress response and that its dephosphorylation is performed by Protein phosphatase 6. The key conclusions of this work are:

- Loss of PLK3 showed to have no relevant effect over the cellular stress response upon hypoxia, osmotic stress and ionizing radiation. The results obtained in our PLK3-KO model were validated trough siRNA Knock-down and in two additional cell lines. Therefore we conclude that PLK3 is disposable during the stress response in transformed and non-transformed human cells.
- Protein phosphatase 6, in complex with the regulatory subunits PP6R1 and PP6R3 were identified as novel interacting partners of PLK3 through mass spectrometry and were confirmed through immunoprecipitation. The PP6 complex showed to interact with PLK3 through the PBD domain and to actively dephosphorylate PLK3 on its T219 residue.

6.2. Aim 2. To identify and describe novel regulators of the cell cycle in mammalian cells.

FAM110A protein was selected from a list of candidate genes generated by a Cell cycle-specific gene expression profiling performed in hTERT-immortalized RPE cells stably expressing the FUCCI system. We employed genetic silencing assays to deplete cells of endogenous FAM110A in order to assess its function during the Cell cycle. The results generated during my PhD studies show the mitotic role of the uncharacterized FAM110A and through direct interaction with the CK1δ and CK1ε isoforms. The key conclusions of this work are:

- FAM110A localizes at the spindle poles and at the proximal spindle microtubules during mitosis.
- Phosphorylation of FAM110A at S252-255 by Casein kinase 1 isoform δ promotes its interaction with tubulin and localization to the spindle poles.
- Depletion of FAM110A or inhibition of CK1 activity lead to chromosomal misalignments, delayed progression through mitosis and spindle position defects.
- A phosphorylation-mimicking FAM110A-S252-255E mutant rescues the defects generated by endogenous FAM110A depletion during chromosomal alignment and the consequent spindle positon defects caused by depletion or inhibition of CK1.
- FAM110A interaction with actin is mediated through its N-terminal domain and it's important for proper chromosomal alignment during metaphase.

7. REFERENCES

Abraham, R. T. (2001). "Cell cycle checkpoint signaling through the ATM and ATR kinases." Genes Dev **15**(17): 2177-2196.

Adams, R. R., H. Maiato, W. C. Earnshaw and M. Carmena (2001). "Essential roles of Drosophila inner centromere protein (INCENP) and aurora B in histone H3 phosphorylation, metaphase chromosome alignment, kinetochore disjunction, and chromosome segregation." J Cell Biol **153**(4): 865-880.

Adler, P., J. Mayne, K. Walker, Z. Ning and D. Figeys (2019). "Therapeutic Targeting of Casein Kinase 1delta/epsilon in an Alzheimer's Disease Mouse Model." J Proteome Res **18**(9): 3383-3393.

Agami, R. and R. Bernards (2000). "Distinct initiation and maintenance mechanisms cooperate to induce G1 cell cycle arrest in response to DNA damage." Cell **102**(1): 55-66.

Aguilera, A. and B. Gomez-Gonzalez (2008). "Genome instability: a mechanistic view of its causes and consequences." Nat Rev Genet **9**(3): 204-217.

Ahn, J. Y., J. K. Schwarz, H. Piwnica-Worms and C. E. Canman (2000). "Threonine 68 phosphorylation by ataxia telangiectasia mutated is required for efficient activation of Chk2 in response to ionizing radiation." Cancer Res **60**(21): 5934-5936.

Aist, J. R., C. J. Bayles, W. Tao and M. W. Berns (1991). "Direct experimental evidence for the existence, structural basis and function of astral forces during anaphase B in vivo." J Cell Sci **100 (Pt 2)**: 279-288.

Alabert, C. and A. Groth (2012). "Chromatin replication and epigenome maintenance." Nat Rev Mol Cell Biol **13**(3): 153-167.

Alberico, E. O., Z. C. Zhu, Y. O. Wu, M. K. Gardner, D. R. Kovar and H. V. Goodson (2016). "Interactions between the Microtubule Binding Protein EB1 and F-Actin." J Mol Biol **428**(6): 1304-1314.

Alberts, G. F. and J. A. Winkles (2004). "Murine FGF-inducible kinase is rapidly degraded via the nuclear ubiquitin-proteosome system when overexpressed in NIH 3T3 cells." Cell Cycle **3**(5): 678-684.

Albertson, R., J. Cao, T. S. Hsieh and W. Sullivan (2008). "Vesicles and actin are targeted to the cleavage furrow via furrow microtubules and the central spindle." J Cell Biol **181**(5): 777-790.

Allen, C., J. Halbrook and J. A. Nickoloff (2003). "Interactive competition between homologous recombination and non-homologous end joining." Mol Cancer Res **1**(12): 913-920.

Anderson, D. J. and M. W. Hetzer (2007). "Nuclear envelope formation by chromatin-mediated reorganization of the endoplasmic reticulum." Nat Cell Biol **9**(10): 1160-1166.

Anderson, D. J. and M. W. Hetzer (2008). "Reshaping of the endoplasmic reticulum limits the rate for nuclear envelope formation." J Cell Biol **182**(5): 911-924.

Anerillas, C., K. Abdelmohsen and M. Gorospe (2020). "Regulation of senescence traits by MAPKs." Geroscience **42**(2): 397-408.

Asaad, N. A., Z. C. Zeng, J. Guan, J. Thacker and G. Iliakis (2000). "Homologous recombination as a potential target for caffeine radiosensitization in mammalian cells: reduced caffeine radiosensitization in XRCC2 and XRCC3 mutants." Oncogene **19**(50): 5788-5800.

Awasthi, P., M. Foiani and A. Kumar (2015). "ATM and ATR signaling at a glance." J Cell Sci **128**(23): 4255-4262.

Babagana, M., J. V. Kichina, H. Slabodkin, S. Johnson, A. Maslov, L. Brown, K. Attwood, M. A. Nikiforov and E. S. Kandel (2020). "The role of polo-like kinase 3 in the response of BRAF-mutant cells to targeted anticancer therapies." Mol Carcinog **59**(1): 5-14.

Bahassi el, M., C. W. Conn, D. L. Myer, R. F. Hennigan, C. H. McGowan, Y. Sanchez and P. J. Stambrook (2002). "Mammalian Polo-like kinase 3 (Plk3) is a multifunctional protein involved in stress response pathways." Oncogene **21**(43): 6633-6640.

Bahassi el, M., D. L. Myer, R. J. McKenney, R. F. Hennigan and P. J. Stambrook (2006). "Priming phosphorylation of Chk2 by polo-like kinase 3 (Plk3) mediates its full activation by ATM and a downstream checkpoint in response to DNA damage." Mutat Res **596**(1-2): 166-176.

Baldin, V., J. Lukas, M. J. Marcote, M. Pagano and G. Draetta (1993). "Cyclin D1 is a nuclear protein required for cell cycle progression in G1." Genes Dev **7**(5): 812-821.

Bao, S., R. S. Tibbetts, K. M. Brumbaugh, Y. Fang, D. A. Richardson, A. Ali, S. M. Chen, R. T. Abraham and X. F. Wang (2001). "ATR/ATM-mediated phosphorylation of human Rad17 is required for genotoxic stress responses." Nature **411**(6840): 969-974.
Bartek, J., C. Lukas and J. Lukas (2004). "Checking on DNA damage in S phase." Nat Rev Mol Cell Biol **5**(10): 792-804.
Bartek, J. and J. Lukas (2003). "Chk1 and Chk2 kinases in checkpoint control and cancer." Cancer Cell **3**(5): 421-429.
Bartek, J. and J. Lukas (2007). "DNA damage checkpoints: from initiation to recovery or adaptation." Curr Opin Cell Biol **19**(2): 238-245.
Bashir, T., N. V. Dorrello, V. Amador, D. Guardavaccaro and M. Pagano (2004). "Control of the SCF(Skp2-Cks1) ubiquitin ligase by the APC/C(Cdh1) ubiquitin ligase." Nature **428**(6979): 190-193.
Baur, T., K. Ramadan, A. Schlundt, J. Kartenbeck and H. H. Meyer (2007). "NSF- and SNARE-mediated membrane fusion is required for nuclear envelope formation and completion of nuclear pore complex assembly in Xenopus laevis egg extracts." J Cell Sci **120**(Pt 16): 2895-2903.
Beaudouin, J., D. Gerlich, N. Daigle, R. Eils and J. Ellenberg (2002). "Nuclear envelope breakdown proceeds by microtubule-induced tearing of the lamina." Cell **108**(1): 83-96.
Behrend, L., D. M. Milne, M. Stoter, W. Deppert, L. E. Campbell, D. W. Meek and U. Knippschild (2000). "IC261, a specific inhibitor of the protein kinases casein kinase 1-delta and -epsilon, triggers the mitotic checkpoint and induces p53-dependent postmitotic effects." Oncogene **19**(47): 5303-5313.
Behrend, L., M. Stoter, M. Kurth, G. Rutter, J. Heukeshoven, W. Deppert and U. Knippschild (2000). "Interaction of casein kinase 1 delta (CK1delta) with post-Golgi structures, microtubules and the spindle apparatus." Eur J Cell Biol **79**(4): 240-251.
Bekker-Jensen, S. and N. Mailand (2010). "Assembly and function of DNA double-strand break repair foci in mammalian cells." DNA Repair (Amst) **9**(12): 1219-1228.
Belmont, L. D., A. A. Hyman, K. E. Sawin and T. J. Mitchison (1990). "Real-time visualization of cell cycle-dependent changes in microtubule dynamics in cytoplasmic extracts." Cell **62**(3): 579-589.
Benada, J., K. Burdova, T. Lidak, P. von Morgen and L. Macurek (2015). "Polo-like kinase 1 inhibits DNA damage response during mitosis." Cell Cycle **14**(2): 219-231.
Bennetzen, M. V., D. H. Larsen, J. Bunkenborg, J. Bartek, J. Lukas and J. S. Andersen (2010). "Site-specific phosphorylation dynamics of the nuclear proteome during the DNA damage response." Mol Cell Proteomics **9**(6): 1314-1323.
Bergman, Z. J., J. D. McLaurin, A. S. Eritano, B. M. Johnson, A. Q. Sims and B. Riggs (2015). "Spatial reorganization of the endoplasmic reticulum during mitosis relies on mitotic kinase cyclin A in the early Drosophila embryo." PLoS One **10**(2): e0117859.
Bermejo, R., Y. Doksani, T. Capra, Y. M. Katou, H. Tanaka, K. Shirahige and M. Foiani (2007). "Top1- and Top2-mediated topological transitions at replication forks ensure fork progression and stability and prevent DNA damage checkpoint activation." Genes Dev **21**(15): 1921-1936.
Bermejo, R., M. S. Lai and M. Foiani (2012). "Preventing replication stress to maintain genome stability: resolving conflicts between replication and transcription." Mol Cell **45**(6): 710-718.
Bertoli, C., J. M. Skotheim and R. A. de Bruin (2013). "Control of cell cycle transcription during G1 and S phases." Nat Rev Mol Cell Biol **14**(8): 518-528.
Bhalla, U. S., P. T. Ram and R. Iyengar (2002). "MAP kinase phosphatase as a locus of flexibility in a mitogen-activated protein kinase signaling network." Science **297**(5583): 1018-1023.
Bhandari, D., J. Zhang, S. Menon, C. Lord, S. Chen, J. R. Helm, K. Thorsen, K. D. Corbett, J. C. Hay and S. Ferro-Novick (2013). "Sit4p/PP6 regulates ER-to-Golgi traffic by controlling the dephosphorylation of COPII coat subunits." Mol Biol Cell **24**(17): 2727-2738.
Bian, L., Y. Meng, M. Zhang and D. Li (2019). "MRE11-RAD50-NBS1 complex alterations and DNA damage response: implications for cancer treatment." Mol Cancer **18**(1): 169.
Bieling, P., I. A. Telley, C. Hentrich, J. Piehler and T. Surrey (2010). "Fluorescence microscopy assays on chemically functionalized surfaces for quantitative imaging of microtubule, motor, and +TIP dynamics." Methods Cell Biol **95**: 555-580.

Blackford, A. N. and S. P. Jackson (2017). "ATM, ATR, and DNA-PK: The Trinity at the Heart of the DNA Damage Response." Mol Cell **66**(6): 801-817.
Blagosklonny, M. V. and A. B. Pardee (2002). "The restriction point of the cell cycle." Cell Cycle **1**(2): 103-110.
Blanchard, A., V. Ohanian and D. Critchley (1989). "The structure and function of alpha-actinin." J Muscle Res Cell Motil **10**(4): 280-289.
Blanchoin, L., R. Boujemaa-Paterski, C. Sykes and J. Plastino (2014). "Actin dynamics, architecture, and mechanics in cell motility." Physiol Rev **94**(1): 235-263.
Blangy, A., H. A. Lane, P. d'Herin, M. Harper, M. Kress and E. A. Nigg (1995). "Phosphorylation by p34cdc2 regulates spindle association of human Eg5, a kinesin-related motor essential for bipolar spindle formation in vivo." Cell **83**(7): 1159-1169.
Blomberg, I. and I. Hoffmann (1999). "Ectopic expression of Cdc25A accelerates the G(1)/S transition and leads to premature activation of cyclin E- and cyclin A-dependent kinases." Mol Cell Biol **19**(9): 6183-6194.
Blow, J. J. and B. Hodgson (2002). "Replication licensing--defining the proliferative state?" Trends Cell Biol **12**(2): 72-78.
Bluemink, J. G. and S. W. de Laat (1973). "New membrane formation during cytokinesis in normal and cytochalasin B-treated eggs of Xenopus laevis. I. Electron microscope observations." J Cell Biol **59**(1): 89-108.
Bornstein, G., J. Bloom, D. Sitry-Shevah, K. Nakayama, M. Pagano and A. Hershko (2003). "Role of the SCFSkp2 ubiquitin ligase in the degradation of p21Cip1 in S phase." J Biol Chem **278**(28): 25752-25757.
Boutros, R., V. Lobjois and B. Ducommun (2007). "CDC25 phosphatases in cancer cells: key players? Good targets?" Nat Rev Cancer **7**(7): 495-507.
Bringmann, H. and A. A. Hyman (2005). "A cytokinesis furrow is positioned by two consecutive signals." Nature **436**(7051): 731-734.
Brockman, J. L., S. D. Gross, M. R. Sussman and R. A. Anderson (1992). "Cell cycle-dependent localization of casein kinase I to mitotic spindles." Proc Natl Acad Sci U S A **89**(20): 9454-9458.
Brooks, W. S., S. Banerjee and D. F. Crawford (2007). "G2E3 is a nucleo-cytoplasmic shuttling protein with DNA damage responsive localization." Exp Cell Res **313**(4): 665-676.
Brooks, W. S., E. S. Helton, S. Banerjee, M. Venable, L. Johnson, T. R. Schoeb, R. A. Kesterson and D. F. Crawford (2008). "G2E3 is a dual function ubiquitin ligase required for early embryonic development." J Biol Chem **283**(32): 22304-22315.
Brouhard, G. J. and A. J. Hunt (2005). "Microtubule movements on the arms of mitotic chromosomes: polar ejection forces quantified in vitro." Proc Natl Acad Sci U S A **102**(39): 13903-13908.
Brust-Mascher, I. and J. M. Scholey (2011). "Mitotic motors and chromosome segregation: the mechanism of anaphase B." Biochem Soc Trans **39**(5): 1149-1153.
Budd, M. E., C. C. Reis, S. Smith, K. Myung and J. L. Campbell (2006). "Evidence suggesting that Pif1 helicase functions in DNA replication with the Dna2 helicase/nuclease and DNA polymerase delta." Mol Cell Biol **26**(7): 2490-2500.
Budini, M., G. Jacob, A. Jedlicki, C. Perez, C. C. Allende and J. E. Allende (2009). "Autophosphorylation of carboxy-terminal residues inhibits the activity of protein kinase CK1alpha." J Cell Biochem **106**(3): 399-408.
Budman, J. and G. Chu (2005). "Processing of DNA for nonhomologous end-joining by cell-free extract." EMBO J **24**(4): 849-860.
Buffin, E., C. Lefebvre, J. Huang, M. E. Gagou and R. E. Karess (2005). "Recruitment of Mad2 to the kinetochore requires the Rod/Zw10 complex." Curr Biol **15**(9): 856-861.
Bulavin, D. V., S. A. Amundson and A. J. Fornace (2002). "p38 and Chk1 kinases: different conductors for the G(2)/M checkpoint symphony." Curr Opin Genet Dev **12**(1): 92-97.
Burdova, K., R. Storchova, M. Palek and L. Macurek (2019). "WIP1 Promotes Homologous Recombination and Modulates Sensitivity to PARP Inhibitors." Cells **8**(10).

Burke, D. J. and P. T. Stukenberg (2008). "Linking kinetochore-microtubule binding to the spindle checkpoint." Dev Cell **14**(4): 474-479.
Burma, S., B. P. Chen, M. Murphy, A. Kurimasa and D. J. Chen (2001). "ATM phosphorylates histone H2AX in response to DNA double-strand breaks." J Biol Chem **276**(45): 42462-42467.
Busino, L., M. Donzelli, M. Chiesa, D. Guardavaccaro, D. Ganoth, N. V. Dorrello, A. Hershko, M. Pagano and G. F. Draetta (2003). "Degradation of Cdc25A by beta-TrCP during S phase and in response to DNA damage." Nature **426**(6962): 87-91.
Byers, B. and D. H. Abramson (1968). "Cytokinesis in HeLa: post-telophase delay and microtubule-associated motility." Protoplasma **66**(4): 413-435.
Byers, T. J., A. H. Beggs, E. M. McNally and L. M. Kunkel (1995). "Novel actin crosslinker superfamily member identified by a two step degenerate PCR procedure." FEBS Lett **368**(3): 500-504.
Cadet, J., A. Grand and T. Douki (2015). "Solar UV radiation-induced DNA Bipyrimidine photoproducts: formation and mechanistic insights." Top Curr Chem **356**: 249-275.
Cardoso, M. C., H. Leonhardt and B. Nadal-Ginard (1993). "Reversal of terminal differentiation and control of DNA replication: cyclin A and Cdk2 specifically localize at subnuclear sites of DNA replication." Cell **74**(6): 979-992.
Carmena, M., M. G. Riparbelli, G. Minestrini, A. M. Tavares, R. Adams, G. Callaini and D. M. Glover (1998). "Drosophila polo kinase is required for cytokinesis." J Cell Biol **143**(3): 659-671.
Casas-Mollano, J. A., B. R. Jeong, J. Xu, H. Moriyama and H. Cerutti (2008). "The MUT9p kinase phosphorylates histone H3 threonine 3 and is necessary for heritable epigenetic silencing in Chlamydomonas." Proc Natl Acad Sci U S A **105**(17): 6486-6491.
Casenghi, M., P. Meraldi, U. Weinhart, P. I. Duncan, R. Korner and E. A. Nigg (2003). "Polo-like kinase 1 regulates Nlp, a centrosome protein involved in microtubule nucleation." Dev Cell **5**(1): 113-125.
Castrillon, D. H. and S. A. Wasserman (1994). "Diaphanous is required for cytokinesis in Drosophila and shares domains of similarity with the products of the limb deformity gene." Development **120**(12): 3367-3377.
Cegielska, A., K. F. Gietzen, A. Rivers and D. M. Virshup (1998). "Autoinhibition of casein kinase I epsilon (CKI epsilon) is relieved by protein phosphatases and limited proteolysis." J Biol Chem **273**(3): 1357-1364.
Chakravarty, A., L. Howard and D. A. Compton (2004). "A mechanistic model for the organization of microtubule asters by motor and non-motor proteins in a mammalian mitotic extract." Mol Biol Cell **15**(5): 2116-2132.
Chan, E. H., A. Santamaria, H. H. Sillje and E. A. Nigg (2008). "Plk1 regulates mitotic Aurora A function through betaTrCP-dependent degradation of hBora." Chromosoma **117**(5): 457-469.
Chang, P., T. H. Giddings, Jr., M. Winey and T. Stearns (2003). "Epsilon-tubulin is required for centriole duplication and microtubule organization." Nat Cell Biol **5**(1): 71-76.
Chatonnet, F., A. Pignarre, A. A. Serandour, G. Caron, S. Avner, N. Robert, A. Kassambara, A. Laurent, M. Bizot, X. Agirre, F. Prosper, J. I. Martin-Subero, J. Moreaux, T. Fest and G. Salbert (2020). "The hydroxymethylome of multiple myeloma identifies FAM72D as a 1q21 marker linked to proliferation." Haematologica **105**(3): 774-783.
Chaudhry, M. A., L. A. Chodosh, W. G. McKenna and R. J. Muschel (2002). "Gene expression profiling of HeLa cells in G1 or G2 phases." Oncogene **21**(12): 1934-1942.
Cheeseman, I. M. (2014). "The kinetochore." Cold Spring Harb Perspect Biol **6**(7): a015826.
Cheeseman, I. M., J. S. Chappie, E. M. Wilson-Kubalek and A. Desai (2006). "The conserved KMN network constitutes the core microtubule-binding site of the kinetochore." Cell **127**(5): 983-997.
Cheeseman, I. M., S. Niessen, S. Anderson, F. Hyndman, J. R. Yates, 3rd, K. Oegema and A. Desai (2004). "A conserved protein network controls assembly of the outer kinetochore and its ability to sustain tension." Genes Dev **18**(18): 2255-2268.
Chen, H., M. Lisby and L. S. Symington (2013). "RPA coordinates DNA end resection and prevents formation of DNA hairpins." Mol Cell **50**(4): 589-600.
Chen, Y., P. L. Chen, C. F. Chen, X. Jiang and D. J. Riley (2008). "Never-in-mitosis related kinase 1 functions in DNA damage response and checkpoint control." Cell Cycle **7**(20): 3194-3201.

Chen, Y. J., C. Dominguez-Brauer, Z. Wang, J. M. Asara, R. H. Costa, A. L. Tyner, L. F. Lau and P. Raychaudhuri (2009). "A conserved phosphorylation site within the forkhead domain of FoxM1B is required for its activation by cyclin-CDK1." J Biol Chem **284**(44): 30695-30707.
Cheong, J. K. and D. M. Virshup (2011). "Casein kinase 1: Complexity in the family." Int J Biochem Cell Biol **43**(4): 465-469.
Ciferri, C., S. Pasqualato, E. Screpanti, G. Varetti, S. Santaguida, G. Dos Reis, A. Maiolica, J. Polka, J. G. De Luca, P. De Wulf, M. Salek, J. Rappsilber, C. A. Moores, E. D. Salmon and A. Musacchio (2008). "Implications for kinetochore-microtubule attachment from the structure of an engineered Ndc80 complex." Cell **133**(3): 427-439.
Cimprich, K. A. (2007). "Probing ATR activation with model DNA templates." Cell Cycle **6**(19): 2348-2354.
Cizmecioglu, O., A. Krause, R. Bahtz, L. Ehret, N. Malek and I. Hoffmann (2012). "Plk2 regulates centriole duplication through phosphorylation-mediated degradation of Fbxw7 (human Cdc4)." J Cell Sci **125**(Pt 4): 981-992.
Clikeman, J. A., G. J. Khalsa, S. L. Barton and J. A. Nickoloff (2001). "Homologous recombinational repair of double-strand breaks in yeast is enhanced by MAT heterozygosity through yKU-dependent and -independent mechanisms." Genetics **157**(2): 579-589.
Clokie, S., H. Falconer, S. Mackie, T. Dubois and A. Aitken (2009). "The interaction between casein kinase Ialpha and 14-3-3 is phosphorylation dependent." FEBS J **276**(23): 6971-6984.
Clute, P. and J. Pines (1999). "Temporal and spatial control of cyclin B1 destruction in metaphase." Nat Cell Biol **1**(2): 82-87.
Conn, C. W., R. F. Hennigan, W. Dai, Y. Sanchez and P. J. Stambrook (2000). "Incomplete cytokinesis and induction of apoptosis by overexpression of the mammalian polo-like kinase, Plk3." Cancer Res **60**(24): 6826-6831.
Connell, J. W., C. Lindon, J. P. Luzio and E. Reid (2009). "Spastin couples microtubule severing to membrane traffic in completion of cytokinesis and secretion." Traffic **10**(1): 42-56.
Convery, E., E. K. Shin, Q. Ding, W. Wang, P. Douglas, L. S. Davis, J. A. Nickoloff, S. P. Lees-Miller and K. Meek (2005). "Inhibition of homologous recombination by variants of the catalytic subunit of the DNA-dependent protein kinase (DNA-PKcs)." Proc Natl Acad Sci U S A **102**(5): 1345-1350.
Cooper, S. and K. Shedden (2003). "Microarray analysis of gene expression during the cell cycle." Cell Chromosome **2**(1): 1.
Cortez, D., Y. Wang, J. Qin and S. J. Elledge (1999). "Requirement of ATM-dependent phosphorylation of brca1 in the DNA damage response to double-strand breaks." Science **286**(5442): 1162-1166.
Cotta-Ramusino, C., E. R. McDonald, 3rd, K. Hurov, M. E. Sowa, J. W. Harper and S. J. Elledge (2011). "A DNA damage response screen identifies RHINO, a 9-1-1 and TopBP1 interacting protein required for ATR signaling." Science **332**(6035): 1313-1317.
Courtheoux, T., A. Diallo, A. P. Damodaran, D. Reboutier, E. Watrin and C. Prigent (2018). "Aurora A kinase activity is required to maintain an active spindle assembly checkpoint during prometaphase." J Cell Sci **131**(7).
Crasta, K., P. Huang, G. Morgan, M. Winey and U. Surana (2006). "Cdk1 regulates centrosome separation by restraining proteolysis of microtubule-associated proteins." EMBO J **25**(11): 2551-2563.
Crawford, D. F. and H. Piwnica-Worms (2001). "The G(2) DNA damage checkpoint delays expression of genes encoding mitotic regulators." J Biol Chem **276**(40): 37166-37177.
Crncec, A. and H. Hochegger (2019). "Triggering mitosis." FEBS Lett **593**(20): 2868-2888.
Cruciat, C. M., C. Dolde, R. E. de Groot, B. Ohkawara, C. Reinhard, H. C. Korswagen and C. Niehrs (2013). "RNA helicase DDX3 is a regulatory subunit of casein kinase 1 in Wnt-beta-catenin signaling." Science **339**(6126): 1436-1441.
Cui, X., Y. Yu, S. Gupta, Y. M. Cho, S. P. Lees-Miller and K. Meek (2005). "Autophosphorylation of DNA-dependent protein kinase regulates DNA end processing and may also alter double-strand break repair pathway choice." Mol Cell Biol **25**(24): 10842-10852.

D'Avino, P. P., T. Takeda, L. Capalbo, W. Zhang, K. S. Lilley, E. D. Laue and D. M. Glover (2008). "Interaction between Anillin and RacGAP50C connects the actomyosin contractile ring with spindle microtubules at the cell division site." J Cell Sci **121**(Pt 8): 1151-1158.
Daley, J. M., R. L. Laan, A. Suresh and T. E. Wilson (2005). "DNA joint dependence of pol X family polymerase action in nonhomologous end joining." J Biol Chem **280**(32): 29030-29037.
Dalvai, M., O. Mondesert, J. C. Bourdon, B. Ducommun and C. Dozier (2011). "Cdc25B is negatively regulated by p53 through Sp1 and NF-Y transcription factors." Oncogene **30**(19): 2282-2288.
Dambournet, D., M. Machicoane, L. Chesneau, M. Sachse, M. Rocancourt, A. El Marjou, E. Formstecher, R. Salomon, B. Goud and A. Echard (2011). "Rab35 GTPase and OCRL phosphatase remodel lipids and F-actin for successful cytokinesis." Nat Cell Biol **13**(8): 981-988.
Davis, A. J., B. P. Chen and D. J. Chen (2014). "DNA-PK: a dynamic enzyme in a versatile DSB repair pathway." DNA Repair (Amst) **17**: 21-29.
Dawlaty, M. M., L. Malureanu, K. B. Jeganathan, E. Kao, C. Sustmann, S. Tahk, K. Shuai, R. Grosschedl and J. M. van Deursen (2008). "Resolution of sister centromeres requires RanBP2-mediated SUMOylation of topoisomerase IIalpha." Cell **133**(1): 103-115.
de Carcer, G., B. Escobar, A. M. Higuero, L. Garcia, A. Anson, G. Perez, M. Mollejo, G. Manning, B. Melendez, J. Abad-Rodriguez and M. Malumbres (2011). "Plk5, a polo box domain-only protein with specific roles in neuron differentiation and glioblastoma suppression." Mol Cell Biol **31**(6): 1225-1239.
de Carcer, G., G. Manning and M. Malumbres (2011). "From Plk1 to Plk5: functional evolution of polo-like kinases." Cell Cycle **10**(14): 2255-2262.
Degenhardt, Y. and T. Lampkin (2010). "Targeting Polo-like kinase in cancer therapy." Clin Cancer Res **16**(2): 384-389.
DeLuca, K. F., S. M. Lens and J. G. DeLuca (2011). "Temporal changes in Hec1 phosphorylation control kinetochore-microtubule attachment stability during mitosis." J Cell Sci **124**(Pt 4): 622-634.
den Elzen, N. and J. Pines (2001). "Cyclin A is destroyed in prometaphase and can delay chromosome alignment and anaphase." J Cell Biol **153**(1): 121-136.
Deng, S., X. Lu, Z. Zhang, R. Meng, M. Li and S. Xia (2021). "Identification and assessment of PLK1/2/3/4 in lung adenocarcinoma and lung squamous cell carcinoma: Evidence from methylation profile." J Cell Mol Med **25**(14): 6652-6663.
DeRan, M., M. Pulvino, E. Greene, C. Su and J. Zhao (2008). "Transcriptional activation of histone genes requires NPAT-dependent recruitment of TRRAP-Tip60 complex to histone promoters during the G1/S phase transition." Mol Cell Biol **28**(1): 435-447.
Deshpande, R. A., J. H. Lee and T. T. Paull (2017). "Rad50 ATPase activity is regulated by DNA ends and requires coordination of both active sites." Nucleic Acids Res **45**(9): 5255-5268.
Devos, D., S. Dokudovskaya, F. Alber, R. Williams, B. T. Chait, A. Sali and M. P. Rout (2004). "Components of coated vesicles and nuclear pore complexes share a common molecular architecture." PLoS Biol **2**(12): e380.
Dewar, J. M., M. Budzowska and J. C. Walter (2015). "The mechanism of DNA replication termination in vertebrates." Nature **525**(7569): 345-350.
Dewar, J. M. and J. C. Walter (2017). "Mechanisms of DNA replication termination." Nat Rev Mol Cell Biol **18**(8): 507-516.
Dogterom, M. and G. H. Koenderink (2019). "Actin-microtubule crosstalk in cell biology." Nat Rev Mol Cell Biol **20**(1): 38-54.
Donjerkovic, D. and D. W. Scott (2000). "Regulation of the G1 phase of the mammalian cell cycle." Cell Res **10**(1): 1-16.
Donohue, P. J., G. F. Alberts, Y. Guo and J. A. Winkles (1995). "Identification by targeted differential display of an immediate early gene encoding a putative serine/threonine kinase." J Biol Chem **270**(17): 10351-10357.
Donzelli, M. and G. F. Draetta (2003). "Regulating mammalian checkpoints through Cdc25 inactivation." EMBO Rep **4**(7): 671-677.

Dultz, E., E. Zanin, C. Wurzenberger, M. Braun, G. Rabut, L. Sironi and J. Ellenberg (2008). "Systematic kinetic analysis of mitotic dis- and reassembly of the nuclear pore in living cells." J Cell Biol **180**(5): 857-865.
Dumaz, N. and D. W. Meek (1999). "Serine15 phosphorylation stimulates p53 transactivation but does not directly influence interaction with HDM2." EMBO J **18**(24): 7002-7010.
Dumaz, N., D. M. Milne and D. W. Meek (1999). "Protein kinase CK1 is a p53-threonine 18 kinase which requires prior phosphorylation of serine 15." FEBS Lett **463**(3): 312-316.
Ebisawa, T. (2007). "Circadian rhythms in the CNS and peripheral clock disorders: human sleep disorders and clock genes." J Pharmacol Sci **103**(2): 150-154.
Egelhoff, T. T., R. J. Lee and J. A. Spudich (1993). "Dictyostelium myosin heavy chain phosphorylation sites regulate myosin filament assembly and localization in vivo." Cell **75**(2): 363-371.
Eide, E. J. and D. M. Virshup (2001). "Casein kinase I: another cog in the circadian clockworks." Chronobiol Int **18**(3): 389-398.
Eisenhardt, N., J. Redolfi and W. Antonin (2014). "Interaction of Nup53 with Ndc1 and Nup155 is required for nuclear pore complex assembly." J Cell Sci **127**(Pt 4): 908-921.
Ekholm, S. V., P. Zickert, S. I. Reed and A. Zetterberg (2001). "Accumulation of cyclin E is not a prerequisite for passage through the restriction point." Mol Cell Biol **21**(9): 3256-3265.
El-Brolosy, M. A. and D. Y. R. Stainier (2017). "Genetic compensation: A phenomenon in search of mechanisms." PLoS Genet **13**(7): e1006780.
Elia, A. E., L. C. Cantley and M. B. Yaffe (2003). "Proteomic screen finds pSer/pThr-binding domain localizing Plk1 to mitotic substrates." Science **299**(5610): 1228-1231.
Elia, A. E., P. Rellos, L. F. Haire, J. W. Chao, F. J. Ivins, K. Hoepker, D. Mohammad, L. C. Cantley, S. J. Smerdon and M. B. Yaffe (2003). "The molecular basis for phosphodependent substrate targeting and regulation of Plks by the Polo-box domain." Cell **115**(1): 83-95.
Ellison, V. and B. Stillman (2001). "Opening of the clamp: an intimate view of an ATP-driven biological machine." Cell **106**(6): 655-660.
Elting, M. W., C. L. Hueschen, D. B. Udy and S. Dumont (2014). "Force on spindle microtubule minus ends moves chromosomes." J Cell Biol **206**(2): 245-256.
Elyada, E., A. Pribluda, R. E. Goldstein, Y. Morgenstern, G. Brachya, G. Cojocaru, I. Snir-Alkalay, I. Burstain, R. Haffner-Krausz, S. Jung, Z. Wiener, K. Alitalo, M. Oren, E. Pikarsky and Y. Ben-Neriah (2011). "CKIalpha ablation highlights a critical role for p53 in invasiveness control." Nature **470**(7334): 409-413.
Ettinger, A. W., M. Wilsch-Brauninger, A. M. Marzesco, M. Bickle, A. Lohmann, Z. Maliga, J. Karbanova, D. Corbeil, A. A. Hyman and W. B. Huttner (2011). "Proliferating versus differentiating stem and cancer cells exhibit distinct midbody-release behaviour." Nat Commun **2**: 503.
Fabbro, M., K. Savage, K. Hobson, A. J. Deans, S. N. Powell, G. A. McArthur and K. K. Khanna (2004). "BRCA1-BARD1 complexes are required for p53Ser-15 phosphorylation and a G1/S arrest following ionizing radiation-induced DNA damage." J Biol Chem **279**(30): 31251-31258.
Falck, J., N. Mailand, R. G. Syljuasen, J. Bartek and J. Lukas (2001). "The ATM-Chk2-Cdc25A checkpoint pathway guards against radioresistant DNA synthesis." Nature **410**(6830): 842-847.
Farina, F., J. Gaillard, C. Guerin, Y. Coute, J. Sillibourne, L. Blanchoin and M. Thery (2016). "The centrosome is an actin-organizing centre." Nat Cell Biol **18**(1): 65-75.
Farina, F., N. Ramkumar, L. Brown, D. Samandar Eweis, J. Anstatt, T. Waring, J. Bithell, G. Scita, M. Thery, L. Blanchoin, T. Zech and B. Baum (2019). "Local actin nucleation tunes centrosomal microtubule nucleation during passage through mitosis." EMBO J **38**(11).
Fededa, J. P. and D. W. Gerlich (2012). "Molecular control of animal cell cytokinesis." Nat Cell Biol **14**(5): 440-447.
Firestein, R., A. J. Bass, S. Y. Kim, I. F. Dunn, S. J. Silver, I. Guney, E. Freed, A. H. Ligon, N. Vena, S. Ogino, M. G. Chheda, P. Tamayo, S. Finn, Y. Shrestha, J. S. Boehm, S. Jain, E. Bojarski, C. Mermel, J. Barretina, J. A. Chan, J. Baselga, J. Tabernero, D. E. Root, C. S. Fuchs, M. Loda, R. A. Shivdasani, M.

Meyerson and W. C. Hahn (2008). "CDK8 is a colorectal cancer oncogene that regulates beta-catenin activity." Nature **455**(7212): 547-551.
Fisher, R. P. (2005). "Secrets of a double agent: CDK7 in cell-cycle control and transcription." J Cell Sci **118**(Pt 22): 5171-5180.
Flajolet, M., G. He, M. Heiman, A. Lin, A. C. Nairn and P. Greengard (2007). "Regulation of Alzheimer's disease amyloid-beta formation by casein kinase I." Proc Natl Acad Sci U S A **104**(10): 4159-4164.
Fleming, E. S., M. Temchin, Q. Wu, L. Maggio-Price and J. S. Tirnauer (2009). "Spindle misorientation in tumors from APC(min/+) mice." Mol Carcinog **48**(7): 592-598.
Flotow, H., P. R. Graves, A. Q. Wang, C. J. Fiol, R. W. Roeske and P. J. Roach (1990). "Phosphate groups as substrate determinants for casein kinase I action." J Biol Chem **265**(24): 14264-14269.
Flotow, H. and P. J. Roach (1991). "Role of acidic residues as substrate determinants for casein kinase I." J Biol Chem **266**(6): 3724-3727.
Foe, I. T., S. A. Foster, S. K. Cheung, S. Z. DeLuca, D. O. Morgan and D. P. Toczyski (2011). "Ubiquitination of Cdc20 by the APC occurs through an intramolecular mechanism." Curr Biol **21**(22): 1870-1877.
Foldynova-Trantirkova, S., P. Sekyrova, K. Tmejova, E. Brumovska, O. Bernatik, W. Blankenfeldt, P. Krejci, A. Kozubik, T. Dolezal, L. Trantirek and V. Bryja (2010). "Breast cancer-specific mutations in CK1epsilon inhibit Wnt/beta-catenin and activate the Wnt/Rac1/JNK and NFAT pathways to decrease cell adhesion and promote cell migration." Breast Cancer Res **12**(3): R30.
Foley, E. A. and T. M. Kapoor (2013). "Microtubule attachment and spindle assembly checkpoint signalling at the kinetochore." Nat Rev Mol Cell Biol **14**(1): 25-37.
Forrest, A. and B. Gabrielli (2001). "Cdc25B activity is regulated by 14-3-3." Oncogene **20**(32): 4393-4401.
Freed, E., K. R. Lacey, P. Huie, S. A. Lyapina, R. J. Deshaies, T. Stearns and P. K. Jackson (1999). "Components of an SCF ubiquitin ligase localize to the centrosome and regulate the centrosome duplication cycle." Genes Dev **13**(17): 2242-2257.
Frouin, I., M. Toueille, E. Ferrari, I. Shevelev and U. Hubscher (2005). "Phosphorylation of human DNA polymerase lambda by the cyclin-dependent kinase Cdk2/cyclin A complex is modulated by its association with proliferating cell nuclear antigen." Nucleic Acids Res **33**(16): 5354-5361.
Fulcher, L. J., P. Bozatzi, T. Tachie-Menson, K. Z. L. Wu, T. D. Cummins, J. C. Bufton, D. M. Pinkas, K. Dunbar, S. Shrestha, N. T. Wood, S. Weidlich, T. J. Macartney, J. Varghese, R. Gourlay, D. G. Campbell, K. S. Dingwell, J. C. Smith, A. N. Bullock and G. P. Sapkota (2018). "The DUF1669 domain of FAM83 family proteins anchor casein kinase 1 isoforms." Sci Signal **11**(531).
Fulcher, L. J., Z. He, L. Mei, T. J. Macartney, N. T. Wood, A. R. Prescott, A. J. Whigham, J. Varghese, R. Gourlay, G. Ball, R. Clarke, D. G. Campbell, C. A. Maxwell and G. P. Sapkota (2019). "FAM83D directs protein kinase CK1alpha to the mitotic spindle for proper spindle positioning." EMBO Rep **20**(9): e47495.
Fulcher, L. J. and G. P. Sapkota (2020). "Functions and regulation of the serine/threonine protein kinase CK1 family: moving beyond promiscuity." Biochem J **477**(23): 4603-4621.
Fullbright, G., H. B. Rycenga, J. D. Gruber and D. T. Long (2016). "p97 Promotes a Conserved Mechanism of Helicase Unloading during DNA Cross-Link Repair." Mol Cell Biol **36**(23): 2983-2994.
Furnari, B., A. Blasina, M. N. Boddy, C. H. McGowan and P. Russell (1999). "Cdc25 inhibited in vivo and in vitro by checkpoint kinases Cds1 and Chk1." Mol Biol Cell **10**(4): 833-845.
Garcia-Higuera, I., E. Manchado, P. Dubus, M. Canamero, J. Mendez, S. Moreno and M. Malumbres (2008). "Genomic stability and tumour suppression by the APC/C cofactor Cdh1." Nat Cell Biol **10**(7): 802-811.
Garcin, C. and A. Straube (2019). "Microtubules in cell migration." Essays Biochem **63**(5): 509-520.
Gautier, J., C. Norbury, M. Lohka, P. Nurse and J. Maller (1988). "Purified maturation-promoting factor contains the product of a Xenopus homolog of the fission yeast cell cycle control gene cdc2+." Cell **54**(3): 433-439.
Gavet, O. and J. Pines (2010). "Progressive activation of CyclinB1-Cdk1 coordinates entry to mitosis." Dev Cell **18**(4): 533-543.

Geley, S., E. Kramer, C. Gieffers, J. Gannon, J. M. Peters and T. Hunt (2001). "Anaphase-promoting complex/cyclosome-dependent proteolysis of human cyclin A starts at the beginning of mitosis and is not subject to the spindle assembly checkpoint." J Cell Biol **153**(1): 137-148.
Gentile, M., L. Latonen and M. Laiho (2003). "Cell cycle arrest and apoptosis provoked by UV radiation-induced DNA damage are transcriptionally highly divergent responses." Nucleic Acids Res **31**(16): 4779-4790.
Georgatos, S. D., A. Pyrpasopoulou and P. A. Theodoropoulos (1997). "Nuclear envelope breakdown in mammalian cells involves stepwise lamina disassembly and microtubule-drive deformation of the nuclear membrane." J Cell Sci **110 (Pt 17)**: 2129-2140.
Gerace, L. and G. Blobel (1980). "The nuclear envelope lamina is reversibly depolymerized during mitosis." Cell **19**(1): 277-287.
Giamas, G., H. Hirner, L. Shoshiashvili, A. Grothey, S. Gessert, M. Kuhl, D. Henne-Bruns, C. E. Vorgias and U. Knippschild (2007). "Phosphorylation of CK1delta: identification of Ser370 as the major phosphorylation site targeted by PKA in vitro and in vivo." Biochem J **406**(3): 389-398.
Glotzer, M. (2009). "The 3Ms of central spindle assembly: microtubules, motors and MAPs." Nat Rev Mol Cell Biol **10**(1): 9-20.
Glover, D. M. (1989). "Mitosis in Drosophila." J Cell Sci **92 (Pt 2)**: 137-146.
Goldberg, M., M. Stucki, J. Falck, D. D'Amours, D. Rahman, D. Pappin, J. Bartek and S. P. Jackson (2003). "MDC1 is required for the intra-S-phase DNA damage checkpoint." Nature **421**(6926): 952-956.
Grant, G. D., L. Brooks, 3rd, X. Zhang, J. M. Mahoney, V. Martyanov, T. A. Wood, G. Sherlock, C. Cheng and M. L. Whitfield (2013). "Identification of cell cycle-regulated genes periodically expressed in U2OS cells and their regulation by FOXM1 and E2F transcription factors." Mol Biol Cell **24**(23): 3634-3650.
Graves, P. R. and P. J. Roach (1995). "Role of COOH-terminal phosphorylation in the regulation of casein kinase I delta." J Biol Chem **270**(37): 21689-21694.
Greer, Y. E., C. J. Westlake, B. Gao, K. Bharti, Y. Shiba, C. P. Xavier, G. J. Pazour, Y. Yang and J. S. Rubin (2014). "Casein kinase 1delta functions at the centrosome and Golgi to promote ciliogenesis." Mol Biol Cell **25**(10): 1629-1640.
Gromley, A., C. Yeaman, J. Rosa, S. Redick, C. T. Chen, S. Mirabelle, M. Guha, J. Sillibourne and S. J. Doxsey (2005). "Centriolin anchoring of exocyst and SNARE complexes at the midbody is required for secretory-vesicle-mediated abscission." Cell **123**(1): 75-87.
Gross, S. D., D. P. Hoffman, P. L. Fisette, P. Baas and R. A. Anderson (1995). "A phosphatidylinositol 4,5-bisphosphate-sensitive casein kinase I alpha associates with synaptic vesicles and phosphorylates a subset of vesicle proteins." J Cell Biol **130**(3): 711-724.
Groth, A., A. Corpet, A. J. Cook, D. Roche, J. Bartek, J. Lukas and G. Almouzni (2007). "Regulation of replication fork progression through histone supply and demand." Science **318**(5858): 1928-1931.
Gu, Y., J. Rosenblatt and D. O. Morgan (1992). "Cell cycle regulation of CDK2 activity by phosphorylation of Thr160 and Tyr15." EMBO J **11**(11): 3995-4005.
Guirouilh-Barbat, J., S. Huck and B. S. Lopez (2008). "S-phase progression stimulates both the mutagenic KU-independent pathway and mutagenic processing of KU-dependent intermediates, for nonhomologous end joining." Oncogene **27**(12): 1726-1736.
Guizetti, J. and D. W. Gerlich (2010). "Cytokinetic abscission in animal cells." Semin Cell Dev Biol **21**(9): 909-916.
Guizetti, J., L. Schermelleh, J. Mantler, S. Maar, I. Poser, H. Leonhardt, T. Muller-Reichert and D. W. Gerlich (2011). "Cortical constriction during abscission involves helices of ESCRT-III-dependent filaments." Science **331**(6024): 1616-1620.
Gunesdogan, U., H. Jackle and A. Herzig (2014). "Histone supply regulates S phase timing and cell cycle progression." Elife **3**: e02443.
Guo, Z. Y., X. H. Hao, F. F. Tan, X. Pei, L. M. Shang, X. L. Jiang and F. Yang (2011). "The elements of human cyclin D1 promoter and regulation involved." Clin Epigenetics **2**(2): 63-76.

Gupta, S., S. Mana-Capelli, J. R. McLean, C. T. Chen, S. Ray, K. L. Gould and D. McCollum (2013). "Identification of SIN pathway targets reveals mechanisms of crosstalk between NDR kinase pathways." Curr Biol **23**(4): 333-338.
Guttinger, S., E. Laurell and U. Kutay (2009). "Orchestrating nuclear envelope disassembly and reassembly during mitosis." Nat Rev Mol Cell Biol **10**(3): 178-191.
Hannak, E., M. Kirkham, A. A. Hyman and K. Oegema (2001). "Aurora-A kinase is required for centrosome maturation in Caenorhabditis elegans." J Cell Biol **155**(7): 1109-1116.
Hara, M. and T. Fukagawa (2018). "Kinetochore assembly and disassembly during mitotic entry and exit." Curr Opin Cell Biol **52**: 73-81.
Harbour, J. W., R. X. Luo, A. Dei Santi, A. A. Postigo and D. C. Dean (1999). "Cdk phosphorylation triggers sequential intramolecular interactions that progressively block Rb functions as cells move through G1." Cell **98**(6): 859-869.
Harel, A., R. C. Chan, A. Lachish-Zalait, E. Zimmerman, M. Elbaum and D. J. Forbes (2003). "Importin beta negatively regulates nuclear membrane fusion and nuclear pore complex assembly." Mol Biol Cell **14**(11): 4387-4396.
Haren, L., T. Stearns and J. Luders (2009). "Plk1-dependent recruitment of gamma-tubulin complexes to mitotic centrosomes involves multiple PCM components." PLoS One **4**(6): e5976.
Hartmann, O., F. Spyratos, N. Harbeck, D. Dietrich, A. Fassbender, M. Schmitt, S. Eppenberger-Castori, V. Vuaroqueaux, F. Lerebours, K. Welzel, S. Maier, A. Plum, S. Niemann, J. A. Foekens, R. Lesche and J. W. Martens (2009). "DNA methylation markers predict outcome in node-positive, estrogen receptor-positive breast cancer with adjuvant anthracycline-based chemotherapy." Clin Cancer Res **15**(1): 315-323.
Harvey, K. J. and J. Newport (2003). "Metazoan origin selection: origin recognition complex chromatin binding is regulated by CDC6 recruitment and ATP hydrolysis." J Biol Chem **278**(49): 48524-48528.
Hauge, H., K. E. Fjelland, M. Sioud and H. C. Aasheim (2009). "Evidence for the involvement of FAM110C protein in cell spreading and migration." Cell Signal **21**(12): 1866-1873.
Hauge, H., S. Patzke and H. C. Aasheim (2007). "Characterization of the FAM110 gene family." Genomics **90**(1): 14-27.
He, G., Z. H. Siddik, Z. Huang, R. Wang, J. Koomen, R. Kobayashi, A. R. Khokhar and J. Kuang (2005). "Induction of p21 by p53 following DNA damage inhibits both Cdk4 and Cdk2 activities." Oncogene **24**(18): 2929-2943.
He, Z., N. Kannan, O. Nemirovsky, H. Chen, M. Connell, B. Taylor, J. Jiang, L. M. Pilarski, M. C. Fleisch, D. Niederacher, M. A. Pujana, C. J. Eaves and C. A. Maxwell (2017). "BRCA1 controls the cell division axis and governs ploidy and phenotype in human mammary cells." Oncotarget **8**(20): 32461-32475.
Heald, R., R. Tournebize, T. Blank, R. Sandaltzopoulos, P. Becker, A. Hyman and E. Karsenti (1996). "Self-organization of microtubules into bipolar spindles around artificial chromosomes in Xenopus egg extracts." Nature **382**(6590): 420-425.
Hebbar, S., M. T. Mesngon, A. M. Guillotte, B. Desai, R. Ayala and D. S. Smith (2008). "Lis1 and Ndel1 influence the timing of nuclear envelope breakdown in neural stem cells." J Cell Biol **182**(6): 1063-1071.
Hegarat, N., A. Crncec, M. F. Suarez Peredo Rodriguez, F. Echegaray Iturra, Y. Gu, O. Busby, P. F. Lang, A. R. Barr, C. Bakal, M. T. Kanemaki, A. I. Lamond, B. Novak, T. Ly and H. Hochegger (2020). "Cyclin A triggers Mitosis either via the Greatwall kinase pathway or Cyclin B." EMBO J **39**(11): e104419.
Helin, K., E. Harlow and A. Fattaey (1993). "Inhibition of E2F-1 transactivation by direct binding of the retinoblastoma protein." Mol Cell Biol **13**(10): 6501-6508.
Helleday, T., J. Lo, D. C. van Gent and B. P. Engelward (2007). "DNA double-strand break repair: from mechanistic understanding to cancer treatment." DNA Repair (Amst) **6**(7): 923-935.
Helmke, C., M. Raab, F. Rodel, Y. Matthess, T. Oellerich, R. Mandal, M. Sanhaji, H. Urlaub, C. Rodel, S. Becker and K. Strebhardt (2016). "Ligand stimulation of CD95 induces activation of Plk3 followed by phosphorylation of caspase-8." Cell Res **26**(8): 914-934.
Hengstschlager, M., K. Braun, T. Soucek, A. Miloloza and E. Hengstschlager-Ottnad (1999). "Cyclin-dependent kinases at the G1-S transition of the mammalian cell cycle." Mutat Res **436**(1): 1-9.

Hentges, P., P. Ahnesorg, R. S. Pitcher, C. K. Bruce, B. Kysela, A. J. Green, J. Bianchi, T. E. Wilson, S. P. Jackson and A. J. Doherty (2006). "Evolutionary and functional conservation of the DNA non-homologous end-joining protein, XLF/Cernunnos." J Biol Chem **281**(49): 37517-37526.
Hetzer, M., D. Bilbao-Cortes, T. C. Walther, O. J. Gruss and I. W. Mattaj (2000). "GTP hydrolysis by Ran is required for nuclear envelope assembly." Mol Cell **5**(6): 1013-1024.
Hetzer, M., H. H. Meyer, T. C. Walther, D. Bilbao-Cortes, G. Warren and I. W. Mattaj (2001). "Distinct AAA-ATPase p97 complexes function in discrete steps of nuclear assembly." Nat Cell Biol **3**(12): 1086-1091.
Hinchcliffe, E. H., C. Li, E. A. Thompson, J. L. Maller and G. Sluder (1999). "Requirement of Cdk2-cyclin E activity for repeated centrosome reproduction in Xenopus egg extracts." Science **283**(5403): 851-854.
Hirao, A., Y. Y. Kong, S. Matsuoka, A. Wakeham, J. Ruland, H. Yoshida, D. Liu, S. J. Elledge and T. W. Mak (2000). "DNA damage-induced activation of p53 by the checkpoint kinase Chk2." Science **287**(5459): 1824-1827.
Ho, A. and S. F. Dowdy (2002). "Regulation of G(1) cell-cycle progression by oncogenes and tumor suppressor genes." Curr Opin Genet Dev **12**(1): 47-52.
Hoar, K., A. Chakravarty, C. Rabino, D. Wysong, D. Bowman, N. Roy and J. A. Ecsedy (2007). "MLN8054, a small-molecule inhibitor of Aurora A, causes spindle pole and chromosome congression defects leading to aneuploidy." Mol Cell Biol **27**(12): 4513-4525.
Hoek, M. and B. Stillman (2003). "Chromatin assembly factor 1 is essential and couples chromatin assembly to DNA replication in vivo." Proc Natl Acad Sci U S A **100**(21): 12183-12188.
Hoekstra, M. F., A. J. DeMaggio and N. Dhillon (1991). "Genetically identified protein kinases in yeast. II: DNA metabolism and meiosis." Trends Genet **7**(9): 293-297.
Hoekstra, M. F., R. M. Liskay, A. C. Ou, A. J. DeMaggio, D. G. Burbee and F. Heffron (1991). "HRR25, a putative protein kinase from budding yeast: association with repair of damaged DNA." Science **253**(5023): 1031-1034.
Holloway, S. L., M. Glotzer, R. W. King and A. W. Murray (1993). "Anaphase is initiated by proteolysis rather than by the inactivation of maturation-promoting factor." Cell **73**(7): 1393-1402.
Holt, L. J., B. B. Tuch, J. Villen, A. D. Johnson, S. P. Gygi and D. O. Morgan (2009). "Global analysis of Cdk1 substrate phosphorylation sites provides insights into evolution." Science **325**(5948): 1682-1686.
Holtrich, U., G. Wolf, J. Yuan, J. Bereiter-Hahn, T. Karn, M. Weiler, G. Kauselmann, M. Rehli, R. Andreesen, M. Kaufmann, D. Kuhl and K. Strebhardt (2000). "Adhesion induced expression of the serine/threonine kinase Fnk in human macrophages." Oncogene **19**(42): 4832-4839.
Honaker, Y. and H. Piwnica-Worms (2010). "Casein kinase 1 functions as both penultimate and ultimate kinase in regulating Cdc25A destruction." Oncogene **29**(23): 3324-3334.
Hopfner, K. P., L. Craig, G. Moncalian, R. A. Zinkel, T. Usui, B. A. Owen, A. Karcher, B. Henderson, J. L. Bodmer, C. T. McMurray, J. P. Carney, J. H. Petrini and J. A. Tainer (2002). "The Rad50 zinc-hook is a structure joining Mre11 complexes in DNA recombination and repair." Nature **418**(6897): 562-566.
Hornbeck, P. V., B. Zhang, B. Murray, J. M. Kornhauser, V. Latham and E. Skrzypek (2015). "PhosphoSitePlus, 2014: mutations, PTMs and recalibrations." Nucleic Acids Res **43**(Database issue): D512-520.
Hu, C. K., M. Coughlin, C. M. Field and T. J. Mitchison (2011). "KIF4 regulates midzone length during cytokinesis." Curr Biol **21**(10): 815-824.
Huang, R., J. Guo, P. Yan, S. Zhai, P. Hu, X. Zhu, J. Zhang, Y. Qiao, Y. Zhang, H. Liu, L. Huang, J. Zhang, D. Yang and Z. Huang (2020). "The Construction of Bone Metastasis-Specific Prognostic Model and Co-expressed Network of Alternative Splicing in Breast Cancer." Front Cell Dev Biol **8**: 790.
Huart, A. S., N. J. MacLaine, D. W. Meek and T. R. Hupp (2009). "CK1alpha plays a central role in mediating MDM2 control of p53 and E2F-1 protein stability." J Biol Chem **284**(47): 32384-32394.
Hustedt, N. and D. Durocher (2016). "The control of DNA repair by the cell cycle." Nat Cell Biol **19**(1): 1-9.
Hutterer, A., M. Glotzer and M. Mishima (2009). "Clustering of centralspindlin is essential for its accumulation to the central spindle and the midbody." Curr Biol **19**(23): 2043-2049.

Hwang, L. H., L. F. Lau, D. L. Smith, C. A. Mistrot, K. G. Hardwick, E. S. Hwang, A. Amon and A. W. Murray (1998). "Budding yeast Cdc20: a target of the spindle checkpoint." Science **279**(5353): 1041-1044.
Hyun, J., I. Becam, C. Yanicostas and D. Bohmann (2006). "Control of G2/M transition by Drosophila Fos." Mol Cell Biol **26**(22): 8293-8302.
Iavarone, A. and J. Massague (1999). "E2F and histone deacetylase mediate transforming growth factor beta repression of cdc25A during keratinocyte cell cycle arrest." Mol Cell Biol **19**(1): 916-922.
Iida, M., M. Matsuda and H. Komatani (2008). "Plk3 phosphorylates topoisomerase IIalpha at Thr(1342), a site that is not recognized by Plk1." Biochem J **411**(1): 27-32.
Iliakis, G., Y. Wang, J. Guan and H. Wang (2003). "DNA damage checkpoint control in cells exposed to ionizing radiation." Oncogene **22**(37): 5834-5847.
Inuzuka, H., A. Tseng, D. Gao, B. Zhai, Q. Zhang, S. Shaik, L. Wan, X. L. Ang, C. Mock, H. Yin, J. M. Stommel, S. Gygi, G. Lahav, J. Asara, Z. X. Xiao, W. G. Kaelin, Jr., J. W. Harper and W. Wei (2010). "Phosphorylation by casein kinase I promotes the turnover of the Mdm2 oncoprotein via the SCF(beta-TRCP) ubiquitin ligase." Cancer Cell **18**(2): 147-159.
Iouk, T., O. Kerscher, R. J. Scott, M. A. Basrai and R. W. Wozniak (2002). "The yeast nuclear pore complex functionally interacts with components of the spindle assembly checkpoint." J Cell Biol **159**(5): 807-819.
Jang, Y. J., J. H. Ji, Y. C. Choi, C. J. Ryu and S. Y. Ko (2007). "Regulation of Polo-like kinase 1 by DNA damage in mitosis. Inhibition of mitotic PLK-1 by protein phosphatase 2A." J Biol Chem **282**(4): 2473-2482.
Jares, P. and J. J. Blow (2000). "Xenopus cdc7 function is dependent on licensing but not on XORC, XCdc6, or CDK activity and is required for XCdc45 loading." Genes Dev **14**(12): 1528-1540.
Jeggo, P. and P. O'Neill (2002). "The Greek Goddess, Artemis, reveals the secrets of her cleavage." DNA Repair (Amst) **1**(9): 771-777.
Jiang, H., H. C. Reinhardt, J. Bartkova, J. Tommiska, C. Blomqvist, H. Nevanlinna, J. Bartek, M. B. Yaffe and M. T. Hemann (2009). "The combined status of ATM and p53 link tumor development with therapeutic response." Genes Dev **23**(16): 1895-1909.
Jiang, N., X. Wang, M. Jhanwar-Uniyal, Z. Darzynkiewicz and W. Dai (2006). "Polo box domain of Plk3 functions as a centrosome localization signal, overexpression of which causes mitotic arrest, cytokinesis defects, and apoptosis." J Biol Chem **281**(15): 10577-10582.
Jin, J., X. L. Ang, X. Ye, M. Livingstone and J. W. Harper (2008). "Differential roles for checkpoint kinases in DNA damage-dependent degradation of the Cdc25A protein phosphatase." J Biol Chem **283**(28): 19322-19328.
Johnson, A. E., J. S. Chen and K. L. Gould (2013). "CK1 is required for a mitotic checkpoint that delays cytokinesis." Curr Biol **23**(19): 1920-1926.
Jonsson, Z. O. and U. Hubscher (1997). "Proliferating cell nuclear antigen: more than a clamp for DNA polymerases." Bioessays **19**(11): 967-975.
Kaestel, C. G., H. O. Madsen, J. U. Prause, A. Jorgensen, Y. Liang, M. la Cour, G. M. Lui, N. Odum, M. H. Nissen and C. Ropke (2001). "Lack of FasL expression in cultured human retinal pigment epithelial cells." Exp Clin Immunogenet **18**(1): 34-41.
Kalinina, I., A. Nandi, P. Delivani, M. R. Chacon, A. H. Klemm, D. Ramunno-Johnson, A. Krull, B. Lindner, N. Pavin and I. M. Tolic-Norrelykke (2013). "Pivoting of microtubules around the spindle pole accelerates kinetochore capture." Nat Cell Biol **15**(1): 82-87.
Kalousi, A., I. Mylonis, A. S. Politou, G. Chachami, E. Paraskeva and G. Simos (2010). "Casein kinase 1 regulates human hypoxia-inducible factor HIF-1." J Cell Sci **123**(Pt 17): 2976-2986.
Kanchanawong, P., G. Shtengel, A. M. Pasapera, E. B. Ramko, M. W. Davidson, H. F. Hess and C. M. Waterman (2010). "Nanoscale architecture of integrin-based cell adhesions." Nature **468**(7323): 580-584.
Kang, D., J. Chen, J. Wong and G. Fang (2002). "The checkpoint protein Chfr is a ligase that ubiquitinates Plk1 and inhibits Cdc2 at the G2 to M transition." J Cell Biol **156**(2): 249-259.
Kapoor, T. M., M. A. Lampson, P. Hergert, L. Cameron, D. Cimini, E. D. Salmon, B. F. McEwen and A. Khodjakov (2006). "Chromosomes can congress to the metaphase plate before biorientation." Science **311**(5759): 388-391.

Kastan, M. B. (2001). "Cell cycle. Checking two steps." Nature **410**(6830): 766-767.
Kastan, M. B. and J. Bartek (2004). "Cell-cycle checkpoints and cancer." Nature **432**(7015): 316-323.
Kawakami, F., K. Suzuki and K. Ohtsuki (2008). "A novel consensus phosphorylation motif in sulfatide- and cholesterol-3-sulfate-binding protein substrates for CK1 in vitro." Biol Pharm Bull **31**(2): 193-200.
Kettenbach, A. N., K. A. Schlosser, S. P. Lyons, I. Nasa, J. Gui, M. E. Adamo and S. A. Gerber (2018). "Global assessment of its network dynamics reveals that the kinase Plk1 inhibits the phosphatase PP6 to promote Aurora A activity." Sci Signal **11**(530).
Kim, J. M., M. Yamada and H. Masai (2003). "Functions of mammalian Cdc7 kinase in initiation/monitoring of DNA replication and development." Mutat Res **532**(1-2): 29-40.
Kimura, K. and T. Hirano (1997). "ATP-dependent positive supercoiling of DNA by 13S condensin: a biochemical implication for chromosome condensation." Cell **90**(4): 625-634.
Kinner, A., W. Wu, C. Staudt and G. Iliakis (2008). "Gamma-H2AX in recognition and signaling of DNA double-strand breaks in the context of chromatin." Nucleic Acids Res **36**(17): 5678-5694.
Kirschner, M. and T. Mitchison (1986). "Beyond self-assembly: from microtubules to morphogenesis." Cell **45**(3): 329-342.
Kita, A. M., Z. T. Swider, I. Erofeev, M. C. Halloran, A. B. Goryachev and W. M. Bement (2019). "Spindle-F-actin interactions in mitotic spindles in an intact vertebrate epithelium." Mol Biol Cell **30**(14): 1645-1654.
Kitagawa, R. and A. M. Rose (1999). "Components of the spindle-assembly checkpoint are essential in Caenorhabditis elegans." Nat Cell Biol **1**(8): 514-521.
Kitamura, E., K. Tanaka, S. Komoto, Y. Kitamura, C. Antony and T. U. Tanaka (2010). "Kinetochores generate microtubules with distal plus ends: their roles and limited lifetime in mitosis." Dev Cell **18**(2): 248-259.
Kiyomitsu, T. and I. M. Cheeseman (2012). "Chromosome- and spindle-pole-derived signals generate an intrinsic code for spindle position and orientation." Nat Cell Biol **14**(3): 311-317.
Klebba, J. E., B. J. Galletta, J. Nye, K. M. Plevock, D. W. Buster, N. A. Hollingsworth, K. C. Slep, N. M. Rusan and G. C. Rogers (2015). "Two Polo-like kinase 4 binding domains in Asterless perform distinct roles in regulating kinase stability." J Cell Biol **208**(4): 401-414.
Kleiblova, P., L. Stolarova, K. Krizova, F. Lhota, J. Hojny, P. Zemankova, O. Havranek, M. Vocka, M. Cerna, K. Lhotova, M. Borecka, M. Janatova, J. Soukupova, J. Sevcik, M. Zimovjanova, J. Kotlas, A. Panczak, K. Vesela, J. Cervenkova, M. Schneiderova, M. Burocziova, K. Burdova, V. Stranecky, L. Foretova, E. Machackova, S. Tavandzis, S. Kmoch, L. Macurek and Z. Kleibl (2019). "Identification of deleterious germline CHEK2 mutations and their association with breast and ovarian cancer." Int J Cancer **145**(7): 1782-1797.
Kleylein-Sohn, J., J. Westendorf, M. Le Clech, R. Habedanck, Y. D. Stierhof and E. A. Nigg (2007). "Plk4-induced centriole biogenesis in human cells." Dev Cell **13**(2): 190-202.
Knight, A. S., M. Notaridou and R. J. Watson (2009). "A Lin-9 complex is recruited by B-Myb to activate transcription of G2/M genes in undifferentiated embryonal carcinoma cells." Oncogene **28**(15): 1737-1747.
Knippschild, U., A. Gocht, S. Wolff, N. Huber, J. Lohler and M. Stoter (2005). "The casein kinase 1 family: participation in multiple cellular processes in eukaryotes." Cell Signal **17**(6): 675-689.
Knippschild, U., D. M. Milne, L. E. Campbell, A. J. DeMaggio, E. Christenson, M. F. Hoekstra and D. W. Meek (1997). "p53 is phosphorylated in vitro and in vivo by the delta and epsilon isoforms of casein kinase 1 and enhances the level of casein kinase 1 delta in response to topoisomerase-directed drugs." Oncogene **15**(14): 1727-1736.
Knippschild, U., S. Wolff, G. Giamas, C. Brockschmidt, M. Wittau, P. U. Wurl, T. Eismann and M. Stoter (2005). "The role of the casein kinase 1 (CK1) family in different signaling pathways linked to cancer development." Onkologie **28**(10): 508-514.
Kops, G. J., B. A. Weaver and D. W. Cleveland (2005). "On the road to cancer: aneuploidy and the mitotic checkpoint." Nat Rev Cancer **5**(10): 773-785.
Kornberg, R. D. (1977). "Structure of chromatin." Annu Rev Biochem **46**: 931-954.

Korns, J., X. Liu and V. Takiar (2022). "A review of Plks: Thinking outside the (polo) box." Mol Carcinog **61**(2): 254-263.
Kotak, S. (2019). "Mechanisms of Spindle Positioning: Lessons from Worms and Mammalian Cells." Biomolecules **9**(2).
Kotak, S., C. Busso and P. Gonczy (2012). "Cortical dynein is critical for proper spindle positioning in human cells." J Cell Biol **199**(1): 97-110.
Kraft, C., F. Herzog, C. Gieffers, K. Mechtler, A. Hagting, J. Pines and J. M. Peters (2003). "Mitotic regulation of the human anaphase-promoting complex by phosphorylation." EMBO J **22**(24): 6598-6609.
Kramer, E. R., N. Scheuringer, A. V. Podtelejnikov, M. Mann and J. M. Peters (2000). "Mitotic regulation of the APC activator proteins CDC20 and CDH1." Mol Biol Cell **11**(5): 1555-1569.
Krenn, V. and A. Musacchio (2015). "The Aurora B Kinase in Chromosome Bi-Orientation and Spindle Checkpoint Signaling." Front Oncol **5**: 225.
Krupczak-Hollis, K., X. Wang, V. V. Kalinichenko, G. A. Gusarova, I. C. Wang, M. B. Dennewitz, H. M. Yoder, H. Kiyokawa, K. H. Kaestner and R. H. Costa (2004). "The mouse Forkhead Box m1 transcription factor is essential for hepatoblast mitosis and development of intrahepatic bile ducts and vessels during liver morphogenesis." Dev Biol **276**(1): 74-88.
Kubota, T., K. Nishimura, M. T. Kanemaki and A. D. Donaldson (2013). "The Elg1 replication factor C-like complex functions in PCNA unloading during DNA replication." Mol Cell **50**(2): 273-280.
Kukimoto, I., H. Igaki and T. Kanda (1999). "Human CDC45 protein binds to minichromosome maintenance 7 protein and the p70 subunit of DNA polymerase alpha." Eur J Biochem **265**(3): 936-943.
Kulikov, R., M. Winter and C. Blattner (2006). "Binding of p53 to the central domain of Mdm2 is regulated by phosphorylation." J Biol Chem **281**(39): 28575-28583.
Kunda, P., A. E. Pelling, T. Liu and B. Baum (2008). "Moesin controls cortical rigidity, cell rounding, and spindle morphogenesis during mitosis." Curr Biol **18**(2): 91-101.
Kunitoku, N., T. Sasayama, T. Marumoto, D. Zhang, S. Honda, O. Kobayashi, K. Hatakeyama, Y. Ushio, H. Saya and T. Hirota (2003). "CENP-A phosphorylation by Aurora-A in prophase is required for enrichment of Aurora-B at inner centromeres and for kinetochore function." Dev Cell **5**(6): 853-864.
Kuo, T. C., C. T. Chen, D. Baron, T. T. Onder, S. Loewer, S. Almeida, C. M. Weismann, P. Xu, J. M. Houghton, F. B. Gao, G. Q. Daley and S. Doxsey (2011). "Midbody accumulation through evasion of autophagy contributes to cellular reprogramming and tumorigenicity." Nat Cell Biol **13**(10): 1214-1223.
Kwon, M., M. Bagonis, G. Danuser and D. Pellman (2015). "Direct Microtubule-Binding by Myosin-10 Orients Centrosomes toward Retraction Fibers and Subcortical Actin Clouds." Dev Cell **34**(3): 323-337.
Laan, L., N. Pavin, J. Husson, G. Romet-Lemonne, M. van Duijn, M. P. Lopez, R. D. Vale, F. Julicher, S. L. Reck-Peterson and M. Dogterom (2012). "Cortical dynein controls microtubule dynamics to generate pulling forces that position microtubule asters." Cell **148**(3): 502-514.
Lacroix, B., J. van Dijk, N. D. Gold, J. Guizetti, G. Aldrian-Herrada, K. Rogowski, D. W. Gerlich and C. Janke (2010). "Tubulin polyglutamylation stimulates spastin-mediated microtubule severing." J Cell Biol **189**(6): 945-954.
Lafarga, V., A. Cuadrado, I. Lopez de Silanes, R. Bengoechea, O. Fernandez-Capetillo and A. R. Nebreda (2009). "p38 Mitogen-activated protein kinase- and HuR-dependent stabilization of p21(Cip1) mRNA mediates the G(1)/S checkpoint." Mol Cell Biol **29**(16): 4341-4351.
Lamb, J. R., C. Petit-Frere, B. C. Broughton, A. R. Lehmann and M. H. Green (1989). "Inhibition of DNA replication by ionizing radiation is mediated by a trans-acting factor." Int J Radiat Biol **56**(2): 125-130.
Lammer, C., S. Wagerer, R. Saffrich, D. Mertens, W. Ansorge and I. Hoffmann (1998). "The cdc25B phosphatase is essential for the G2/M phase transition in human cells." J Cell Sci **111 (Pt 16)**: 2445-2453.
Lampe, P. D. and A. F. Lau (2004). "The effects of connexin phosphorylation on gap junctional communication." Int J Biochem Cell Biol **36**(7): 1171-1186.
Lampson, M. A. and I. M. Cheeseman (2011). "Sensing centromere tension: Aurora B and the regulation of kinetochore function." Trends Cell Biol **21**(3): 133-140.
Landsverk, H. B., M. Kirkhus, M. Bollen, T. Kuntziger and P. Collas (2005). "PNUTS enhances in vitro chromosome decondensation in a PP1-dependent manner." Biochem J **390**(Pt 3): 709-717.

Lane, H. A. and E. A. Nigg (1996). "Antibody microinjection reveals an essential role for human polo-like kinase 1 (Plk1) in the functional maturation of mitotic centrosomes." J Cell Biol **135**(6 Pt 2): 1701-1713.
Lange, B. M. and K. Gull (1995). "A molecular marker for centriole maturation in the mammalian cell cycle." J Cell Biol **130**(4): 919-927.
Laoukili, J., M. R. Kooistra, A. Bras, J. Kauw, R. M. Kerkhoven, A. Morrison, H. Clevers and R. H. Medema (2005). "FoxM1 is required for execution of the mitotic programme and chromosome stability." Nat Cell Biol **7**(2): 126-136.
Larochelle, S., J. Pandur, R. P. Fisher, H. K. Salz and B. Suter (1998). "Cdk7 is essential for mitosis and for in vivo Cdk-activating kinase activity." Genes Dev **12**(3): 370-381.
Lawson, C., S. T. Lim, S. Uryu, X. L. Chen, D. A. Calderwood and D. D. Schlaepfer (2012). "FAK promotes recruitment of talin to nascent adhesions to control cell motility." J Cell Biol **196**(2): 223-232.
Lechler, T. and M. Mapelli (2021). "Spindle positioning and its impact on vertebrate tissue architecture and cell fate." Nat Rev Mol Cell Biol **22**(10): 691-708.
Lee, J., A. Kumagai and W. G. Dunphy (2001). "Positive regulation of Wee1 by Chk1 and 14-3-3 proteins." Mol Biol Cell **12**(3): 551-563.
Lee, K. S., J. E. Park, Y. H. Kang, T. S. Kim and J. K. Bang (2014). "Mechanisms underlying Plk1 polo-box domain-mediated biological processes and their physiological significance." Mol Cells **37**(4): 286-294.
Lee, S. Y., C. Jang and K. A. Lee (2014). "Polo-like kinases (plks), a key regulator of cell cycle and new potential target for cancer therapy." Dev Reprod **18**(1): 65-71.
Lenart, P., M. Petronczki, M. Steegmaier, B. Di Fiore, J. J. Lipp, M. Hoffmann, W. J. Rettig, N. Kraut and J. M. Peters (2007). "The small-molecule inhibitor BI 2536 reveals novel insights into mitotic roles of polo-like kinase 1." Curr Biol **17**(4): 304-315.
Leung, G. C., J. W. Hudson, A. Kozarova, A. Davidson, J. W. Dennis and F. Sicheri (2002). "The Sak polo-box comprises a structural domain sufficient for mitotic subcellular localization." Nat Struct Biol **9**(10): 719-724.
Li, M., J. P. York and P. Zhang (2007). "Loss of Cdc20 causes a securin-dependent metaphase arrest in two-cell mouse embryos." Mol Cell Biol **27**(9): 3481-3488.
Li, X. and W. D. Heyer (2008). "Homologous recombination in DNA repair and DNA damage tolerance." Cell Res **18**(1): 99-113.
Liao, S., M. Tammaro and H. Yan (2016). "The structure of ends determines the pathway choice and Mre11 nuclease dependency of DNA double-strand break repair." Nucleic Acids Res **44**(12): 5689-5701.
Lim, D. S., S. T. Kim, B. Xu, R. S. Maser, J. Lin, J. H. Petrini and M. B. Kastan (2000). "ATM phosphorylates p95/nbs1 in an S-phase checkpoint pathway." Nature **404**(6778): 613-617.
Lin, C., S. Bai, T. Du, Y. Lai, X. Chen, S. Peng, X. Ma, W. Wu, Z. Guo and H. Huang (2019). "Polo-like kinase 3 is associated with poor prognosis and regulates proliferation and metastasis in prostate cancer." Cancer Manag Res **11**: 1517-1524.
Lindqvist, A., H. Kallstrom, A. Lundgren, E. Barsoum and C. K. Rosenthal (2005). "Cdc25B cooperates with Cdc25A to induce mitosis but has a unique role in activating cyclin B1-Cdk1 at the centrosome." J Cell Biol **171**(1): 35-45.
Lindqvist, A., V. Rodriguez-Bravo and R. H. Medema (2009). "The decision to enter mitosis: feedback and redundancy in the mitotic entry network." J Cell Biol **185**(2): 193-202.
Lindqvist, A., W. van Zon, C. Karlsson Rosenthal and R. M. Wolthuis (2007). "Cyclin B1-Cdk1 activation continues after centrosome separation to control mitotic progression." PLoS Biol **5**(5): e123.
Liu, D., M. Vleugel, C. B. Backer, T. Hori, T. Fukagawa, I. M. Cheeseman and M. A. Lampson (2010). "Regulated targeting of protein phosphatase 1 to the outer kinetochore by KNL1 opposes Aurora B kinase." J Cell Biol **188**(6): 809-820.
Liu, S., S. O. Opiyo, K. Manthey, J. G. Glanzer, A. K. Ashley, C. Amerin, K. Troksa, M. Shrivastav, J. A. Nickoloff and G. G. Oakley (2012). "Distinct roles for DNA-PK, ATM and ATR in RPA phosphorylation and checkpoint activation in response to replication stress." Nucleic Acids Res **40**(21): 10780-10794.

Liu, X. S., H. Li, B. Song and X. Liu (2010). "Polo-like kinase 1 phosphorylation of G2 and S-phase-expressed 1 protein is essential for p53 inactivation during G2 checkpoint recovery." EMBO Rep **11**(8): 626-632.
Liu, Y., J. Kim, R. Philip, V. Sridhar, M. Chandrashekhar, J. Moffat, M. van Breugel and L. Pelletier (2020). "Direct interaction between CEP85 and STIL mediates PLK4-driven directed cell migration." J Cell Sci **133**(8).
Lobjois, V., C. Froment, E. Braud, F. Grimal, O. Burlet-Schiltz, B. Ducommun and J. P. Bouche (2011). "Study of the docking-dependent PLK1 phosphorylation of the CDC25B phosphatase." Biochem Biophys Res Commun **410**(1): 87-90.
Lobjois, V., D. Jullien, J. P. Bouche and B. Ducommun (2009). "The polo-like kinase 1 regulates CDC25B-dependent mitosis entry." Biochim Biophys Acta **1793**(3): 462-468.
Locke, W. J. and S. J. Clark (2012). "Epigenome remodelling in breast cancer: insights from an early in vitro model of carcinogenesis." Breast Cancer Res **14**(6): 215.
Lolli, G. and L. N. Johnson (2005). "CAK-Cyclin-dependent Activating Kinase: a key kinase in cell cycle control and a target for drugs?" Cell Cycle **4**(4): 572-577.
Lopez-Colome, A. M., I. Lee-Rivera, R. Benavides-Hidalgo and E. Lopez (2017). "Paxillin: a crossroad in pathological cell migration." J Hematol Oncol **10**(1): 50.
Lopez-Girona, A., B. Furnari, O. Mondesert and P. Russell (1999). "Nuclear localization of Cdc25 is regulated by DNA damage and a 14-3-3 protein." Nature **397**(6715): 172-175.
Lopez-Sanchez, I., M. Sanz-Garcia and P. A. Lazo (2009). "Plk3 interacts with and specifically phosphorylates VRK1 in Ser342, a downstream target in a pathway that induces Golgi fragmentation." Mol Cell Biol **29**(5): 1189-1201.
Lowe, M., N. K. Gonatas and G. Warren (2000). "The mitotic phosphorylation cycle of the cis-Golgi matrix protein GM130." J Cell Biol **149**(2): 341-356.
Lowery, D. M., D. Lim and M. B. Yaffe (2005). "Structure and function of Polo-like kinases." Oncogene **24**(2): 248-259.
Lu, L., M. S. Ladinsky and T. Kirchhausen (2009). "Cisternal organization of the endoplasmic reticulum during mitosis." Mol Biol Cell **20**(15): 3471-3480.
Lu, M. S. and C. A. Johnston (2013). "Molecular pathways regulating mitotic spindle orientation in animal cells." Development **140**(9): 1843-1856.
Lu, X., B. Nannenga and L. A. Donehower (2005). "PPM1D dephosphorylates Chk1 and p53 and abrogates cell cycle checkpoints." Genes Dev **19**(10): 1162-1174.
Lukas, C., J. Bartkova, L. Latella, J. Falck, N. Mailand, T. Schroeder, M. Sehested, J. Lukas and J. Bartek (2001). "DNA damage-activated kinase Chk2 is independent of proliferation or differentiation yet correlates with tissue biology." Cancer Res **61**(13): 4990-4993.
Lukas, C., V. Savic, S. Bekker-Jensen, C. Doil, B. Neumann, R. S. Pedersen, M. Grofte, K. L. Chan, I. D. Hickson, J. Bartek and J. Lukas (2011). "53BP1 nuclear bodies form around DNA lesions generated by mitotic transmission of chromosomes under replication stress." Nat Cell Biol **13**(3): 243-253.
Lukas, C., C. S. Sorensen, E. Kramer, E. Santoni-Rugiu, C. Lindeneg, J. M. Peters, J. Bartek and J. Lukas (1999). "Accumulation of cyclin B1 requires E2F and cyclin-A-dependent rearrangement of the anaphase-promoting complex." Nature **401**(6755): 815-818.
Lukasik, P., M. Zaluski and I. Gutowska (2021). "Cyclin-Dependent Kinases (CDK) and Their Role in Diseases Development-Review." Int J Mol Sci **22**(6).
Ly, T., A. Whigham, R. Clarke, A. J. Brenes-Murillo, B. Estes, D. Madhessian, E. Lundberg, P. Wadsworth and A. I. Lamond (2017). "Proteomic analysis of cell cycle progression in asynchronous cultures, including mitotic subphases, using PRIMMUS." Elife **6**.
Ma, R. Y., T. H. Tong, A. M. Cheung, A. C. Tsang, W. Y. Leung and K. M. Yao (2005). "Raf/MEK/MAPK signaling stimulates the nuclear translocation and transactivating activity of FOXM1c." J Cell Sci **118**(Pt 4): 795-806.
Ma, S., J. Charron and R. L. Erikson (2003). "Role of Plk2 (Snk) in mouse development and cell proliferation." Mol Cell Biol **23**(19): 6936-6943.

Mackay, D. R., M. Makise and K. S. Ullman (2010). "Defects in nuclear pore assembly lead to activation of an Aurora B-mediated abscission checkpoint." J Cell Biol **191**(5): 923-931.
Macurek, L., J. Benada, E. Mullers, V. A. Halim, K. Krejcikova, K. Burdova, S. Pechackova, Z. Hodny, A. Lindqvist, R. H. Medema and J. Bartek (2013). "Downregulation of Wip1 phosphatase modulates the cellular threshold of DNA damage signaling in mitosis." Cell Cycle **12**(2): 251-262.
Macurek, L., A. Lindqvist, D. Lim, M. A. Lampson, R. Klompmaker, R. Freire, C. Clouin, S. S. Taylor, M. B. Yaffe and R. H. Medema (2008). "Polo-like kinase-1 is activated by aurora A to promote checkpoint recovery." Nature **455**(7209): 119-123.
Macurek, L., A. Lindqvist, O. Voets, J. Kool, H. R. Vos and R. H. Medema (2010). "Wip1 phosphatase is associated with chromatin and dephosphorylates gammaH2AX to promote checkpoint inhibition." Oncogene **29**(15): 2281-2291.
Magidson, V., C. B. O'Connell, J. Loncarek, R. Paul, A. Mogilner and A. Khodjakov (2011). "The spatial arrangement of chromosomes during prometaphase facilitates spindle assembly." Cell **146**(4): 555-567.
Mailand, N., J. Falck, C. Lukas, R. G. Syljuasen, M. Welcker, J. Bartek and J. Lukas (2000). "Rapid destruction of human Cdc25A in response to DNA damage." Science **288**(5470): 1425-1429.
Major, M. L., R. Lepe and R. H. Costa (2004). "Forkhead box M1B transcriptional activity requires binding of Cdk-cyclin complexes for phosphorylation-dependent recruitment of p300/CBP coactivators." Mol Cell Biol **24**(7): 2649-2661.
Makela, T. P., J. P. Tassan, E. A. Nigg, S. Frutiger, G. J. Hughes and R. A. Weinberg (1994). "A cyclin associated with the CDK-activating kinase MO15." Nature **371**(6494): 254-257.
Maller, J. L. (1986). "Mitogenic signalling and protein phosphorylation in Xenopus oocytes." J Cyclic Nucleotide Protein Phosphor Res **11**(7): 543-555.
Malumbres, M. and M. Barbacid (2005). "Mammalian cyclin-dependent kinases." Trends Biochem Sci **30**(11): 630-641.
Malumbres, M. and M. Barbacid (2009). "Cell cycle, CDKs and cancer: a changing paradigm." Nat Rev Cancer **9**(3): 153-166.
Manfredi, M. G., J. A. Ecsedy, K. A. Meetze, S. K. Balani, O. Burenkova, W. Chen, K. M. Galvin, K. M. Hoar, J. J. Huck, P. J. LeRoy, E. T. Ray, T. B. Sells, B. Stringer, S. G. Stroud, T. J. Vos, G. S. Weatherhead, D. R. Wysong, M. Zhang, J. B. Bolen and C. F. Claiborne (2007). "Antitumor activity of MLN8054, an orally active small-molecule inhibitor of Aurora A kinase." Proc Natl Acad Sci U S A **104**(10): 4106-4111.
Manke, I. A., A. Nguyen, D. Lim, M. Q. Stewart, A. E. Elia and M. B. Yaffe (2005). "MAPKAP kinase-2 is a cell cycle checkpoint kinase that regulates the G2/M transition and S phase progression in response to UV irradiation." Mol Cell **17**(1): 37-48.
Manning, G., D. B. Whyte, R. Martinez, T. Hunter and S. Sudarsanam (2002). "The protein kinase complement of the human genome." Science **298**(5600): 1912-1934.
Mao, Z., M. Bozzella, A. Seluanov and V. Gorbunova (2008). "Comparison of nonhomologous end joining and homologous recombination in human cells." DNA Repair (Amst) **7**(10): 1765-1771.
Marin, O., V. H. Bustos, L. Cesaro, F. Meggio, M. A. Pagano, M. Antonelli, C. C. Allende, L. A. Pinna and J. E. Allende (2003). "A noncanonical sequence phosphorylated by casein kinase 1 in beta-catenin may play a role in casein kinase 1 targeting of important signaling proteins." Proc Natl Acad Sci U S A **100**(18): 10193-10200.
Marin, O., F. Meggio, S. Sarno, M. Andretta and L. A. Pinna (1994). "Phosphorylation of synthetic fragments of inhibitor-2 of protein phosphatase-1 by casein kinase-1 and -2. Evidence that phosphorylated residues are not strictly required for efficient targeting by casein kinase-1." Eur J Biochem **223**(2): 647-653.
Marino, M., F. Acconcia and A. Trentalance (2003). "Biphasic estradiol-induced AKT phosphorylation is modulated by PTEN via MAP kinase in HepG2 cells." Mol Biol Cell **14**(6): 2583-2591.
Martinez-Balbas, M. A., A. Dey, S. K. Rabindran, K. Ozato and C. Wu (1995). "Displacement of sequence-specific transcription factors from mitotic chromatin." Cell **83**(1): 29-38.
Masai, H., N. Sato, T. Takeda and K. Arai (1999). "CDC7 kinase complex as a molecular switch for DNA replication." Front Biosci **4**: D834-840.

Matlashewski, G., P. Lamb, D. Pim, J. Peacock, L. Crawford and S. Benchimol (1984). "Isolation and characterization of a human p53 cDNA clone: expression of the human p53 gene." EMBO J **3**(13): 3257-3262.
Matsumura, F. (2005). "Regulation of myosin II during cytokinesis in higher eukaryotes." Trends Cell Biol **15**(7): 371-377.
Matsuoka, S., M. Huang and S. J. Elledge (1998). "Linkage of ATM to cell cycle regulation by the Chk2 protein kinase." Science **282**(5395): 1893-1897.
Mayer, T. U., T. M. Kapoor, S. J. Haggarty, R. W. King, S. L. Schreiber and T. J. Mitchison (1999). "Small molecule inhibitor of mitotic spindle bipolarity identified in a phenotype-based screen." Science **286**(5441): 971-974.
McAinsh, A. D. and P. Meraldi (2011). "The CCAN complex: linking centromere specification to control of kinetochore-microtubule dynamics." Semin Cell Dev Biol **22**(9): 946-952.
McIntosh, J. R. (2016). "Mitosis." Cold Spring Harb Perspect Biol **8**(9).
McKenzie, L., S. King, L. Marcar, S. Nicol, S. S. Dias, K. Schumm, P. Robertson, J. C. Bourdon, N. Perkins, F. Fuller-Pace and D. W. Meek (2010). "p53-dependent repression of polo-like kinase-1 (PLK1)." Cell Cycle **9**(20): 4200-4212.
Medema, R. H. and L. Macurek (2012). "Checkpoint control and cancer." Oncogene **31**(21): 2601-2613.
Meek, K. (2020). "Activation of DNA-PK by hairpinned DNA ends reveals a stepwise mechanism of kinase activation." Nucleic Acids Res **48**(16): 9098-9108.
Melchionna, R., X. B. Chen, A. Blasina and C. H. McGowan (2000). "Threonine 68 is required for radiation-induced phosphorylation and activation of Cds1." Nat Cell Biol **2**(10): 762-765.
Melixetian, M., D. K. Klein, C. S. Sorensen and K. Helin (2009). "NEK11 regulates CDC25A degradation and the IR-induced G2/M checkpoint." Nat Cell Biol **11**(10): 1247-1253.
Mendoza, M., C. Norden, K. Durrer, H. Rauter, F. Uhlmann and Y. Barral (2009). "A mechanism for chromosome segregation sensing by the NoCut checkpoint." Nat Cell Biol **11**(4): 477-483.
Meng, Z., L. Capalbo, D. M. Glover and W. G. Dunphy (2011). "Role for casein kinase 1 in the phosphorylation of Claspin on critical residues necessary for the activation of Chk1." Mol Biol Cell **22**(16): 2834-2847.
Miller, R. K., S. D'Silva, J. K. Moore and H. V. Goodson (2006). "The CLIP-170 orthologue Bik1p and positioning the mitotic spindle in yeast." Curr Top Dev Biol **76**: 49-87.
Milne, D. M., P. Looby and D. W. Meek (2001). "Catalytic activity of protein kinase CK1 delta (casein kinase 1delta) is essential for its normal subcellular localization." Exp Cell Res **263**(1): 43-54.
Mimori-Kiyosue, Y., I. Grigoriev, H. Sasaki, C. Matsui, A. Akhmanova, S. Tsukita and I. Vorobjev (2006). "Mammalian CLASPs are required for mitotic spindle organization and kinetochore alignment." Genes Cells **11**(8): 845-857.
Min, M., Y. Rong, C. Tian and S. L. Spencer (2020). "Temporal integration of mitogen history in mother cells controls proliferation of daughter cells." Science **368**(6496): 1261-1265.
Mishima, M., S. Kaitna and M. Glotzer (2002). "Central spindle assembly and cytokinesis require a kinesin-like protein/RhoGAP complex with microtubule bundling activity." Dev Cell **2**(1): 41-54.
Mitchison, T., L. Evans, E. Schulze and M. Kirschner (1986). "Sites of microtubule assembly and disassembly in the mitotic spindle." Cell **45**(4): 515-527.
Mitra, J. and G. H. Enders (2004). "Cyclin A/Cdk2 complexes regulate activation of Cdk1 and Cdc25 phosphatases in human cells." Oncogene **23**(19): 3361-3367.
Mitsushima, M., K. Aoki, M. Ebisuya, S. Matsumura, T. Yamamoto, M. Matsuda, F. Toyoshima and E. Nishida (2010). "Revolving movement of a dynamic cluster of actin filaments during mitosis." J Cell Biol **191**(3): 453-462.
Mogessie, B. and M. Schuh (2017). "Actin protects mammalian eggs against chromosome segregation errors." Science **357**(6353).
Molinari, M., C. Mercurio, J. Dominguez, F. Goubin and G. F. Draetta (2000). "Human Cdc25 A inactivation in response to S phase inhibition and its role in preventing premature mitosis." EMBO Rep **1**(1): 71-79.

Moreno, S. P., R. Bailey, N. Campion, S. Herron and A. Gambus (2014). "Polyubiquitylation drives replisome disassembly at the termination of DNA replication." Science **346**(6208): 477-481.
Morris, E. J., J. Y. Ji, F. Yang, L. Di Stefano, A. Herr, N. S. Moon, E. J. Kwon, K. M. Haigis, A. M. Naar and N. J. Dyson (2008). "E2F1 represses beta-catenin transcription and is antagonized by both pRB and CDK8." Nature **455**(7212): 552-556.
Mueller, P. R., T. R. Coleman, A. Kumagai and W. G. Dunphy (1995). "Myt1: a membrane-associated inhibitory kinase that phosphorylates Cdc2 on both threonine-14 and tyrosine-15." Science **270**(5233): 86-90.
Mukherjee, P., S. L. Winter and M. G. Alexandrow (2010). "Cell cycle arrest by transforming growth factor beta1 near G1/S is mediated by acute abrogation of prereplication complex activation involving an Rb-MCM interaction." Mol Cell Biol **30**(3): 845-856.
Muller, H., M. C. Moroni, E. Vigo, B. O. Petersen, J. Bartek and K. Helin (1997). "Induction of S-phase entry by E2F transcription factors depends on their nuclear localization." Mol Cell Biol **17**(9): 5508-5520.
Murphy, A. C. and P. W. Young (2015). "The actinin family of actin cross-linking proteins - a genetic perspective." Cell Biosci **5**: 49.
Nakajima, H., F. Toyoshima-Morimoto, E. Taniguchi and E. Nishida (2003). "Identification of a consensus motif for Plk (Polo-like kinase) phosphorylation reveals Myt1 as a Plk1 substrate." J Biol Chem **278**(28): 25277-25280.
Neef, R., C. Preisinger, J. Sutcliffe, R. Kopajtich, E. A. Nigg, T. U. Mayer and F. A. Barr (2003). "Phosphorylation of mitotic kinesin-like protein 2 by polo-like kinase 1 is required for cytokinesis." J Cell Biol **162**(5): 863-875.
Nicklas, R. B., M. S. Campbell, S. C. Ward and G. J. Gorbsky (1998). "Tension-sensitive kinetochore phosphorylation in vitro." J Cell Sci **111 (Pt 21)**: 3189-3196.
Nigg, E. A. (2001). "Mitotic kinases as regulators of cell division and its checkpoints." Nat Rev Mol Cell Biol **2**(1): 21-32.
Nurse, P. (1990). "Universal control mechanism regulating onset of M-phase." Nature **344**(6266): 503-508.
O'Connell, K. F., C. Caron, K. R. Kopish, D. D. Hurd, K. J. Kemphues, Y. Li and J. G. White (2001). "The C. elegans zyg-1 gene encodes a regulator of centrosome duplication with distinct maternal and paternal roles in the embryo." Cell **105**(4): 547-558.
O'Connell, M. J., J. M. Raleigh, H. M. Verkade and P. Nurse (1997). "Chk1 is a wee1 kinase in the G2 DNA damage checkpoint inhibiting cdc2 by Y15 phosphorylation." EMBO J **16**(3): 545-554.
Oakes, V., W. Wang, B. Harrington, W. J. Lee, H. Beamish, K. M. Chia, A. Pinder, H. Goto, M. Inagaki, S. Pavey and B. Gabrielli (2014). "Cyclin A/Cdk2 regulates Cdh1 and claspin during late S/G2 phase of the cell cycle." Cell Cycle **13**(20): 3302-3311.
Oh, K. S., M. Bustin, S. J. Mazur, E. Appella and K. H. Kraemer (2011). "UV-induced histone H2AX phosphorylation and DNA damage related proteins accumulate and persist in nucleotide excision repair-deficient XP-B cells." DNA Repair (Amst) **10**(1): 5-15.
Ohama, T., L. Wang, E. M. Griner and D. L. Brautigan (2013). "Protein Ser/Thr phosphatase-6 is required for maintenance of E-cadherin at adherens junctions." BMC Cell Biol **14**: 42.
Ohtsubo, M., A. M. Theodoras, J. Schumacher, J. M. Roberts and M. Pagano (1995). "Human cyclin E, a nuclear protein essential for the G1-to-S phase transition." Mol Cell Biol **15**(5): 2612-2624.
Okamura, H., C. Garcia-Rodriguez, H. Martinson, J. Qin, D. M. Virshup and A. Rao (2004). "A conserved docking motif for CK1 binding controls the nuclear localization of NFAT1." Mol Cell Biol **24**(10): 4184-4195.
Okazaki, R., T. Okazaki, K. Sakabe, K. Sugimoto and A. Sugino (1968). "Mechanism of DNA chain growth. I. Possible discontinuity and unusual secondary structure of newly synthesized chains." Proc Natl Acad Sci U S A **59**(2): 598-605.
Ou, B., H. Sun, J. Zhao, Z. Xu, Y. Liu, H. Feng and Z. Peng (2019). "Polo-like kinase 3 inhibits glucose metabolism in colorectal cancer by targeting HSP90/STAT3/HK2 signaling." J Exp Clin Cancer Res **38**(1): 426.

Ouyang, B., H. Pan, L. Lu, J. Li, P. Stambrook, B. Li and W. Dai (1997). "Human Prk is a conserved protein serine/threonine kinase involved in regulating M phase functions." J Biol Chem **272**(45): 28646-28651.
Pagano, M., R. Pepperkok, F. Verde, W. Ansorge and G. Draetta (1992). "Cyclin A is required at two points in the human cell cycle." EMBO J **11**(3): 961-971.
Panbianco, C., D. Weinkove, E. Zanin, D. Jones, N. Divecha, M. Gotta and J. Ahringer (2008). "A casein kinase 1 and PAR proteins regulate asymmetry of a PIP(2) synthesis enzyme for asymmetric spindle positioning." Dev Cell **15**(2): 198-208.
Pardee, A. B. (1989). "G1 events and regulation of cell proliferation." Science **246**(4930): 603-608.
Park, J. E., N. K. Soung, Y. Johmura, Y. H. Kang, C. Liao, K. H. Lee, C. H. Park, M. C. Nicklaus and K. S. Lee (2010). "Polo-box domain: a versatile mediator of polo-like kinase function." Cell Mol Life Sci **67**(12): 1957-1970.
Parker, L. L. and H. Piwnica-Worms (1992). "Inactivation of the p34cdc2-cyclin B complex by the human WEE1 tyrosine kinase." Science **257**(5078): 1955-1957.
Patzke, S., T. Stokke and H. C. Aasheim (2006). "CSPP and CSPP-L associate with centrosomes and microtubules and differently affect microtubule organization." J Cell Physiol **209**(1): 199-210.
Pavicic-Kaltenbrunner, V., M. Mishima and M. Glotzer (2007). "Cooperative assembly of CYK-4/MgcRacGAP and ZEN-4/MKLP1 to form the centralspindlin complex." Mol Biol Cell **18**(12): 4992-5003.
Pearson, G., F. Robinson, T. Beers Gibson, B. E. Xu, M. Karandikar, K. Berman and M. H. Cobb (2001). "Mitogen-activated protein (MAP) kinase pathways: regulation and physiological functions." Endocr Rev **22**(2): 153-183.
Peeper, D. S., T. M. Upton, M. H. Ladha, E. Neuman, J. Zalvide, R. Bernards, J. A. DeCaprio and M. E. Ewen (1997). "Ras signalling linked to the cell-cycle machinery by the retinoblastoma protein." Nature **386**(6621): 177-181.
Peng, C. Y., P. R. Graves, R. S. Thoma, Z. Wu, A. S. Shaw and H. Piwnica-Worms (1997). "Mitotic and G2 checkpoint control: regulation of 14-3-3 protein binding by phosphorylation of Cdc25C on serine-216." Science **277**(5331): 1501-1505.
Peng, Y., M. Moritz, X. Han, T. H. Giddings, A. Lyon, J. Kollman, M. Winey, J. Yates, 3rd, D. A. Agard, D. G. Drubin and G. Barnes (2015). "Interaction of CK1delta with gammaTuSC ensures proper microtubule assembly and spindle positioning." Mol Biol Cell **26**(13): 2505-2518.
Perez-Moreno, M., C. Jamora and E. Fuchs (2003). "Sticky business: orchestrating cellular signals at adherens junctions." Cell **112**(4): 535-548.
Perez, D. I., C. Gil and A. Martinez (2011). "Protein kinases CK1 and CK2 as new targets for neurodegenerative diseases." Med Res Rev **31**(6): 924-954.
Perpelescu, M. and T. Fukagawa (2011). "The ABCs of CENPs." Chromosoma **120**(5): 425-446.
Peter, M. (1997). "The regulation of cyclin-dependent kinase inhibitors (CKIs)." Prog Cell Cycle Res **3**: 99-108.
Peters, J. M. (2002). "The anaphase-promoting complex: proteolysis in mitosis and beyond." Mol Cell **9**(5): 931-943.
Peters, J. M. (2006). "The anaphase promoting complex/cyclosome: a machine designed to destroy." Nat Rev Mol Cell Biol **7**(9): 644-656.
Petersen, B. O., J. Lukas, C. S. Sorensen, J. Bartek and K. Helin (1999). "Phosphorylation of mammalian CDC6 by cyclin A/CDK2 regulates its subcellular localization." EMBO J **18**(2): 396-410.
Petojevic, T., J. J. Pesavento, A. Costa, J. Liang, Z. Wang, J. M. Berger and M. R. Botchan (2015). "Cdc45 (cell division cycle protein 45) guards the gate of the Eukaryote Replisome helicase stabilizing leading strand engagement." Proc Natl Acad Sci U S A **112**(3): E249-258.
Petrovic, A., S. Pasqualato, P. Dube, V. Krenn, S. Santaguida, D. Cittaro, S. Monzani, L. Massimiliano, J. Keller, A. Tarricone, A. Maiolica, H. Stark and A. Musacchio (2010). "The MIS12 complex is a protein interaction hub for outer kinetochore assembly." J Cell Biol **190**(5): 835-852.
Pfleger, C. M. and M. W. Kirschner (2000). "The KEN box: an APC recognition signal distinct from the D box targeted by Cdh1." Genes Dev **14**(6): 655-665.

Piao, S., S. J. Lee, Y. Xu, J. Gwak, S. Oh, B. J. Park and N. C. Ha (2011). "CK1epsilon targets Cdc25A for ubiquitin-mediated proteolysis under normal conditions and in response to checkpoint activation." Cell Cycle **10**(3): 531-537.
Pichierri, P., F. Rosselli and A. Franchitto (2003). "Werner's syndrome protein is phosphorylated in an ATR/ATM-dependent manner following replication arrest and DNA damage induced during the S phase of the cell cycle." Oncogene **22**(10): 1491-1500.
Piekny, A. J. and M. Glotzer (2008). "Anillin is a scaffold protein that links RhoA, actin, and myosin during cytokinesis." Curr Biol **18**(1): 30-36.
Piekny, A. J. and A. S. Maddox (2010). "The myriad roles of Anillin during cytokinesis." Semin Cell Dev Biol **21**(9): 881-891.
Pines, J. (1994). "Protein kinases and cell cycle control." Semin Cell Biol **5**(6): 399-408.
Pines, J. and T. Hunter (1989). "Isolation of a human cyclin cDNA: evidence for cyclin mRNA and protein regulation in the cell cycle and for interaction with p34cdc2." Cell **58**(5): 833-846.
Pines, J. and T. Hunter (1994). "The differential localization of human cyclins A and B is due to a cytoplasmic retention signal in cyclin B." EMBO J **13**(16): 3772-3781.
Plessner, M., J. Knerr and R. Grosse (2019). "Centrosomal Actin Assembly Is Required for Proper Mitotic Spindle Formation and Chromosome Congression." iScience **15**: 274-281.
Pohl, C. and S. Jentsch (2009). "Midbody ring disposal by autophagy is a post-abscission event of cytokinesis." Nat Cell Biol **11**(1): 65-70.
Poon, R. Y. and T. Hunter (1995). "Dephosphorylation of Cdk2 Thr160 by the cyclin-dependent kinase-interacting phosphatase KAP in the absence of cyclin." Science **270**(5233): 90-93.
Poteryaev, D., J. M. Squirrell, J. M. Campbell, J. G. White and A. Spang (2005). "Involvement of the actin cytoskeleton and homotypic membrane fusion in ER dynamics in Caenorhabditis elegans." Mol Biol Cell **16**(5): 2139-2153.
Powers, J., E. M. Pinto, T. Barnoud, J. C. Leung, T. Martynyuk, A. V. Kossenkov, A. H. Philips, H. Desai, R. Hausler, G. Kelly, A. N. Le, M. M. Li, S. P. MacFarland, L. C. Pyle, K. Zelley, K. L. Nathanson, S. M. Domchek, T. P. Slavin, J. N. Weitzel, J. E. Stopfer, J. E. Garber, V. Joseph, K. Offit, J. S. Dolinsky, S. Gutierrez, K. McGoldrick, F. J. Couch, B. Levin, M. C. Edelman, C. F. Levy, S. L. Spunt, R. W. Kriwacki, G. P. Zambetti, R. C. Ribeiro, M. E. Murphy and K. N. Maxwell (2020). "A Rare TP53 Mutation Predominant in Ashkenazi Jews Confers Risk of Multiple Cancers." Cancer Res **80**(17): 3732-3744.
Powers, R. E., S. Wang, T. Y. Liu and T. A. Rapoport (2017). "Reconstitution of the tubular endoplasmic reticulum network with purified components." Nature **543**(7644): 257-260.
Price, M. A. (2006). "CKI, there's more than one: casein kinase I family members in Wnt and Hedgehog signaling." Genes Dev **20**(4): 399-410.
Pyrpasopoulou, A., J. Meier, C. Maison, G. Simos and S. D. Georgatos (1996). "The lamin B receptor (LBR) provides essential chromatin docking sites at the nuclear envelope." EMBO J **15**(24): 7108-7119.
Ramachandran, S. and S. Henikoff (2015). "Replicating Nucleosomes." Sci Adv **1**(7).
Raman, M., S. Earnest, K. Zhang, Y. Zhao and M. H. Cobb (2007). "TAO kinases mediate activation of p38 in response to DNA damage." EMBO J **26**(8): 2005-2014.
Reimann, J. D., B. E. Gardner, F. Margottin-Goguet and P. K. Jackson (2001). "Emi1 regulates the anaphase-promoting complex by a different mechanism than Mad2 proteins." Genes Dev **15**(24): 3278-3285.
Reinhardt, H. C., A. S. Aslanian, J. A. Lees and M. B. Yaffe (2007). "p53-deficient cells rely on ATM- and ATR-mediated checkpoint signaling through the p38MAPK/MK2 pathway for survival after DNA damage." Cancer Cell **11**(2): 175-189.
Reinhardt, H. C., P. Hasskamp, I. Schmedding, S. Morandell, M. A. van Vugt, X. Wang, R. Linding, S. E. Ong, D. Weaver, S. A. Carr and M. B. Yaffe (2010). "DNA damage activates a spatially distinct late cytoplasmic cell-cycle checkpoint network controlled by MK2-mediated RNA stabilization." Mol Cell **40**(1): 34-49.

Renshaw, M. J., J. J. Ward, M. Kanemaki, K. Natsume, F. J. Nedelec and T. U. Tanaka (2010). "Condensins promote chromosome recoiling during early anaphase to complete sister chromatid separation." Dev Cell **19**(2): 232-244.
Rhind, N. and P. Russell (2000). "Chk1 and Cds1: linchpins of the DNA damage and replication checkpoint pathways." J Cell Sci **113 (Pt 22)**: 3889-3896.
Rieder, C. L., R. W. Cole, A. Khodjakov and G. Sluder (1995). "The checkpoint delaying anaphase in response to chromosome monoorientation is mediated by an inhibitory signal produced by unattached kinetochores." J Cell Biol **130**(4): 941-948.
Ritchie, M. E., B. Phipson, D. Wu, Y. Hu, C. W. Law, W. Shi and G. K. Smyth (2015). "limma powers differential expression analyses for RNA-sequencing and microarray studies." Nucleic Acids Res **43**(7): e47.
Rizzelli, F., M. G. Malabarba, S. Sigismund and M. Mapelli (2020). "The crosstalk between microtubules, actin and membranes shapes cell division." Open Biol **10**(3): 190314.
Robinson, L. C., M. M. Menold, S. Garrett and M. R. Culbertson (1993). "Casein kinase I-like protein kinases encoded by YCK1 and YCK2 are required for yeast morphogenesis." Mol Cell Biol **13**(5): 2870-2881.
Rogers, S. L., G. C. Rogers, D. J. Sharp and R. D. Vale (2002). "Drosophila EB1 is important for proper assembly, dynamics, and positioning of the mitotic spindle." J Cell Biol **158**(5): 873-884.
Roll-Mecak, A. and R. D. Vale (2008). "Structural basis of microtubule severing by the hereditary spastic paraplegia protein spastin." Nature **451**(7176): 363-367.
Roovers, K. and R. K. Assoian (2003). "Effects of rho kinase and actin stress fibers on sustained extracellular signal-regulated kinase activity and activation of G(1) phase cyclin-dependent kinases." Mol Cell Biol **23**(12): 4283-4294.
Rosenberg, L. H., J. L. Cleveland, W. R. Roush and D. R. Duckett (2016). "CK1delta: an exploitable vulnerability in breast cancer." Ann Transl Med **4**(23): 474.
Rothstein, R., B. Michel and S. Gangloff (2000). "Replication fork pausing and recombination or "gimme a break"." Genes Dev **14**(1): 1-10.
Ruan, Q., Q. Wang, S. Xie, Y. Fang, Z. Darzynkiewicz, K. Guan, M. Jhanwar-Uniyal and W. Dai (2004). "Polo-like kinase 3 is Golgi localized and involved in regulating Golgi fragmentation during the cell cycle." Exp Cell Res **294**(1): 51-59.
Sadasivam, S., S. Duan and J. A. DeCaprio (2012). "The MuvB complex sequentially recruits B-Myb and FoxM1 to promote mitotic gene expression." Genes Dev **26**(5): 474-489.
Sakaue-Sawano, A., H. Kurokawa, T. Morimura, A. Hanyu, H. Hama, H. Osawa, S. Kashiwagi, K. Fukami, T. Miyata, H. Miyoshi, T. Imamura, M. Ogawa, H. Masai and A. Miyawaki (2008). "Visualizing spatiotemporal dynamics of multicellular cell-cycle progression." Cell **132**(3): 487-498.
Sakaue-Sawano, A., M. Yo, N. Komatsu, T. Hiratsuka, T. Kogure, T. Hoshida, N. Goshima, M. Matsuda, H. Miyoshi and A. Miyawaki (2017). "Genetically Encoded Tools for Optical Dissection of the Mammalian Cell Cycle." Mol Cell **68**(3): 626-640 e625.
Salina, D., K. Bodoor, D. M. Eckley, T. A. Schroer, J. B. Rattner and B. Burke (2002). "Cytoplasmic dynein as a facilitator of nuclear envelope breakdown." Cell **108**(1): 97-107.
Santra, M. K., N. Wajapeyee and M. R. Green (2009). "F-box protein FBXO31 mediates cyclin D1 degradation to induce G1 arrest after DNA damage." Nature **459**(7247): 722-725.
Sartori, A. A., C. Lukas, J. Coates, M. Mistrik, S. Fu, J. Bartek, R. Baer, J. Lukas and S. P. Jackson (2007). "Human CtIP promotes DNA end resection." Nature **450**(7169): 509-514.
Sato, N., K. Arai and H. Masai (1997). "Human and Xenopus cDNAs encoding budding yeast Cdc7-related kinases: in vitro phosphorylation of MCM subunits by a putative human homologue of Cdc7." EMBO J **16**(14): 4340-4351.
Saurin, A. T., J. Durgan, A. J. Cameron, A. Faisal, M. S. Marber and P. J. Parker (2008). "The regulated assembly of a PKCepsilon complex controls the completion of cytokinesis." Nat Cell Biol **10**(8): 891-901.
Saxton, W. M. and J. R. McIntosh (1987). "Interzone microtubule behavior in late anaphase and telophase spindles." J Cell Biol **105**(2): 875-886.

Saxton, W. M., D. L. Stemple, R. J. Leslie, E. D. Salmon, M. Zavortink and J. R. McIntosh (1984). "Tubulin dynamics in cultured mammalian cells." J Cell Biol **99**(6): 2175-2186.
Schalbetter, S. A., S. Mansoubi, A. L. Chambers, J. A. Downs and J. Baxter (2015). "Fork rotation and DNA precatenation are restricted during DNA replication to prevent chromosomal instability." Proc Natl Acad Sci U S A **112**(33): E4565-4570.
Schiel, J. A., K. Park, M. K. Morphew, E. Reid, A. Hoenger and R. Prekeris (2011). "Endocytic membrane fusion and buckling-induced microtubule severing mediate cell abscission." J Cell Sci **124**(Pt 9): 1411-1424.
Schittek, B. and T. Sinnberg (2014). "Biological functions of casein kinase 1 isoforms and putative roles in tumorigenesis." Mol Cancer **13**: 231.
Schroeder, T. E. (1972). "The contractile ring. II. Determining its brief existence, volumetric changes, and vital role in cleaving Arbacia eggs." J Cell Biol **53**(2): 419-434.
Schultz, L. B., N. H. Chehab, A. Malikzay and T. D. Halazonetis (2000). "p53 binding protein 1 (53BP1) is an early participant in the cellular response to DNA double-strand breaks." J Cell Biol **151**(7): 1381-1390.
Scolnick, D. M. and T. D. Halazonetis (2000). "Chfr defines a mitotic stress checkpoint that delays entry into metaphase." Nature **406**(6794): 430-435.
Seemann, J., M. Pypaert, T. Taguchi, J. Malsam and G. Warren (2002). "Partitioning of the matrix fraction of the Golgi apparatus during mitosis in animal cells." Science **295**(5556): 848-851.
Seki, A. and G. Fang (2007). "CKAP2 is a spindle-associated protein degraded by APC/C-Cdh1 during mitotic exit." J Biol Chem **282**(20): 15103-15113.
Seldin, L., A. Muroyama and T. Lechler (2016). "NuMA-microtubule interactions are critical for spindle orientation and the morphogenesis of diverse epidermal structures." Elife **5**.
Severson, A. F., D. L. Baillie and B. Bowerman (2002). "A Formin Homology protein and a profilin are required for cytokinesis and Arp2/3-independent assembly of cortical microfilaments in C. elegans." Curr Biol **12**(24): 2066-2075.
Shah, K. and S. Rossie (2018). "Tale of the Good and the Bad Cdk5: Remodeling of the Actin Cytoskeleton in the Brain." Mol Neurobiol **55**(4): 3426-3438.
Shangary, S. and S. Wang (2008). "Targeting the MDM2-p53 interaction for cancer therapy." Clin Cancer Res **14**(17): 5318-5324.
She, Q. B., N. Chen and Z. Dong (2000). "ERKs and p38 kinase phosphorylate p53 protein at serine 15 in response to UV radiation." J Biol Chem **275**(27): 20444-20449.
Sheehan, M. A., A. D. Mills, A. M. Sleeman, R. A. Laskey and J. J. Blow (1988). "Steps in the assembly of replication-competent nuclei in a cell-free system from Xenopus eggs." J Cell Biol **106**(1): 1-12.
Sheikh-Hamad, D. and M. C. Gustin (2004). "MAP kinases and the adaptive response to hypertonicity: functional preservation from yeast to mammals." Am J Physiol Renal Physiol **287**(6): F1102-1110.
Shi, Y. and J. Massague (2003). "Mechanisms of TGF-beta signaling from cell membrane to the nucleus." Cell **113**(6): 685-700.
Shibata, A., D. Moiani, A. S. Arvai, J. Perry, S. M. Harding, M. M. Genois, R. Maity, S. van Rossum-Fikkert, A. Kertokalio, F. Romoli, A. Ismail, E. Ismalaj, E. Petricci, M. J. Neale, R. G. Bristow, J. Y. Masson, C. Wyman, P. A. Jeggo and J. A. Tainer (2014). "DNA double-strand break repair pathway choice is directed by distinct MRE11 nuclease activities." Mol Cell **53**(1): 7-18.
Shieh, S. Y., M. Ikeda, Y. Taya and C. Prives (1997). "DNA damage-induced phosphorylation of p53 alleviates inhibition by MDM2." Cell **91**(3): 325-334.
Shorter, J. and G. Warren (2002). "Golgi architecture and inheritance." Annu Rev Cell Dev Biol **18**: 379-420.
Siegel, P. M. and J. Massague (2003). "Cytostatic and apoptotic actions of TGF-beta in homeostasis and cancer." Nat Rev Cancer **3**(11): 807-821.
Silva Cascales, H., K. Burdova, A. Middleton, V. Kuzin, E. Mullers, H. Stoy, L. Baranello, L. Macurek and A. Lindqvist (2021). "Cyclin A2 localises in the cytoplasm at the S/G2 transition to activate PLK1." Life Sci Alliance **4**(3).

Sivan, G., N. Kedersha and O. Elroy-Stein (2007). "Ribosomal slowdown mediates translational arrest during cellular division." Mol Cell Biol **27**(19): 6639-6646.
Skop, A. R., D. Bergmann, W. A. Mohler and J. G. White (2001). "Completion of cytokinesis in C. elegans requires a brefeldin A-sensitive membrane accumulation at the cleavage furrow apex." Curr Biol **11**(10): 735-746.
Skop, A. R., H. Liu, J. Yates, 3rd, B. J. Meyer and R. Heald (2004). "Dissection of the mammalian midbody proteome reveals conserved cytokinesis mechanisms." Science **305**(5680): 61-66.
Skop, A. R. and J. G. White (1998). "The dynactin complex is required for cleavage plane specification in early Caenorhabditis elegans embryos." Curr Biol **8**(20): 1110-1116.
Skoufias, D. A., S. DeBonis, Y. Saoudi, L. Lebeau, I. Crevel, R. Cross, R. H. Wade, D. Hackney and F. Kozielski (2006). "S-trityl-L-cysteine is a reversible, tight binding inhibitor of the human kinesin Eg5 that specifically blocks mitotic progression." J Biol Chem **281**(26): 17559-17569.
Slep, K. C. (2010). "Structural and mechanistic insights into microtubule end-binding proteins." Curr Opin Cell Biol **22**(1): 88-95.
Slevin, L. K., J. Nye, D. C. Pinkerton, D. W. Buster, G. C. Rogers and K. C. Slep (2012). "The structure of the plk4 cryptic polo box reveals two tandem polo boxes required for centriole duplication." Structure **20**(11): 1905-1917.
Smith, E., N. Hegarat, C. Vesely, I. Roseboom, C. Larch, H. Streicher, K. Straatman, H. Flynn, M. Skehel, T. Hirota, R. Kuriyama and H. Hochegger (2011). "Differential control of Eg5-dependent centrosome separation by Plk1 and Cdk1." EMBO J **30**(11): 2233-2245.
Smits, V. A. (2006). "Spreading the signal: dissociation of Chk1 from chromatin." Cell Cycle **5**(10): 1039-1043.
Smits, V. A., R. Klompmaker, L. Arnaud, G. Rijksen, E. A. Nigg and R. H. Medema (2000). "Polo-like kinase-1 is a target of the DNA damage checkpoint." Nat Cell Biol **2**(9): 672-676.
Speck, C., Z. Chen, H. Li and B. Stillman (2005). "ATPase-dependent cooperative binding of ORC and Cdc6 to origin DNA." Nat Struct Mol Biol **12**(11): 965-971.
Srivastava, S., E. Zasadzinska and D. R. Foltz (2018). "Posttranslational mechanisms controlling centromere function and assembly." Curr Opin Cell Biol **52**: 126-135.
Stearns, T. (2001). "Centrosome duplication. a centriolar pas de deux." Cell **105**(4): 417-420.
Steen, R. L., S. B. Martins, K. Tasken and P. Collas (2000). "Recruitment of protein phosphatase 1 to the nuclear envelope by A-kinase anchoring protein AKAP149 is a prerequisite for nuclear lamina assembly." J Cell Biol **150**(6): 1251-1262.
Steigemann, P. and D. W. Gerlich (2009). "Cytokinetic abscission: cellular dynamics at the midbody." Trends Cell Biol **19**(11): 606-616.
Steigemann, P., C. Wurzenberger, M. H. Schmitz, M. Held, J. Guizetti, S. Maar and D. W. Gerlich (2009). "Aurora B-mediated abscission checkpoint protects against tetraploidization." Cell **136**(3): 473-484.
Stewart, G. S., B. Wang, C. R. Bignell, A. M. Taylor and S. J. Elledge (2003). "MDC1 is a mediator of the mammalian DNA damage checkpoint." Nature **421**(6926): 961-966.
Stewart, S. and G. Fang (2005). "Destruction box-dependent degradation of aurora B is mediated by the anaphase-promoting complex/cyclosome and Cdh1." Cancer Res **65**(19): 8730-8735.
Stoter, M., A. M. Bamberger, B. Aslan, M. Kurth, D. Speidel, T. Loning, H. G. Frank, P. Kaufmann, J. Lohler, D. Henne-Bruns, W. Deppert and U. Knippschild (2005). "Inhibition of casein kinase I delta alters mitotic spindle formation and induces apoptosis in trophoblast cells." Oncogene **24**(54): 7964-7975.
Su, T. T. and B. Jaklevic (2001). "DNA damage leads to a Cyclin A-dependent delay in metaphase-anaphase transition in the Drosophila gastrula." Curr Biol **11**(1): 8-17.
Subramanian, R., E. M. Wilson-Kubalek, C. P. Arthur, M. J. Bick, E. A. Campbell, S. A. Darst, R. A. Milligan and T. M. Kapoor (2010). "Insights into antiparallel microtubule crosslinking by PRC1, a conserved nonmotor microtubule binding protein." Cell **142**(3): 433-443.
Sudakin, V., G. K. Chan and T. J. Yen (2001). "Checkpoint inhibition of the APC/C in HeLa cells is mediated by a complex of BUBR1, BUB3, CDC20, and MAD2." J Cell Biol **154**(5): 925-936.

Sumara, I., M. Quadroni, C. Frei, M. H. Olma, G. Sumara, R. Ricci and M. Peter (2007). "A Cul3-based E3 ligase removes Aurora B from mitotic chromosomes, regulating mitotic progression and completion of cytokinesis in human cells." Dev Cell **12**(6): 887-900.
Sun, J., Y. Shi, R. E. Georgescu, Z. Yuan, B. T. Chait, H. Li and M. E. O'Donnell (2015). "The architecture of a eukaryotic replisome." Nat Struct Mol Biol **22**(12): 976-982.
Sung, P. and H. Klein (2006). "Mechanism of homologous recombination: mediators and helicases take on regulatory functions." Nat Rev Mol Cell Biol **7**(10): 739-750.
Sunkel, C. E. and D. M. Glover (1988). "polo, a mitotic mutant of Drosophila displaying abnormal spindle poles." J Cell Sci **89 (Pt 1)**: 25-38.
Swingle, M., L. Ni and R. E. Honkanen (2007). "Small-molecule inhibitors of ser/thr protein phosphatases: specificity, use and common forms of abuse." Methods Mol Biol **365**: 23-38.
Sy, S. M., M. S. Huen and J. Chen (2009). "PALB2 is an integral component of the BRCA complex required for homologous recombination repair." Proc Natl Acad Sci U S A **106**(17): 7155-7160.
Symington, L. S. and J. Gautier (2011). "Double-strand break end resection and repair pathway choice." Annu Rev Genet **45**: 247-271.
Taal, K., J. Tuvikene, G. Rullinkov, M. Piirsoo, M. Sepp, T. Neuman, R. Tamme and T. Timmusk (2019). "Neuralized family member NEURL1 is a ubiquitin ligase for the cGMP-specific phosphodiesterase 9A." Sci Rep **9**(1): 7104.
Takai, N., R. Hamanaka, J. Yoshimatsu and I. Miyakawa (2005). "Polo-like kinases (Plks) and cancer." Oncogene **24**(2): 287-291.
Takayama, Y., Y. Kamimura, M. Okawa, S. Muramatsu, A. Sugino and H. Araki (2003). "GINS, a novel multiprotein complex required for chromosomal DNA replication in budding yeast." Genes Dev **17**(9): 1153-1165.
Takeda, D. Y. and A. Dutta (2005). "DNA replication and progression through S phase." Oncogene **24**(17): 2827-2843.
Takizawa, C. G. and D. O. Morgan (2000). "Control of mitosis by changes in the subcellular location of cyclin-B1-Cdk1 and Cdc25C." Curr Opin Cell Biol **12**(6): 658-665.
Tame, M. A., J. A. Raaijmakers, P. Afanasyev and R. H. Medema (2016). "Chromosome misalignments induce spindle-positioning defects." EMBO Rep **17**(3): 317-325.
Tan, S. T., C. Dai, H. T. Liu and H. W. Xue (2013). "Arabidopsis casein kinase1 proteins CK1.3 and CK1.4 phosphorylate cryptochrome2 to regulate blue light signaling." Plant Cell **25**(7): 2618-2632.
Tan, Y., P. Raychaudhuri and R. H. Costa (2007). "Chk2 mediates stabilization of the FoxM1 transcription factor to stimulate expression of DNA repair genes." Mol Cell Biol **27**(3): 1007-1016.
Tanaka, T. U., N. Rachidi, C. Janke, G. Pereira, M. Galova, E. Schiebel, M. J. Stark and K. Nasmyth (2002). "Evidence that the Ipl1-Sli15 (Aurora kinase-INCENP) complex promotes chromosome bi-orientation by altering kinetochore-spindle pole connections." Cell **108**(3): 317-329.
Taneja, N., A. M. Fenix, L. Rathbun, B. A. Millis, M. J. Tyska, H. Hehnly and D. T. Burnette (2016). "Focal adhesions control cleavage furrow shape and spindle tilt during mitosis." Sci Rep **6**: 29846.
Tanenbaum, M. E., L. Macurek, N. Galjart and R. H. Medema (2008). "Dynein, Lis1 and CLIP-170 counteract Eg5-dependent centrosome separation during bipolar spindle assembly." EMBO J **27**(24): 3235-3245.
Terasaki, M., P. Campagnola, M. M. Rolls, P. A. Stein, J. Ellenberg, B. Hinkle and B. Slepchenko (2001). "A new model for nuclear envelope breakdown." Mol Biol Cell **12**(2): 503-510.
Thadani, R., F. Uhlmann and S. Heeger (2012). "Condensin, chromatin crossbarring and chromosome condensation." Curr Biol **22**(23): R1012-1021.
Torvaldson, E., V. Kochin and J. E. Eriksson (2015). "Phosphorylation of lamins determine their structural properties and signaling functions." Nucleus **6**(3): 166-171.
Toyoshima-Morimoto, F., E. Taniguchi and E. Nishida (2002). "Plk1 promotes nuclear translocation of human Cdc25C during prophase." EMBO Rep **3**(4): 341-348.
Toyoshima, F. and E. Nishida (2007). "Integrin-mediated adhesion orients the spindle parallel to the substratum in an EB1- and myosin X-dependent manner." EMBO J **26**(6): 1487-1498.

Tsai, I. C., M. Woolf, D. W. Neklason, W. W. Branford, H. J. Yost, R. W. Burt and D. M. Virshup (2007). "Disease-associated casein kinase I delta mutation may promote adenomatous polyps formation via a Wnt/beta-catenin independent mechanism." Int J Cancer **120**(5): 1005-1012.
Tsuruta, H., G. W. Verhaegh and J. A. Schalken (2014). "The Expression and Function of Fam110a in Human Prostate Cancer." Journal of Urology **191**(4): E327-E327.
Tsvetkov, L. M., K. H. Yeh, S. J. Lee, H. Sun and H. Zhang (1999). "p27(Kip1) ubiquitination and degradation is regulated by the SCF(Skp2) complex through phosphorylated Thr187 in p27." Curr Biol **9**(12): 661-664.
Uehara, R. and G. Goshima (2010). "Functional central spindle assembly requires de novo microtubule generation in the interchromosomal region during anaphase." J Cell Biol **191**(2): 259-267.
Uehara, R., R. S. Nozawa, A. Tomioka, S. Petry, R. D. Vale, C. Obuse and G. Goshima (2009). "The augmin complex plays a critical role in spindle microtubule generation for mitotic progression and cytokinesis in human cells." Proc Natl Acad Sci U S A **106**(17): 6998-7003.
Uetake, Y. and G. Sluder (2010). "Prolonged prometaphase blocks daughter cell proliferation despite normal completion of mitosis." Curr Biol **20**(18): 1666-1671.
Uhlen, M., L. Fagerberg, B. M. Hallstrom, C. Lindskog, P. Oksvold, A. Mardinoglu, A. Sivertsson, C. Kampf, E. Sjostedt, A. Asplund, I. Olsson, K. Edlund, E. Lundberg, S. Navani, C. A. Szigyarto, J. Odeberg, D. Djureinovic, J. O. Takanen, S. Hober, T. Alm, P. H. Edqvist, H. Berling, H. Tegel, J. Mulder, J. Rockberg, P. Nilsson, J. M. Schwenk, M. Hamsten, K. von Feilitzen, M. Forsberg, L. Persson, F. Johansson, M. Zwahlen, G. von Heijne, J. Nielsen and F. Ponten (2015). "Proteomics. Tissue-based map of the human proteome." Science **347**(6220): 1260419.
Uhlmann, F. (2001). "Chromosome cohesion and segregation in mitosis and meiosis." Curr Opin Cell Biol **13**(6): 754-761.
Utz, A. C., H. Hirner, A. Blatz, A. Hillenbrand, B. Schmidt, W. Deppert, D. Henne-Bruns, D. Fischer, D. R. Thal, F. Leithauser and U. Knippschild (2010). "Analysis of cell type-specific expression of CK1 epsilon in various tissues of young adult BALB/c Mice and in mammary tumors of SV40 T-Ag-transgenic mice." J Histochem Cytochem **58**(1): 1-15.
Vagnarelli, P., D. F. Hudson, S. A. Ribeiro, L. Trinkle-Mulcahy, J. M. Spence, F. Lai, C. J. Farr, A. I. Lamond and W. C. Earnshaw (2006). "Condensin and Repo-Man-PP1 co-operate in the regulation of chromosome architecture during mitosis." Nat Cell Biol **8**(10): 1133-1142.
Vainio, P., M. Wolf, H. Edgren, T. He, P. Kohonen, J. P. Mpindi, F. Smit, G. Verhaegh, J. Schalken, M. Perala, K. Iljin and O. Kallioniemi (2012). "Integrative genomic, transcriptomic, and RNAi analysis indicates a potential oncogenic role for FAM110B in castration-resistant prostate cancer." Prostate **72**(7): 789-802.
van Leen, E. V., F. di Pietro and Y. Bellaiche (2020). "Oriented cell divisions in epithelia: from force generation to force anisotropy by tension, shape and vertices." Curr Opin Cell Biol **62**: 9-16.
Van Rechem, C., F. Ji, S. Mishra, D. Chakraborty, S. E. Murphy, M. E. Dillingham, R. I. Sadreyev and J. R. Whetstine (2020). "The lysine demethylase KDM4A controls the cell-cycle expression of replicative canonical histone genes." Biochim Biophys Acta Gene Regul Mech **1863**(10): 194624.
van Vugt, M. A., A. Bras and R. H. Medema (2004). "Polo-like kinase-1 controls recovery from a G2 DNA damage-induced arrest in mammalian cells." Mol Cell **15**(5): 799-811.
van Vugt, M. A., V. A. Smits, R. Klompmaker and R. H. Medema (2001). "Inhibition of Polo-like kinase-1 by DNA damage occurs in an ATM- or ATR-dependent fashion." J Biol Chem **276**(45): 41656-41660.
Venerando, A., M. Ruzzene and L. A. Pinna (2014). "Casein kinase: the triple meaning of a misnomer." Biochem J **460**(2): 141-156.
Vigneron, S., L. Sundermann, J. C. Labbe, L. Pintard, O. Radulescu, A. Castro and T. Lorca (2018). "Cyclin A-cdk1-Dependent Phosphorylation of Bora Is the Triggering Factor Promoting Mitotic Entry." Dev Cell **45**(5): 637-650 e637.
Walter, J. and J. Newport (2000). "Initiation of eukaryotic DNA replication: origin unwinding and sequential chromatin association of Cdc45, RPA, and DNA polymerase alpha." Mol Cell **5**(4): 617-627.

Walther, T. C., A. Alves, H. Pickersgill, I. Loiodice, M. Hetzer, V. Galy, B. B. Hulsmann, T. Kocher, M. Wilm, T. Allen, I. W. Mattaj and V. Doye (2003). "The conserved Nup107-160 complex is critical for nuclear pore complex assembly." Cell **113**(2): 195-206.
Walther, T. C., P. Askjaer, M. Gentzel, A. Habermann, G. Griffiths, M. Wilm, I. W. Mattaj and M. Hetzer (2003). "RanGTP mediates nuclear pore complex assembly." Nature **424**(6949): 689-694.
Wandke, C., M. Barisic, R. Sigl, V. Rauch, F. Wolf, A. C. Amaro, C. H. Tan, A. J. Pereira, U. Kutay, H. Maiato, P. Meraldi and S. Geley (2012). "Human chromokinesins promote chromosome congression and spindle microtubule dynamics during mitosis." J Cell Biol **198**(5): 847-863.
Wang, I. C., Y. J. Chen, D. Hughes, V. Petrovic, M. L. Major, H. J. Park, Y. Tan, T. Ackerson and R. H. Costa (2005). "Forkhead box M1 regulates the transcriptional network of genes essential for mitotic progression and genes encoding the SCF (Skp2-Cks1) ubiquitin ligase." Mol Cell Biol **25**(24): 10875-10894.
Wang, J. C. (2002). "Cellular roles of DNA topoisomerases: a molecular perspective." Nat Rev Mol Cell Biol **3**(6): 430-440.
Wang, L., W. Dai and L. Lu (2007). "Stress-induced c-Jun activation mediated by Polo-like kinase 3 in corneal epithelial cells." J Biol Chem **282**(44): 32121-32127.
Wang, L., W. Dai and L. Lu (2011). "Hyperosmotic stress-induced corneal epithelial cell death through activation of Polo-like kinase 3 and c-Jun." Invest Ophthalmol Vis Sci **52**(6): 3200-3206.
Wang, L., W. Dai and L. Lu (2014). "Osmotic stress-induced phosphorylation of H2AX by polo-like kinase 3 affects cell cycle progression in human corneal epithelial cells." J Biol Chem **289**(43): 29827-29835.
Wang, L., J. Gao, W. Dai and L. Lu (2008). "Activation of Polo-like kinase 3 by hypoxic stresses." J Biol Chem **283**(38): 25928-25935.
Wang, L., R. Payton, W. Dai and L. Lu (2011). "Hyperosmotic stress-induced ATF-2 activation through Polo-like kinase 3 in human corneal epithelial cells." J Biol Chem **286**(3): 1951-1958.
Wang, S., H. Tukachinsky, F. B. Romano and T. A. Rapoport (2016). "Cooperation of the ER-shaping proteins atlastin, lunapark, and reticulons to generate a tubular membrane network." Elife **5**.
Wang, Y., T. B. Liu, S. Patel, L. Jiang and C. Xue (2011). "The casein kinase I protein Cck1 regulates multiple signaling pathways and is essential for cell integrity and fungal virulence in Cryptococcus neoformans." Eukaryot Cell **10**(11): 1455-1464.
Watanabe, K., T. Umeda, K. Niwa, I. Naguro and H. Ichijo (2018). "A PP6-ASK3 Module Coordinates the Bidirectional Cell Volume Regulation under Osmotic Stress." Cell Rep **22**(11): 2809-2817.
Watanabe, N., H. Arai, J. Iwasaki, M. Shiina, K. Ogata, T. Hunter and H. Osada (2005). "Cyclin-dependent kinase (CDK) phosphorylation destabilizes somatic Wee1 via multiple pathways." Proc Natl Acad Sci U S A **102**(33): 11663-11668.
Weberruss, M. and W. Antonin (2016). "Perforating the nuclear boundary - how nuclear pore complexes assemble." J Cell Sci **129**(24): 4439-4447.
Werner, M., E. Munro and M. Glotzer (2007). "Astral signals spatially bias cortical myosin recruitment to break symmetry and promote cytokinesis." Curr Biol **17**(15): 1286-1297.
Whalley, H. J. and A. Malliri (2015). "Centrosome separation; a careful balancing act." Cell Cycle **14**(19): 3001-3002.
Willems, E., M. Dedobbeleer, M. Digregorio, A. Lombard, P. N. Lumapat and B. Rogister (2018). "The functional diversity of Aurora kinases: a comprehensive review." Cell Div **13**: 7.
Williams, G. J., S. P. Lees-Miller and J. A. Tainer (2010). "Mre11-Rad50-Nbs1 conformations and the control of sensing, signaling, and effector responses at DNA double-strand breaks." DNA Repair (Amst) **9**(12): 1299-1306.
Wilson, K. L. and J. Newport (1988). "A trypsin-sensitive receptor on membrane vesicles is required for nuclear envelope formation in vitro." J Cell Biol **107**(1): 57-68.
Winter, M., D. Milne, S. Dias, R. Kulikov, U. Knippschild, C. Blattner and D. Meek (2004). "Protein kinase CK1delta phosphorylates key sites in the acidic domain of murine double-minute clone 2 protein (MDM2) that regulate p53 turnover." Biochemistry **43**(51): 16356-16364.

Wisdom, R., R. S. Johnson and C. Moore (1999). "c-Jun regulates cell cycle progression and apoptosis by distinct mechanisms." EMBO J **18**(1): 188-197.
Wolfe, B. A., T. Takaki, M. Petronczki and M. Glotzer (2009). "Polo-like kinase 1 directs assembly of the HsCyk-4 RhoGAP/Ect2 RhoGEF complex to initiate cleavage furrow formation." PLoS Biol **7**(5): e1000110.
Woodcock, S. A., H. J. Rushton, E. Castaneda-Saucedo, K. Myant, G. R. White, K. Blyth, O. J. Sansom and A. Malliri (2010). "Tiam1-Rac signaling counteracts Eg5 during bipolar spindle assembly to facilitate chromosome congression." Curr Biol **20**(7): 669-675.
Woolner, S., L. L. O'Brien, C. Wiese and W. M. Bement (2008). "Myosin-10 and actin filaments are essential for mitotic spindle function." J Cell Biol **182**(1): 77-88.
Xi, T. and G. Zhang (2018). "Integrated analysis of tumor differentiation genes in pancreatic adenocarcinoma." PLoS One **13**(3): e0193427.
Xiao, Z., Z. Chen, A. H. Gunasekera, T. J. Sowin, S. H. Rosenberg, S. Fesik and H. Zhang (2003). "Chk1 mediates S and G2 arrests through Cdc25A degradation in response to DNA-damaging agents." J Biol Chem **278**(24): 21767-21773.
Xie, M., L. Cai, J. Li, J. Zhao, Y. Guo, Z. Hou, X. Zhang, H. Tian, A. Li and Y. Miao (2020). "FAM110B Inhibits Non-Small Cell Lung Cancer Cell Proliferation and Invasion Through Inactivating Wnt/beta-Catenin Signaling." Onco Targets Ther **13**: 4373-4384.
Xie, S., Q. Wang, Q. Ruan, T. Liu, M. Jhanwar-Uniyal, K. Guan and W. Dai (2004). "MEK1-induced Golgi dynamics during cell cycle progression is partly mediated by Polo-like kinase-3." Oncogene **23**(21): 3822-3829.
Xie, S., H. Wu, Q. Wang, J. P. Cogswell, I. Husain, C. Conn, P. Stambrook, M. Jhanwar-Uniyal and W. Dai (2001). "Plk3 functionally links DNA damage to cell cycle arrest and apoptosis at least in part via the p53 pathway." J Biol Chem **276**(46): 43305-43312.
Xu, B., A. H. O'Donnell, S. T. Kim and M. B. Kastan (2002). "Phosphorylation of serine 1387 in Brca1 is specifically required for the Atm-mediated S-phase checkpoint after ionizing irradiation." Cancer Res **62**(16): 4588-4591.
Xu, X. and D. F. Stern (2003). "NFBD1/KIAA0170 is a chromatin-associated protein involved in DNA damage signaling pathways." J Biol Chem **278**(10): 8795-8803.
Yamagishi, Y., C. H. Yang, Y. Tanno and Y. Watanabe (2012). "MPS1/Mph1 phosphorylates the kinetochore protein KNL1/Spc7 to recruit SAC components." Nat Cell Biol **14**(7): 746-752.
Yang, H. W., M. Chung, T. Kudo and T. Meyer (2017). "Competing memories of mitogen and p53 signalling control cell-cycle entry." Nature **549**(7672): 404-408.
Yang, Y., J. Bai, R. Shen, S. A. Brown, E. Komissarova, Y. Huang, N. Jiang, G. F. Alberts, M. Costa, L. Lu, J. A. Winkles and W. Dai (2008). "Polo-like kinase 3 functions as a tumor suppressor and is a negative regulator of hypoxia-inducible factor-1 alpha under hypoxic conditions." Cancer Res **68**(11): 4077-4085.
Yu, J., X. Sun, J. Y. G. Goie and Y. Zhang (2020). "Regulation of Host Immune Responses against Influenza A Virus Infection by Mitogen-Activated Protein Kinases (MAPKs)." Microorganisms **8**(7).
Yuan, J. and J. Chen (2010). "MRE11-RAD50-NBS1 complex dictates DNA repair independent of H2AX." J Biol Chem **285**(2): 1097-1104.
Yuce, O., A. Piekny and M. Glotzer (2005). "An ECT2-centralspindlin complex regulates the localization and function of RhoA." J Cell Biol **170**(4): 571-582.
Zemp, I., F. Wandrey, S. Rao, C. Ashiono, E. Wyler, C. Montellese and U. Kutay (2014). "CK1delta and CK1epsilon are components of human 40S subunit precursors required for cytoplasmic 40S maturation." J Cell Sci **127**(Pt 6): 1242-1253.
Zetterberg, A., O. Larsson and K. G. Wiman (1995). "What is the restriction point?" Curr Opin Cell Biol **7**(6): 835-842.
Zhang, X., L. Lin, H. Guo, J. Yang, S. N. Jones, A. Jochemsen and X. Lu (2009). "Phosphorylation and degradation of MdmX is inhibited by Wip1 phosphatase in the DNA damage response." Cancer Res **69**(20): 7960-7968.

Zhang, Z., K. Shibahara and B. Stillman (2000). "PCNA connects DNA replication to epigenetic inheritance in yeast." Nature **408**(6809): 221-225.
Zhao, F., W. Kim, J. A. Kloeber and Z. Lou (2020). "DNA end resection and its role in DNA replication and DSB repair choice in mammalian cells." Exp Mol Med **52**(10): 1705-1714.
Zhao, H., J. L. Watkins and H. Piwnica-Worms (2002). "Disruption of the checkpoint kinase 1/cell division cycle 25A pathway abrogates ionizing radiation-induced S and G2 checkpoints." Proc Natl Acad Sci U S A **99**(23): 14795-14800.
Zhao, W., J. B. Steinfeld, F. Liang, X. Chen, D. G. Maranon, C. Jian Ma, Y. Kwon, T. Rao, W. Wang, C. Sheng, X. Song, Y. Deng, J. Jimenez-Sainz, L. Lu, R. B. Jensen, Y. Xiong, G. M. Kupfer, C. Wiese, E. C. Greene and P. Sung (2017). "BRCA1-BARD1 promotes RAD51-mediated homologous DNA pairing." Nature **550**(7676): 360-365.
Zheng, L., U. Baumann and J. L. Reymond (2004). "An efficient one-step site-directed and site-saturation mutagenesis protocol." Nucleic Acids Res **32**(14): e115.
Zheng, Z., H. Zhu, Q. Wan, J. Liu, Z. Xiao, D. P. Siderovski and Q. Du (2010). "LGN regulates mitotic spindle orientation during epithelial morphogenesis." J Cell Biol **189**(2): 275-288.
Zhou, T., J. P. Aumais, X. Liu, L. Y. Yu-Lee and R. L. Erikson (2003). "A role for Plk1 phosphorylation of NudC in cytokinesis." Dev Cell **5**(1): 127-138.
Zimmerman, W. C. and R. L. Erikson (2007). "Polo-like kinase 3 is required for entry into S phase." Proc Natl Acad Sci U S A **104**(6): 1847-1852.
Zimmermann, M. and T. de Lange (2014). "53BP1: pro choice in DNA repair." Trends Cell Biol **24**(2): 108-117.
Zitouni, S., C. Nabais, S. C. Jana, A. Guerrero and M. Bettencourt-Dias (2014). "Polo-like kinases: structural variations lead to multiple functions." Nat Rev Mol Cell Biol **15**(7): 433-452.
Ziv, Y., D. Bielopolski, Y. Galanty, C. Lukas, Y. Taya, D. C. Schultz, J. Lukas, S. Bekker-Jensen, J. Bartek and Y. Shiloh (2006). "Chromatin relaxation in response to DNA double-strand breaks is modulated by a novel ATM- and KAP-1 dependent pathway." Nat Cell Biol **8**(8): 870-876.
Zou, L. and S. J. Elledge (2003). "Sensing DNA damage through ATRIP recognition of RPA-ssDNA complexes." Science **300**(5625): 1542-1548.

8. PUBLICATIONS

This thesis is mainly based on the following publications:

Phosphorylation of PLK3 is controlled by Protein Phosphatase 6.
Cecilia Aquino Perez, Matous Palek, Lenka Stolarova, Patrick von Morgen and Libor Macůrek.
Cells. 2020 June 17: 9, 1506; DOI: 10.3390/cells9061506.

IF: 6.600 (2021)

Author Contributions: CAP conducted most of the experiments; acquired and analyzed the confocal microscopy, FACS, immunoprecipitation, knock-down and stress-induction data. MP performed ScanR microscopy data acquirement and analysis, LS performed the qPCR analysis for KO cell lines validation. PvM generated the ectopic expression stable cell lines and performed preliminary experiments. LM conceptualized and supervised the project, generated KO cell lines, performed kinases assays and analyzed and curated the data, wrote the first draft of the manuscript and acquired funding for the project. All authors read and edited the final version of the manuscript.

CK1-mediated phosphorylation of FAM110A promotes its interaction with mitotic spindle and controls chromosomal alignment.
Cecilia Aquino Perez, Monika Burocziova, Gabriela Jenikova and Libor Macůrek.
EMBO reports. 2021 May 5: e51847; DOI: 10.15252/embr.202051847

IF: 8.807 (2021)

Author Contributions: CAP conducted most of the experiments; generated stable cell lines, acquired, analyzed and quantified the confocal microscopy, time-lapse microscopy, FACS, immunoprecipitation, knock-down, spindle measurement and actin dynamics data. MB and GJ performed the expression profiling and qPCR confirmation of the hits. LM conceptualized and supervised the project, designed and generated mutant constructs, performed kinase assays, analyzed the data, wrote the first draft of the manuscript and acquired funding for the project. All authors read and edited the final version of the manuscript.

APPENDIX

Original publications attached.